Kombikraftwerk 2

Final Report

August 2014


The translation from German into English was kindly provided by Stellenbosch University and reviewed by the authors.

Authors:

Fraunhofer IWES: Kaspar Knorr, Britta Zimmermann, Dirk Kirchner, Markus Speckmann, Raphael Spieckermann, Martin Widdel, Manuela Wunderlich, Dr. Reinhard Mackensen, Dr. Kurt Rohrig

Siemens AG: Dr. Florian Steinke, Dr. Philipp Wolfrum

Institut für Energieversorgung und Hochspannungstechnik, Fachgebiet Elektrische Energieversorgung der Universität Hannover: Thomas Leveringhaus, Thomas Lager, Prof. Dr.-Ing. habil. Lutz Hofmann

CUBE Engineering GmbH: Dirk Filzek, Tina Göbel, Bettina Kusserow, Lars Nicklaus, Peter Ritter

The project underlying this report was funded by the Federal Ministry for the Environment, Nature Conservation, Building and Nuclear Safety under the funding codes 0325248A-D. The responsibility for the contents of this publication lies with the authors.

Gefördert durch:

Bundesministerium
für Umwelt, Naturschutz,
Bau und Reaktorsicherheit

aufgrund eines Beschlusses
des Deutschen Bundestages

Summary

In the autumn of 2007, the project “Kombikraftwerk 1” proved that a purely regenerative power supply is basically feasible. With the specially developed regenerative virtual power plant, the ‘Kombikraftwerk’, intelligently interlinking power producer and user and storage, a plant park of 36 renewable energy plants was able to meet the actual German electricity requirements in a ratio of 1:10.000.

After it had been proved that renewable energy sources (RE) when combined with storage were able to make power available on demand at any time, the question arose whether the grid stability indispensable for security of supply in a power system using 100% renewable sources could be guaranteed at all times.

It involves ensuring that the voltage and frequency lie within designated limits at any place within the grid and at all times. Major deviations of voltage can only be remedied locally, i.e., by nearby plants, deviations in frequency require especially a very rapid response. These measures to maintain grid stability are called ancillary services. Thus for our future power supply, the following questions arise: whether the plants likely to be available to the system are connected to the grid at the correct places in order to maintain the voltage and whether their technical abilities are sufficiently well developed to react rapidly to deviations in frequency. In many quarters it is feared that a power supply system based 100% on renewable energies could not cope with these tasks. The research project “Kombikraftwerk 2” had the task of investigating what future demands of ancillary services there would probably be and how a purely RE-based power system could deliver these in future.

In order to adequately model grid stability, initially a consistent future scenario of power producers, consumers, storages and the grid was modelled with a high temporal and singularly high spatial resolution regarding the position of power producers and storage. Within the framework of this scenario and using simulations, tests were carried out to determine whether the system could deliver sufficient control reserve to maintain frequency, and reactive power to maintain voltage stability, whether grid congestions can be avoided or else rectified and whether producers of renewables could possibly take over the restoration of supply if the grid were to break down. At the same time, possibilities were explored how RE-plants could deliver these services necessary for grid stability. The solutions were demonstrated at the actual wind energy, photovoltaic and bio-energy installations of the regenerative Kombikraftwerk.

The result of the project shows: Grid stability can be ensured at any time! These theoretical conclusions were successfully confirmed by a laboratory test on the restoration of supply as well as several field tests.

However, to reach the goal of an energy transition, several political, economic and technical efforts will have to be made during the next years and decades. The challenges of maintaining grid stability which are raised by the change in electricity supply are less to be seen in RE which, in principle, fulfil the necessary technical requirements now already. The new types of structure of prospective power production and distribution demands require rather a rethinking of the organisation of the system. It is a matter of transformation of the system, which will put the fluctuating feed-in from wind power

and photovoltaic (PV) facilities in the centre, as an essential supporting pillar. Flexible biomass facilities (biogas and solid mass) and bio-methane facilities form an important part of the energy system and contribute to a secure service. An appropriately adapted expansion of the grid with all its components, adapting regulations and the creation of both adequate flexibilities and a power storage system are important pillars for the turnaround in electricity supply.

In summary, the most important outcomes of the project are the following:

- A secure and stable future electricity supply for Germany from 100% renewable sources is technically possible if renewable production, storage and backup power plants with renewable gas work together intelligently.
- Even now, RE can provide technically important ancillary services. At the same time, they are able to react extremely quickly.
  However, the general conditions of market and system integration would have to be adapted so that market participation is possible for all RE-installations.
- In order to guarantee grid security, decentralised RE-plants, too, would have to be monitored and steered by secure and efficient communication standards. Linking virtual power plants will increase the room for manoeuvre. The disadvantages of the individual plants, such as faulty forecasts, schedule deviations or outages can be absorbed by the group and thus the services offered can be rendered reliably, with a minimum of external communication requirements.

The project was supported by the Federal Ministry for the Environment and built upon the project Kombikraftwerk 1 which was implemented in 2007. The duration of the project was in excess of three years and ended in December 2013. The project consortium comprised representatives from the areas of research, industry and services. CUBE Engineering, the German Weather Service (DWD), ÖKOBIT GmbH, SIEMENS AG, SMA AG, SolarWorld AG, the Institute for Energy Supply and High Voltage Technology of Leibnitz University Hannover (IEH) and the Agency for Renewable Energy (AEE) worked together as project partners under the leadership of the Fraunhofer Institute for Wind Energy and Energy System Technology (IWES).

Table of contents

Summary 5

List of figures 10

List of tables 16

List of abbreviations 17

Preface 21

1 Introduction 22

2 The 100%-RE-scenario 24

2.1 Dimensioning and unit commitment 27

2.2 Overview of scenario data 30

Annual 31

2.3 Power consumption 33

2.3.1 Modelling spatial distribution 35

2.3.2 Production and evaluation of time series 35

2.4 Producers 39

2.4.1 Wind energy 39

2.4.2 Photovoltaics 51

2.4.3 Bioenergy 59

2.4.4 Hydro energy 68

2.4.5 Geothermal energy 71

2.4.6 Methane power plants 72

2.5 The grid 77

2.6 Energy storages 83

2.6.1 Power-to-gas 83

2.6.2 Pumped hydro storage 85

2.6.3 Batteries 89

2.6.4 Electricity imports and exports 91

2.7 Conclusions and recommendations 93

3 Power system stability and ancillary services 94

3.1 Control reserve for maintaining frequency stability 96

3.1.1 Current framework conditions 96

3.1.2 Field tests for delivery of control reserve 100

3.1.3 Simulations of the revenue situation for control reserve delivery by flexible energy plants 119

3.1.4 Simulation for reducing control reserve demand through improved forecasts 135

3.1.5 Simulation of control reserve demand in 100% RE scenario 143
3.1.6 Simulation of meeting demand for control reserve in the 100% RE scenario 155
3.1.7 Simulation of dynamic frequency stability in 100% RE-scenario 161
3.1.8 Conclusions and recommendations 166
3.2 Voltage stability and reactive power management 169
3.2.1 Current general conditions 171
3.2.2 Complete power flow calculations 171
3.2.3 Simulation of voltage bands at the highest voltage nodes in the 100% RE scenario 173
3.2.4 Simulation of reactive power demand in highest voltage in the 100% RE scenario 173
3.2.5 Reactive power delivery in extra high voltage level 175
3.2.6 Conclusions and recommendations 184
3.3 Grid congestion management 185
3.3.1 Current general conditions 186
3.3.2 Simulations 186
3.3.3 Conclusions and recommendations 192
3.4 Restoration of supply 193
3.4.1 Current general conditions 193
3.4.2 Laboratory test 194
3.4.3 Conclusions and recommendations 207
4 Summary, recommendations and outlook 209
5 Definition 212
6 References 213

List of figures

Figure 1: Cover of power needs by the plants of Kombikraftwerk 1 22

Figure 2: Set power mix of the scenario..... 24

Figure 3: Determination of potential RE areas..... 26

Figure 4: Spatial distribution of annual energy production and consumption in the scenario 27

Figure 5: Simulation steps in design and unit commitment planning calculations of the flexible producers 28

Figure 6: Characteristics of simulated future feed-in from renewable energies across Germany 32

Figure 7: Standard load profile of households 35

Figure 8: Excerpt from the aggregated power consumption time series for Germanyof the scenario 36

Figure 9: Period with changing weather-dependent energy feed-in, consumption deficit and surplus 36

Figure 10: Annual peak loads 37

Figure 11: Installed wind capacities in the Bundesländer in the scenario [MW]..... 40

Figure 12: Development of an onshore-wind energy scenario..... 41

Figure 13: Selection of WT locations exemplified in a grid-section 42

Figure 14: Size of wind farms in the scenario..... 42

Figure 15: Offshore scenario (above: North Sea below: Baltic) 44

Figure 16: Types of wind turbines in the 100% RE scenario 45

Figure 17: Power curves and thrust coefficient curves of wind turbines in the scenario..... 46

Figure 18: Characteristics of the simulated wind energy feed-in 47

Figure 19: Windy weeks in January 49

Figure 20: a)Connection between the simulated wind energy feed-in across Germany and consumption (left) and b) the curtailment of WT (right) 49

Figure 21: a) Regional distribution of annual curtailment (GWh) with a loss-optimizing (left) or b) equal regulation (right) 50

Figure 22: Calculation of PV areas..... 52

Figure 23: Determining the future PV installations under the assumption of a saturation process („S-Kurve“)..... 53

Figure 24: Distribution curve for production density for various development conditions and orientation of PV pitched roof installtions of a postal code area 54

Figure 25: Diurnal variations of simulated PV feed-in and consumption throughout Germany 56

Figure 26: Relationship between the simulated PV feed-in and power consumption in Germany..... 57

Figure 27: Six selected weeks in the simulated power production in all of Germany 57

Figure 28: Diurnal variation in simulated feed-in from PV and wind energy for all of Germany 58

Figure 29: Diurnal variation in simulated feed-in from PV and wind energy for a) North and b) South Germany 58

Figure 30: Spatial distribution of different bio-energy potentials in the scenario..... 62

Figure 31: Positioning of energy potentials and conversion to power or gas of residual forest wood, waste wood and biogenic waste (locations of crops as at 2010)..... 63

Figure 32: section of the set heat requirement time series, aggregated for all of Germany 64

Figure 33: Meeting the residual load by controllable producers and storage in the last two weeks of the year. For purposes of illustration, the heat load progression is sketched qualitatively. In order to meet this heat load, biogas and biomass installations cannot be switched off completely..... 65

Figure 34: Relationship between the simulated power feed-in from local biomass installations and the residual load for all hours of the year..... 66

Figure 35: Diurnal energies of local bio-energy feed-in 67

Figure 36: Simulated local bio-energy feed-in over heat load 67

Figure 37: Connection between simulated residual load and heat load 68

Figure 38: Spatial distribution of installed hydropower output in scenario 69

Figure 39: Hydropower curve used 70

Figure 40: Frequency distribution of simulated feed-in from hydropower 70

Figure 41: Spatial distribution of geothermic installations in the scenario 72

Figure 42: Number of HV-network nodes with methane power plants and their installed capacity in the scenario divided into classes of capacity 74

Figure 43: Meeting the residual load with controllable producers and storages in the last week of January. The maximum residual load and simultaneous maximum capacity utilization of the methane power plants occurs on 25 January..... 75

Figure 44: Two weeks in winter with the longest duration of use of methane power plants during the scenario year 76

Figure 45: Connection between the simulated operation of methane power plants and the residual load (left) and b) the capacity imports and exports (right)..... 76

Figure 46: The scenario's extra high voltage grid model 79

Figure 47: Modelled catchment areas of the HV nodes..... 81

Figure 48: Simulated grid load dependent on wind and solar energy 82

Figure 49: Required capacity of power-to-gas installations as function of bio-methane produced 84

Figure 50: Regional distribution of the simulated power-to-gas installations..... 84

Figure 51: a) Simulated connection between methanization and residual load (left) and b) power import and export respectively (right) for every hour of the scenario-year and for all of Germany ... 85

Figure 52: The pumped hydro storage power plants in the scenario 86

Figure 53: Average diurnal course of a pumped hydro storage operation, power consumption and photovoltaic feed-in 87

Figure 54: Simulated connection between the operation of pumped hydro storage power plants and residual load 88

Figure 55: Simulated feed-in and feedback daily energy quantities of pumped hydro storage power plants 88

Figure 56: Example of a calculated battery usage plan for a HV network node with a regional PV penetration of household load of an annual average of 66 % and an associated battery capacity of 276 MWh 90

Figure 57: Share of PV daily energy fed into batteries 90

Figure 58: Simulated PV own usage with and without batteries in dependence on the local, energetic share of PV production in the load 91

Figure 59: Simulated daily imports (positive) and exports (negative) 92

Figure 60: Explanations of the concept of grid stability 95

Figure 61: Temporal progress of the three qualities of control reserve [49] 98

Figure 62: Illustration of the “schedule method” 101

Figure 63: Control reserve delivery of a wind farm according to “schedule-method” [60] 102

Figure 64: Illustration of the method “available active power” 102

Figure 65: Locations of the RE plants for the control reserve tests 105

Figure 66: Structure of VPP for delivery of control reserve 106

Figure 67: The three phases of the desired value signal for control reserve 108

Figure 68: Record of demonstration of control reserve delivery by the VPP on 30/10/2013 109

Figure 69: Approach of control reserve deliverd to reference value plateau 112

Figure 70: Accuracy in adherence to constant control reserve reference values 114

Figure 71: Record of a test for control reserve delivery with a wind farm on 11/10/2013 116

Figure 72: Record of a test for control reserve delivery with two biogas installations on 25.9.2013 117

Figure 73: Record of a test for control reserve delivery with photovoltaic installations on 09/10/2013 (screen shots) A group of 11 small and one larger roof-installed plant was used (totalling 970 kW). It shows a good coverage of the reference value (red) derived from the control reserve reference value for PV installation feed-in (green) and the recorded actual feed-in from the PV installations (blue).118

Figure 74: Overview of offer strategies 133

Figure 75: Illustration of probabilistic day-ahead forecast (orange) and 1-h forecast (blue) for a reliability of 99.994 % for the German pool of wind farms (30 GW) 134

Figure 76: Scheme of analysis 1 136

Figure 77: Scheme of analysis 2 136

Figure 78: Overview of wind farms used and table 137

Figure 79: Characteristic output curve depending on temperature 137

Figure 80: Correlation between forecast and observation 138

Figure 81: a) The difference between observation and forecast (set out in % of nominal capacity), smaller than 5 %. b) Difference between observation and forecast (set out in % of the nominal capacity) smaller than 10 % (in case of wind farm 3 – forecast year 2011)..... 138

Figure 82: 5% and 10% value of all wind farms..... 139

Figure 83: RMSE of the 5 % and 10 %-value of all parks 140

Figure 84: RMSE of the forecast for wind farm 4 – 2011 141

Figure 85: RMSE of forecast for all parks 141

Figure 86: Wind-class specific RMSE for Park 4..... 142

Figure 87: Method for dimensioning the static and dynamic demand for control reserve..... 144

Figure 88: Illustration of a two-dimensional kernel density estimation for the wind forecast error . 147

Figure 89: Progress for positive total reserve demand for the scenario year according to the dynamic (continuous line) and the static (dotted line) method..... 149

Figure 90: Progress for positive total negative reserve demand for the scenario year according to the dynamic (continuous line) and the static (dotted line) method 150

Figure 91: Illustration of the positive reserve demand and the demand for the individual errors 152

Figure 92: Illustration of the negative reserve demand and the demand for the individual errors... 152

Figure 93: Control reserve demand with varying degrees of balancing the 1-h forecast error for wind energy and photovoltaics on the level of balancing responsible parties, utilizing the static method 154

Figure 94: Average part of the various sources in producing the six simulated types of control reserves 157

Figure 95: Simulated exploitation of existing potential for the delivery of control reserve from different sources 158

Figure 96: Distribution of simulated control reserve output for a point in time (1st Jan. 2:00) according to various locations and sources..... 159

Figure 97: Simulated utilization of the existing potential for control reserve output of various sources for dynamic dimensioning of reserve power availability. 159

Figure 98: Average share of various sources in producing the six simulated types of control reserve, in case batteries are not included in control reserve production..... 160

Figure 99: Simulated utilization of existing potential for producing control reserve of various sources, without taking batteries into account..... 160

Figure 100: Frequency function and minimum requirements for primary control reserve delivery.. 162

Figure 101: Sorted progression of grid time constants for the scenario year 163

Figure 102: Frequency and output power progression in construction of conventional primary control reserve delivery. 164

Figure 103: Frequency and delivery progress with changed primary control reserve delivery with identification of the major parts: converters, wind energy, rotating masses 166

Figure 104: Single-phase π-equivalent circuit diagram of a transmission line 169

Figure 105: Reactive power demand in a 10 km long 380-kV transmission line in dependence on transmitted active power 170

Figure 106: (n-0) voltage bands of all nodes for all points in time of the scenario year 173

Figure 107: (n-0) voltage bands for all hours of the scenario year at all nodes 173

Figure 108: Simulated average reactive power demand of loads and the highest voltage grid in the 100% RE scenario and the balance. Positive reactive power implies an inductive reactive power, negative reactive power a capacitive reference. 174

Figure 109: Simulated total reactive power reference of the highest voltage grid as function of the transport performance of the grid (negative values imply capacitive reactive power receipt) 174

Figure 110: Schematic illustration of reactive power delivery of central and decentralized energy producers in the transport and distribution grid 176

Figure 111: Grid model showcasing secondary voltage levels of a highest voltage node 179

Figure 112: Voltage band of the example grid for the basic load situation 180

Figure 113: Voltage band in the example grid for the basic load case with changed transformer step range 181

Figure 114: Voltage band of example grid in 4 production variants 181

Figure 115: Voltage band of the example grid in 5 production variants with changed transformer steps. 182

Figure 116: Grid losses through reactive power delivery in secondary voltage levels. 183

Figure 117: Grid losses through reactive power delivery in secondary voltage levels 183

Figure 118: Necessary re-dispatch performance per point in time to eliminate all (n-0)- and (n-1)-congestions in the KK2 (n-1)-scenario 187

Figure 119: Number of congestions per energy source for a year in KK2-(n-1)-scenario 188

Figure 120: Process for optimization of multiple congestions 189

Figure 121: Required re-dispatch power per point in time for elimination of all (n-0) and (n-1) congestions in KK2-(n-1) scenario 190

Figure 122: Annual re-dispatch quantities in depending on further network expansion 191

Figure 123: Annual number of congestion hours depending on further network expansion 191

Figure 124: The Design Centre for Modular Supply Technology (DeMoTec) 195

Figure 125: Structure of the laboratory test for the restoration of supply 196

Figure 126: Communication and control infrastructure of the laboratory test 197

Figure 127: Set P/Q diagram of the biogas installation 199

Figure 128: Set statics of the biogas plant 200

Figure 129: The 80 kVA machine unit as replica of a wind energy plant 202
Figure 130: Set PQ diagram of wind energy plant 202
Figure 131: Set ΔP/Δf-static of the wind energy plant 203
Figure 132: Status transition diagram of wind energy plant 203
Figure 133: Set ΔP/Δf-static for controllable loads 204
Figure 134: Status transition diagram of load shedding 205
Figure 135: Progression of tests for the restoration of supply 206
Figure 136: Progression of energy usage 207

List of tables

Table 1: Final benchmark data of the 100%-RE scenario 31

Table 2: Composition of annual power consumption in Kombikraftwerk 2-scenario 34

Table 3: Properties of the wind energy installations in the scenario 45

Table 4: Key data of the wind energy scenario (rounded) 47

Table 5: Rounded area and delivery potential of PV installations and their value in the scenario 55

Table 6: Key data of photovoltaic scenario (rounded) 55

Table 7: Distribution of power generation from biomass in 2012 in separate fractionations 60

Table 8: Distribution of bio-energy in the scenario 61

Table 9: Set electrical parameters of the grid model for a simplified power flow calculation 78

Table 10: Total line lengths of the different upgrade steps of the modelled German supergrid (mostly several lines per route!) 80

Table 11: Comparison of the three types of control reserve [85], [86], [87], [48], [88], [31], [77], [89]) 99

Table 12: Evaluation of response time of control reserve delivery 111

Table 13: Simulation results for market participation of the electrical battery related to the model year 122

Table 14: Simulation results on market participation of the power-to-heat plant related to the model year 123

Table 15: Simulation results for market participation of the electrolyser related to the model year 124

Table 16: Simulation results for market participation of the electrolyser related to the model year 126

Table 17: Simulation results for market participation of biogas plant related to the model year 130

Table 18: Comparison of the total reserve demand and the demand for tertiary control reserve, primary and secondary control reserve. The demands according to the static and the dynamic method are compared with the demand during the 4th quarter of 2012 151

Table 19: Comparison of average demand of total reserve with different nRMSE values of wind and photovoltaic forecast errors 153

Table 20: Distribution of nominal capacity throughout Germany according to the Power Plant list 2013 [80] and the EEG Statistics Report 2011 [81] as well as the 100% RE scenario for the different energy producing technologies on grid or transformer level 177

Table 21: Distribution of total nominal capacities from Table 20 to the grid or conversion levels of the connection 178

List of abbreviations

Abbreviation	Meaning
a	year
AC	alternating current
BAT	battery
BGP	biogas plant
CHP	combined heat and power
ct	Eurocent
DA	day-ahead
DC	direct current
DeMoTec	Design Centre Modular Supply Technology
DSL	digital subscriber line
DSM	demand side management
EEG	Erneuerbare-Energien-Gesetz (Act for the Priority of Renewable Energies)
EEX	European Energy Exchange
EHV	Extra high voltage level
EPEX	European Power Exchange
f	frequency
FACTS	flexible AC transmission System
RCT	remote control terminal
FLM	free cable monitoring
RCS	trade, commerce, services
Gvar	Gigavar (unit of reactive power)
GW	gigawatt
GWh	gigawatt hours
h	hour
HV	high voltage
Hz	Hertz
ID	intraday
ICT	information and communication technology
IWES	Fraunhofer Institute for Wind Energy and Energy System Technology
k	constant
KK2	Kombikraftwerk 2
km	kilometer
KRI	communikations and control infragstructure
kV	kilovolt
kVA	kilovolt ampere (unit of apparent power)
kW	kilowatt
m	meter
TCR	tertiary control reserve
MV	medium voltage
ms	milli second
Mvar	megavar (unit of reactive power)
MW	megawatt
MWh	megawatt hour
LV	low voltage
OPC	open process control
P2H	power-to-heat

PJ	petajoule
PLZ	postal code
PCR	primary control reserve
PSW	pumped hydro storage plant
PV	photovoltaics
Q	reactive power
RE	renewable energy
CR	control reserve
RMSE	root-mean-square error
s	second
SCR	secondary control reserve
T	time
TCS	trade, commerce, service
TSO	transmission grid operator
TWh	terrawatt hour
û	voltage
UCTE	Union for the Co-ordination of Transmission of Electricity
V	volt
WT	wind turbine
Ω	ohm
EUR	Euro
°C	degree Celsius

Preface

The regenerative virtual power plant (‘Kombikraftwerk’) is the symbol for tomorrow's power supply. A climate-friendly, reliable and economical supply of electricity and heat can only be achieved by intelligently linking all renewable energies. The basic idea of the Kombikraftwerk rests on this interplay and interaction with storage and consumers.

The idea of the Kombikraftwerk was born as a bet between representatives of the renewable energy branch – Alois Wobben (Enercon), Frank Asbeck (Solarworld) and Ulrich Schmack (Schmack Biogas) – and the Federal Chancellor Angela Merkel at the last Energy Summit in 2006. The industrial representatives promised the Chancellor that by the next energy summit they would demonstrate the complete power supply with renewable energies. Thus in the autumn of 2007, the feasibility of a purely regenerative electricity supply system was impressively demonstrated with the Kombikraftwerk plant. In 2009, the Kombikraftwerk was awarded the German Climate Protection Award “for the development of a sustainable future energy system”.

The Kombikraftwerk is more than a simulation. It allows the active control of renewable energy power plants in real-time operation. The variation of individual general conditions – such as power requirements or wind resources – directly changes the interplay of the linked installations. In this way, the Kombikraftwerk demonstrates the capability and the simple controllability of renewable energies. Together they guarantee a need-based power supply.

After the impressive prelude of the first project, in the follow-up project Kombikraftwerk 2 presented here, an expanded consortium researched and proved the question of system stability in a purely regenerative electricity supply. Renewable power plants are often regarded unsuitable for the provision of frequency and voltage control, which today require the operation of conventional power plants in high wind or solar feed-in conditions. I am delighted that the project team consisting of the Agency for Renewable Energies, Enercon, Solarworld, Ökobit, SIEMENS, SMA, CUBE Engineering, the IEH of Hanover University and the Fraunhofer IWES were able to prove and demonstrate how the system stability can be guaranteed in a future power system based on 100% renewable energy sources. Kombikraftwerk 2 provides solutions for two of the three competing objectives of the energy-policy triangle. Providing solutions for the objectives climate-friendliness and system stability encourages tackling the third aspect of cost effectiveness.

Kurt Rohrig, May 2014

1 Introduction

When the Kombikraftwerk 1 [1] was introduced in 2007, it drew great public attention and triggered a wow effect in many people. As until then the power feed-in from wind and solar energy was seen as too unstable to handle supplying power to a large degree. Kombikraftwerk 1 showed that not only weather-dependent fluctuations and forecast errors could be compensated by bio-energy and storage but also a 100% regenerative power supply for Germany is also achievable. The demonstration was based on a simple concept: Germany's electricity supply was scaled down to 1:10.000. Intelligent control and communications technologies of the Kombikraftwerk 1 power plant were used to orchestrate fluctuating RE, biomass and storages to satisfy the electricity demand. The composition of the plants reflected the production potential for wind, solar and bio-energy in Germany and thus represented a reduced image of a possible 100% power supply for Germany [1].

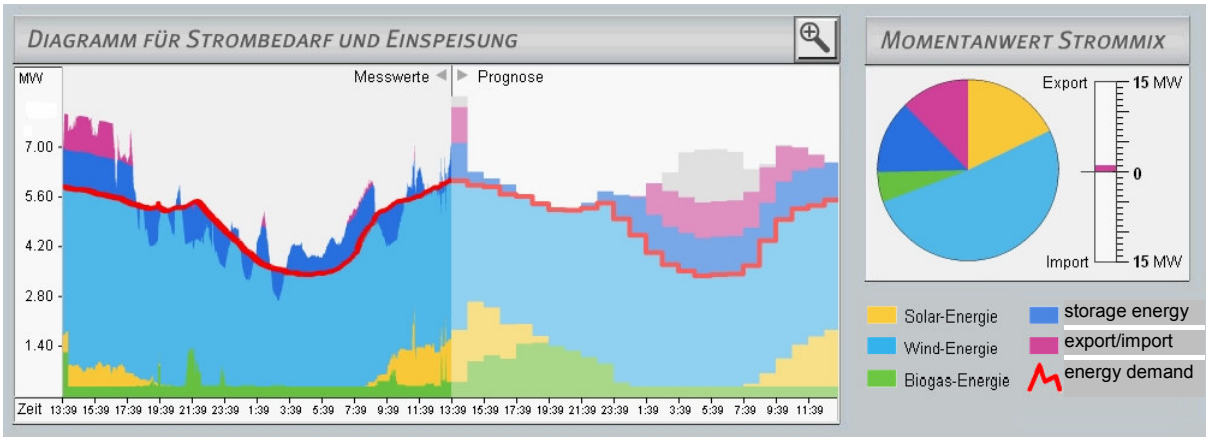

Figure 1: Cover of power needs by the plants of Kombikraftwerk 1

Today, renewable energies have left their niche as electricity providers in Germany. They have experienced continuous growth and provide a quarter of Germany's electricity supply on an annual basis (state: 2013). The official goals of the government aim at increasing this share towards a predominantly renewable power supply, building upon a large societal support. As a reward for the "Energiewende", a clean and sustainable power supply can be achieved and this increasing added value. The Energiewende is a task of truly Herculean proportions. Its game changing dimension will require a huge effort and bring up contradictions, which ultimately show in the fiercely fought political debates. One of the great themes discussed is the potentially threatened grid stability. This can only be maintained by power supply components that are deemed relevant to the power system. The technical challenges of the Energiewende cannot be discussed without the necessary technical background knowledge, the technical details behind it are too profound. The question of grid stability cannot be answered in brief, since every single power line and plant has an influence on it.

It is insufficient to only have enough power in the power system and provide electricity without gaps, as in Kombikraftwerk 1. It is paramount that the security of supply is guaranteed. The quality of supply is an essential part of a modern power system [2]. The so-called voltage quality describes how the power supply can only function if the preferably sinusoidal system voltage lies within certain tolerances. Deviations of the frequency and amplitude of the voltage from its narrow operational margins would cause the loss of grid stability. Building the power system on 100 % renewable

sources requires proving that reliability of supply can be maintained alongside whilst maintaining grid stability. Following this logic, a detailed scenario of a possible 100% RE-power supply was designed in the project Kombikraftwerk 2 (chapter 2) and the grid stability investigated (chapter 3). Theoretical modelling of a purely renewable power supply was supported by a technical demonstration with real installations (section 3.1.2). Through this, all proven features of Kombikraftwerk 1 were retained in Kombikraftwerk 2. The main objectives are:

- Assessment of the technical feasibility of a model-based 100% renewable power supply of Germany.
- Linking real RE power plants with state-of-the-art communications technology to a Kombikraftwerk/virtual power plant and demonstrate its future-proof operation capabilities.
- Dissemination of the content and results of the project in a transparent and clear manner on www.kombikraftwerk.de.

In the project Kombikraftwerk 2, the objectives were applied to the question of grid stability as a basic requirement for supply security in the area of electricity. Since the focus is on the electricity supply, the project only briefly discusses on heat and mobility issues. Economic aspects, such as the design of the electricity market or a cost-benefit-analysis of the Energiewende were not taken into account.

2 The 100%-RE-scenario

In order to investigate the grid stability of a 100% RE electricity supply, the nature of the grid itself, the location and properties of the producers and the consumers as well as the power flows within the grid must be known. Since latter are heavily dependent on the weather, a detailed, spatially highly differentiated scenario of a possible 100% renewable power supply for Germany is modelled. The power flows within the grid are gathered from models for the feed-in from weather-dependent RE, the power consumption including load management and unit commitment of power plants and storages. The generated time series and the underlying meteorological data have a temporal resolution of one hour.

The starting point for modelling the scenarios are assumptions about the future annual power consumption in TWh for all of Germany and its coverage by various types of RE. The contribution of the different types of renewable energies to a future power supply depends on their abundant potential, their technical abilities, their economic viability, the framework conditions and the general acceptance. Counterbalancing numerous unforeseeable future influences requires a balanced and transparent share between the different RE generators. For the scenario of the Kombikraftwerk 2 this share is predefined in such way that it easily comprehensible reflects the proportion of a particular RE participation in the electricity supply in rounded figures. As shown in Figure 2, it is assumed that 90 % of the power supply would be sourced from three types of renewable energies with the greatest potential in Germany. Wind energy has 60 %, photovoltaics (PV) 20 % and bio-energy 10 %. The remaining 10 % are allocated to water and geothermal energy.

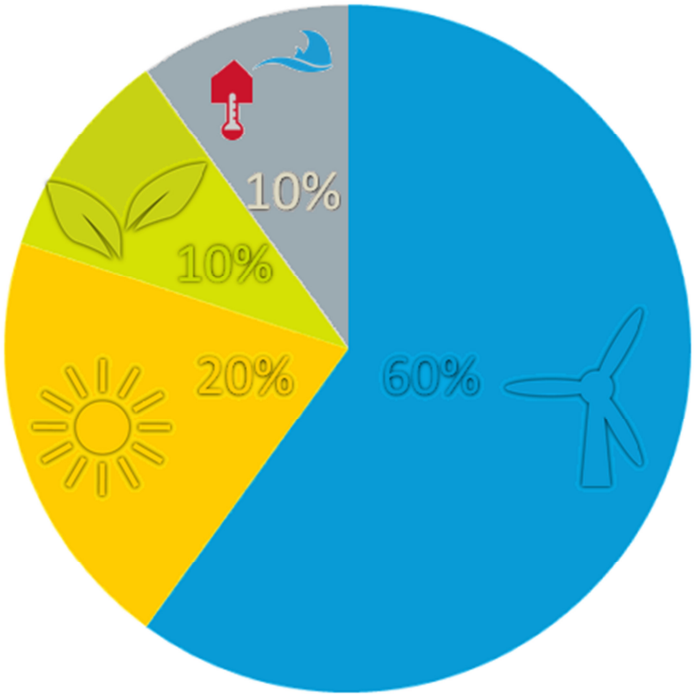

Figure 2: Set power mix of the scenario

Once production proportions have been set, their energy yields and installed capacities emerge, taking into account annual power consumption, the losses in the grid and storages and estimated full-load hours respectively. Given these benchmarks, the main challenge of making the scenario is

the modelling of the positions and the temporal behaviour of consumers, producers and storage are modelled. The behaviour over time of weather-dependent power producers and consumers is simulated in a temporal resolution of one hour, based on the weather model data and consumption data from the year 2007. Thus the scenario describes a power supply as it would take place in future, if the modelled producers and consumers existed and the weather and the weekday series of the year 2007 were to prevail. The modelling methodology is described in the subsequent sections of the following sub-chapters. Firstly, the power consumption is described, followed by the different power-producers, and lastly the energy storage. Each subchapter is divided into a description of the modelling of the spatial distribution and a description of the modelling of the temporal behaviour (production of time series). The sections describing the generation of time series also include an evaluation of the time series. The sub-chapters are organized as following:

- Power consumption (Chapter 2.3)
- Wind energy (section 2.4.1)
- Photovoltaics (section 2.4.2)
- Bio-energy (section 2.4.3)
- Methane power plants (section 2.4.6)
- Hydro energy (section 2.4.4)
- Geothermal (section 2.4.5)
- Electricity grid (Chapter 2.5)
- Power-to-gas (section 2.6.1)
- Pumped hydro storage (section 2.6.2)
- Batteries (section 2.6.3)
- Energy imports and exports (section 2.6.4)

The modelling of the consumption, the generation and the storages has a very high spatial distribution, which has not been used previously. The spatial information is mostly based on the land cover data „CORINE Land Cover“ [3] which shows a spatial resolution of 100 x 100 meters; the spatial resolution of the scenario is correspondingly high. Where topographical object data [4] is used for the modelling, the spatial resolution is sufficient to locate single RE power plants, which is the case in the scenario for wind energy and open area PV installations. Run-off hydro power plants, pumped hydro storage, waste incineration and biomass thermal power plants are located at their current location.

In a first step, the potential sites for three main power producers of the scenario, wind energy, photovoltaics and bio-energy are identified. Figure 3 provides an overview of the main data sources for the determination of areas with potential RE locations and the spatial allocation of consumers. The right-hand side Figure 3 shows that the input data is used for the different types of RE and consumption. Each group is divided into sub-groups, which are addressed individually.

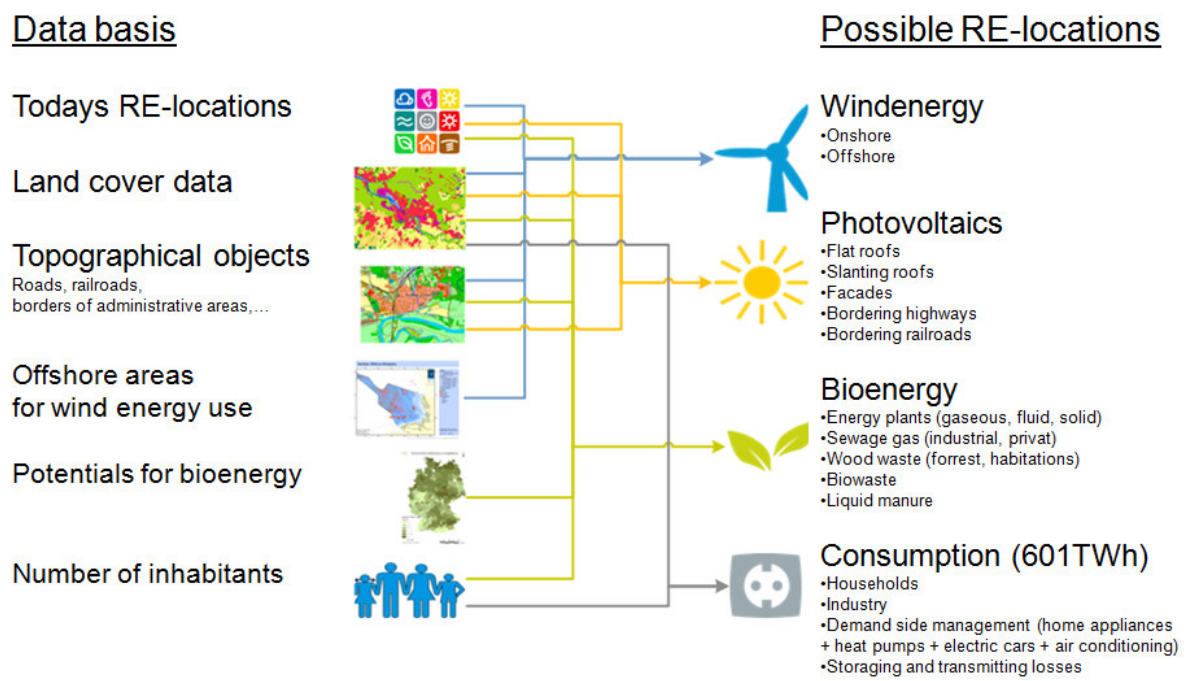

Figure 3: Determination of potential RE areas

Figure 4 shows the resulting spatial distribution of the annual energy yields of wind energy, photovoltaics and biomass as well as the consumption are shown aggregated for pixels with the size of approximately 10 km x 10 km. The spatial distribution of the photovoltaics feed-in and the bio-energy potential are correlating with the power consumption. This essentially reflects urban agglomerations. In the case of photovoltaics, the reason for this is that a large number of PV-installations are placed on rooftops or nearby settlements. Bio-energy has a high density in urban areas, although energy crops are grown rurally. This is due to the fact bio-energy contains other forms of bio-energy that exist in especially highly populated areas. The forms of bio-energy are e.g. bio-waste from households and wood residues. Figure 4 shows those locations where the electrical energy yield from bio-energy accumulates. The generation of electricity is concentrated in even higher degree in urban agglomerations (see also section 2.4.6). The annual wind energy feed-in is highly concentrated in the coastal areas of Germany. This results both from the higher installed wind capacities and from the on average higher wind speeds in the North of Germany.

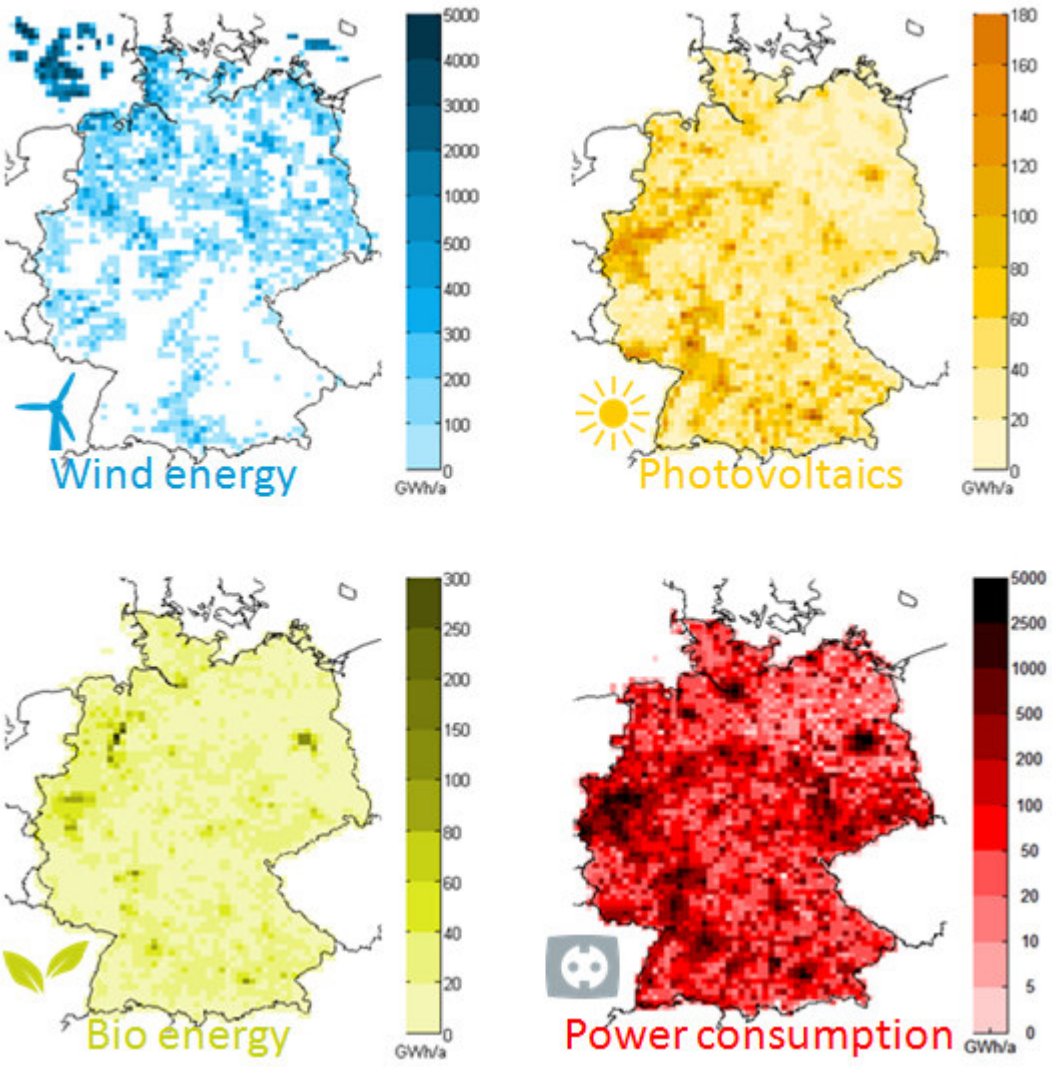

Figure 4: Spatial distribution of annual energy production and consumption in the scenario

2.1 Dimensioning and unit commitment

The installed capacities and the operations time series of the flexible generators and storage are not pre-defined in the scenario and can be obtained with a unit commitment model. The model provides the optimal operation of controllable generators and consumers. The dimensioning of important system components such as the capacities of back-up power plants can be derived from this. The following results are calculated in an aggregated form for each grid node:

- Capacities (described in the respective sections “Modelling of spatial distribution”):
  - Methane power plants (fuelled with bio-methane and renewable methane)
  - Power-to-gas plants
  - Solid biomass
  - Local biogas
  - Three-phase grids (without (n-1)-safety assessment, cf. Chapter 3.3)

- Operation (described in the respective sections “generation and evaluation time series“):
  - Storage: Pumped hydro storage, batteries, power-to-gas plants, methane power plants, load management
  - Bio-energy: Solid biomass, biogas, methane power plants
  - High voltage direct current transmission system (HVDC)-grids, import/export
  - Other: Wind/PV-curtailments

The determination of an optimal operation and suitable performance capacities is an optimization problem. This can be formulated and solved with the aid of the description language GAMS and the optimizer CPLEX. Solving this problem in a single step would pose a large optimizing problem with 8.760 time increments, 501 grid nodes and approximately 10 flexible power producers and consumers. The addition of the optimal distribution of the control reserve together with the unit commitment for each time increment (see section 3.1.6), would further increase the complexity. In order to make the problem more manageable it was subdivided into several sequential steps. Some of the steps use the full coverage of temporal dimensions and simplify the spatial distribution to a point distribution model, whereas others work with the full spatial complexity whilst reducing the timely complexity (see Figure 5). Combining these steps allows approximating an overall optimum for the characteristics of the power system operation.

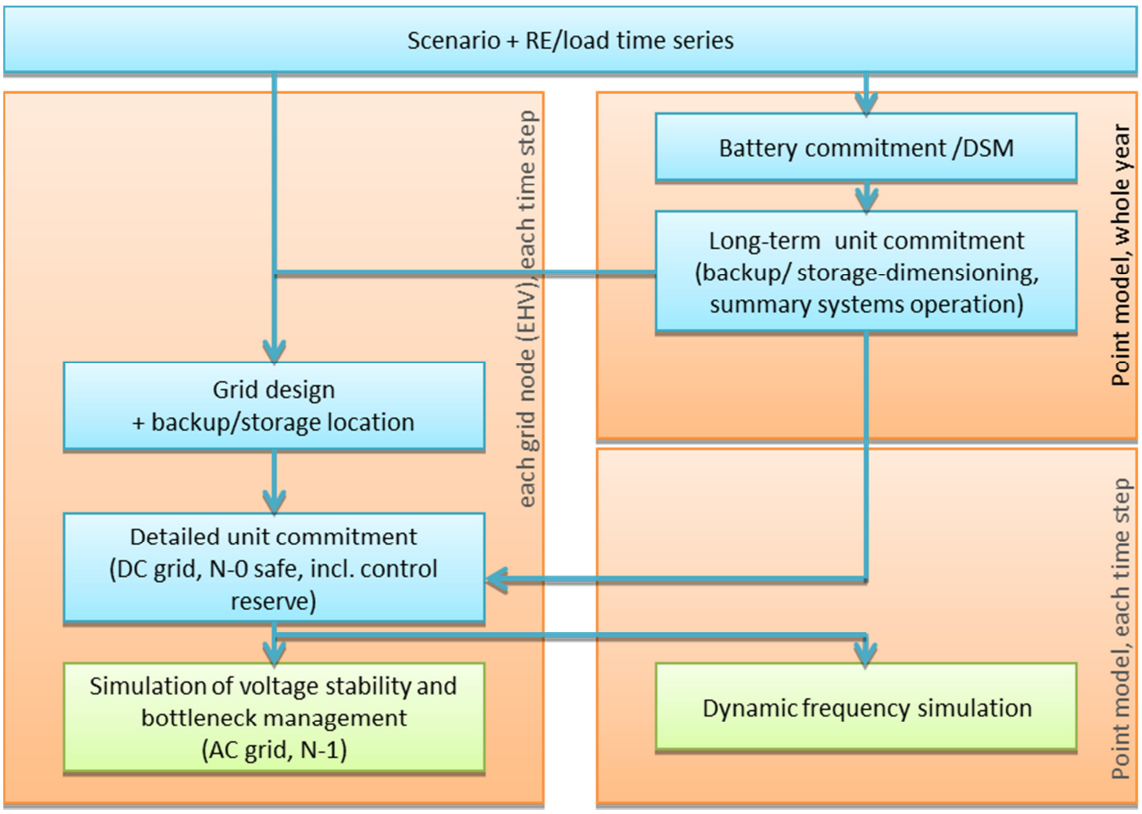

Figure 5: Simulation steps in design and unit commitment planning calculations of the flexible producers

The individual simulation steps (blue boxes in Figure 5) are structured as follows:

1. Battery commitment: The usage of household batteries was optimized with regard to an increased self-consumption. The commitment of batteries took place in a forward-looking optimization over a full year (see section 2.6.3).

2. Load management: Forward-looking simulation of important flexible loads, based on a point residual load across the whole of Germany (in section 2.3.2).

3. Long-term simulation: Using an optimization, both the necessary total capacities of the free backup power plants and storage as well as the hour-exact aggregated commitment time series of all flexible producers and consumers across the whole of Germany were determined for a point model. In detail, these are the capacities and application time series of
   - power-to-gas plants (section 2.6.1)
   - methane power plants (section 2.4.6)
   - biogas plants (section 2.4.3)
   - cogeneration plants (solid biomass) (section 2.4.3)

   as well as the time series for
   - operation of the pumped hydro storage
   - import/export (section 2.6.4),

   for the respective capacities which had been given in the scenario. The operational planning was carried out with the optimization goal of minimizing the consumption of renewable methane (from wind or PV power) and bio-methane. Based on that, and bearing in mind minimum capacities and minimum full load hours, the dimensioning calculation minimized the respective installed capacities.
   A forward-looking commitment planning was carried out for a whole year. In this way, flexible producers are optimally deployed and unnecessary backup capacities (see below) are avoided. The reduction of the computational intensity required the use of an aggregated point model calculation for Germany.

4. Grid design: It was attempted to spatially distribute residual load (consumption minus RE-generation) for each time step in a way that lacking electricity generation in some regions are balanced by surpluses in other regions. The grid flows are calculated with a DC approximation of the full load flow equations (“simplified power flow calculations”). Lines were fully loaded (n-0) and unnecessary electricity transport (e.g. transport of North German wind power to the South, if there is no load left to be covered) was avoided. Subsequently, the grids are extended iteratively. The regional distribution of available generation and storage capacities is determined through long-term optimization. These capacities are allocated based on the remaining average RE surpluses and shortages.

5. Detailed system simulation: The final commitment optimization for all producers and consumers was implemented individually for each time step. Taking into account long-term planning, a spatially distributed calculation was made. Grid flows were calculated using a DC approximation of the full load flow equation (simplified power flow calculation) again. Lines were loaded (n-0)-safe. Concurrently to this step, the capacities to be available for providing control reserve were distributed cost-optimally to the available installations (see section 3.1.6).

The individual steps of the simulation and the quantitative general conditions of the particular technologies are described in detail in the following sections as far as it is necessary for understanding the time series calculation.

The system stability and the ancillary services required were investigated with the help results of these simulations, as shown in Chapter 3. This was done using the following steps (green blocks in Figure 5):

1. Simulation of the voltage stability and congestion management: Using the full power flow calculations and certain assumptions about the delivery of reactive power for any point in time, the voltage in the grid and the following amount of reactive power needed were investigated. Simultaneously the remaining (especially (n-1)-) congestions were removed by redispatch measures (see Chapter 3.3).

2. Dynamic frequency simulation: It was simulated how the grid frequency would behave after a grid failure for every point in time during the scenario-year. It was assessed whether frequency stability can be guaranteed and how this could be achieved (see section 3.1.7).

2.2 Overview of scenario data

Table 1 summarizes the final key parameters of Kombikraftwerk 2 scenario. These are the results of the calculations described further down. This includes the precise local weather-dependent feed-in simulation, the power plant and storage commitment modelling and the calculations of power flows through the power grid (high-voltage). Some parameters in the table are based on educated guesses. Since grid expansion, storage capacities and unused surplus energy have an interdependency with each other, trade-offs and reasonable scales had to be found. The number of calculated influences on production and consumption results in the final RE-share in the electricity supply in Table 1. The calculated shares differ from the numbers in the initial starting point in Figure 2. The shares of photovoltaics and bio-energy (composed of bio-energy with local conversion and the bio-methane converted in methane power plants) approximate the delivery initial assumption of 20 % and 10 % respectively. The share of wind energy of approximately 54 % falls short of the initial value of 60 %. This is mainly because a part of the wind energy yield in the scenario is not used for satisfying the electricity demand (see section 2.4.1.2). This share, together with contributions from photovoltaics, is reported as excess production in Table 1.

Table 1: Final benchmark data of the 100%-RE scenario

Production	Annual energy yield (TWh)	Installed capacity [GW]	Annual full load hours [h]	Share of power production [%]	Consumption	Annual energy consumption [TWh]	Installed capacity [GW]	Annual full load hours [h]	Share in power consumption [%]
Import	11,5	20****	575		Export	11,5	36,6	314	
Excess	58,5								
Onshore wind energy	213,9*	87	2584**	35,58					
Offshore wind energy	108,7*	40	3862**	18,08					
Photovoltaics	119,7*	133,7	909**	19,91					
Bioenergy local	34,5	17,3	2000	5,74					
Bio methane	26	***		4,33					
Geothermal	41	4,7	8760	6,82	Existing and new consumers	523,6			87,09
Hydro energy	25	4,8	5253	4,16	Grid losses	8,7			1,45
pumped hydro storage	11,1	12,6	883	1,85	Pumped hydro storage	14,8	11,2	1318	2,46
Batteries	2,7	55	49	0,45	Batteries	3,2	55	58	0,53
Methane power plants	18,5	53,8***	828***	3,08	Power-to-gas	50,9	13,1	3869	8,47
Σ	601,2		Σ	100	Σ	601,2		Σ	100

**: The annual energy yields are listed without the surplus proportion*

***: The annual full load hours refer to the annual energy yield incl. surpluses*

****: In the methane power plants bio-methane is also converted to power (see section 2.4.6.)*

*****: Assumed restriction*

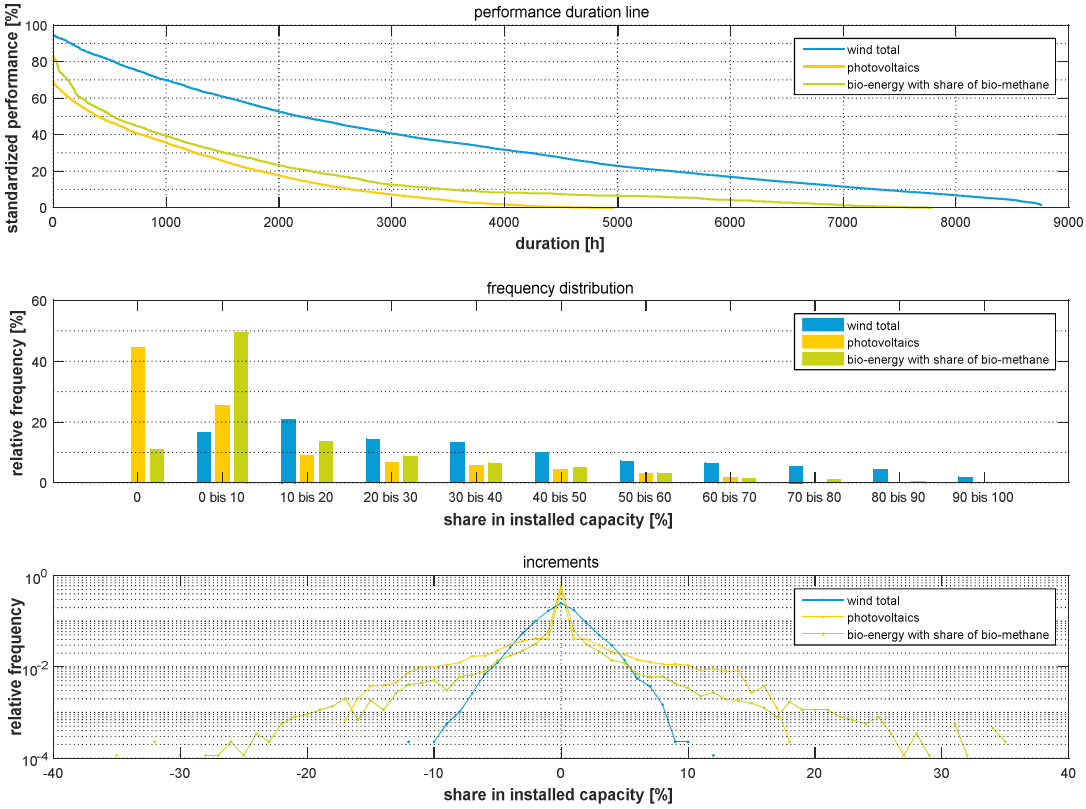

Figure 6: Characteristics of simulated future feed-in from renewable energies across Germany

In the upper part of Figure 6 the power duration curves (see also Figure 18) for the three main forms of renewable energy (wind energy, photovoltaics and bioenergy) simulated for the scenario are represented. The curves are applicable to the entire feed-in throughout Germany. Bioenergy feed-in partially includes the feed-in from methane power plant, since bio-methane if fired alongside RE methane. The feed-in of wind energy covers the largest part of the duration curves with up to 95 % of the nominal capacity. The maximal feed-in is the highest value. In comparison, the highest feed-in from bioenergy is above 80 % and almost 70 % from photovoltaics. Feed-in from wind energy can be observed in nearly 8.760 hours over the entire year. The feed-in biogas plants stay well below 8,000 hours, and the feed-in from photovoltaic lies below 5,000 hours.

These proportions can also be observed when the frequency distribution of feed-ins is compared to the installed capacity. This can be seen in the middle section of Figure 6. While 60 % of the feed-in of wind energy is distributed over up to 40 % of the installed capacities, 60 % of the bioenergy and photovoltaics show a utilization of below 20 %. In the case of photovoltaics, this is mainly due to nighttime hours without PV feed-in. In the case of biogas installations and methane power plants, this is caused by low-demand periods when the plants are underutilized.

In the lowest part of Figure 6 the capacity increments are shown, i.e. the changes of the feed-in values from one hour to the next. It is apparent that the wind energy feed-in across Germany is the most steady, which only fluctuates by a maximum of 12 %. The bio-energy and photovoltaics have fluctuations of up to 35 %. The fact that the increments photovoltaics and biogas reach zero more

often than the increments of wind energy is due to higher the number of hours without feed-in, which does not happen for wind.

Further evaluations of the time series of wind energy, photovoltaics and bio-energy may be found in the sections 2.4.1.2, 2.4.2.2 and 2.4.3.2.

The following sub-chapters describe the creation of the scenarios in detail, beginning with power consumption over the RE feed-in and the grid and ultimately leading up to energy storages. Based on the results of the simplified power flow calculations in Chapter 2.1 conclusions are drawn and recommendations regarding the structure of a future power supply are made.

2.3 Power consumption

The starting point for the creation of the 100%-RE-scenario is the determination of power consumption that shall be supplied completely by RE. The power consumption is divided into two different parts. The first part is the conventional consumption, as we know it today. The latter part consists of shiftable loads. In the scenario, the annual energy consumption of the first part is set at 523.6 TWh. Latter part results from the dimensioning and the commitment of energy storages (see Chapter 2.6) as well as grid losses which occur due to the power flows through the electricity grid (see section 2.5.1.2). In total the annual power consumption for the Kombikraftwerk 2 scenario is 601.2 TWh. This value includes all stored energy end-to-end; if only the storage losses were rated as consumption, the annual consumption in the scenario would amount to about 569 TWh. Both values lie below the present annual gross electricity consumption, which was 615 TWh in 2008. The reason for the reduction is an assumed increase in efficiency on the consumer side. The efficiency goal of the German government according to their energy concept [5] requires a 25 % reduction in electricity consumption by 2050. In relation to the gross electricity consumption of the reference year 2008, a gross electricity consumption of 461 TWh would be the result. Grid losses and self-consumption of power plants account for approximately 35 TWh, leading to a net electricity consumption of 426 TWh. Based upon conservative assumptions concerning the implementation of possible efficiency measures, the Kombikraftwerk 2-scenario assumes a net electricity consumption of 450 TWh. This net electricity consumption only relates to conventional consumers (existing applications). Parts of these existing consumers are the so-called DSM-applications (Demand Side Management) with the capability to shift the electricity consumption in time. This includes washing machines, tumble dryers and dishwashers in households. Industrial appliances and trade have a great potential to shift loads in time and allow adjusting the consumption to the power production. The part of the 450 TWh of existing consumers that can be shifted is at an annual energy volume of 43.2 TWh, which corresponds to roughly 10 %. Innovative power consumers will accompany the existing power consumers. These new power consumers will increasingly be used for heating/cooling or for transport/mobility applications. Among them are heat pumps, air conditioning and electric cars with a total energy consumption of 73.6 TWh per year. If heating and transport sectors where to be supplied by renewable energies as well, an even higher consumption for heating and transport can be expected. However, this aspect was not addressed in detail in the project. Table 2 delivers an

overview of the expected power consumption (red) as well as the power consumption resulting from the use of storage and power flow calculations.

Table 2: Composition of annual power consumption in Kombikraftwerk 2-scenario

Conventional net electricity consumption			450 TWh
Heat	E-heat pumps		20,7 TWh
	Air-conditioning		10,1 TWh
	Other power-to-heat applications (electric heating, heating elements)		*
Transport	E-mobility		42,8 TWh
	other power-to-transport applications (RE methane, hydrogen)		*
Storage consumption (absorbed energy)		RE methane	50,9 TWh
		Pumped hydro	14,8 TWh
		Batteries	3,2 TWh
Grid losses			8,7 TWh
			601,2 TWh

*: No scenario assumptions were made for these future consumers. The power surpluses (see Table 1) could contribute to covering this demand.

According to [6], the value of 43 TWh for **electrical-mobility** equals approximately 57 % of motorized individual transport. **Electric heat pumps** are beneficial for the future energy supply because they can use surplus RE energy efficiently. Their power consumption is set at 20.7 TWh in the scenario. In comparison, the power consumption of night storage heaters is currently approximately 29 TWh in Germany. It is difficult to estimate the additional **air-conditioning** and cooling demands in the commercial sector (TCS) due to high uncertainties regarding the technical situation of the buildings (shadowing, passive cooling). According to the assumptions in [6] and [7] approximately 10 TWh are assigned to this.

The net electricity consumption (450 TWh) is allocated to the three sectors, “industry”, “trade, commerce, services” (TCS) and “households”. The proportions between the sectors are taken from [8] and subsequently applied to the to the power consumption of 2009. The resulting shares are 46 % for industry, 15 percent for TCS and 39 % for the household sector.

2.3.1 Modelling spatial distribution

The information gained from CORINE-land-cover [3] about the spatial position of residential and industrial areas enable a differentiated assessment of power consumption in households and industry according to their spatial positioning. The consumption in households is distributed evenly to the residential areas of each relevant community, according to the share of each community in relation to the overall number of inhabitants in Germany. The CORINE-type "continuous urban settlement structures" is weighted twice as high as the CORINE-type "non-continuous urban settlement structures". Half of the power consumption in the TCS sector is treated in the same way.

Industrial consumption is distributed evenly over the industrial areas of the relevant district (from [9]). The total numbers are gained from of each district's share of the consumption in Germany. Half of the power consumption in the commercial sector is treated in the same way.

2.3.2 Production and evaluation of time series

The chronological course of power consumption in households is compiled from standard load profiles for different weekdays, holidays and seasons (see Figure 7). The profiles are scaled to match the annual power consumption of to 39% * 450 TWh = 175.5 TWh. This time series is subtracted from the consumption time series for all of Germany in 2007 [10] and scaled to 450 TWh. This allows to model the chronological course of the power consumption in the industry (with an annual energy 46% * 450 TWh = 207 TWh) and TCS (with an annual energy 15% * 450 TWh).

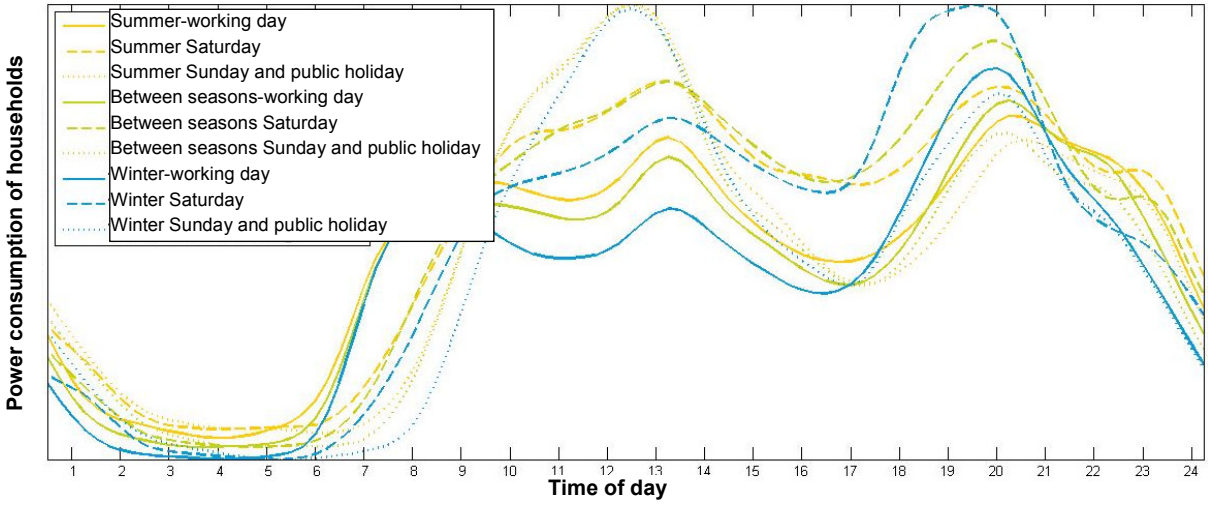

Figure 7: Standard load profile of households

The load management is factored in, using methods from [6]. For this, initially the non-managed load requirements for DSM applications were modelled using weekday and time-of-day dependent load profiles. This was carried out for each individual type of DSM applications and "cut out" of the total load from [10]. As frame parameters for the optimization of applications with storage facilities (such as electrical cars, heat pumps and coolers or freezers for air-conditioning), the nominal capacity and storage sizes are crucial. Shiftable loads (e.g. household appliances, washing machines, driers and dishwashers) require the information of both the nominal capacity [6] and of the average duration of time shift per application. Taking into account all side conditions (meeting demand, max. duration of shift, nominal capacity, etc.) the load profile for each application is optimized. The aim of this optimization is to minimize the variance of the residual load that results from the difference between the power consumption and the feed-in from wind energy, photovoltaics, hydro and geothermal

energy. As a result, the residual load fluctuates as little as possible. The load management measures for household equipment, electrical cars and heat pumps are added to the time series of power consumption of the households; the load management measures for air-conditioning are added to the time series of power consumption of TCS. Figure 8 shows an excerpt from the modelled time series of power consumption for Germany.

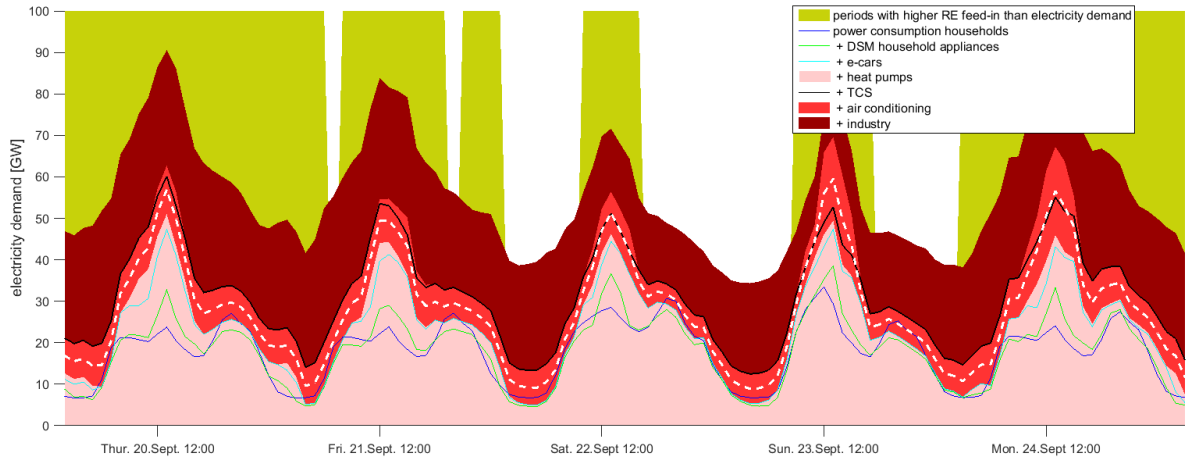

Figure 8: Excerpt from the aggregated power consumption time series for Germany of the scenario

As described in the previous chapter, these time series are distributed to residential and industrial areas in Germany. As for the purposes of this investigation no spatial information for TCS-locations is available, the time series for this sector is allocated to residential areas and industrial areas in equal parts. The broken white line in Figure 8 illustrates the distribution of the time series over residential areas (area below the line) and industrial areas (area above the line).

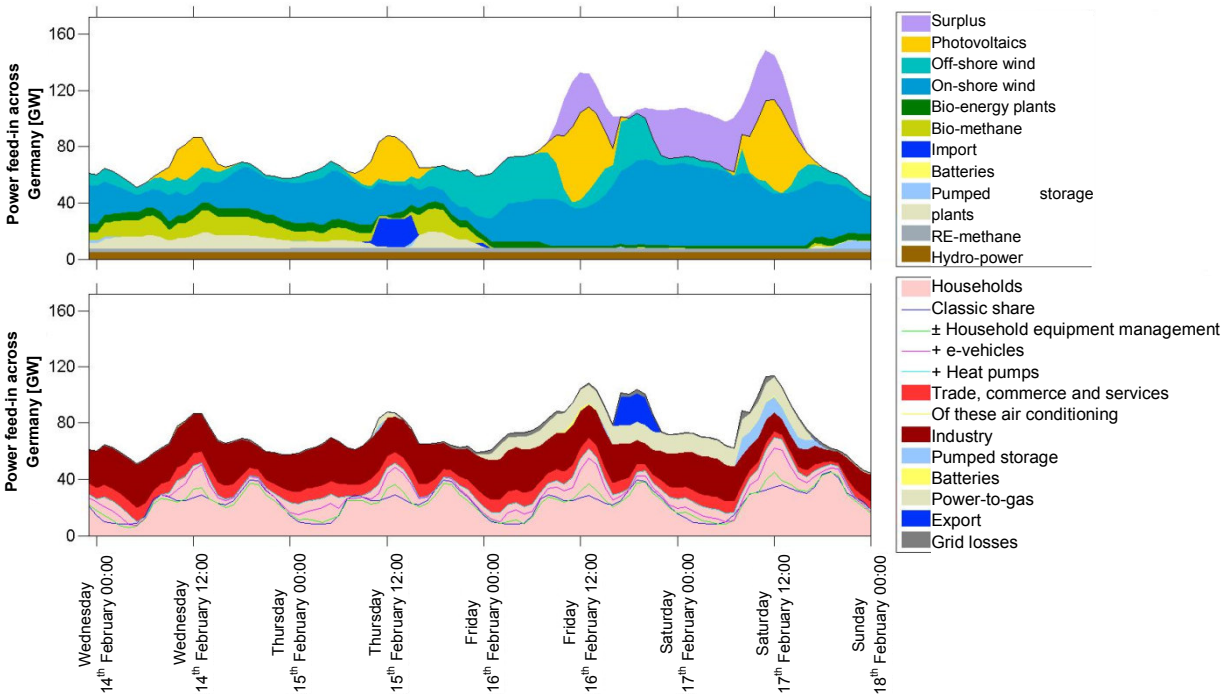

Figure 9: Period with changing weather-dependent energy feed-in, consumption deficit and surplus

Figure 9 shows a period of four days in which all simulated production and consumption types appear. The diagram is the result of all models that will be described further down. It is shown at this stage to illustrate the interaction of power production and consumption in a 100% RE-scenario. The first two days illustrate the case where the consumption in Germany (lower image) is higher than the weather-dependent RE generation (see upper image). The last two days dominated by a high weather-dependent RE generation. Here the renewable energies produce so much electricity that part of is exported to neighbouring countries, as well as it is converted into RE-methane through the power-to-gas process and subsequently and stored for long term storage. Additionally pumped hydro storages and batteries (lower image) are used. Some of the excess electricity cannot be used. During the first two days shown, the feed-in from wind energy and photovoltaics is so low that bio-energy plants, bio-methane and RE-methane have to be utilized in order to meet power needs. For a short period, energy is imported from a neighbouring country. Comparing the encapsulating curves in the upper and lower images, and disregarding surpluses in the upper image, reveals the finding that the energy production and consumption for the whole of Germany are balanced at all times.

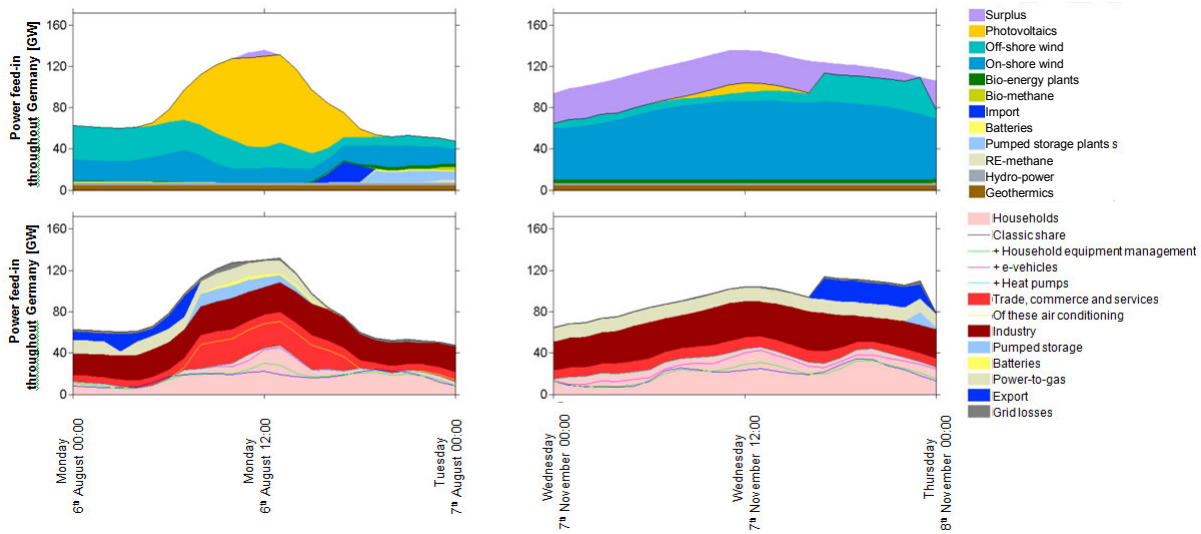

Figure 10: Annual peak loads

The images on the left in Figure 10 illustrate the power production and consumption on the day of the simulated year, which shows the highest consumption. The power consumption without storage consumption and grid losses amounts to approximately 109 GW at 13:00 in the beginning of August. Now there is so much feed-in from PV and wind energy available that the pumped hydro storage and batteries can be filled and RE-methane be produced. The increased operation of air-conditioning systems explains why the power consumption reaches its highest level throughout the year. In 2012, the peak load occurred at the beginning of February at 19:15h, which is an evening in winter, with almost 82 GW. [96]

The two images on the right in Figure 10 show the power production and consumer situation on the day with the highest conventional net electricity consumption, thus disregarding the rest of the consumers from Table 2. This occurs on the 7th November and amounts to approximately 71 GW (add approximately another 8 GW for the novel temporally shiftable consumers). The demand is met

entirely by renewable feed-in. The feed-in from wind energy is high enough that surpluses cannot be absorbed by power-to-gas installations defined in the scenario.

2.4 Producers

2.4.1 Wind energy

Wind energy has the lion's share of a power supply from 100% renewable energies. The reason for that is the high-level technological maturity and its cost effectives under the German weather conditions. It is almost the most abundant resource of renewable energy. At sea, wind conditions are even better suited for wind energy utilization. For this reason there are ambitious goals regarding the construction of offshore wind farms. In the future, a significant expansion of wind energy on land, and the construction of large offshore farms can be expected.

2.4.1.1 Modelling spatial distribution

Onshore

As of today, wind energy has a share of 40 % of the total power supply from renewable energies. Large-scale use of wind energy in Germany began in the 1990s, initiated by the Renewable Energy Act (EEG) and its precursor, the Electricity Feed-in Law. Since then, every year additional wind farms were built throughout Germany, especially in the north and northeast. By 2013, approximately 24.000 wind energy installations with a total of 34 GW could be counted. This makes Germany one of the leaders in wind energy usage and makes it possible for wind energy to supply approximately 9 % of the overall power supply for Germany. On a regional scale, the share of wind energy in the power supply clearly differs. Apart from the regionally highly differing power consumption, this share is highly influenced by the spatial distribution of the installed wind generation.

The location of existing and newly built wind farms depend on numerous factors. In principle, areas for wind energy use have to be approved, which in general depends on local politics and legal requirements, such as the minimum distance from settlements. In [11] potential locations for wind energy installations of the 5-MW-class within Germany were determined, taking into account types of terrain, nature reserves and minimum distances. The large number of potential wind turbine (WT) locations on agriculture areas, grasslands and forests outside of nature reserves from [11] is reduced in relation to the deployment targets of the different federal states (Bundesländer). The scenario of Kombikraftwerk 2 balances the states' individual targets between each other as well as the extent of the expansion plans for the Bundesländer for based on targets for 2020 [12]:

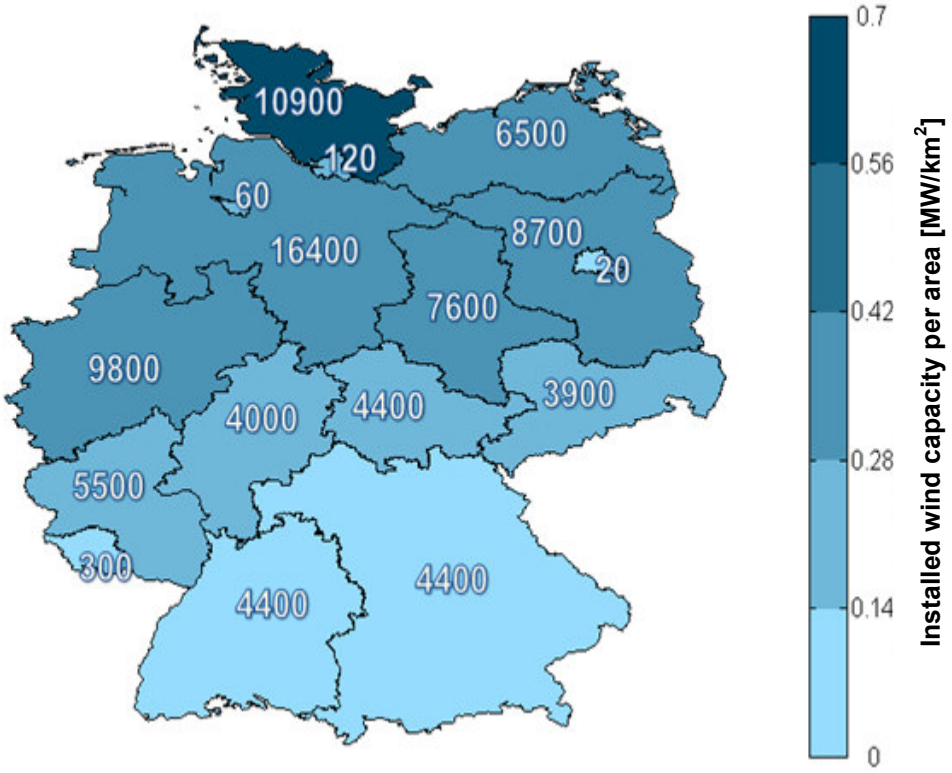

Figure 11: Installed wind capacities in the Bundesländer in the scenario [MW]

The total installed capacity of onshore wind in the scenario amounts to approximately 87 GW. Comparing this value to the current installed capacity, it becomes apparent that the assumed expansion in onshore wind energy capacity is relatively low. This value could already be reached by replacing present wind installations with newer and larger turbines. However, larger turbines would also require larger areas. The assumed wind energy expansion is quite moderate compared to the available potential. The expansion includes areas so far not utilized, such as areas in southern Germany. By using of 2 % of the area of each of the state, as shown in [11], a total capacity of 198 GW could be installed. A more recent study [13] identified an even larger potential.

In reducing the potential WT locations from [11] to the WT locations of the scenario, Germany is initially divided into a grid with a mesh size of 0.125° x 0.125° (longitude and latitude). For each of the grid square the average wind speed is calculated based on the weather model COSMO-EU [14], as well as the already installed wind capacity and the potentially installable wind capacity. The following steps are implemented for each Bundesland separately.

Initially, the additional wind capacities are distributed to classes of wind speeds. The distribution of the average wind speeds (grey columns in Figure 12, upper section) and the distribution of the existing wind capacity (green column) are scaled in such way that their sum corresponds to the capacity to be installed in each Bundesland according to the scenario. Then, beginning with the highest wind speed class, the larger of the grey or green columns is chosen for each wind speed class is chosen. This value is chosen if they are smaller than the spatial potential of this class (yellow columns); otherwise, its column size is adopted. This selection is continued down to smaller wind speed classes until the sum of the selected columns (the blue columns) equals the target capacity value of each Bundesland. This method ensures that the present relationship between the installed wind capacity and the average wind speed is continued in the future if an equal distribution does not

yield a utilization of more favourable winds and the spatial potential is available. Figure 12 explains this process as well as the spatial data, for the example of all of Germany.

After these steps, it is known how much wind capacity should be installed in the various wind speed classes in each Bundesland. The next step is the distribution of the capacity to be installed per grid square of a Bundesland. The share of a grid square in the total capacity of the appropriate class of wind speed to be installed is then set in relation to the potential with the share of the grid surface within the total potential of the wind speed class; grid surfaces with high spatial potential are therefore assigned more wind capacity than grid surfaces with low potential.

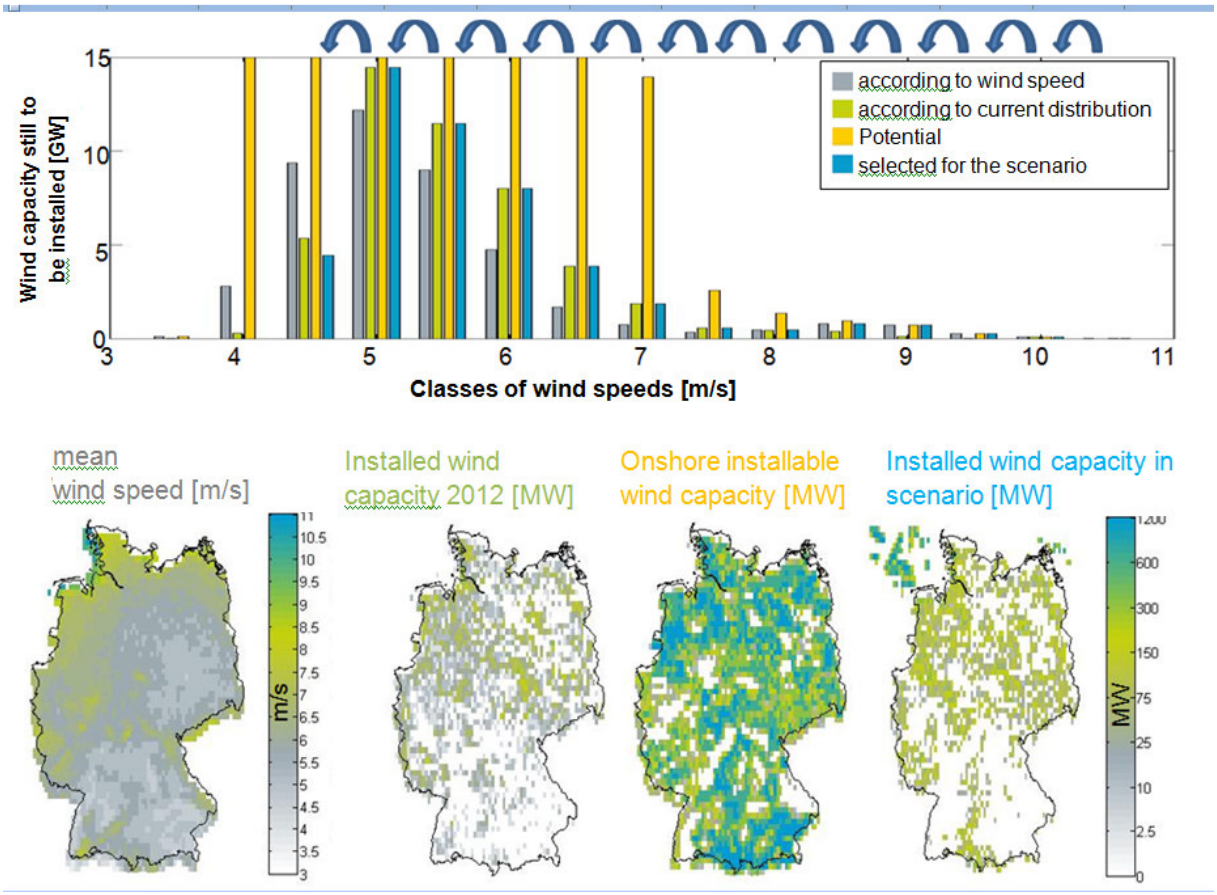

Figure 12: Development of an onshore-wind energy scenario

For the selection of potential WT locations within the grid surface, another, finer grid of 0,025° x 0,025° is applied. This grid has the same resolution as the grid of the weather model COSMO-DE [15], which is also used for the creation of the wind energy feed-in time series. Initially those COSMO-DE grid squares are selected that currently have wind energy installations, foremost those with presently high WT numbers. All potential WTs within a selected COSMO-DE grid square are used as scenario-WTs. If after this selection no WTs remain in the main 0,125° x 0,125°- grid squares, the COSMO-DE grid surfaces with the greatest number of potential WTs are included. Overall COSMO-DE grid squares are added until the designated capacity value for the 0,125° x 0,125°- grid squares has been met or exceeded for the first time. If after the last addition the difference between the sum of the nominal capacity of all WTs and the target value is greater than before, the last addition is removed.

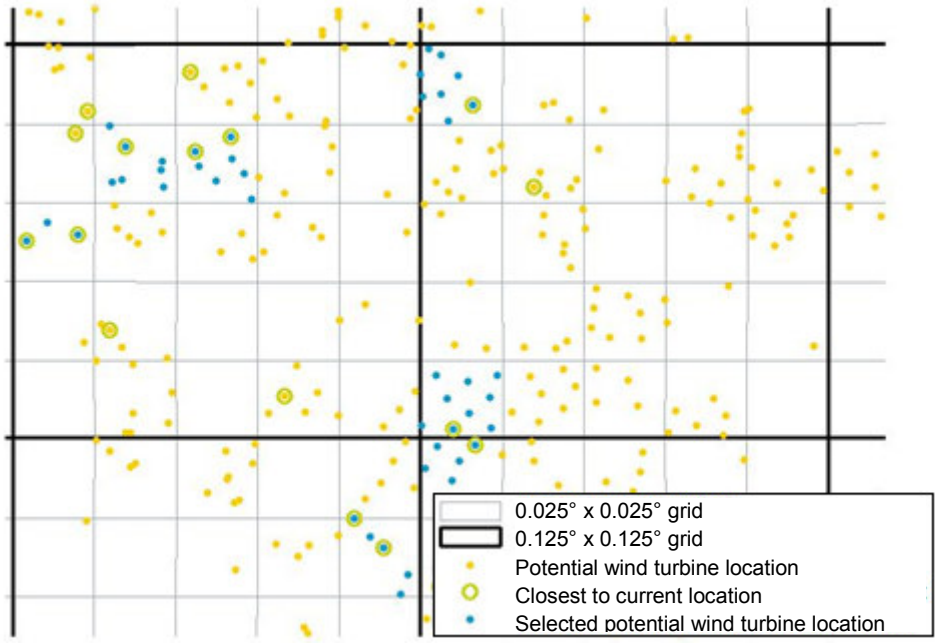

Figure 13: Selection of WT locations exemplified in a grid-section

Through this approach, rather large and more compact wind farms are modelled. They lie near existing WTs as far as these exist in the larger grid squares. Due to the applied selection method, some of the present WTs are not shown in the scenario. However, these are partly old WTs, which are very isolated, and it is very likely that they cease to function or being replaced by newer turbines. A weakness of the selection method is the use of discrete grid squares. This can lead to the fact that WTs are excluded from the scenario since they lie just outside of a selected grid square. Alternative clustering methods can illustrate features like WT distances and sizes of wind farms. They provide a promising opportunity for an improved selection methodology. The strength of the selected methodology is the low number of selected COSMO-DE grid squares. Later on, this reduces the computational intensity to account for wake effects of the WTs. Figure 14 presents an overview of the size and number of wind farms modelled in the scenario.

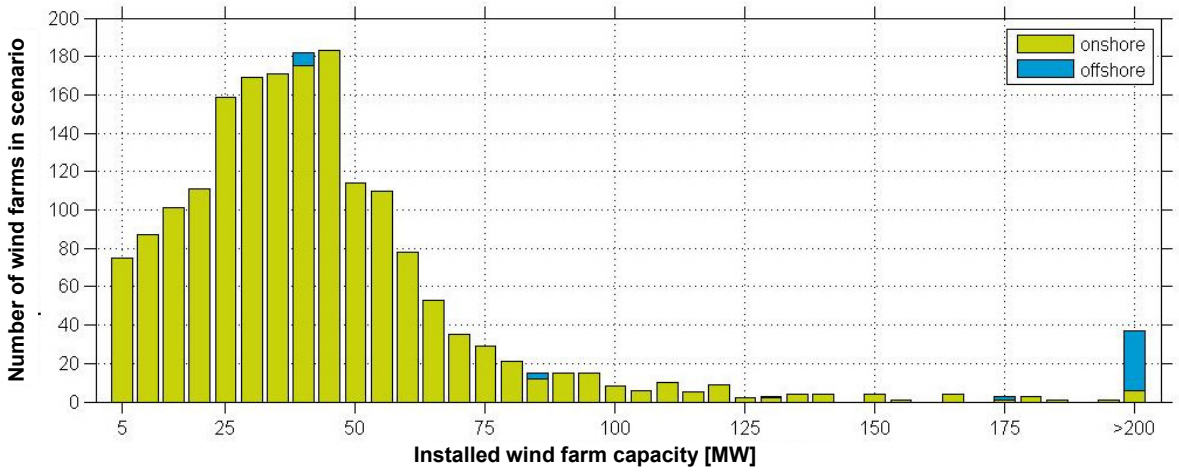

Figure 14: Size of wind farms in the scenario

Offshore

The use of wind energy on the high sea is still in the early stages of development. A start was made in 2010 with the commissioning of the research wind farm „Alpha Ventus“. By the end of 2013, there are now four offshore wind farms with approximately 600 MW installed capacity in German waters. A great future is predicted for the use of offshore of wind energy even though its development lags behind earlier goals. The reasons for this are the favourable wind conditions at sea. The wind is stronger, more frequent and more continuous than onshore. This can be seen in full load hours of approximately 4.000 hours per year [5], [7], [16] or from section 2.4.1.2. Due to the favourable wind conditions and the assumption that building and cabling of wind farms and causes less public acceptance issues, it is assumed that all of the planned offshore wind energy areas will be realited as planned.

In [17] and [18] the planning status, project names, the geographical positions and the extent of the planned German offshore wind farms are shown. In some cases the planned nominal capacities, WT types, hub height and rotor diameter are given. In some cases where the planned offshore wind farm projects in [17] and [18] overlap spatially, the overlapping offshore wind farms are adjusted to obtain the greatest possible suitable area. In Figure 15 black lines show the offshore areas designated for wind energy use that have been identified in this way as of January 2011.

In total 97 offshore wind farms with a total area of approximately 4.560 km² accrue. One of these wind farms, which is situated far offshore in the middle of the North Sea near the Doggerbank, is not shown in the diagram. It has been earmarked for the on-site production of hydrogen and is not to be connected to the grid. Without this wind farm, the total area is approximately 4.440 km². In order to deliver this area with wind capacity for the scenario, initially the grid of the weather model used is considered. It consists of cells, which show an area of approximately 4.5 km² in these latitudes. Assuming typical WT distances (e.g. like those of alpha-ventus) and a rotor diameter of 160 m, four installations can be erected on a weather model grid square as is shown in the enlarged section in Figure 15. This regular and concentric alignment of the WTs to the four main points of the compass reflects the model character of the 100%-RE-scenario in their simplicity but is very comparable to the WT-layout of alpha-ventus. Naturally, in reality the installations will be arranged somewhat differently so as best to avoid wind-dependent WT-wake effects.

Figure 15: Offshore scenario (above: North Sea below: Baltic)

Using this WT-layout, 4.000 plants could be placed in the offshore wind energy areas currently planned. The total installed offshore wind capacity is dependent on the nominal capacity of the wind turbines. For the scenario, a flat 10 MW capacity for each WT is set. This ensures a realistic rotor area/nominal capacity ratio and an installed offshore capacity of 40 GW. 36 GW are located in the North Sea and 4 GW in the Baltic Sea. The resulting space requirement of 444.000 ha / 40.000 MW = 11.1 ha/MW needed also lies within a realistic range when compared to Alpha Ventus.

The wind energy installations in the scenario

For the onshore- wind energy installations of Kombikraftwerk 2 parameters were adopted from [19], in its long version [11]. In case wind conditions at the onshore locations allow for an equivalent number of full load hours of at least 1.600, a rotor diameter of 129 m was set. If the equivalent full load hours lie under 1.600 and the location is thus not a strong wind location, the rotor diameter was set at 149 m. Dependent on the rotor diameter and whether it is situated in a forest, the hub heights of these wind turbines were set at 120, 150, 155 and 175 m. Including the offshore turbines, the Kombikraftwerk 2 scenario provides five types of wind turbines as is illustrated in Figure 16.

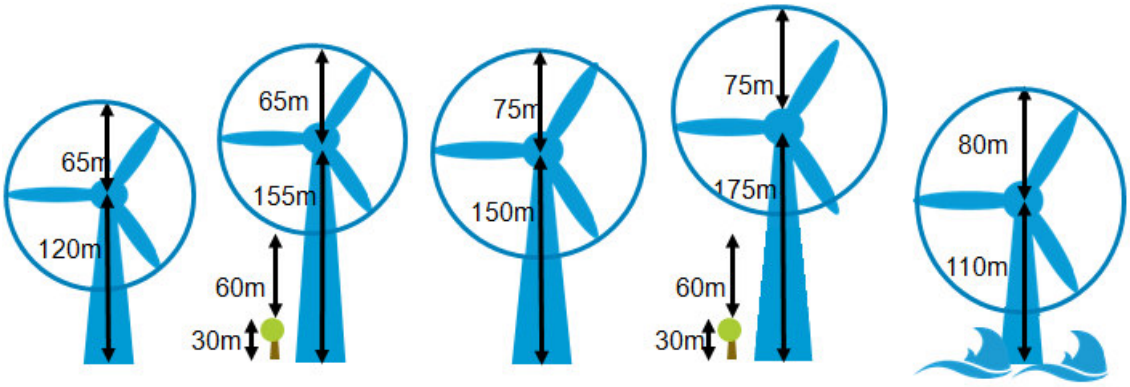

Figure 16: Types of wind turbines in the 100% RE scenario

Even if these installations appear large compared to today's WT; they are significantly lower than the technical threshold established in [20]. Their dimensions and can be viewed as a conservative estimation for a future 100% RE scenario. The properties of the wind turbine types can be seen in Table 3.

Table 3: Properties of the wind energy installations in the scenario

location	grassland / arable acreage	forest	grassland / arable acreage	forest	offshore
wind conditions	strong wind	strong wind	weak wind	weak wind	offshore
nominal capacity	5 MW	5 MW	5 MW	5 MW	10 MW
rotor diameter	129 m	129 m	149 m	149 m	160 m
hub height	120 m	155 m	150 m	175 m	110 m
Rotor area / generator	2,61 $\frac{m^2}{kW}$	2,61 $\frac{m^2}{kW}$	3,49 $\frac{m^2}{kW}$	3,49 $\frac{m^2}{kW}$	2,01 $\frac{m^2}{kW}$
Share in onshore WT	56 %	14 %	20 %	10 %	0 %

Figure 17 shows the power curves set in the scenario as well as the thrust coefficient curve for modelling shading effects. The power curves of existing wind turbines with comparable rotor area / nominal power rating and of existing offshore turbines were used. The power curves show a continuous curtailment for wind speeds exceeding 27 m/s opposed to the currently implemented abrupt shutdown.

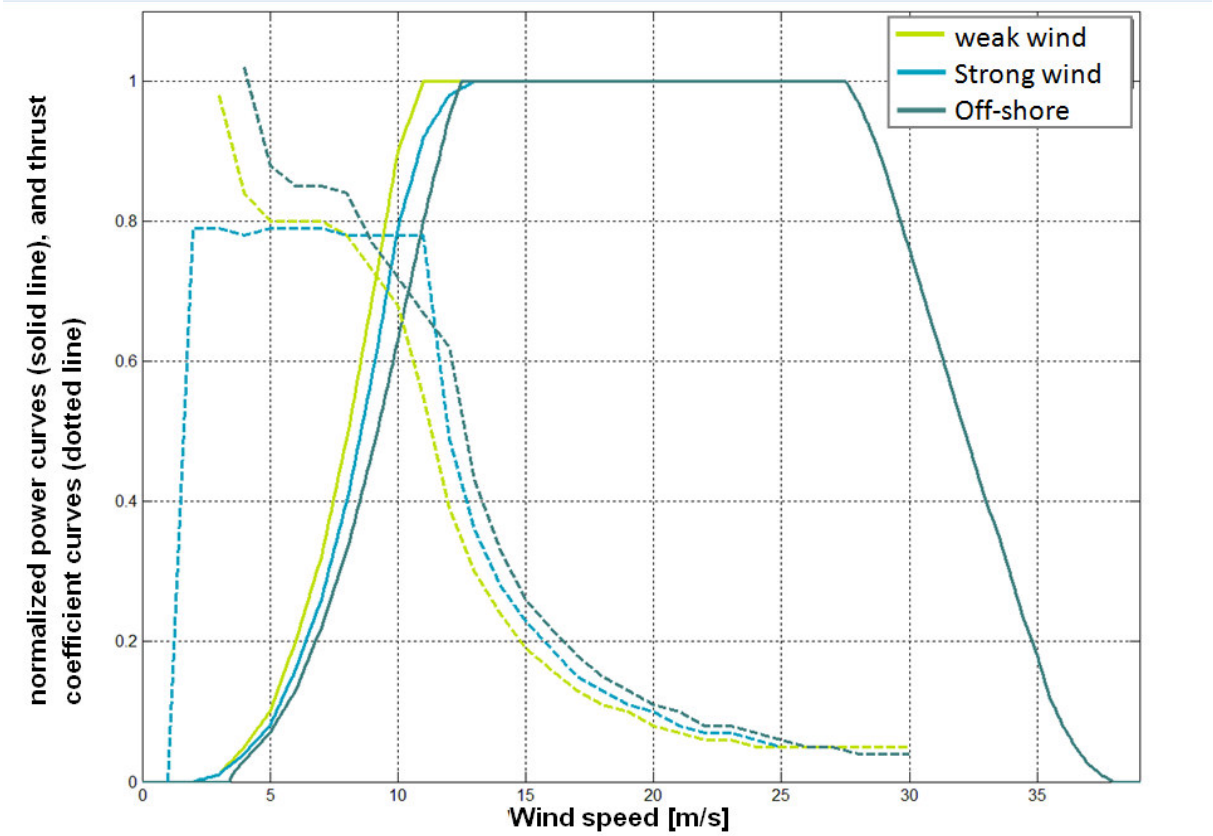

Figure 17: Power curves and thrust coefficient curves of wind turbines in the scenario

2.4.1.2 Production and evaluation of time series

For each individual WT in the scenario, a feed-in time series in a temporal resolution of one hour based on the analysis-data of the spatial highly resolved COSMO-DE [15] of 2007 was generated using the characteristics the previous section. WT wind direction dependent wake effects caused by near-by WTs were taken into account, using the Jensen model [21]. Apart from the WT-precise wake effects that provide an important improvement, the simulation methodology and the parameters are validated by approximately 150 reference measurements from [16]. The wind energy feed-in in the scenario yield the following characteristics for all of Germany:

Table 4: Key data of the wind energy scenario (rounded)

	Onshore	North Sea	Baltic
installed capacity	87 GW	36 GW	4 GW
full load hours	2584 h	3907 h	3463 h
annual energy yield	225 TWh	141 TWh	14 TWh

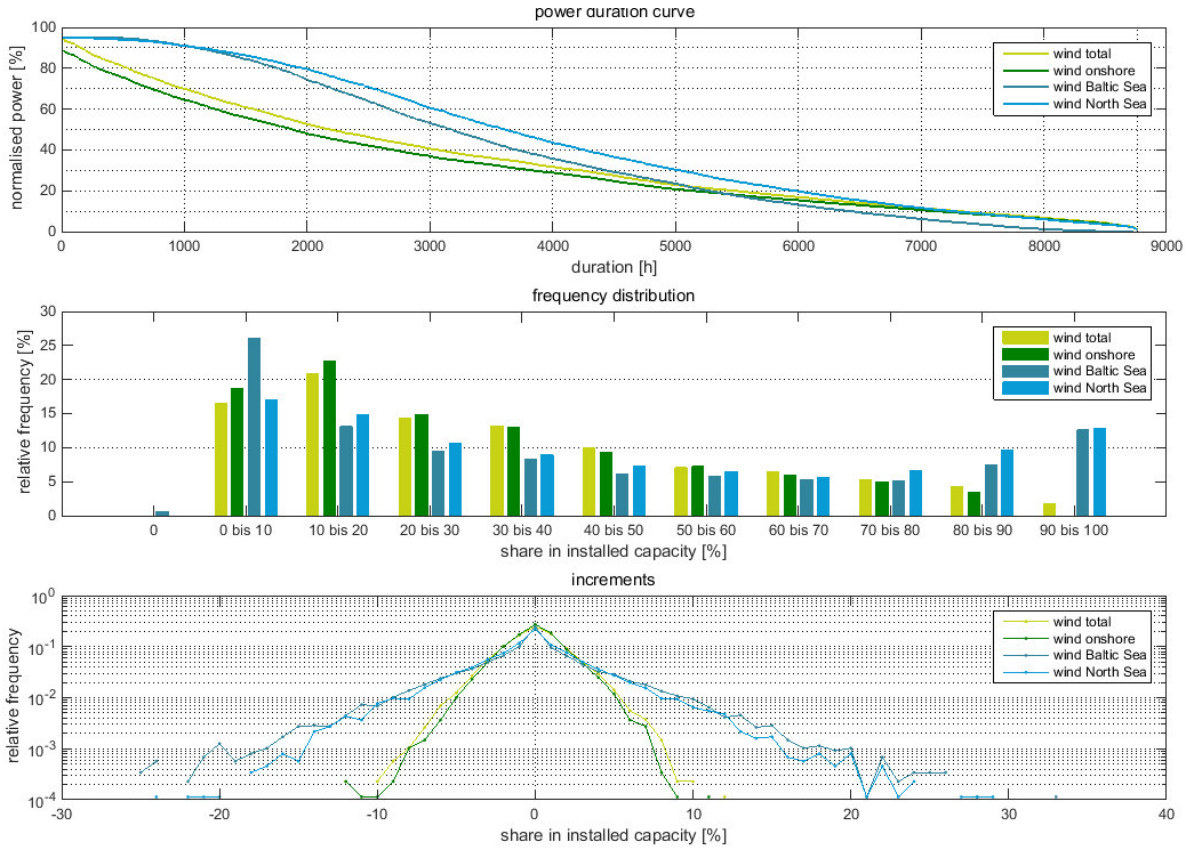

Figure 18: Characteristics of the simulated wind energy feed-in

A look at the power duration curves in the top part of Figure 18 shows that the total and the onshore wind energy have fewer hours with high feed-in than offshore wind energy. Thus during 2000 hours per year, 75 to 80 % of the installed capacity is reached in the offshore area while the onshore, for all installations, only approximately 50 % are reached. The reason for this is the greater spatial distribution of the installed capacities onshore so that the spatial smoothing effect is greater than offshore. Wind energy feed-in in the North Sea shows higher values than in the Baltic Sea, since average wind speeds are higher in the North Sea than in the Baltic Sea. The power duration curve of

the total wind energy feed-in is higher than the one of onshore installations since the offshore wind energy ensures higher total performance.

The middle of Figure 18 shows the amount of hours per year that the wind energy feed-in in certain areas (classes) lies within the relevant capacity classes. The numbers are provided as relative frequency distributions. It can be seen how the onshore feed-in becomes less frequent with an increasing share in the nominal capacity, while the offshore installations show the least frequency in a share of 60 to 70 % of installed capacity (North Sea) and 70 to 80 % (Baltic) and clearly increases again to a higher share. Since wind conditions in the North Sea are more favourable (cf. full load hours), the frequencies in all classes lie above 20 % beyond those of the Baltic Sea. The Baltic Sea feed-in is also the only distribution that occasionally has no wind energy feed-in at all. The comparatively high proportions in the lower capacities are also due to the low spatial distribution of the wind turbines the Baltic Sea. Smoothing effects are therefore not applicable. In the highest range (90-100 %) the relative frequency for North Sea and Baltic in each case lie clearly above the frequency for the total offshore feed-in (not shown here) which allows the conclusion that these high feed-in values occur extremely seldom in the North Sea and the Baltic at the same time.

With the capacity increments in the lower section of Figure 18, the effect of smoothing can also clearly be seen. The wind turbines in the Baltic Sea show little spatial distribution and therefore show extreme values in fluctuations more often. The North Sea turbines follow as second-smallest area and fluctuate less, followed by the feed-in of onshore turbines. The combination of onshore and offshore wind farms has the greatest spatial dispersion, which leads to the most even feed-in.

Figure 19 shows the first three-and-a-half weeks of the scenario year. For the largest part of these days, the large surplus (purple) from on- and offshore wind energy (dark and pale blue) can be noticed. It cannot be absorbed by the energy storage set in the scenario. The reason for these surpluses is the extraordinary weather in January of the weather year 2007 that was used, when the hurricane Kyrill was responsible for high winds. The storages were dimensioned in such a way that they have sufficient storage facilities for average high surpluses, not for extreme weather conditions. This ensures that the utilization of storages is kept high during the rest of the year (see section2.6.1).

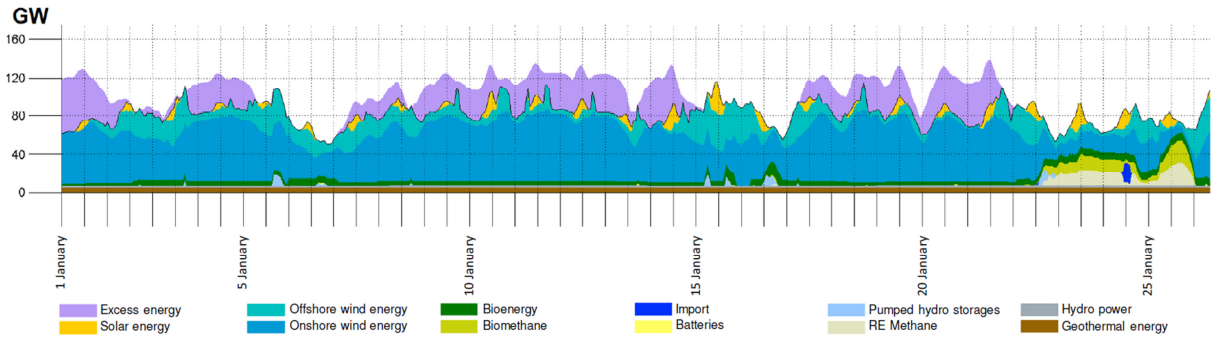

Figure 19: Windy weeks in January

The high wind speeds as in Figure 19 occur more frequently during wintertime, which is a typical phenomenon. It could be sensible to use the winter's surplus power from wind energy for heating purposes since there is a higher demand for heating.

Altogether a share of 85 % of the possible feed-in from wind per year can be utilized, and 15 % are surpluses which cannot be used in the scenario which is limited to the power sector. For the following reason, only 70 % of the offshore wind energy feed-in is used in the scenario in hand: The surpluses were located in the model in such a way that grid losses would remain as small as possible. Thus, the part of unused wind energy is especially high for offshore because higher grid losses occur with its transport than with onshore wind energy, which is usually situated closer to, where it is utilized.

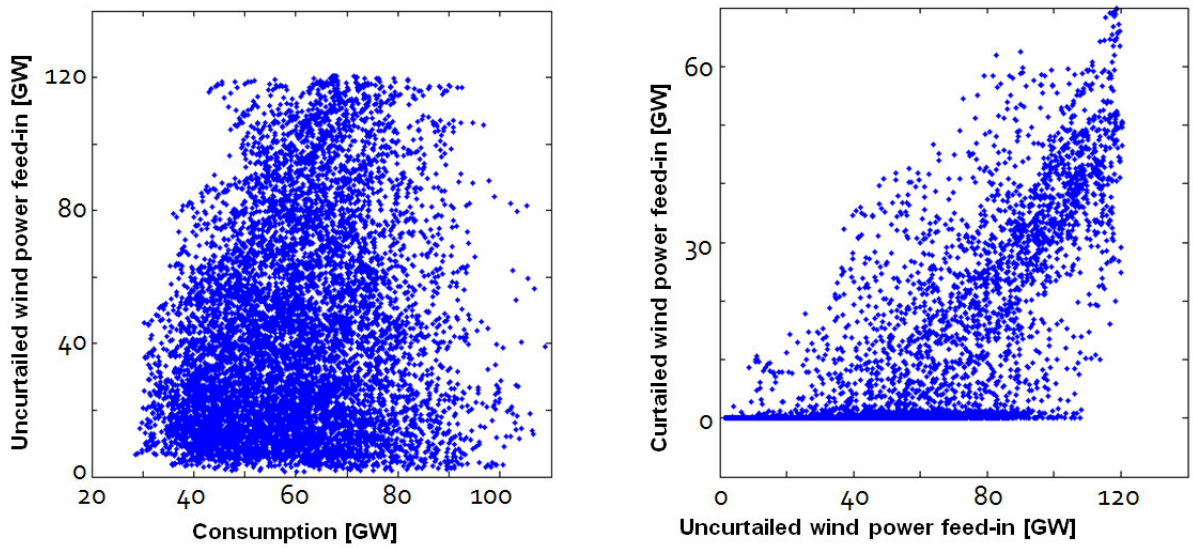

Figure 20: a)Connection between the simulated wind energy feed-in across Germany and consumption (left) and b) the curtailment of WT (right)

In the Figure 20 a) the relation between Germany's consumption and the "uncurtailed" wind feed-in (incl. the surpluses) is shown. The low correlation between these two profiles has correlation co-efficient of 19.21 %. Consumption usually varies between 30 and 90 GW and the wind energy feed-in does not depend on it. There are times of high consumption with little wind feed-in and times of low consumption with much wind feed-in.

The connection between uncurtailed and curtailed (not used) wind energy feed-in is clear in Figure 20 b). The higher the uncurtailed wind energy feed-in, the more the feed-in is curtailed. At times of very high possible feed-in of around 120 GW, the curtailment amounts to 70 GW, occasionally up to 58.33 %. This high value suggests that alternative forms of utilization of surpluses from wind energy should have an important role to play outside of the electricity sector, possibly in the areas of heating and transport.

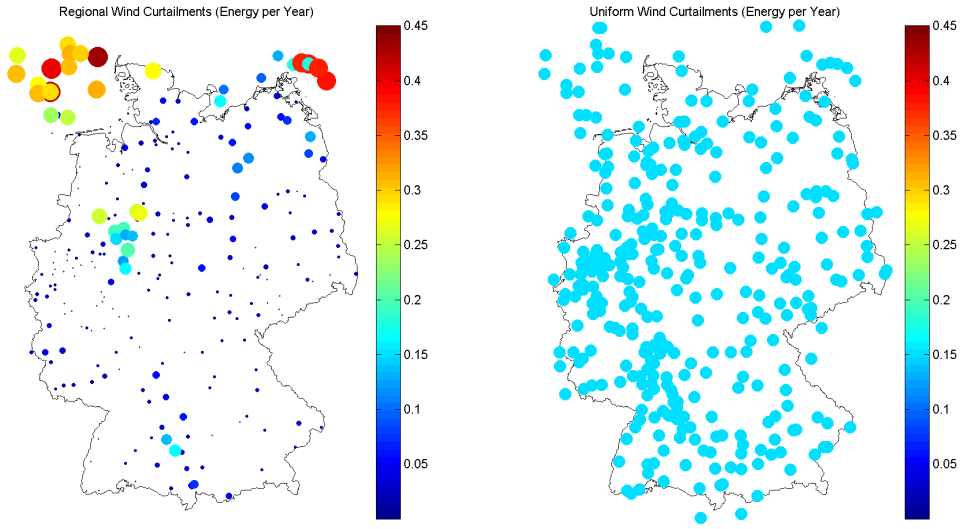

Figure 21: a) Regional distribution of annual curtailment (GWh) with a loss-optimizing (left) or b) equal regulation (right)

Currently curtailment is only exercised due to grid constraints, not due to energy surpluses in Germany or Europe. Depending on future regulations for curtailment due to excessive energy, a different picture emerges for regional distribution of annual curtailments. From the point of view of minimizing losses, obviously locations far from the loads should be curtailed first, for instance in the offshore wind farms (see Figure 21 a). At the same time, the wind farms should be treated equally, regardless their location. Seeing that the question is not one of grid congestion, no single wind farms or cluster of wind farms is predominantly causing the surplus. The surplus is caused by all WTs simultaneously. Therefore the regulation could be shaped in such a way that all producers in a region are reduced equally by a certain percentage (see Figure 21 b). However, in the calculations of this project the regionally differentiated approach was used.

In the presented discussion on curtailment, it should be kept in mind that this study is focussed on the electricity sector only. One could and would probably use such excess wind energy, which cannot be utilized in the electricity sector, for value creation in other sectors. Especially a thermal usage of north German surpluses [79] or the utilization for the production of synthetic fuels would be sensible.

2.4.2 Photovoltaics

The conversion of sunlight to electrical energy, called photovoltaics (PV), has experienced fast growth in Germany during the last ten years. By now, PV installations on rooftops of houses are an every-day sight as well as large areas of ground-mounted installations on the perimeter of towns. With almost 36 GW of installed capacity, photovoltaics supplied approximately 5 % of the electricity needed in Germany during 2013. As progressively lower prices for PV-installations can be foreseen, their number will not only increase but also will find more applications that are not optimally aligned to the sun, e.g. façade installations. For the purely regenerative scenario of Kombikraftwerk 2, the current number is roughly quadrupled and has a share of 20 % or 133 GW_p of installed capacity of PV in the electricity supply. The installations include pitched and flat roof installations with a total capacity of approximately 83 GW_p, façade installations with approximately 5 GW_p and ground mounted installations with approximately 45 GW_p. The latter are divided into areas alongside highways and railway tracks. Together with the land marked for redevelopment, these are the areas suitable for the erection of ground-mounted installations, according to the EEG- amendment of 2012. However, the area for redevelopment is difficult to estimate.

2.4.2.1 Modelling spatial distribution

In order to determine the possible location of different PV installations, a number of calculations are made, which are shown in Figure 22.

Initially all settlement and industrial areas from land cover data with a resolution of 100 m x 100 m [3] are classified as suitable for rooftop and façade installations. In order to determine possible ground mounted installations, areas are identified with the aid of topographical object data in vector format [4]. Based on the vector information, a stretch of 100 m alongside national highways and railway tracks is identified as suitable, if the ground cover type allows the installation [3]. More than 90 % of the ground cover type is identified as potential areas for ground mounted installations along national highways and railway tracks. The ground cover types are “arable land” and “meadows and pastures”.

In a second step, available areas identified in this way are reduced to technically usable ones. This allows taking into account that settlement and industrial areas from [3] do not consist by 100 % of rooftops and façades suitable for roof and façade installations. The implemented deductions are based on satellite pictures of settlements and industrial areas as well as on [22]. The resulting deductions are 90 % for rooftop and 98 % for façade installations. The available areas identified for ground-mounted installations are reduced by a flat 50 % to account for the fact that many areas are ruled due to unfavourable conditions such as shadowing or slopes. Further reductions are caused by buildings such as bridges and tunnels that account for 6 %. In total, the ratio of areas alongside railway tracks to areas alongside national highways amounts to about 2:1.

In a third step, the available technically usable rooftop areas are divided into pitched and flat roof groups. Bearing in mind [22], the settlement areas are set at 90 % pitched and 10 % flat roofs and for industrial areas at 30 % pitched and 70 % flat roofs.

The area utilization level set in the fourth step describes the ratio of installable module area to usable rooftop area. It takes into account the loss of areas due to design-related limitations, e.g., fixed dimensions of modules.

In the fifth step the uniform distribution of the orientation of pitched rooftops is assumed [BSW 2009] [= Bundesverband Solarwirtschaft = Federal Association of Solar Technology]. This is likewise applied for the direction of the house façades across the various points of the compass. For the further assessment only pitched roofs and façades whose alignment (azimuth) deviate to a maximum of ±100° and/or ±90° from 0° (south) are designated for PV installations. For the frequency distribution of the roof angles, an empirically obtained function is set [22]. For flat rooftops and ground-mounted installations, an alignment to the south and an angle of 30° is set.

For the calculation of the theoretically installable PV capacity, step six assumes an overall conservative efficiency of 14 % for all PV installations. If a ground-mounted installation has less than 100 kW_p it is rejected since it is being too small.

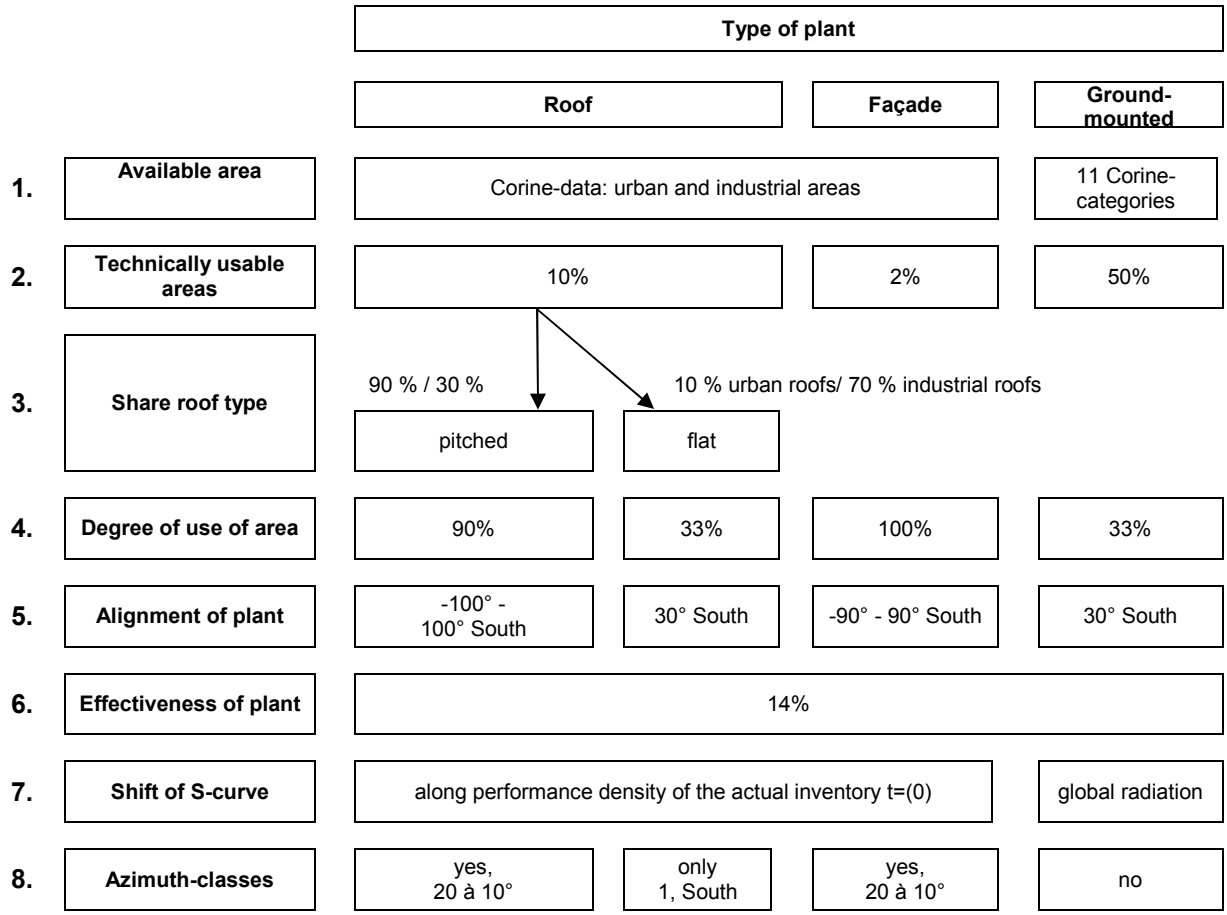

Figure 22: Calculation of PV areas

After step six, potentially installable capacities emerge. These lie, for all types of installations investigated, clearly above the installed capacities needed for the scenario. Initially present PV installations from [23] were investigated with regard to their dependence on local solar irradiation and regionally average income per inhabitant. This would have facilitated the selection of areas from the multitude of usable areas. No clear correlation between the factors could be established, leading to a large number of unpredictable influencing factors. Alternately, a growth process with saturation is used for the modelling of the temporal development. The spatial distribution of PV installations of carried out based on postal-code areas. The PV capacity density I (installed capacity per area) for

every postal-code area (PLZ-area) over time is described as logistic function ("S-curve") with convergence of the potentially possible capacity density $I_{Potential}$.

$$S(t) = \frac{I_{Potential}}{1 + \left(\frac{I_{Potential}}{I_{today}} - 1\right) \cdot e^{-k \cdot t \cdot I_{Potential}}}$$

The current state of the PV installation densities of the individual types of plants from [23] within the postal code areas are increased by the same time interval Δt for each postal code area. This allows determining the expansion in the scenario in line with the S-curve approach until the total installed capacity of the scenario is reached (step 7 in Figure 22). For each postal code area, the same constant *k* is used. Figure 23 illustrates this procedure schematically, using the PV installation values of two postal code areas x and y.

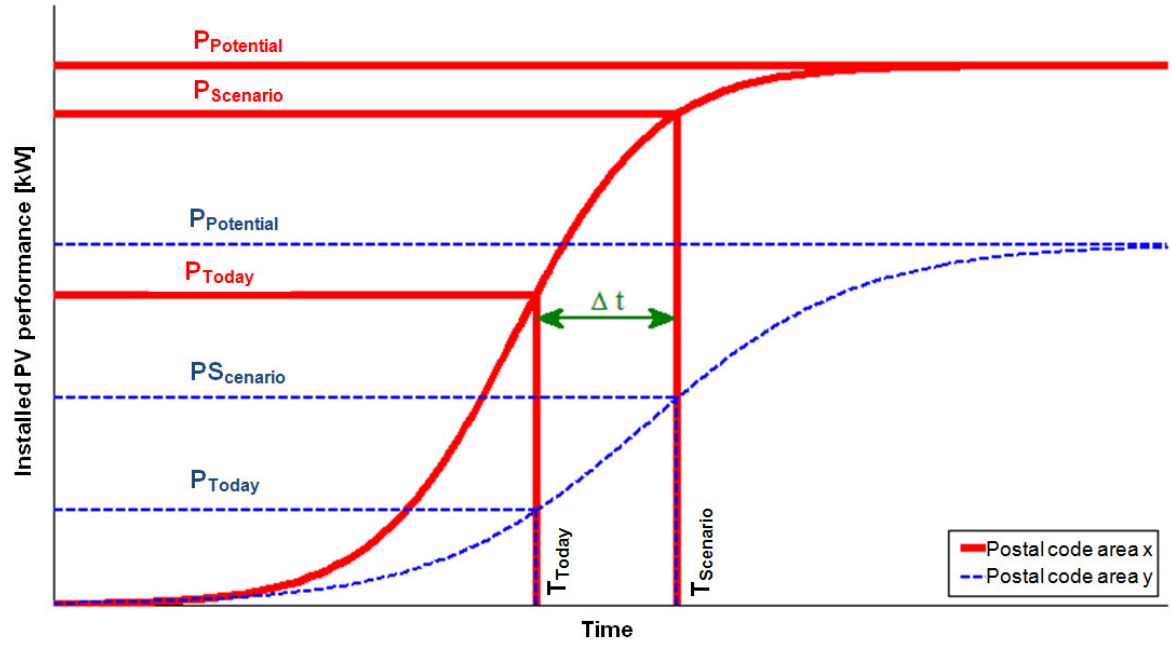

Figure 23: Determining the future PV installations under the assumption of a saturation process („S-Curve")

In step 8, the determined capacity increase of PV will possibly be distributed to plants having different orientation. For this purpose, 20 azimuth-classes of - 100° to 100° are formed for PV installations on pitched roofs and façades. For the current distribution of the orientation of pitched and façade installations a Gaussian distribution is used. This was identified for the pitched roof installations based on the data from [23]. Pitched roofs oriented towards the South currently occur most frequently according to the Gaussian distribution and are therefore most advanced in their saturation process; installations with different orientations are less utilized. Figure 23 shows the distribution of installed PV pitched roof installations to one postal code area to the various azimuth classes and their increase according to the saturation curve set. It can be observed that in the beginning the addition is strongly concentrated towards the south. In case of great installation densities, the units orientated towards the South reach saturation before the others. Consequently, this leads to substantial additions of PV installations towards the east and west until a saturation is reached as well.

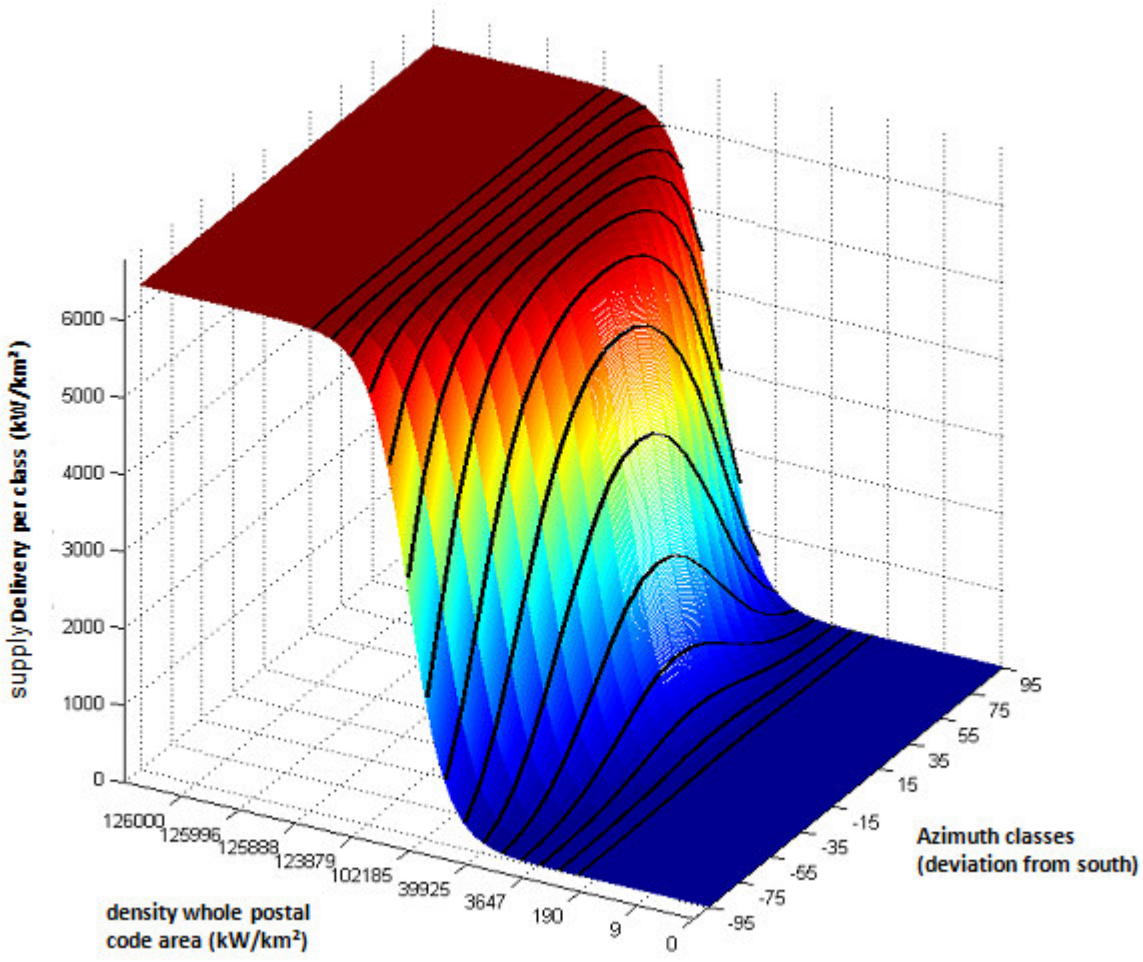

Figure 24: Distribution curve for production density for various development conditions and orientation of PV pitched roof installations of a postal code area

For flat roofs and ground-mounted installations, no distribution of the orientation is made. An orientation to the south and an angle of 30° is assumed. For the addition of flat roof installations, it is assumed that per postal code area progress along the S-curve is equal to the progress of the installations on pitched roofs that are oriented towards the south. The observed development for the addition of ground-mounted installations cannot be used to forecast the future development. This is because the subsidy situation for such plants has been changed repeatedly and significantly by the EEG. It is assumed that factors such as ownership or income distributions will be playing a comparably insignificant role in the addition of open terrain installations. Investors who want to build a ground-mounted PV installation will primarily choose their area based on potential profit. For these reasons, the shift in the S curve is set exclusively in dependence on the solar resource. It is also assumed that the additions will begin in the area with the highest irradiation (average values 2006-09 from [24]) and the area with the least irradiation last. In order to calculate the shift of the curve between the additions in the last-mentioned to the first-mentioned area, starting conditions are formulated for the latter area. The starting conditions demand that the additions in the area with the highest irradiation must have advanced to the stage where half of the possible capacity density has been achieved. Only then will additions in the latter area begin. The starting point for all other postal code areas follows from the linear interpolation in relation to the particular irradiation values.

In Table 5 the results achieved with the aforementioned methods are shown. It contains the values for the area used in the scenario, the capacity potential and the installed capacity in the scenario. For the scenario in installed PV capacity of 83 GW_p on rooftops and 45 GW_p on open spaces has been set. The distribution of 83 GW_p on pitched and flat roofs results from the approach to equal progression along the S curve per postal code area in step 7. The distribution of the 45 GW_p alongside railway tracks and Federal highways coincides with the ratio of their area potential of 2 by 1.

Table 5: Rounded area and delivery potential of PV installations and their value in the scenario

	pitched roofs	**flat roofs**	**façades**	**Federal highways**	**railway tracks**
technically usable areas [km²]	approximately 2.450	approximately 400	approximately 550	approximately 2.050	approximately 4.400
Actually / sensible usable areas [km²]	approximately 1.350	approximately 400	approximately 300	approximately 1.050	approximately 2.200
areas used in the scenario [km²]	approximately 550	approximately 250	approximately 40	approximately 300	approximately 600
potential delivery [GWp]	approximately 170	approximately 20	approximately 40	approximately 50	approximately 100
installed capacity in scenario [GWp]	70	13	5	15	30

2.4.2.2 Production and evaluation of time series

The feed-in time series are created taking into account the capacity installation curves determined in the previous step. The feed-in time series are based on the hourly global radiation data for each grid area with a spatial distribution of 10*14 km^2 for the year 2007 [24]. Corresponding temperature data [14] allows to model losses by PV module heating. For the calculation of the global irradiation on sloped module, approaches from Orgill-Hollands [25],[26] are used. The model covers various configurations of installations (alignment, angle, mounting type etc.). The modelling of the power inverters is based on the model of [27]. The modules are modelled according to [28]. Standard polycrystalline modules are assumed they currently have the predominant share of approximately 60 % of all installed PV installation. In addition, an under-dimensioning of PV power converts compared to the PV module capacity according to EEG Amendment of 2012 was considered, but not pursued any further, due to the small positive effects regarding storage reduction and grid extension needs. For the feed-in time series of the PV scenario, the characteristics result from Table 6 for all of Germany.

Table 6: Key data of photovoltaic scenario (rounded)

	pitched roofs	flat roofs	façades	national highways	railway tracks
installed capacity	70 GW	13 GW	5 GW	15 GW	30 GW
full load hours	909 h		605 h	942 h	947 h
annual energy yield	75 TWh		3 TWh	14 TWh	28 TWh

Figure 25 shows diurnal variation of photovoltaic feed-in and power consumption. The continuous lines represent the average diurnal development over the whole year (annual averages of individual hours of the day) and the dotted lines during the course of the 1st May, which is the day of the highest ratio between photovoltaic feed-in and power consumption.

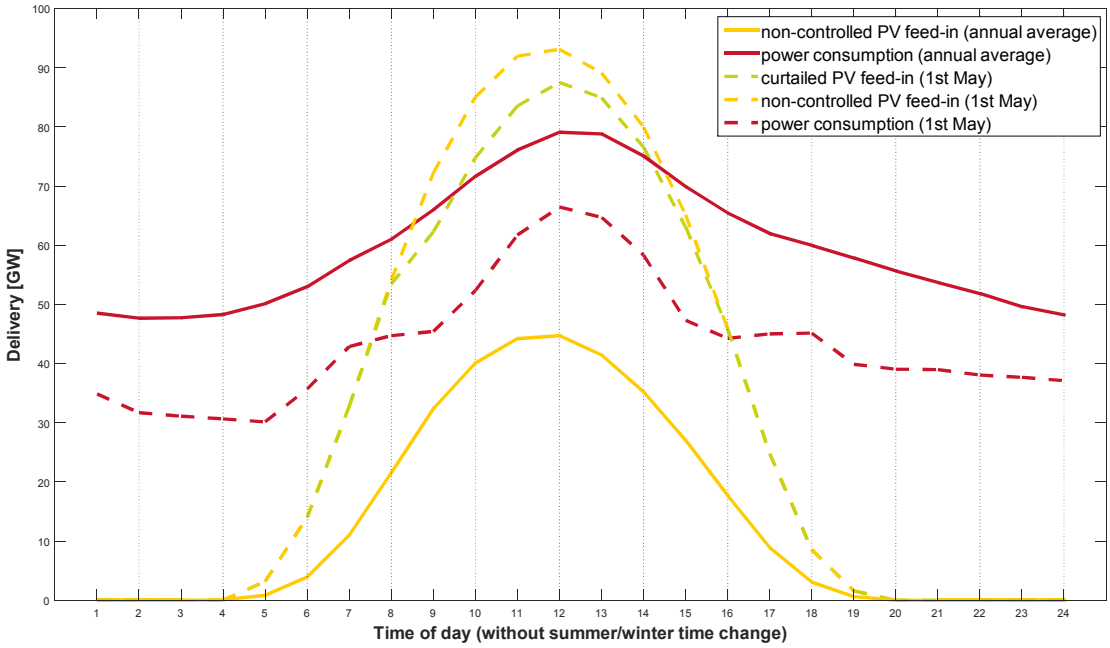

Figure 25: Diurnal variations of simulated PV feed-in and consumption throughout Germany

On this day, the PV feed-in is so high that it cannot be totally used or stored. The real feed-in which is limited for that reason is shown in the dotted green line. Across the year, 98.37 % of the photovoltaic feed-in can be utilized; only 1.63 % of the energy has to be curtailed. It can easily be seen that all diurnal development are at their maximum at 12 noon. On average, the photovoltaic feed-in falls precisely on the load peak (as it does for the 1st May). The diurnal course of PV feed-in has favourable effects on the power supply because its maximum coincides with the high consumption at midday. This is also shown in the value of 57.3 % for the correlation coefficient between the time series of power consumption in Germany and unregulated photovoltaic feed-in. An improvement in the correlation between consumption and PV feed-in can be obtained through PV installations, which do not face directly south because in that way the feed-in in the morning and evening are increased.

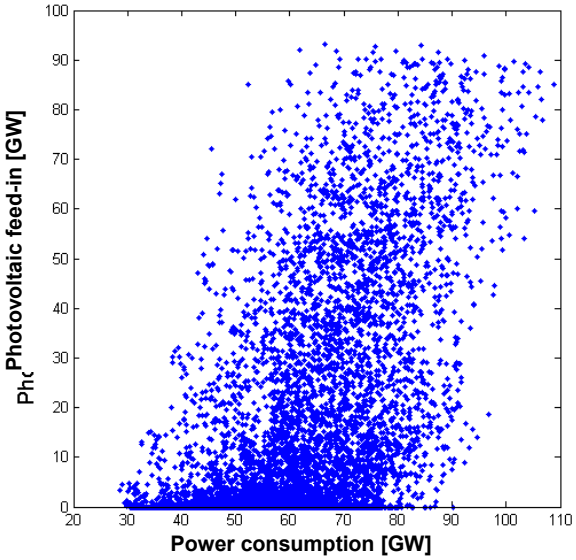

Figure 26: Relationship between the simulated PV feed-in and power consumption in Germany

In the diagram, the simulated relationship between the total power consumption and the PV feed-in for all of Germany is shown as a scatter plot. High PV feed-in very often coincides with high power consumption.

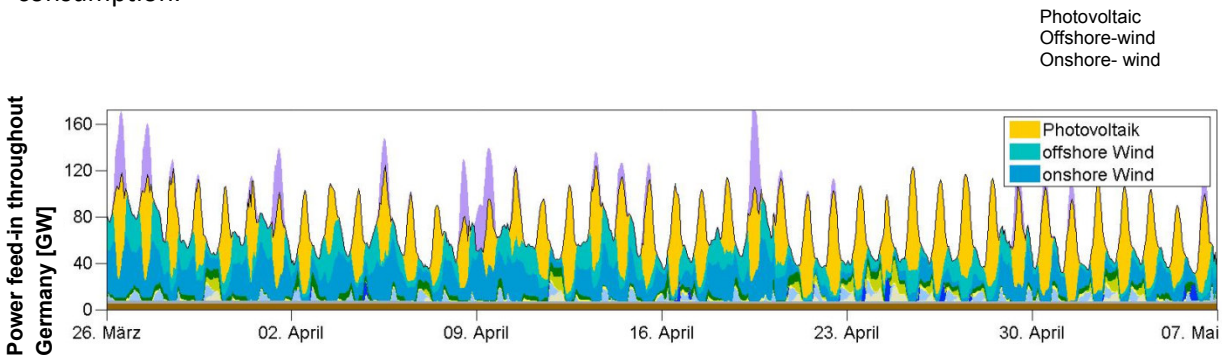

Figure 27: Six selected weeks in the simulated power production in all of Germany

In Figure 27an excerpt of six weeks of the simulated power production throughout Germany in the spring can be seen. Photovoltaic feed-in is concentrated around midday, as it would be expected. The highest feed-in from wind can be observed during the evening and night. Only occasionally does the feed-in from and PV occur simultaneously, which results in overproduction and subsequent curtailment of WTs (see section2.4.1.2). The curtailments are marked with the purple areas in the figure. The other colours in the diagram correspond to those inFigure 9. On all other days, wind energy and photovoltaic feed-in alternate favourably for the consumption. This alternation of PV and wind energy, which is so favourable for the power supply, deserves a closer look.

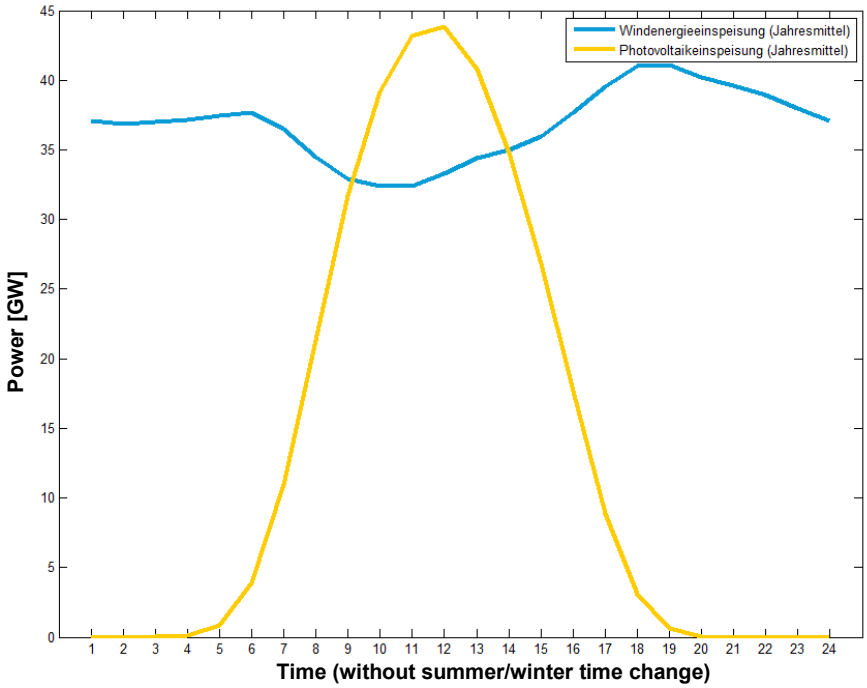

Figure 28: Diurnal variation in simulated feed-in from PV and wind energy for all of Germany

In Figure 28this alternation in the average day (average of all values for all hours of the day and year) of both producers, as shown here, is easy to recognize. On average, between 6h and 16h there is the least wind and precisely in middle of this period we find the peak of photovoltaic feed-in at 12 o'clock. On average, most wind energy is fed into the grid in the evenings between 18h and 19h, while on average, the photovoltaic feed-in disappears completely from 20h in the annual average.

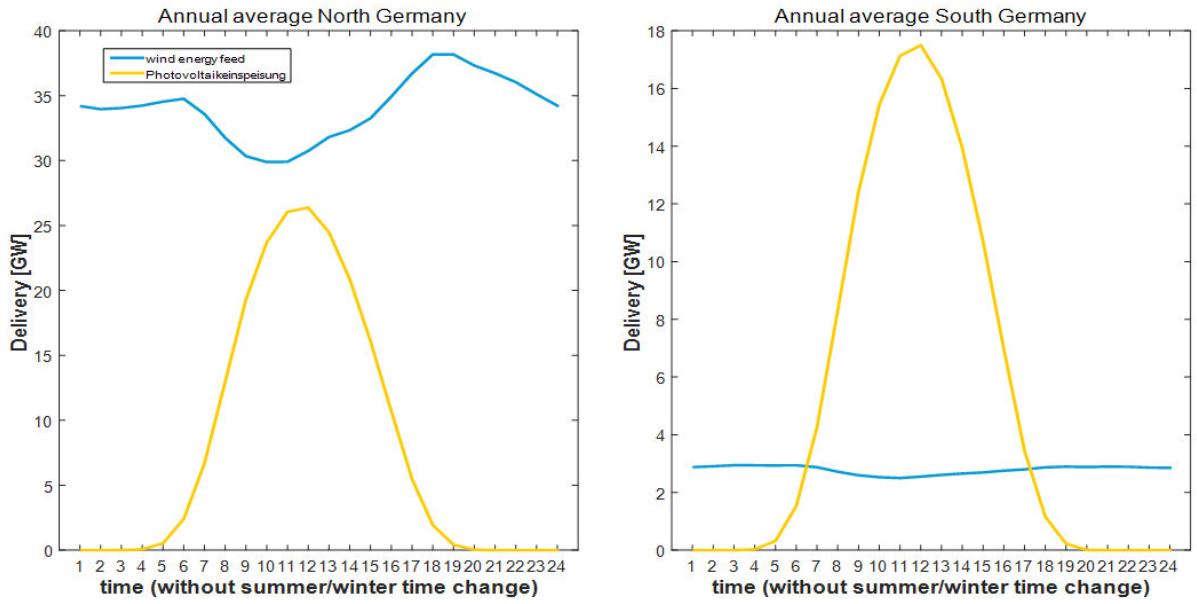

Figure 29: Diurnal variation in simulated feed-in from PV and wind energy for a) North and b) South Germany

Looking and North and South Germany separately (the 50° latitude is taken as the border), this alternating feed-in during average days can easily be distinguished for North Germany and is present in the same way throughout Germany. This leads to the assumption that the most striking characteristic of the diurnal rhythm of wind energy is caused by a meteorological phenomenon near

the coast, such a sea winds. However, in the south of Germany this effect is hardly noticeable due to the clearly lower share of wind energy feed-in, even if slightly lower wind energy feed-in is evident in the morning. Both figures show clearly that the wind feed-in on average surpasses the average photovoltaic feed-in in the north of Germany and vice versa in the south. The different heights of the values in the performance axis are due to the difference in area sites in the north and south Germany and thus having different installed capacities.

2.4.3 Bioenergy

Bio-energy can be used in various forms, e.g. heat, electricity or fuels and is generated by a large number of different energy sources. Its utilization and application are just as varied. The number of its energy sources is collectively called “bio-mass”. Among it are energy crops, which are used in solid form, as a liquid or a gas after being treated. Additionally sewage gas, slurry, wood and bio waste is considered. They all have in common that their energy is stored chemically. The direct storability of bio-energy is a crucial advantage over the weather-dependent wind or solar energy. Bio-energy can be converted to power exactly when it is needed (demand-based feed-in), although certain limits regarding the storage capacities and self-consumption have to be applied. Depending on the stored and available amount of energy and on the installed generator capacity, bio-energy is capable of short-term and long-term balancing of weather dependent energy feed-in. These days, bio-energy installations are generally run in base-load operation mode, i.e. that a relatively constant feed-in is provided. Currently, some biogas installations have more than 8.000 full load hours per year and high technical system availability between 92 and 98 %.

The system availability is similarly high for liquid biomass, and slightly lower for solid biomass. Installations for electricity generation of solid and liquid biomass are usually used for co-generation of heat and power. Their operation is mostly heat-controlled, which results in approximately 5,000 full load hours per year. While solid biomass has been used for power generation for over 100 years, bio-gas is a new addition. It has been used since the beginning of the 1990’s and has an increased utilization since the EEG Amendment of 2004. By 2012, 7.5 GW of installed capacity using bio-energy crops had been installed that generated 43 TWh of electrical energy during this year [82]. This corresponded to a share of 30.6 % of the electricity produced from renewable energy sources. The largest part of energy from biomass was delivered by biogas installations (24.8 TWh).

Table 7: Distribution of power generation from biomass in 2012 in separate fractionations

Input material	Number of installations [83]	installed capacity in GW	electrical energy generation in TWh
Biomass heat and power plants	540	2.2	11.6
biogas installations with on-site conversion to electricity	7,515 [83]	3.21 [83]	23.7
biogas installations with feed-in into the gas grid	116 [83]	0.2 [83]	1.1 [83]
liquid biomass	1,000	0.2	0.4
sewage gas	1,200	0.24	1.3
biogenic fraction of waste		1.4	4.9
landfill gas		0.13	0.6

The main input materials in biogas installations are 52.8 % of renewable raw materials (energy crops), 43 % of animal excrement, 3.8 % of bio-waste and 0.3 % of industrial and agricultural residues, given as a proportion of the mass. Based on the energy content, energy crops have a share of 81.5 %. Energy crops used in 2012 were mainly maize silage. The share of maize silage in relation to all energy crops is 73 %. In biomass, heat and power plants burn mainly residual forest wood (38 % of all installations) as well as waste wood (24 % of all installations).

For the bio-energy part of the Kombikraftwerk 2scenario a total energy potential for power generation of 60.5 TWh_{el} per year is set, which is sourced from Germany only [6],[37]. This equals approximately 10 % of the gross power supply of the entire scenario. In the referenced potential studies, food security and the production of bio fuels was taken into consideration. The total energy related primary energy utilization potential lies at 1.535 PJ. This includes power generation, heat generation as well as the bio-fuels. Further studies on the usable bio-energy potential assume a biomass potential between 1.000 PJ to 1.700 PJ. Table 8 shows how the scenario the total energy potential is divided amongst the ten different biomass technologies 10 technologies, including bio-methane.

Table 8: Distribution of bio-energy in the scenario

		Annual energy [$TWh_{el.}$]	local potential	converted to electricity in:
Biogas	energy crops	10,2	in fields and grass land	bio-energy installations & methane power crops (40% locally in villages, 60% via the natural gas grid)
	slurry	14,1	in villages	
	private sewage gas	1,3	in urban areas	bio-energy installations & methane power crops (40% locally in industrial areas, 60% via the natural gas grid)
	industrial sewage gas	0,3	in industrial areas	
solid biomass	energy crops	6,0	on fields	bio-energy installations locally in villages
	residual forest wood	12,2	in forests	wood heat and power station (approximately 40% via conversion to gas to the natural gas grid)
	wood waste	9,1	in urban areas	wood waste power plants (approximately 60% via conversion to gas to the natural gas grid)
	biogenic waste	5,9	in urban areas	waste-to-energy plants
liquid biomass	energy crops	1,5	on fields	bio-energy installations locally in villages
total		**60,5**		
	of this bio methane	26		

2.4.3.1 Modelling spatial distribution

In [37] a distribution of the potential of energy crops for use in (local) bio-energy plants was determined for the individual districts and published in a chart. Based on the contribution shares given in the chart, the energy crop potential for all of Germany was distributed over the individual districts. By evenly distributing district potentials to the district's grasslands and fields, an increase of the spatial distribution of the potentials was achieved. The CORINE-area-type "non-irrigated arable land" is interpreted as fields as well as half of the available areas of the types "complex parcel structures" and "agricultural land with natural ground cover". Grasslands are identified by using half of the available space of the ground cover types "meadows and grazing" and half if the type "complex parcel structures". Furthermore, it is assumed that energy crops for biogas production grow on fields and grasslands, the energy crops for the production of solid and liquid biomass however only on fields. The potential of slurry is distributed based on statistical surveys of the Federal state (Bundesländer) [9] and the animal population in each province. Within a state, the particular states' potential is again equally distributed in relation to the settlement areas with less than 10.000 inhabitants (villages) since livestock and poultry farms are usually situated in sparsely populated areas. Villages are designated locations where the conversion of slurry and biomass takes place, both liquid and gaseous biomass. However, it is assumed that only 40 % of slurry and biogas are converted to electricity nearby the villages of a district. The rest is fed into the natural gas grid. It is assumed that the part that is fed into the natural gas grid. It is therefore usable throughout

Germany and can be converted into electricity at required locations; mainly in towns with local bio-energy power plants (see section 2.4.3.2 and 2.4.6). Sewage gases are treated similarly. Sewage gases originate in sewage treatment plants, which use a preceding aerobic digestion stage and a subsequent anaerobic digestion stage. The largest potential here is in the densely populated areas. The distribution of the potential to the districts is carried out based on the wastewater volume in the individual districts from [9]. Sewerage is differentiated into industrial sewage and public sewage from dwellings, public buildings etc. Within a district, the potential of wastewater from the industry and trade in a particular district is distributed equally to industrial areas. The potential of sewage from public buildings is distributed evenly to the settlement areas. For the conversion of sewage gas, from either the industry or dwellings, it is assumed that 40% is converted into electricity in the industrial areas of the particular district. The rest is fed into the natural gas grid.

Figure 30 shows the spatial distribution of the different bio-energy potentials based on grid surfaces of 7 km x 7 km.

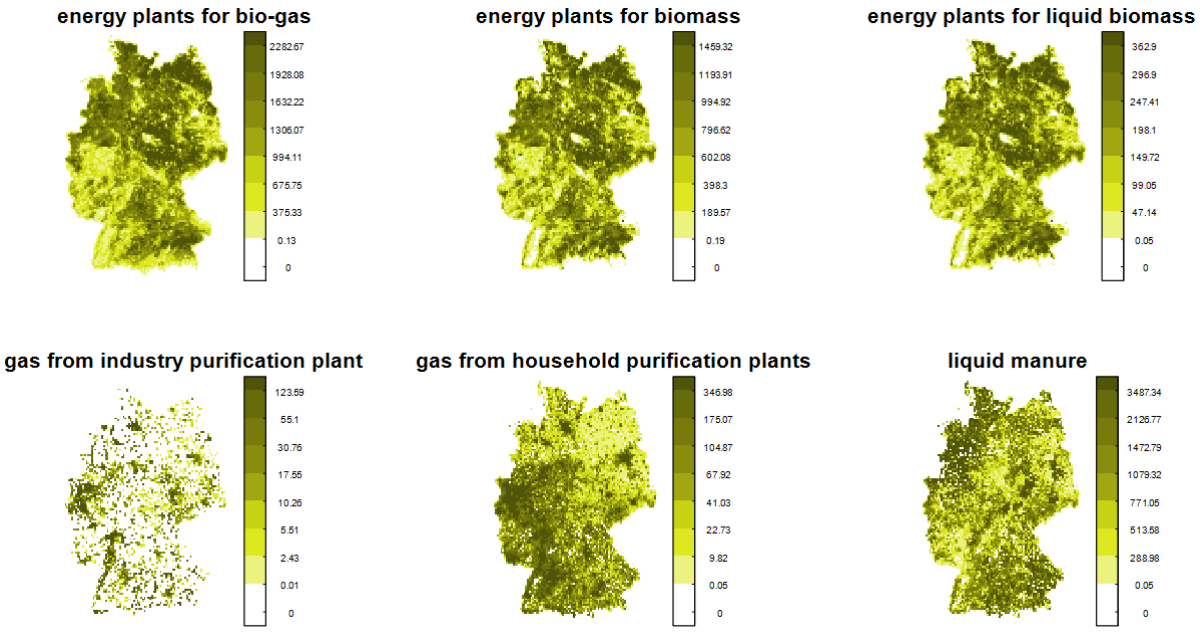

Figure 30: Spatial distribution of different bio-energy potentials in the scenario

Residual forest wood occurs mainly in forested areas**.** In the Kombikraftwerk 2 scenario, the assumed energy potential of 12.2 TWh_{el} per year is distributed equally over all of Germany's forested areas. For the conversion of this residual wood to electricity, each forested area is allocated to the wood heat power plant closest to it. For this, locations of 126 existing wood heat power plants with mixed and forest wood from [36] are used. As of 2010, 600 wood heat power plants are connected to the grid. Waste wood from industrial processes and households are usually found in towns. In the scenario, its energy potential is distributed between settlement areas according to the population. For the location of the conversion of waste wood, each settlement area is allocated to the closest existing waste wood power plant (in total 68 from [36]). Biogenic waste is the biodegradable part of the general waste that is burnt rubbish incineration plants with the rest of general household waste. In the scenario, its energy potential of 5.9 TWh_{el} per year is distributed to the population in Germany's urban areas, on a percentage basis. Biogenic waste is converted in waste-to-energy plants. The annual energy yields of 78 waste-to-energy plants [38] are used for the localization of the conversion of biogenic waste to electricity.

Figure 31 shows the areas in which residual forest wood (green), waste wood and biogenic waste (red) occur. It shows as well the locations and annual energy yields of the power plants used for the conversion into electricity.

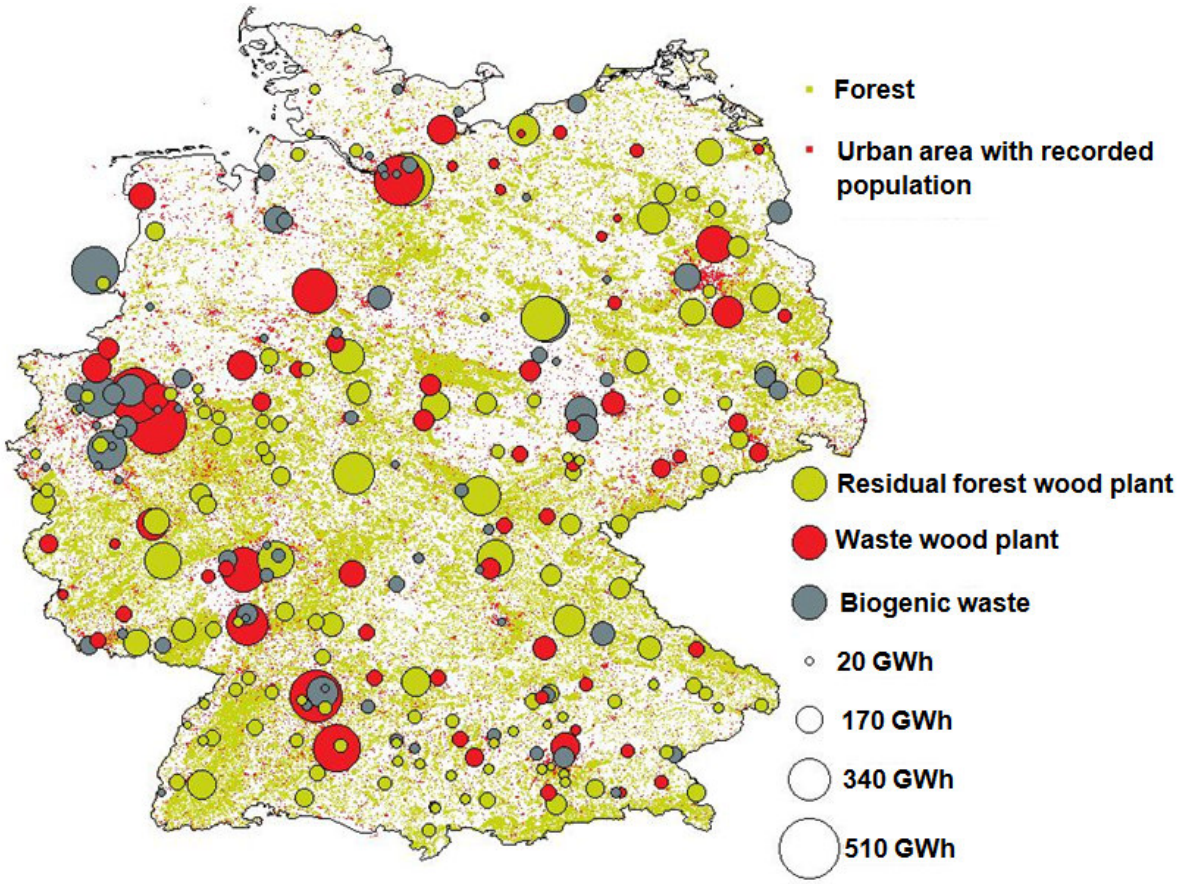

Figure 31: Positioning of energy potentials and conversion to power or gas of residual forest wood, waste wood and biogenic waste (locations of crops as at 2010)

In this section, the location of the annual electrical yields of the various forms of bio-energy was described. The installed capacity of bio-energy power plants is based on the models for time series generation, which are described in the following section.

2.4.3.2 Production and evaluation of time series

For the production of feed-in time series, bio-energy is divided into three groups. One group is bio-methane with approximately 26 TWh_{el}. For this type of bio-energy, it is assumed that it is fed into the natural gas grid that is no spatial restrictions, such as gas grid congestions. Bio-methane is converted into electricity in methane power plants (see section 2.4.6). The two other groups are spatially restricted in the scenario. Their biological energy potential has to be converted into electricity on-site. They are therefore allocated to certain grid nodes, as in Chapter 2.5**.** In the following, they will be called “biogas installations” and “biomass installations” and joined under the term “local bio-energy feed-in”.

A seasonally constant gas production is assumed for the biogas power plants with a total potential of 10.3 TWh_{el}. Furthermore, it is assumed that 30 % of the average heat production is used for heating

the fermenters and the sanitation of the waste installations as well as other applications. The part of agricultural biogas plants without sanitisation predominates which requires that the scenario assumes a seasonal heat requirement. In the model, the maximum heat produced can be stored for up to 24 hours, i.e., the fermenters can get by without additional heating for up to 24 hours. It is also assumed that a gas storage facility of 24 hours is available. In the scenario, power plants are only installed if they have at least 2.000 full load hours.

It is predefined that 75 % of heat produced by solid biomass installations is used. A maximum of 25 % may be discarded (i.e. that they are primarily heat-driven; flexibility is lower than for biogas plants). The total energy content of solid biomass in the scenario is 24.2 TWh_{el}. The time series for the heat requirement, which has to be supplied by the biomass, is assumed proportional to the thermal load profile of the general supply (see Figure 32). Heat storage of 6 hours has been set for biomass. Since solid biomass is easier to store, no limit for the supply of fuel is assumed modelled. The total annual energy is naturally determined by the available solid biomass.

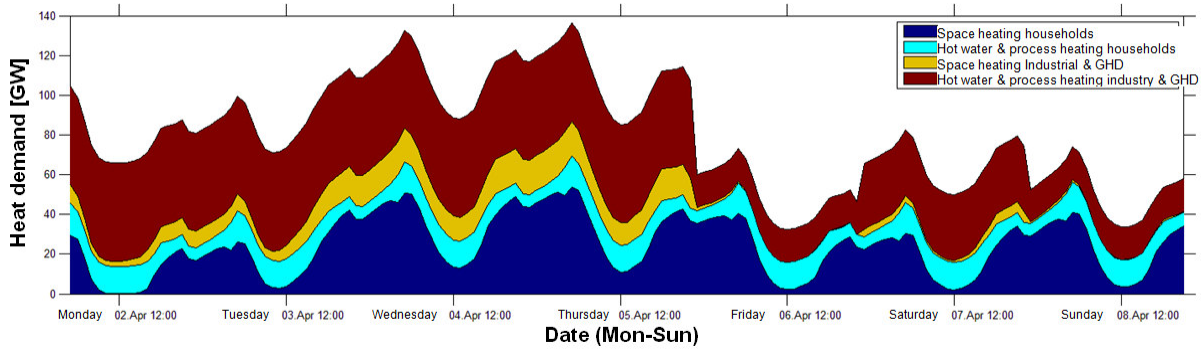

Figure 32: section of the set heat requirement time series, aggregated for all of Germany

Under the conditions that

- the minimum full load hours are met,
- the heat demand could be supplied together with heat storages,
- fuel could be stored and
- the total power demand in Germany is met,

the use of biogas and biomass power plants is planned. The main objective of the planning shall guarantee that the total energy consumption of the system and the required capacities are minimized. This is accomplished with long-term simulations (see Chapter2.1).

The following capacities of bio-energy installations throughout Germany were identified:

- Bio-gas power plants: 5.16 GW
- Biomass power plants: 12.11 GW

The results of the unit commitment show that bio-energy power plants can provide flexibility to the power system in the short term. In the medium term, they have to meet the heat demand, for which they are responsible (see Figure 32). By using seasonal heat storages and power-to-heat installations, the flexibility of biomass power plants could be increased. However, this was not the objective of the investigation. Figure 33 shows the residual load for two particularly critical weeks, i.e. the residual

load, which has to be met after weather-dependent power producers such as PV and wind, and DSM-controlled batteries have already been accounted for.

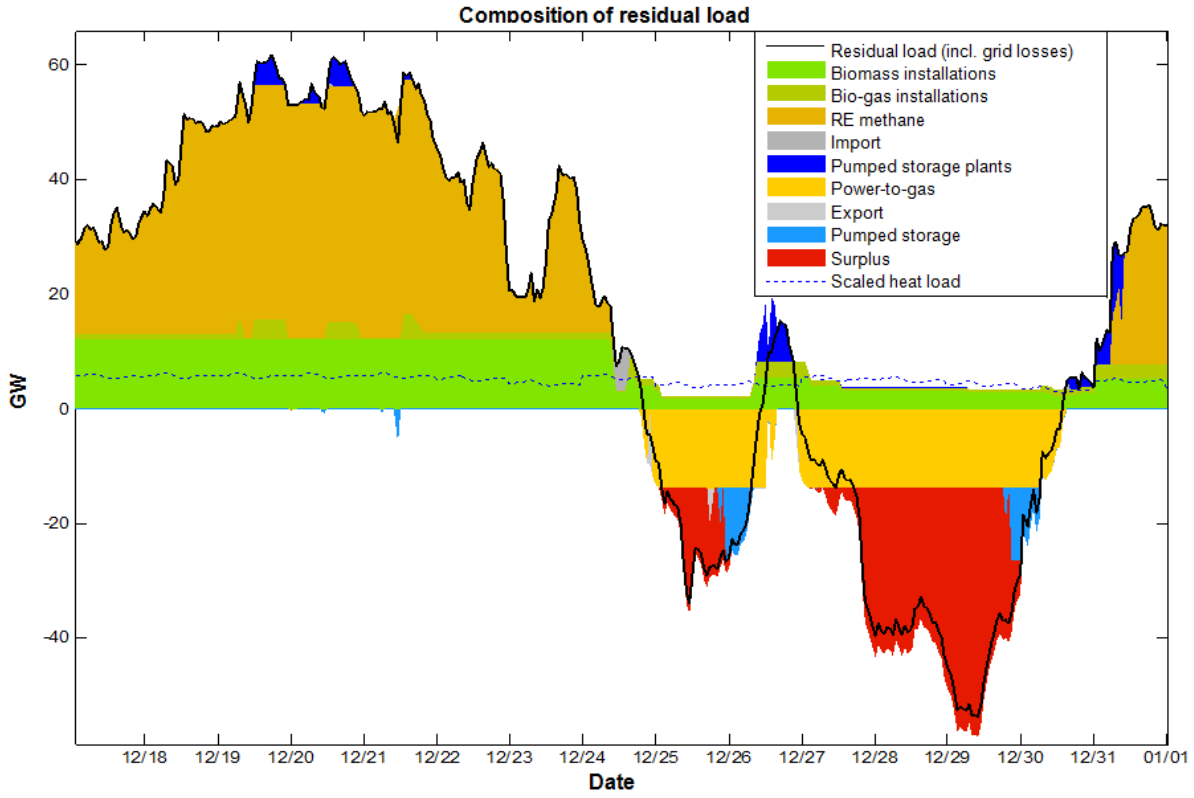

Figure 33: Meeting the residual load by controllable producers and storage in the last two weeks of the year. For purposes of illustration, the heat load progression is sketched qualitatively. In order to meet this heat load, biogas and biomass installations cannot be switched off completely.

As it can be seen in the latter week, there are a few days with a high surplus of wind and PV energy. Consequently, at these times the optimal unit commitment decides to store as much electricity as possible using power-to-gas installation and pumped hydro storages. Nevertheless, a large part of the power has to be curtailed. At times of such surpluses, biogas and biomass installations are operational at a very low level. The reason for this is the relatively constant heat requirement they have to meet. It can be seen very clearly how flexibility is improved with increasing heat storage. The biogas installations with their relatively large heat storage can be turned off completely during the first phase of the over production. Later they still manage to maintain a low output level.

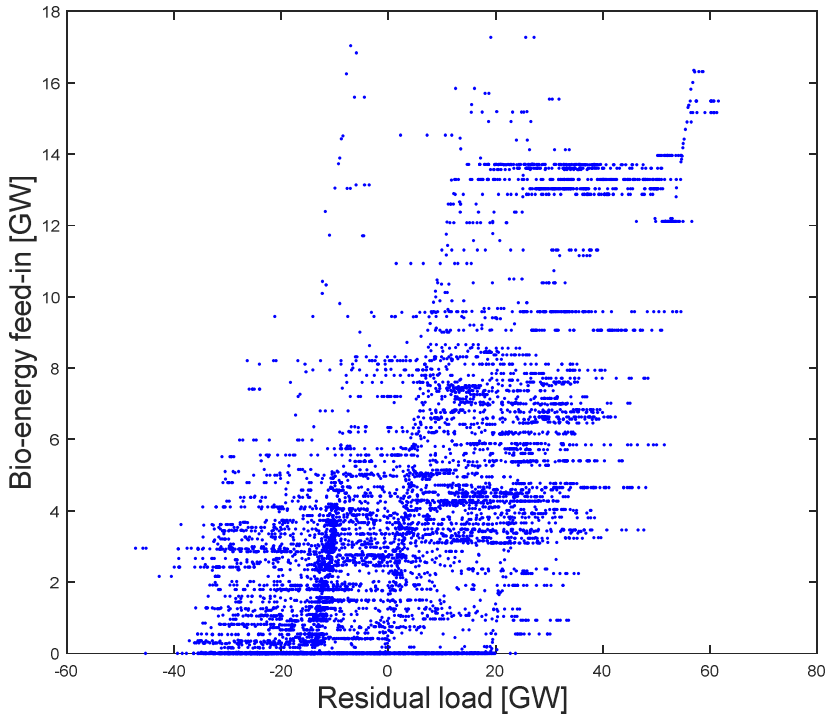

Figure 34: Relationship between the simulated power feed-in from local biomass installations and the residual load for all hours of the year

In order to analyse the behaviour of the local bio-energy feed-in for the whole year, the feed-in of power from local biomass installations is plotted in Figure 34. It is shown in relation to the residual load for all hours of the year, aggregated for all of Germany. Residual load is defined as power the consumption minus the sum of feed-in of the weather-dependent renewable energy sources, which are wind, photovoltaics and run-off-hydro power plants. The highest feed-in from biomass installations with local conversion is seen, as expected, during hours with a positive residual load, when consumption cannot be met by weather-dependent renewable energies. The reason why the feed-in of power from biomass installations with local conversion does not disappear entirely is the installation's operational mode, even during hours with negative residual load. As biomass installations must supply heat, they are switched off very rarely.

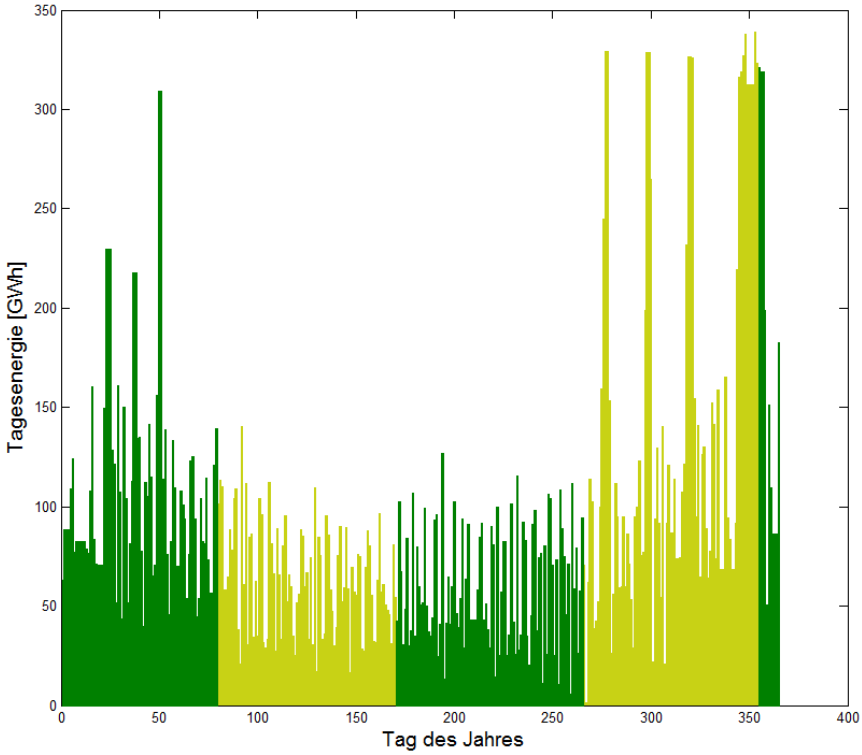

Figure 35: Diurnal energies of local bio-energy feed-in

Figure 35 displays the diurnal energies of local bio-energy feed-in for a complete year and all of Germany. The dark green colour represents the seasons of winter and summer and the pale green colour spring and autumn. It can be seen that there is not a single day on which there is no local feed-in from bio-energy. By looking at the individual hours of the year, there are 1.436 hours without power feed-in from local biomass installations. This represents a share of 16.4 %. The feed-in is clearly higher during autumn and winter than in spring and summer. A reason for this is the evidently lower photovoltaic feed-in during autumn and winter and the resulting increased positive residual load.

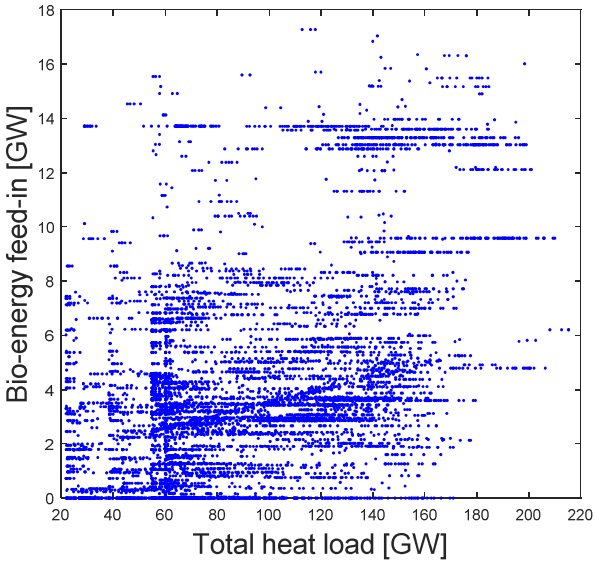

Figure 36: Simulated local bio-energy feed-in over heat load

Figure 36 shows the hourly data of local bio-energy feed-in in relation to the heat demand for all of Germany. It is noticeable that there is hardly any local bio-energy feed-ins during times of low heat load. However, local bio-energy feed-in of up to 8 GW takes place with differing heat loads. The correlation coefficient is 49.8 %. A tendency for higher feed-in of bio-energy with higher heat load is thus given.

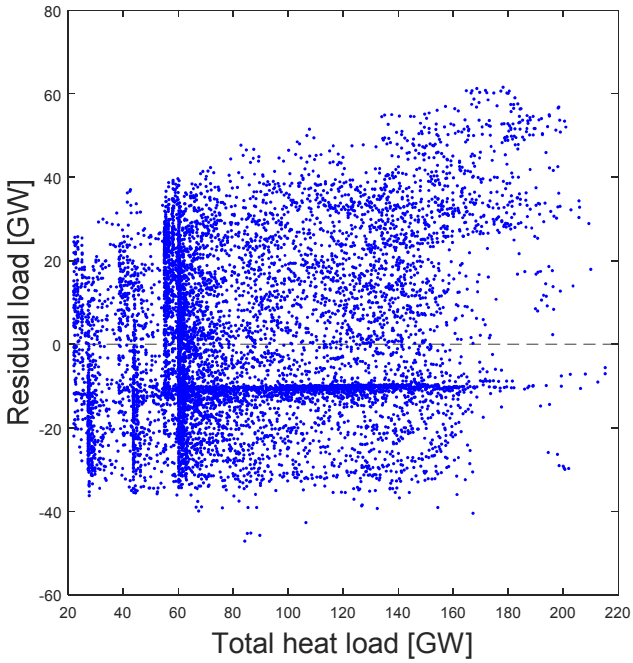

Figure 37: Connection between simulated residual load and heat load

The connection between the simulated heat load and residual load for each hour of the scenario-year and for all of Germany is shown in Figure 37. In most cases, the residual load takes on a high positive value with a high heat load, i.e., there is a demand for energy. Surplus from renewable energy sources (negative residual load) however, coincide with different heat loads. No noteworthy surpluses during low heat demand can be observed. The correlation coefficient of minus 23.6 % (total heat load) is also lower than the coefficient of the bio-energy feed-in.

2.4.4 Hydro energy

There have been hydro energy plants in Germany for many decades. Presently there are approximately 7,700 plants, which have a share of approximately 3.5 % in the power supply [6]. It is assumed that in future small hydro power plants will be added, however, the greatest increase of energy will be obtained from the modernization of existing large hydro power plants. The assumed possible annual energy yields of hydro power ranges between 24 TWh ([7], [6]) and 31.9 TWh [50]. For the Kombikraftwerk scenario 25 TWh are set, according to [6].

2.4.4.1 Modelling spatial distribution

In order to determine the geographical distribution of future capacities of hydro power plants, a list of the installations with an installed capacity of more than 1 MW is used: This list from 2004 contains the locations of hydro power plants, their annual energy yield (in GWh), the installed capacity (in MW) and the flow rate in (in m^3/s), subdivided into different types of power plants. In Kombikraftwerk 2, only the run-of-river power plants are considered since data on storage capacities

and operation modes of hydroelectric storage plants are unavailable. The negligible share of approximately 5% of the annual output from hydro energy allows disregarding this circumstance. Only the hydro power plants in the states of Bavaria, Baden-Wuerttemberg, Rhineland-Palatinate and North Rhine-Westphalia are taken into account. These states have a total share of 96.2 % of the total capacity of all run-of-river and storage hydroelectric plants in Germany. Bavaria has a share of 66.05 %, Baden-Wuerttemberg 22.14 %, Rhineland-Palatinate 5.68 % and North Rhine Westphalia 2.31 % [51]. The installed capacity is approximately 2,730 MW, which is about 58 % of installed capacity in 2007 [50]. The remaining 42 % come from additional hydroelectric plants that have been built after 2004 and from hydroelectric plants that have not been included since they are below the threshold of 1 MW of nominal capacity. The total number of these small plants reaches 7,300. However, they only supply approximately 10 % of the energy. Taking into account the above percentages of the states' annual energy yield, the installed nominal capacity of the recorded installations is scaled up so that the annual hydroelectric electricity produced is 25 TWh, maintaining full load hours in each plant. This upscaling of the captured hydroelectric plants corresponds to the aforementioned assumption that energy generated by hydro power plants can be increased mainly by modernizing the existing large hydroelectric plants. An installed capacity of approximately 4.8 GW of hydropower results for the scenario.

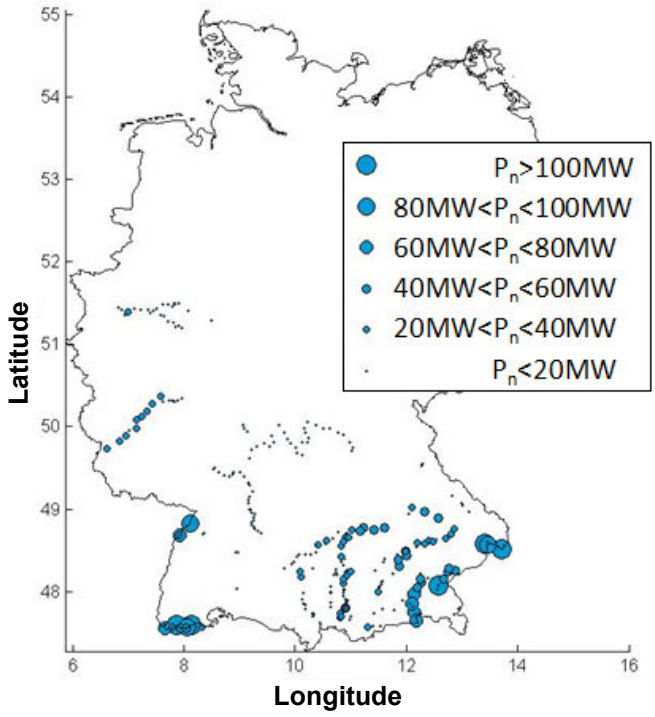

Figure 38: Spatial distribution of installed hydropower output in scenario

2.4.4.2 Production and evaluation of time series

The power output by each captured hydro power plant is simulated as a function of the water flow through the power plant. This is based on the power curve shown in Figure 39. One can observe proportional relation between the power output and the water flow through the plant until the designed maximum water flow is reached, which is the nominal capacity of the power plant. Exceeding the designated maximum water flow leads to a linear power decrease due to the decrease of waterfall heights with high flow rates. The degree of decrease is specific to each location and each power plant. It is assumed equal for all hydroelectric plants, since detailed information is unavailable. The value of the decrease is calculated based on production data available for the project and by calibrating the simulation results with data of the monthly production of hydropower in Bavaria.

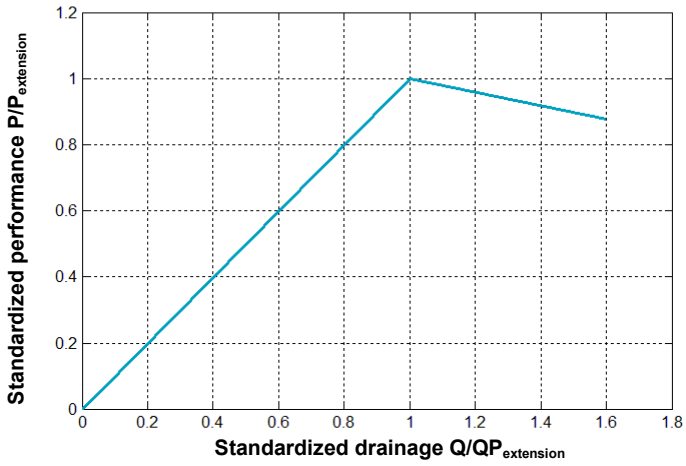

Figure 39: Hydropower curve used

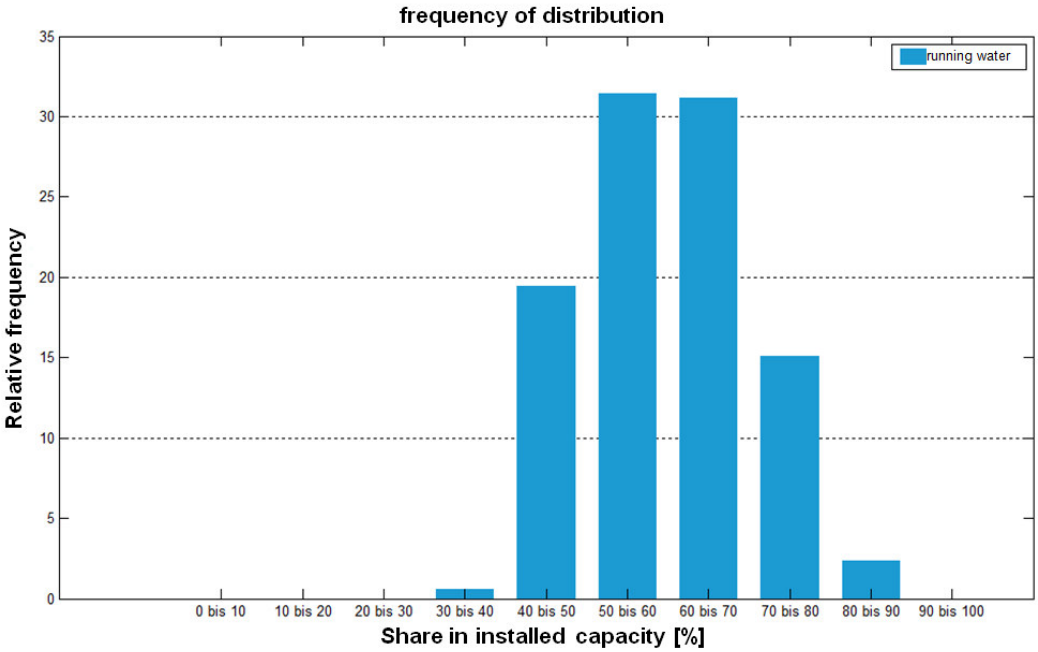

Figure 40: Frequency distribution of simulated feed-in from hydropower

As can be seen inFigure 40, most of the hydropower plants in the scenario are operated slightly above half of their installed capacity, which can also be seen in the number of full load hours of 5,253, which approximates 60 %. A simultaneous utilization of the full installed capacities in Germany does not occur.

2.4.5 Geothermal energy

Apart from supplying heat, the use of geothermal energy provides weather-independent power production. This allows providing electricity to meet the demand during low feed-on of wind and solar. So far, geothermal energy has had little use for the power production in Germany. Just five geothermal energy installations with a total capacity of 12.5 MW_{el} were in operation in 2013 [52]. However, larger installations are being planned and built. Building geothermal installations is associated with economic and ecological risks the expensive drilling operation might have to be stopped due to geological instabilities or minor earthquakes. According to [39], the total technical potential for geothermal power production in Germany is 600 times higher than the German annual electricity demand. About 95 % of the potential are located in crystalline rocks, geological faults account for approximately 4 % and hot water aquifers for 1 %. Even the potential of the smallest resource (hot water aquifers) equals about five times the German annual electricity requirement. The sustainable potential of geothermal power production, i.e. the energy withdrawal from the rock, which does not cause long-term cooling, is estimated to be only 300 TWh/a. Cost effectiveness of geothermal energy is significantly better when power co-produced with heat. The usable potential is further reduced to approximately 66 TWh/a due to the limited heat demand. The value set in the scenario of 40 TWh for annual electrical energy production from geothermal energy is relatively high but possible.

2.4.5.1 Modelling spatial distribution

Particularly hot water aquifers are considered technologically feasible for the use of geothermics for power production in the near future. They are located in the north German basin, the Upper Rhine rift valley and the south German Molasse basin. In the Kombikraftwerk 2 scenario, the geothermic installations are simply distributed equally to positions of network nodes (see section 2.5.1.1) of these areas (see Figure 41). 165 network node locations result, which contribute equally to the set annual energy production.

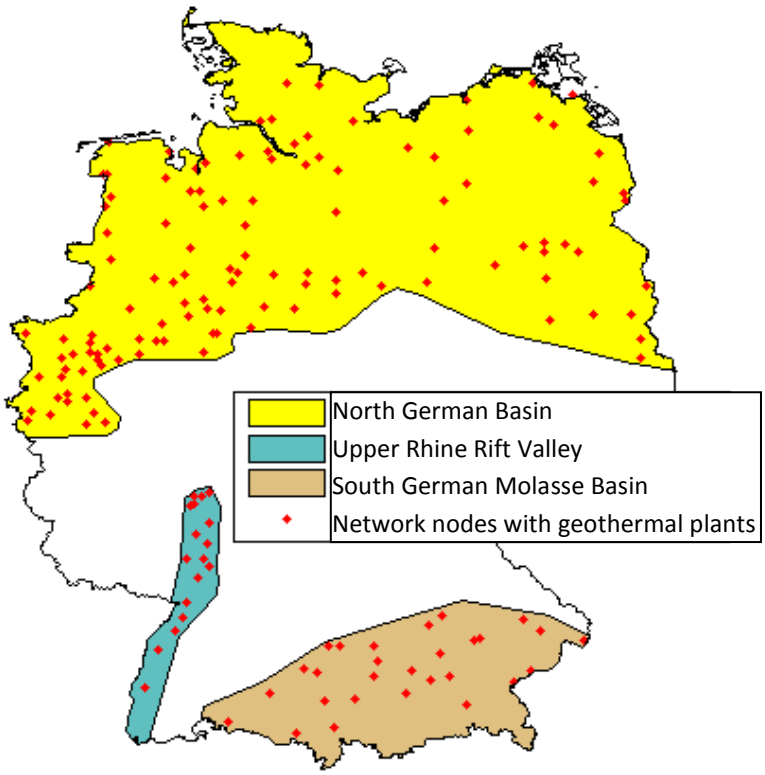

Figure 41: Spatial distribution of geothermic installations in the scenario

2.4.5.2 Production and evaluation of time series

The power feed-in from geothermal energy is simulated as temporally constant for the scenario. The set annual energy production of 40 TWh yields an output of approximately 4.7 GW.

2.4.6 Methane power plants

In the project report, the term “methane power plant” is used for power plants of any size in which methane is converted to power. These could be small combined heat and power units (CHP) in the basements of houses (see 100.000 power units at home by Lichtblick, with 2 kW nominal capacity) or large gas turbines (GTS) or combined cycle gas-and-steam (CCGT) power plants. The term “methane power plant” shows that the fuel is methane from the natural gas grid but not fossil natural gas. In the scenario, this methane is composed by approximately 58 % of bio-methane, which is produced by bio-energy plants (“bio-methane plants”) (section 2.4.3). This bio-methane is purified to meet natural gas standards and fed into the gas grid. Almost 42 % of renewable methane is generated in power-to-gas installations (section 2.6.1), which is in turn a renewable energy source.

Methane power plants are seen as the ideal supplement to wind and solar power plants since they are particularly fast and flexible and can compensate weather-dependent energy production. A smaller variant of a methane power plant is a CHP. Due to their connection to lower voltage levels and their resulting spatial distribution, they are a decentralized form of energy generation. Modern power plants of this kind have an electric efficiency of up to 44 %. Due to the co-generation of power and heat, the primary energy input is used by approximately 90 %. Through the local use of the energy, grid losses can be minimized. In a 100% RE-scenario, the large methane power plants, the gas turbines (GTs) and combined cycle gas turbines (CCGTs), are technically identical to today’s

conventional generation technology. Despite this fact, they are converting renewable methane into electricity. They have all the typical characteristics as in the current power supply, such as nominal capacity, generator type or connection to the highest voltage grid. They can therefore contribute to grid stability in the proven way and allow decreasing the otherwise necessary grid extension and renovation of the grid with all its components. Modern CCGT power plants have an electric efficiency of approximately 60 %.

2.4.6.1 Modelling spatial distribution

In the scenario, the total capacity of methane power plants is derived from the annual unit commitment planning (long-term simulation in Chapter 2.1). It ensures that at any point in time of the scenario the remaining residual load can be met by an appropriate number of methane power plants. This also takes into account the use of storages. The maximum residual load is the load that has to be met if non-controllable producers like wind and solar and the use of DSM applications and batteries are deducted. The capacity has to be provided by flexible producers and storages like methane power plants. The maximum residual load in the scenario is 40.96 GW (see Figure 43). This number is the results of the unit commitment, which is applied for the historic weather year in the scenario. In order to be prepared for years with extreme weather conditions the total capacity of methane power plants is increased. Apart from that, methane power plants must be able to provide the required positive control reserve, which cannot be supplied directly by biomass power plants. In the simulated scenario, the storages were adequately dimensioned to provide positive control reserve. However, in practice a situation might arise in which the storages are empty and thus cannot deliver positive control reserve. For this reason, the entire capacity of methane power plants in the scenario is set to 54 GW. This adjustment was made for the methane power plants (and not for the biogas installations) since they are the most flexibly type of power plant in the scenario. This is mainly due to the fact they have no co-generation of heat and power. This allows them to bridge times of maximum residual load.

Regardless of how the security mark-up of approximately 13 GW is calculated, the installed capacity of the weather-independent producers should correspond to the maximum load. This has been mentioned in various studies, e.g. [57]. In this way, the fact is taken into account that the secured capacity from direct RE feed-in from wind and solar is very low and that storage have a very limited energetic capacity, apart from the power-to-gas option. Methane power plants, as part of the power-to-gas-to-power cycle, can deliver secure reserves independent of weather conditions in the long term.

The spatial distribution of methane power plants is determined jointly with the network expansion assessment. The distribution follows the optimal trans-regional balancing. The total capacity is allocated in proportion to the maximum remaining residual load. Methane power plants are close to the load centres, just as today. This ensures that the network load in times of the greatest demand for residual load is kept as low as possible.

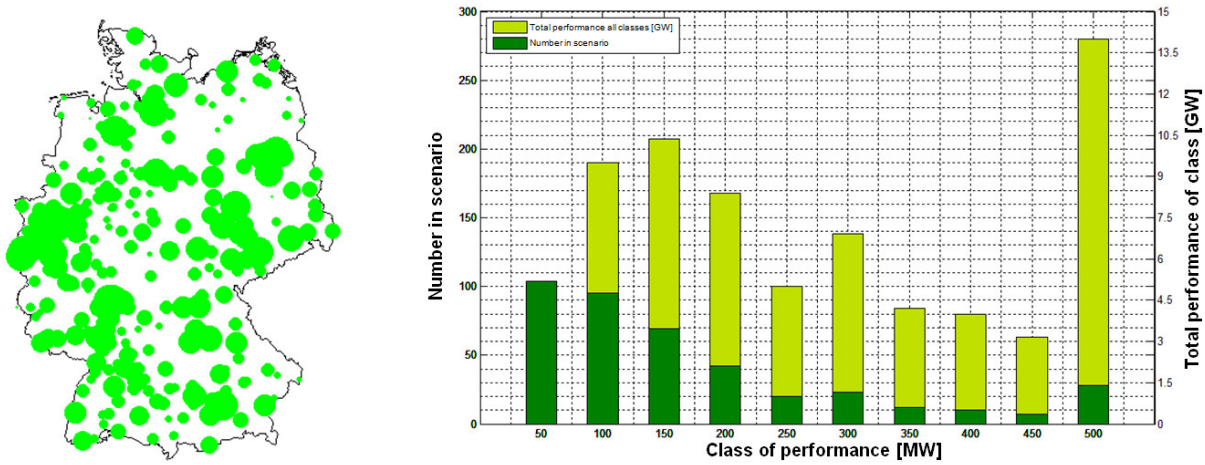

Figure 42: Number of HV-network nodes with methane power plants and their installed capacity in the scenario divided into classes of capacity

Figure 42 shows the total capacity available from methane power plants at each grid node of the highest voltage (HV) network. It is not assessed how this capacity is distributed between large and small power plants. It is possible that the capacities located close to each other are combined in larger blocks. However, this is primarily an economic consideration, which is not investigated in this project.

2.4.6.2 Production and evaluation of time series

The maximum residual load, which influences the dimensioning of the capacities of methane power plants, occurs on 25 January in the year studied. Figure 43 shows the coverage of the residual load during this period.

While in the period before and after this the typical mix of production and storage prevails, on 25 January, all available producers have to contribute to meeting the residual load. Biogas and biomass-plants produce at their maximum. The fore looking unit commitment ensures that all storages are fully loaded and are able to deliver their maximum power output. The rest of the residual load has to be supplied by the methane power plants, which in turn is the aforementioned minimum capacity of 40.96 GW.

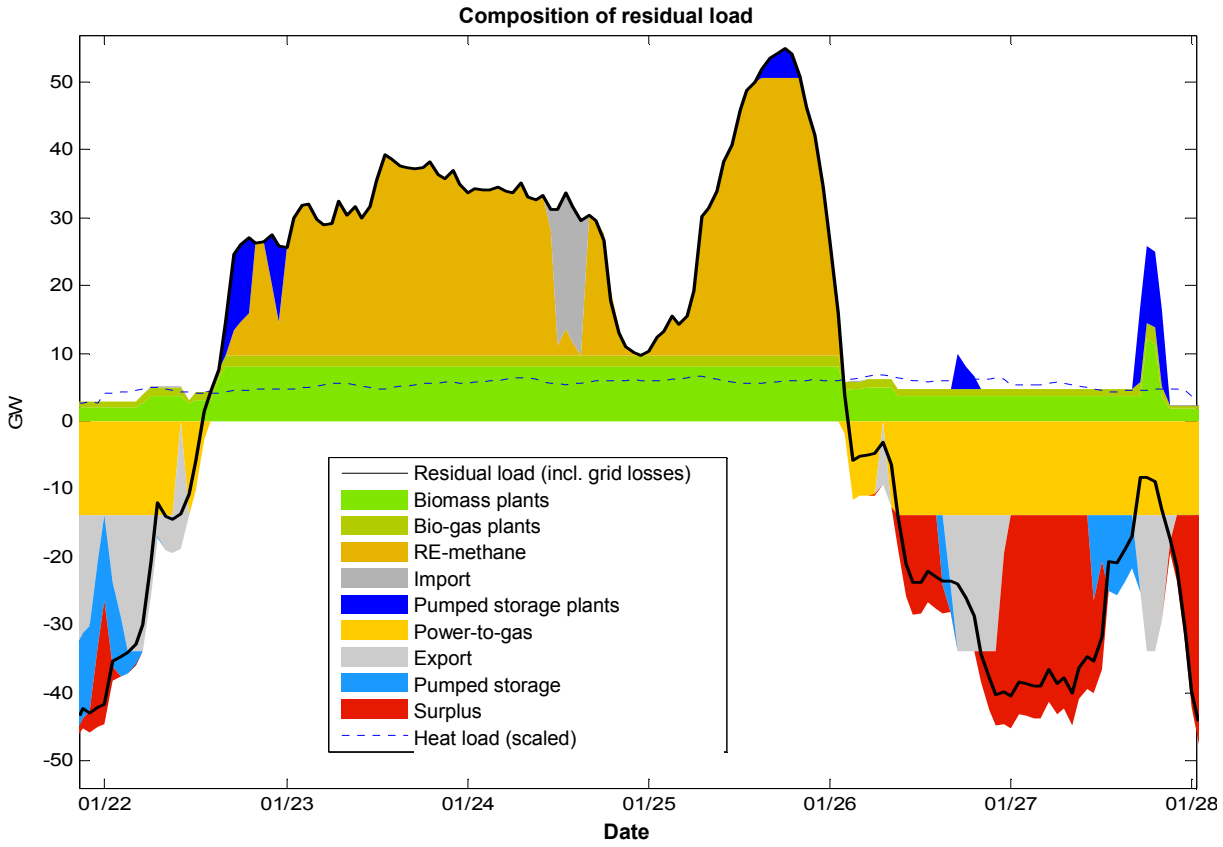

Figure 43: Meeting the residual load with controllable producers and storages in the last week of January. The maximum residual load and simultaneous maximum capacity utilization of the methane power plants occurs on 25 January

The methane power plants are assumed fully flexible without any further time constraints. Their use is thus directly derived from the unit commitment planning with the goal of minimizing the use of methane. Spatial limitations regarding the use of methane, such as congestions in the natural gas grid, were not taken into consideration. In the model, methane is fully available at times and places with the only condition that its sum must be balanced over the year. Figure 44 shows the period in the scenario with the longest continuous use of methane for power production.

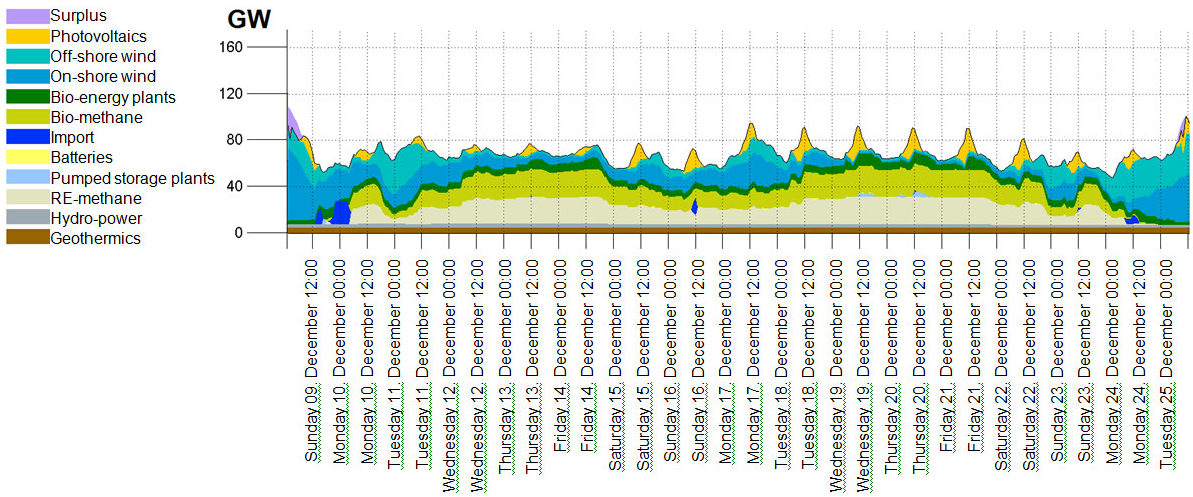

Figure 44: Two weeks in winter with the longest duration of use of methane power plants during the scenario year

As shown in Figure 44, the underlying weather patterns are responsible for the extremely low feed-in from wind and sun during two weeks in winter. The pumped hydro storage facilities are temporally limited because their energetic capacity can only contribute little to load coverage. Instead, the methane power plants and the local bio-energy plants are almost fully used over a longer period, converting RE methane and bio-methane into power.

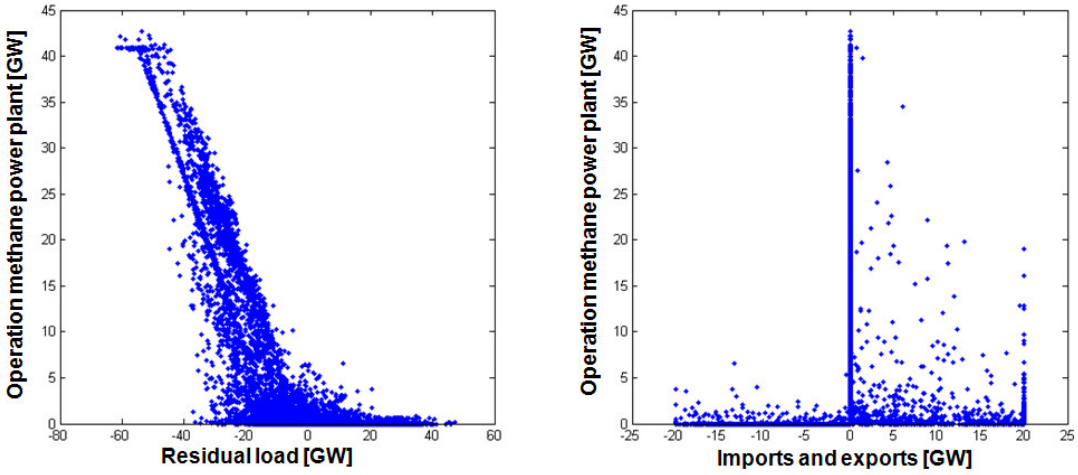

Figure 45: Connection between the simulated operation of methane power plants and the residual load (left) and b) the capacity imports and exports (right)

Those methane power plants are mainly operated during periods with particularly high residual load, as shown in Figure 45 a). At times when the production of renewable energies is not sufficient to meet the load (negative values of the residual load), methane power plants are operated to a high degree. The opposite is true when renewable energy production predominates (positive values of residual load). A similar trend is visible in imports and exports in Figure 45 b). In times of high power exports to the rest of Europe (negative values), the excess power results in hardly any operation of methane power plants. During electricity shortages, which are compensated by imports (positive values), methane power plants are operated to a greater extent.

2.5 The grid

The nature of the high and highest voltage grid, also called transmission network or transport grid, is key to a future energy system and its stability. Assessing long-term network expansion plans for the next few decades is challenging due to uncertainties. On the one other hand, not only economic but also political stipulations are a particular issue. The network expansion suggested in studies [42], [16], [43] is currently meeting resistance in certain parts of the population. Therefore it is uncertain to what extent these measures can be implemented. On the other hand, the grid and its dimensions have a strong interdependency with the other assumptions of the scenario, especially concerning the size and structure of future storages. Nonetheless, for the project in hand a detailed model of a future highest voltage grid is a basic precondition for the investigation of power system stability. The methods used in modelling of this network are described in what follows.

2.5.1.1 Modelling spatial distribution

For the extra high voltage level maps and geographical information exist including information on the location of network nodes/substations, their line connections, the length of lines, the voltage levels (220 or 380 kV) and the number of circuits per line section (e.g. in [40], [41]). In part, the grid maps include lines already planned, e.g. those from [42]. Newer network extension plans also are shown in [43]. All these data are taken into account for the grid modelled in the scenario. A completely new part of the grid is situated offshore (see e.g., [16]). Currently so-called stubs without any interconnections are planned which are shown like that in the net model, i.e., each offshore wind farm in the scenario has its own connection to the onshore grid, usually in form of high voltage direct current (HVDC).

In addition, a further network expansion of the HV grid is designed so that a 100 % renewable scenario could sensibly be modelled. In principle, such calculations always cause a conflict between more network expansion with its economic, political and ecological consequences and a better operation of the power system, i.e. fewer curtailments and re-dispatch measures. In the scenario, an attempt is made to minimize network expansion during normal operation. In this n-0 situations an optimal balance of weather-dependent RE feed-in can be achieved and congestions avoided. At each time step, the grid should therefore be adequately sized so that RE energy curtailment would not be curtailed due to grid constraints and there is a need for this electricity. This approach ensures that the power flows in the scenario are within reasonable boundaries. However, future grid problems are not trivialized. Bottlenecks will still occur, especially in n-1 situations. Where suitable these are alleviated by re-dispatch measures (see section 3.3.2). One of the main aims of the investigations is meeting the challenges (e.g., management of congestions, voltage stability) of a 100 % RE supply. Nevertheless, this goal should not be achieved solely by extensive network expansion.

The optimizing network expansion is limited to the addition of further 380 kV three-phase systems on existing routes and/or the upgrading of 220 kV lines to 380 kV. It was important to optimise the assumed transformer stations from the 220 kV to the 380 kV level. The precise location of transformer stations is not available in sources open to the public. When considering network expansion the transformers were individually modelled and sized in such way that no islanded circuits or single supply line networks occurred.

The connections to foreign countries were assumed to be without change. In total, there are 34 of such interconnectors and 67 transmission systems on the 220 kV and 380 kV level with a nominal transmission capacity of 62 GW. Foreign grids with their possible congestions are not modelled in detail. In all simulations, the total interconnector capacity was therefore limited to 29 GW.

Apart from the modelled characteristics of the high voltage grid, further properties for calculating the power flows through the grid are necessary. In the Kombikraftwerk 2 study, the calculation of power flows is carried out in two separate ways. First are the so-called simplified power flow calculation (see Chapter 2.1) and the so-called complete power flow calculations (see Chapter 3.2 and 3.3). For the simplified power flow calculations, it is important that the electrical parameters of the lines have the standard values from [45]. The values set in the scenario for each alternate current (AC) line; direct current (DC) line and each transformer are summarized in the following table:

Table 9: Set electrical parameters of the grid model for a simplified power flow calculation

	Resistor	Reactance	Transferable power
220 kV-AC-line	0.08 in Ω/km	0.32 in Ω/km	500 in MW
380 kV-AC-line	0.03 in Ω/km	0.25 in Ω/km	1.800 in MW
DC- line	0.01 in Ω/km	0 in Ω/km	400 to 2.000 in MW
Transformer	0.12 in Ω	24 in Ω	600 in MW

Based on these values the following extra high voltage grid model of a 100 % renewable energies power supply is designed for the Kombikraftwerk 2 scenario.

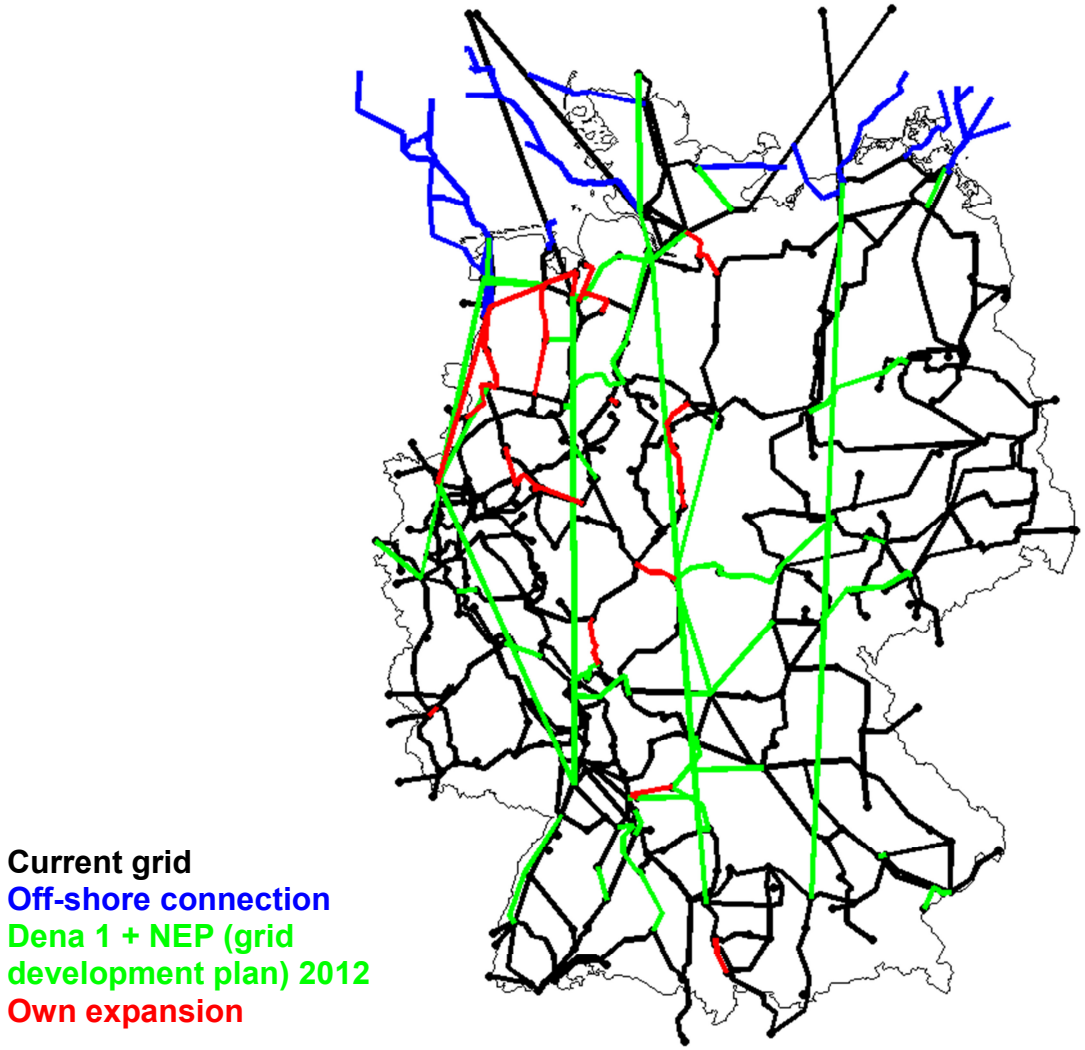

Figure 46: The scenario's extra high voltage grid model

In total, the following line lengths for voltages between 220 kV and the 380 kV resulted. The total number of the transformers is 93. Figure 46 and Table 10 show that the resulting grid is very similar to plans of the transmission system operators in Scenario B 2032 [43]. It can therefore be regarded as a plausible basis for further considerations with regard to power system stability.

Table 10: Total line lengths of the different upgrade steps of the modelled German supergrid (mostly several lines per route!)

Length of line (1.000 km)	220 kV	380 kV	DC	total
Currently	16,2	25,7	1,2	43,1
According to [43] (B 2032)	-5,9	+10,1	+17,4	+50%
100% RE scenario according to simplified power flow calculations, addition for (n-0)- freedom from congestions*		+3,8		+7%
KK2-(n-1)-scenario after addition for (n-1)-freedom from congestions *		+1,1		+2%

*: see section 3.3.2.

A certain additional capacity compared to scenario B 2032 of [43] is necessary to increase the share of renewables from 66 % (scenario B 2032) to 100 % in the Kombikraftwerk 2 scenario. The bulk of the new lines are concentrated regionally in areas where the additional offshore wind capacities are connected to the load centres. Altogether, the additionally simulated network expansion is moderate compared to the scenario B 2032 [43]. There are two important reasons for this. Firstly, the high voltage direct current transmission lines (HVDC or DC lines), like those in [43], connecting the north of the country with the south have a very positive effect on the possible transmission capacity. Due to their lower energy losses, when compared to the longer alternating current lines, cost-optimizing unit commitment planning prefers to use of controllable HVDC lines. Secondly, in scenario B 2032 in [43] the bulk of the south German load can be met by north German wind power. A further addition of wind capacities in the north, as assumed in this project, leads to additional production of methane in power-to-gas plants during peak periods. In the scenario, those power-to-gas plants are located in the north of Germany, which avoids any additional network loads.

The simulated grid expansion could be smaller in reality. New technologies like continuous monitoring of transmission line temperatures (dynamic line rating, DLR) could temporarily increase the available transmission capacity. Moreover, additional restrictions for the system operation could be accepted, which in turn could has implications on the operating costs and environmental effects. Balancing those requirements against network expansion could lead to less additional transmission capacity. However, these considerations are not examined in detail.

Catchment areas are modelled for the allocation of consumption and weather-dependent production time series, the production potentials from bio-energy and the pumped hydro storage power plants associated with the nodes of the HV grid model. It is assumed that all consumers, producers and energy storages withdraw or feed-in power from the HV or their respective catchment. Due to lack of available network data, the distribution networks, from which most consumers and in future also producers are connected to the HV grid, can only be taken into account in the modelling in a relatively simple way. For this, information is used on the areas, voltage levels and possibly upstream grids of the approximately 900 German distribution system operators (DSO) (e.g. [44]). Each spatial point is allocated to the closest HV node, assuming that this is located in the same network area or in

its subordinate grid area. This allocation via the closest distance within the grid areas produces the straight edges of the catchment areas in the following Figure 47. The uneven catchment area borders are the result of either the borders of larger (110 kV) grid areas or of borders of smaller medium voltage network areas which are not split up but are allocated as a whole to the HV node that is closest to them or is within their borders. Apart from this designation of the catchment areas to the HV nodes and in the exemplary distribution model shown in section 3.2.5 the subordinated networks of voltages less or equal to 110 kV are not investigated further in this project.

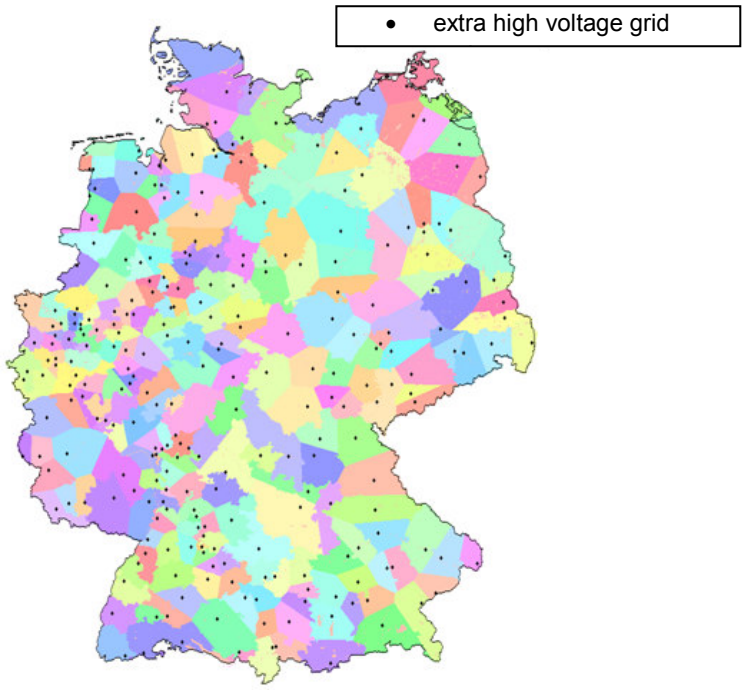

Figure 47: Modelled catchment areas of the HV nodes

Through the partly very large catchment areas, power feed-ins and consumption are balanced for each of the HV nodes. The high spatial resolution and level of detail of the scenario is therefore offset to a certain degree.

2.5.1.2 Time series production and evaluation

The power flows via the modelled HV grid are calculated with both the simplified power flow calculations according to Chapter 2.1 and with the complete power flow calculations according to section 3.2.2. An interesting evaluation of the power flows (calculated with the simplified power flow calculation) is illustrated in Figure 48.

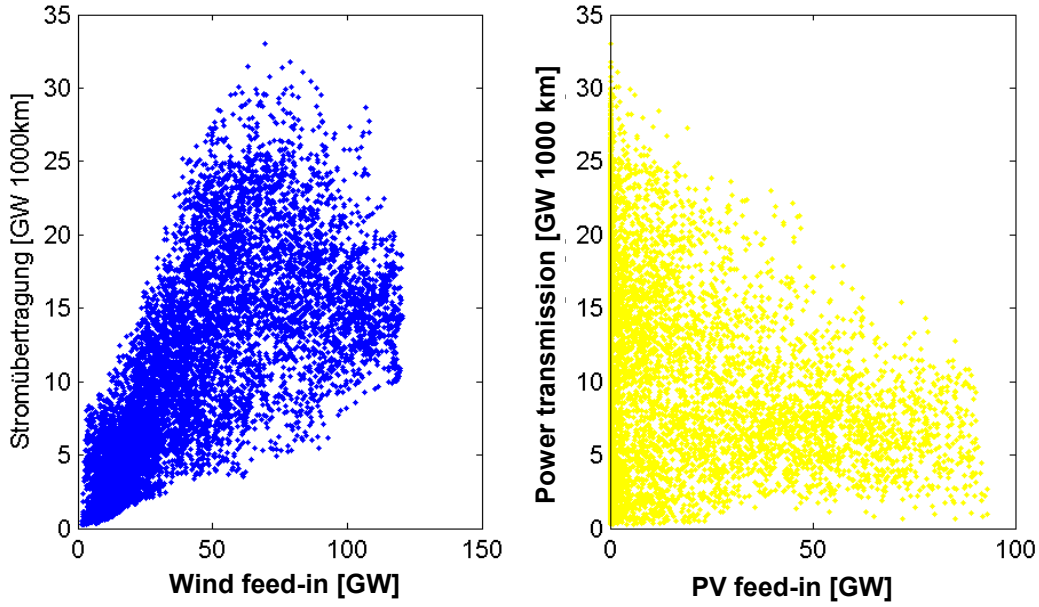

Figure 48: Simulated grid load dependent on wind and solar energy

As is illustrated in Figure 48, the grid load correlates strongly with the available wind production. The grid load is calculated as the product of transmitted power times the length of line totalled for all lines. As the bulk of this production takes place in the north and with the consumption mostly being located in the middle and the south this is well explainable. By contrast, this correlation cannot be observer for photovoltaics. Electricity from PV has to be transported regionally between rural regions and the urban load centres but not outside of the region. During high PV feed-in, even the trans-regional transport is reduced because the southern power demand is already met and the north German wind energy is used in the storages installed in the north.

The important role of DC lines becomes evident when the share in power transmission, again in GW times km, of DC and AC lines is compared. While only 23 % of the transmission grid, in GW times km, is laid out as DC route, these lines transport 45 % of all volumes transported.

2.6 Energy storages

Creating storage capacities is one of the most important and biggest challenges of the energy turnaround ("Energiewende"). As the bulk of power production depends on the weather, consumption however occurs even at times with little wind or sun. There must be means to store the power surpluses, which will be increasingly frequent in the future, when the weather is favourable, and release them when needed. A variety of different concepts for the storages of electrical energy exists. Depending on their "volume", i.e. their storage capacity, energy storages are either designed as long or short-term storages. Short time storages, such as batteries (see section 2.6.3), can only supply provide electricity for a few hours. This is used for instance, to level out the diurnal variations of PV installations and consumption. Long-term storages, such as the natural gas grid (see section 2.6.1), can serve to store power surpluses for weeks or months and release it when need for an extended period of time. Depending on their number, their nominal capacity and their grid connection level, similar to power producers, electric storages are differentiated. Central bulk electricity storages are pumped hydro storage (section2.6.2), compressed air reservoirs, and large power-to-gas installations. Decentralized small storage units are batteries, and small power-to-gas installations.

2.6.1 Power-to-gas

In times with high wind and solar feed-in, surpluses will arise in the future. These surpluses will possibly be needed several weeks or months later, when their feed-in is low. Such times with little wind or sun could last for several days or weeks and usually occur in winter (see Figure 44). Power surpluses due to more sun would arise in summer. Seasonal energy storages in Germany are currently limited to the transformation of surplus electricity into chemical energy carriers and the use of the existing natural gas grid. The natural gas grid has storages for natural gas with very high volumes that would be sufficient for storing future electricity surpluses. The total energetic capacity is 220 TWh_{th} and 65 TWh_{th} additional capacities from [6]. Hydrogen, obtained from water by electrolysis with renewable power surpluses, could be fed into the natural gas grid. However, hydrogen in the natural gas grid affects various materials negatively, leading to permeation and corrosion, increasing the ignition range and lowers the gas mixture's calorific value. Hydrogen has only about a third of its calorific value when compared to natural gas. For this and additional reasons the feed-in of hydrogen is limited to five volume percentages in current regulations [96]. However, technically there is the possibility of combining hydrogen with CO_2. The energy from renewable surpluses can be used to synthesize hydrogen and CO_2 into methane. From this synthesis, the natural gas substitute methane is produced, CH_4. This "renewable methane" or "RE-gas" together with bio-methane from bio-energy installations can be fed into the existing natural gas grid in unlimited amounts. The degree of efficiency of the conversion of surplus RE-power into methane ("power-to-gas") is set to 60 %, allowing for technological developments in the future. For conversion back into electricity, using methane power plants, the degree of efficiency is also set at 60 % (see section 2.4.6). The efficiency of the conversion chain of power to methane to power is therefore 36 % in the model.

2.6.1.1 Modelling spatial distribution

Determining the overall capacity of power-to-gas installations, investment costs of the plants, the volume of methane produced and the remaining quantities of curtailed electricity needs to be weighed. This is illustrated in Figure 49, where for different assumptions of available bio-methane the power-to-gas plant output is dimensioned. It is dimensioned in the way that the total methane usage by the methane power plants is met for the year. In the scenario, it is assumed that annually 26 TWh of bio-methane are available. This leads to a sensible trade-off between unused energy and installed power-to-gas plant capacity. The result is a surplus of almost 60 TWh per year and an installed power-to-gas capacity of 13 GW.

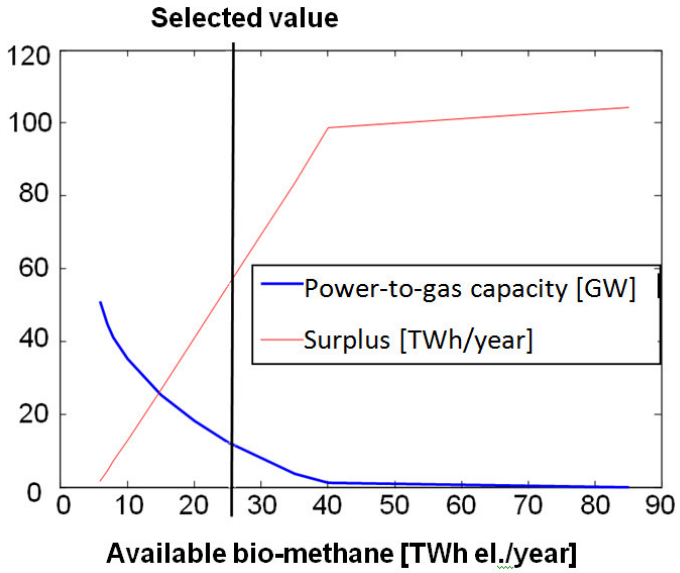

Figure 49: Required capacity of power-to-gas installations as function of bio-methane produced

The power-to-gas plants were positioned where wind and solar regional surpluses persisted after rebalancing renewable energies. The assumed total capacity was then distributed proportionately to the average annual surpluses at each location. This ensures a capacity utilization of the plants as high as possible without additional transport costs. The resulting regional distribution is shown in Figure 50.

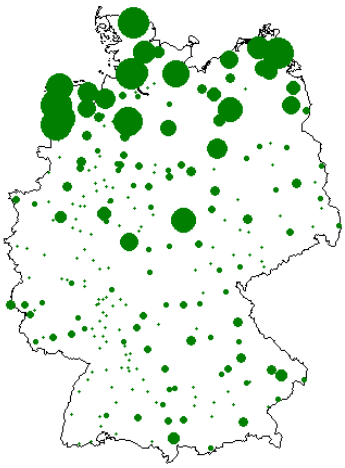

Figure 50: Regional distribution of the simulated power-to-gas installations

Most of the modelled power-to-gas installations are situated in the north, close to the large wind farms. The positioning reduces the need for transport to other areas in the south, especially at times of strong wind, when the transport grids are already working at maximum capacity with directly used wind energy. The influence of the geological potential for the erection of underground storage for the modelled power-to-gas plant locations was not taken into account in this project. Interestingly, in the area where the modelled large power-to-gas installations are located also subterranean saline reservoirs and salt domes are located. Their development as potential future gas storage is a possibility. In modelling the locations for power-to-gas installations the possible availability of CO_2, which is necessary for the process of producing methane, was not considered either. CO_2, emitted from methane power plants or from biogas installations could be used. Additionally other sources are possible, so that in the power-to-gas-to-power concept the storage and supply location of this seasonal storage system can be chosen freely – a huge advantage of this technology.

2.6.1.2 Time series production and evaluation

The utilization of power-to-gas installations was set using long-term unit commitment planning (see Chapter 2.1).

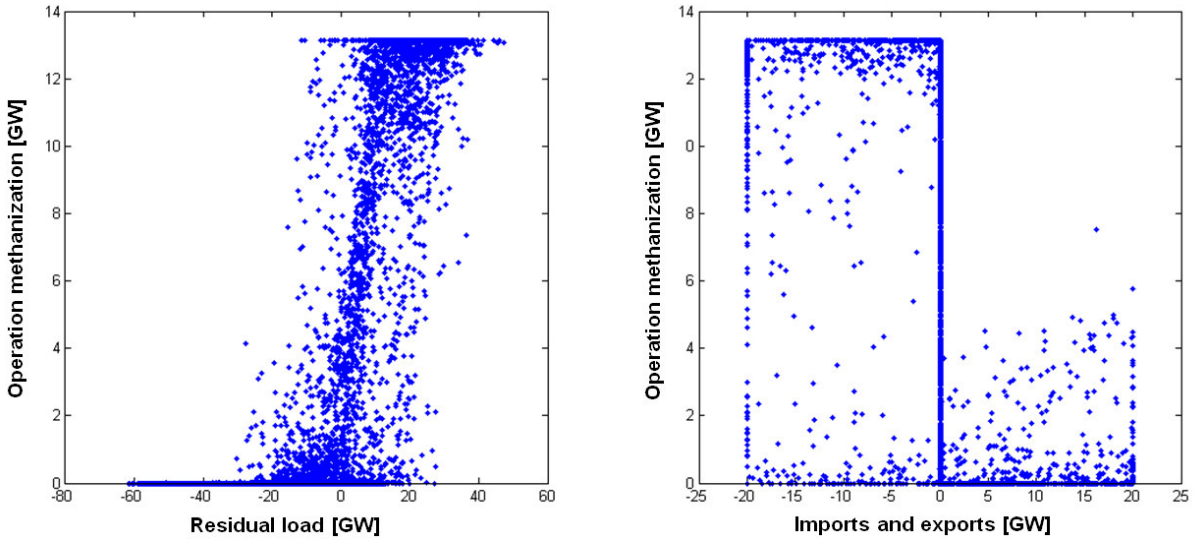

Figure 51: a) Simulated connection between methanization and residual load (left) and b) power import and export respectively (right) for every hour of the scenario-year and for all of Germany

The results shows that the power-to-gas installations are essentially operated at times when the residual load is positive, i.e. when the weather-dependent renewable production predominates (Figure 51 a). In the same way, the operation of the installations coincides with high power exports to other European countries (negative value in the Figure 51 b) since the surplus of electricity in the German grid can be reduced with by both measures.

2.6.2 Pumped hydro storage

Pumped hydro storage power plants pump water into a basin at a higher level and produce power by releasing the water, which then drives turbines and generators. Compared to other energy storages (apart from gas storages), pumped hydro storages can store relatively large amounts of energy, depending on the size of the basin and the height of the storage basin. To what extent pumped hydro storages can contribute to the future power supply depends also on the geographical conditions. While these are comparatively unfavourable in Germany, Norway, for instance, possesses

a considerable geographical potential for building pumped hydro storage power plants. For this project however, the Norwegian pumped hydro potential is not included since the feasibility of a 100 % renewable power supply for Germany based on German potential is studied.

2.6.2.1 Modelling spatial distribution

For the Kombikraftwerk 2 scenario, the pumped hydro storage plants existing in Germany and those planned for 2020 are determined. The installed capacity is 9.6 GW in total. In addition, pumped hydro storage power plants with an installed capacity of approximately 1.5 GW that are not located close to the German borders in Austria and Luxemburg are included in the scenario since they are directly connected to the German HV grid. In the scenario, there are is total of 39 pumped hydro storage power plants with a nominal generator capacity of 11.1 GW and a nominal pumping capacity of about 12.2 GW. The storage capacity of the pumped hydro storage power plants amounts to approximately 83.7 GWh. In addition, the scenario includes two compressed air energy storage plants in Niedersachsen and Sachsen-Anhalt with a nominal generator capacity of approximately 0.4 GW, a nominal pumping capacity of approximately 0.2 GW and a storage capacity of approximately 1 GWh. These plants are treated in the same way as pumped hydro storage power plants. The average storage efficiency is set at 75 %, which reflects possible efficiency gains through modernization.

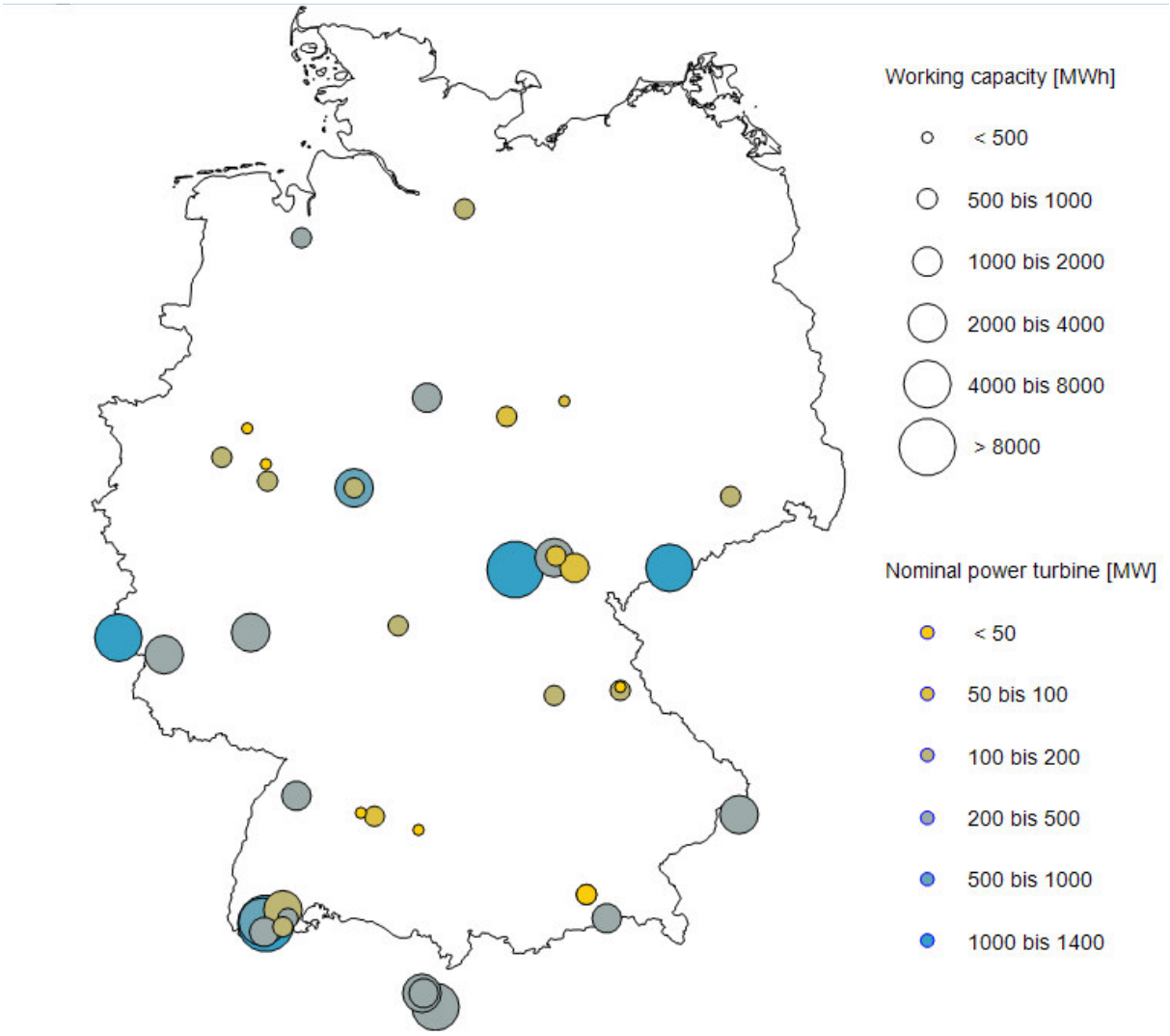

Figure 52: The pumped hydro storage power plants in the scenario

2.6.2.2 Time series production and evaluation

In Figure 53 the typical course of a day of a pumped hydro storage operation with the diurnal patterns of power consumption and the feed-in from photovoltaics is compared (for wind energy see Figure 28). Negative values of the pumped hydro storage line indicate energy feed-in and positive values electricity generation. On many days, the mid-day PV production is used to fill up the pumped hydro storage in order to balance the photovoltaic feed-in which disappears in the evening.

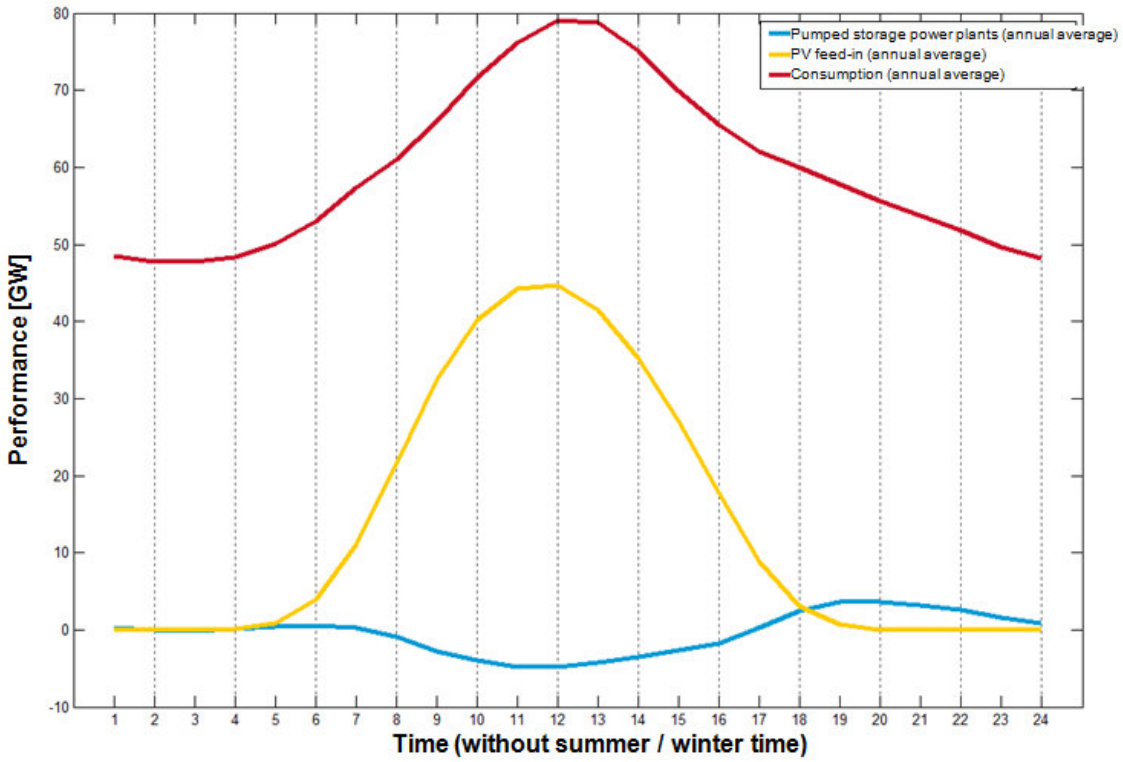

Figure 53: Average diurnal course of a pumped hydro storage operation, power consumption and photovoltaic feed-in

The operation of pumped hydro storage plants is shown in relation to the residual load in Figure 54 for each hour of the scenario-year and for all of Germany. There are four distinct areas. In case of a negative residual load, there is net power consumption. As can be expected this often coincides with positive values for the pumped hydro storage operation, when power production meets the demand and therefore seldom with the feed-in process (negative values of the pumped hydro storage operation). Contrarily, with a positive residual load leads to energy stored by the pumped hydro storage power plants. Despite this general finding, there are cases in the other two areas, which may be connected to spatial distribution and existing regional differences in consumption and production.

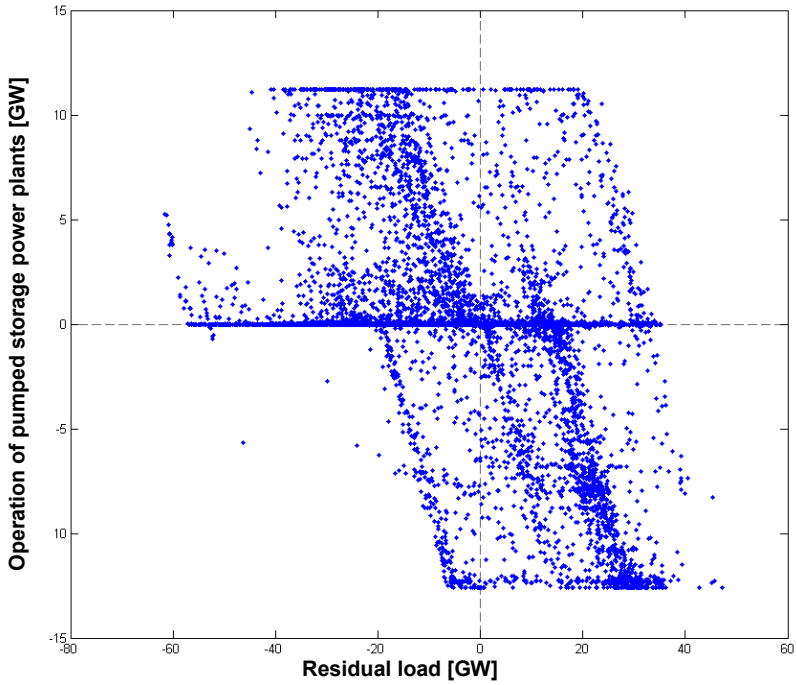

Figure 54: Simulated connection between the operation of pumped hydro storage power plants and residual load

Figure 55 illustrates the feed-in and feedback of daily energy quantities of pumped hydro storage in all of Germany.

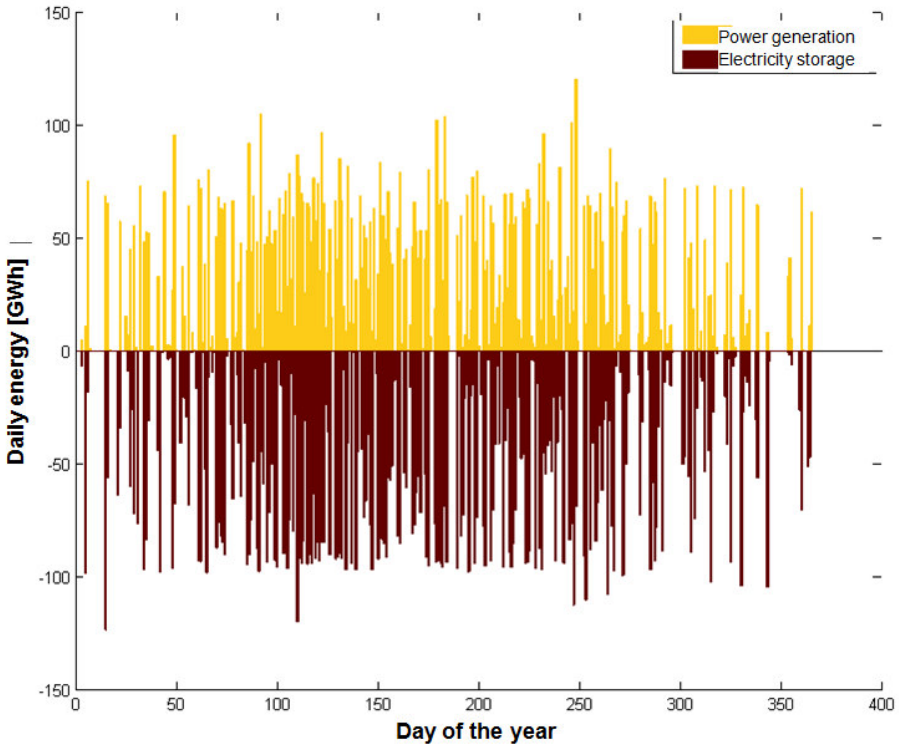

Figure 55: Simulated feed-in and feedback daily energy quantities of pumped hydro storage power plants

In summer, an increased activity of pumped hydro storage power plants is can be observed. Almost every feed-in and feedback balanced the solar feed-in. In winter the operation is less determined by this factor. This reinforces the assumption gained from studying the diurnal courses that pumped hydro storage power plants primarily help to evenly distribute the photovoltaic feed-in across the day. Furthermore, the data indicates that there are very few days in a year when no feed-in and feedback occurs. Only on 22 days (equal to 6 %) only feed-in occurs and on 44 days (12 %) there is only feedback. Most of the year pumped hydro storage power plants balance out fluctuations within a day.

2.6.3 Batteries

Decentralized battery storages can serve as buffer for energy volumes from the grid. This allows stabilising the production of solar energy, which depends on the weather and the time of day. Most owners of solar energy plants have electronic control devices that can optimize their self-consumption, using PV batteries. In the future, many PV plants will probably be linked to batteries, when battery systems are more economical since battery prices are likely to decrease.

2.6.3.1 Modelling and spatial distribution

For Kombikraftwerk 2 it is assumed that approximately 1/3 of all PV installations on houses will feature batteries. Together with a set storage capacity of 2 kWh per installed kilowatt of PV, a total of approximately 55 GWh of storage capacity results for the scenario. It is typical for batteries that the electric capacity and the energy storage capacity are firmly linked. A typical ratio of one between the two values is assumed, resulting in an installed battery capacity of 55 GW. The spatial distribution of batteries equals the spatial distribution of the PV installations on buildings (pitched and flat roof installations, façade installations). The cycle efficiency of the batteries is set to 85 %.

2.6.3.2 Time series production and evaluation

In the scenario, batteries are used to optimizing self-consumption of the PV installations. Thereafter they are not centrally optimized. For each network node, batteries are separately controlled to allow that self-consumption of the PV installations is maximized. The resulting time series for a chosen region and a distinctively interesting week is illustrated in Figure 56.

The batteries store the largest part of the local PV production during the day and meet the power demand for the evening and the night. The use is optimized locally, which allows keeping the network load by PV as low as possible. The red line shows the load/feedback from the network node after the use of batteries. For most of the week, only feedback (negative values) occurs.

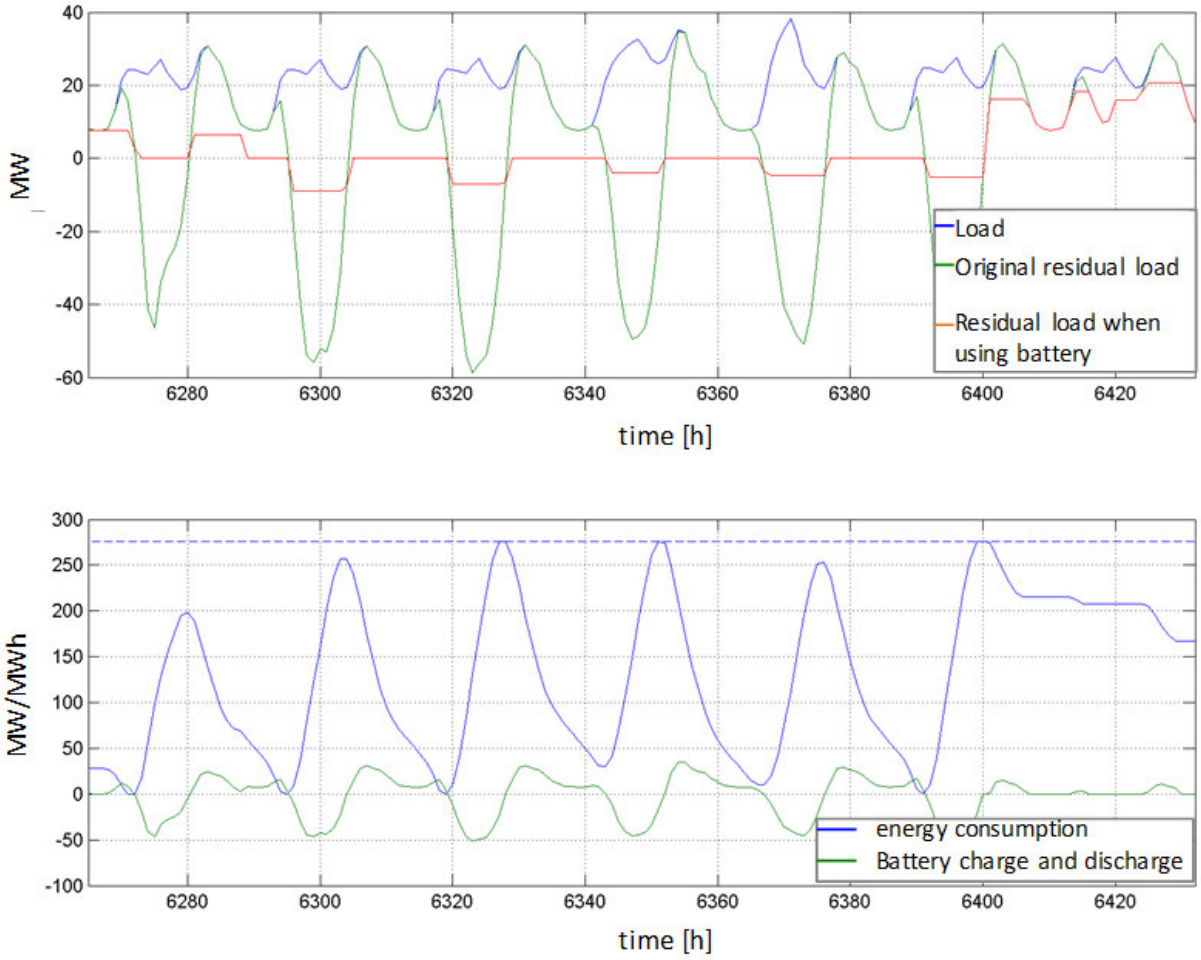

Figure 56: Example of a calculated battery usage plan for a HV network node with a regional PV penetration of household load of an annual average of 66 % and an associated battery capacity of 276 MWh

In the scenario, battery usage for all days of the year is shown in Figure 57.

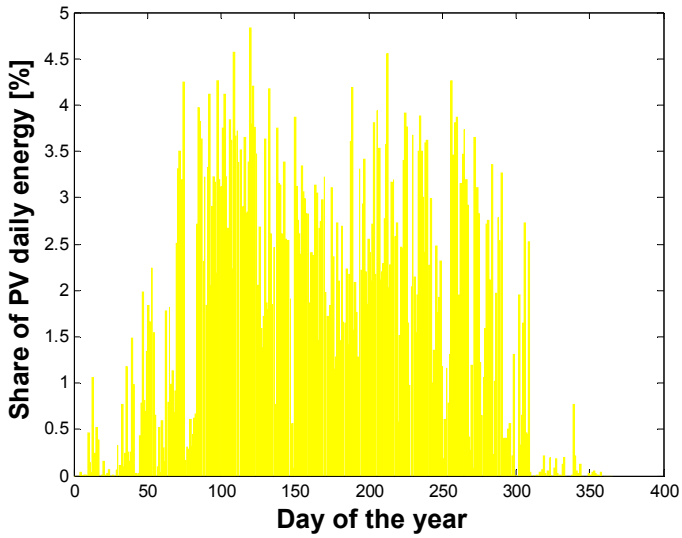

Figure 57: Share of PV daily energy fed into batteries

As the batteries in the scenario are optimized according to decentralized criteria, their total energy turnover (3 TWh per year) is clearly lower than that of pumping storage plants (15 TWh per year), despite the fact that both technologies have a comparable energy content. For instance, the existing PV feed-in during winter can usually be used locally so that storage with high losses is not necessary. This allows the conclusion the central control of local battery storages seems paramount. However, it is not used in this scenario.

Battery usage is simulated with regional network node time series. If the batteries were used completely de-centrally in households, the load profiles of individual households – with clearly greater fluctuations – would have to be taken as a basis. This calculation would increase the battery flow rate slightly. The total picture underutilized storages in winter months would sustain.

Depending on the ratio between the installed PV capacity and the local load, an increase of the own usage share of up to 30 % results as can be seen in Figure 58.

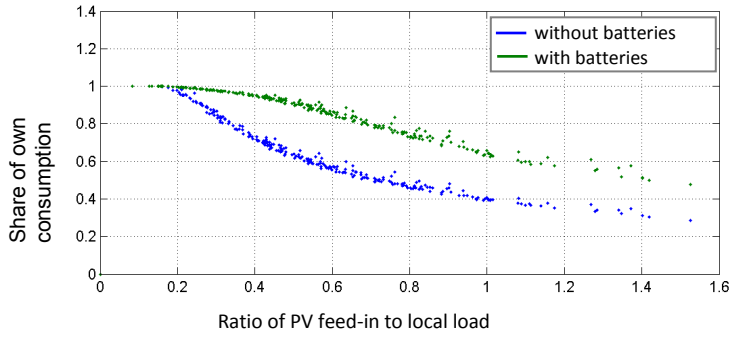

Figure 58: Simulated PV own usage with and without batteries in dependence on the local, energetic share of PV production in the load

2.6.4 Electricity imports and exports

The energy production scenario of Kombikraftwerk 2 is to investigate the possibility of a 100% renewable power supply from exclusively German energy sources. Treating Germany as an island without electrical connections to foreign countries is, however, not the reality and is not further investigated for the scenario. Energy imports and exports are modelled with an annual zero balance and additional limitations.

For the simulation of energy imports and exports to and from Germany, it is assumed that the rest of Europe, i.e., Europe without Germany, fully supplies itself from the renewable sources of sun and wind. Existing time series [46] for the European production potential of these two generation types and the European load curves are used to calculate the residual load for the rest of Europe. In the simulation, whenever the rest of Europe has a temporary energy surplus Germany can take advantage of it. Whenever there is additional demand in the rest of Europe, Germany can export its surplus energy. If this however is not the case, the rest of Europe cannot offer temporary support of the German energy market. This modelling ensures that energy is exchanged with foreign countries only if this is possible, assuming that all of Europe has a fully renewable power system. The use of import and export to the rest of Europe is planned within the cost-based planning simulation.

Imports are earlier on in the merit order and are therefore used more likely than biomass (i.e., for avoidance of biomass incineration but not for loading of storage), exports have lower priority than loading the internal German storage.

2.6.4.1 Modelling and spatial distribution

For the calculation of possible imports and exports, other European countries are simulated as point model. In the simulation, imports and exports from and to the German grid can take place via every existing interconnector with its respective nominal capacity. Network congestions in surrounding European countries are not taken into account. Furthermore, no new lines to foreign countries are planned. The total exchange capacity with foreign countries was limited to 20 GW in each time step.

2.6.4.2 Time series production and evaluation

An evaluation of daily import/export energies is illustrated in Figure 59. A seasonal trend cannot be identified. The exchange of electricity foremost depends on the weather conditions over a few days.

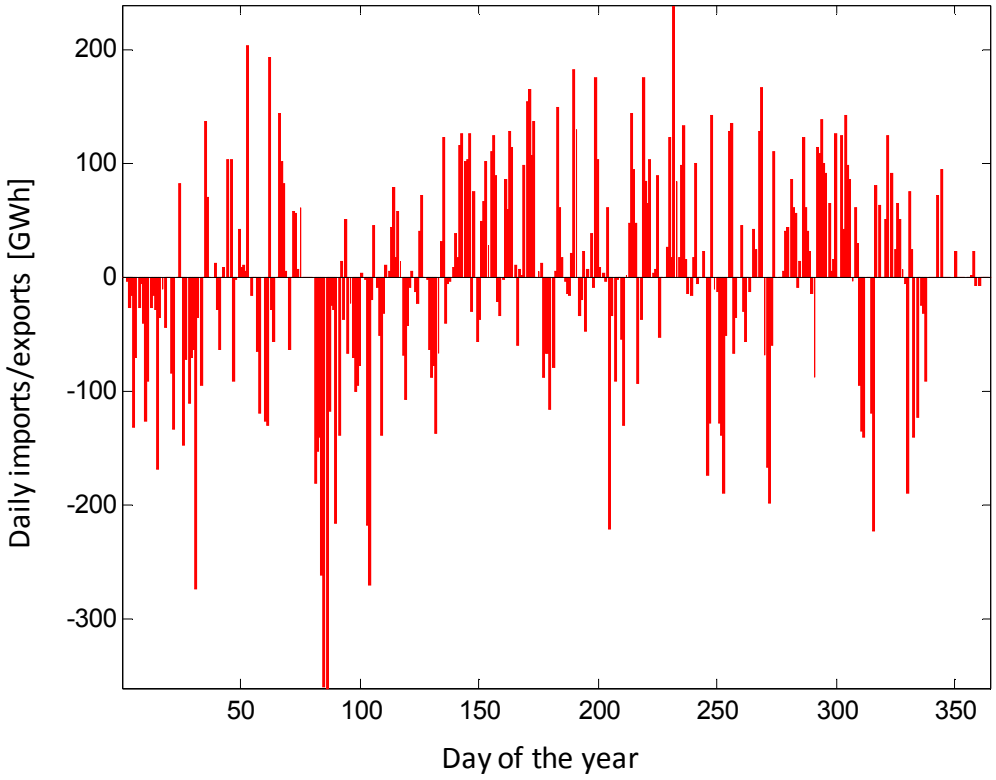

Figure 59: Simulated daily imports (positive) and exports (negative)

2.7 Conclusions and recommendations

For the subsequent investigations of power system stability, previous chapters described a consistent model for a future power supply for Germany purely from renewable sources.

The results of the simulated model suggest that a power supply based 100 % on renewable energies in Germany is possible, both energetically and in capacity. Using the modelled production and storage facilities and the simulated HV grid, power demand can be met anywhere and at any time.

The model developed for the study in hand is distinguished by a uniquely high degree of detail with regard to its spatial resolution and variety of technologies. The modelling techniques applied to master the high temporal and spatial resolution can be seen as innovative.

The modelled possible future power supply is distinctly different to the current one. The power supply has become significantly de-centralized; however, with regard to renewable energies the potential areas are far from being completely exhausted.

Especially the planned DC lines from [43] affect the modelled grid positively and enable the intelligent interaction of renewable generation, storages and back-up power plants using renewable methane. Power-to-gas plants and methane power plants are positioned in the model in a way that network loads are minimized. This favourable approach requires less re-dispatch and network expansion, which is not supported by the current network-independent energy market regulations. From a current point of view, the required storage size is certainly considerable. A realistic load management potential was considered in the model but on its own is not adequate for bringing production and consumption in line. Building energy storages for a 100 % renewable energy supply is clearly necessary. Therefore, it is recommended to further research and develop new storage technologies such as power-to-gas. The precise magnitude of future energy storages depends on a number of other parameters. The storage expansion and usage, network expansion, extent of re-dispatch measures and the use of curtailment of energy surpluses are interdependent Therefore, significant opportunities for influencing the structure of a purely renewable power supply scenario exist here.

The scale of weather-independent power producers set out in the report is partly adapted to the weather year studied and the studied/modelled power consumption. If extreme weather conditions and consumption occur, the scenario delivers an installed capacity from weather-independent producers for the maximum load (excluding storage and demand side management).

The modelled power supply functions by combining the various different elements (producers, storage, consumers, grid). To implement this interaction in real operation, a communication technology infrastructure and regulation concepts are necessary. Hence, the technical requirement to monitor even small decentralized installations and to control them as a Kombikraftwerk – a VPP – should be created.

3 Power system stability and ancillary services

The power system stability, also referred to as grid stability, requires that at any point of the network and at any time the voltage and frequency lie within a given narrow range. They have to be restored within a short specified period after faults or switching operations of grid infrastructure. On the lowest voltage level, the single-phase nominal value of voltage is the 230 volt, commonly known the household sockets. The extra high voltage level is 380,000 volt. The nominal value for the frequency on all levels and throughout Europe is 50 Hertz. Deviations from these values outside a very narrow operational band can lead to power failures or even damages to electrical appliances that are designed for certain tolerances. If the voltage, frequency and rotor angle stability is available in a system it can be safely said that power system stability is given. This is a common methodology ([47]) for a more detailed explanation of the concept of power system stability. It allows subdividing these three concepts further and explaining them. Simplified, power system stability can be illustrated by comparing the green sinus curve with the red dotted one in Figure 60.

In the first 20 ms the peak value of the red curve deviates from the nominal value û of the voltage level. Both too low and too high voltage amplitudes can violate the voltage stability criterion. It must be noted that voltage amplitudes can be different at different points of the grid. Voltage stability of a power grid exists only if the voltage amplitudes lie within the tolerance levels around the particular nominal value at all points of the grid. The frequency, however, is almost identical in the entire grid. An electricity supply system does not fulfil the criteria of frequency stability when its frequency deviates from the nominal value of 50 Hz by more than 200 mHz. The red curve in Figure 60 illustrates this deviation as the second curve of 20 ms has a shorter period duration.

The rotor angle stability is not investigated in detail in this project but briefly explained lower down. It exists when the rotor angles of the generators' rotors in the grid are sufficiently close to each other. During a fault, the difference of the rotor angle between a generator and the grid changes. Within a short period after a network fault, the difference in the angle should again lie within a specific range. If a loss of this synchronicity establishes, the criterion of rotor angle stability has been violated, as shown in Figure 60 in the last 20 ms section. Using the rotor angle stability to monitor power system stability was appropriate in the past as the bulk of power production took place in generators directly linked to the grid (synchronous generators). However, the share of generators directly linked to the grid will decrease significantly in future. The 100% renewable power supply of the Kombikraftwerk 2 scenario includes the synchronous generators of methane, bio-energy, pumped hydro storage, hydro and geothermic power plants for which rotor angle stability can continue to serve as a measure of stability. The large share of wind energy installations are linked directly to the grid but do not supply information on the rotor angle stability in the classical sense, since the double-fed induction generators (DFIGI) have different electric characteristics than synchronous generators. In contrast to today, a much larger share of power producers will be linked to the grid through power inverters. They have no longer a direct linked to the grid (PV, Batteries, and Power-to-Gas facilities will be linked by full power converters to the grid). Depending on the weather and the area under observation, the share of power producers not directly linked to the grid can amount up to 100 %, thus in the Kombikraftwerk 2 scenario, for instance, in the weather year studied, the power consumption of all of Germany is met by more than 91 % by PV on the sunny midday of 21 April. For power inverters rotor angle stability in the classical sense no longer applies.

Measurement of the widely controllable power inverters could be used to define a criterion for defining power system stability in a way that is comparable to rotor angle stability criterion. During the studies of the frequency stability in Kombikraftwerk 2 only the angular velocity was considered (see section 3.1.7). A comprehensive assessment of rotor angle stability with 100 % RE still needs extensive research and is not an object of Kombikraftwerk 2. In [84] for instance, the classical methods for studying angular stability and also suitable methods for inverter-dominated grids are investigated and improved.

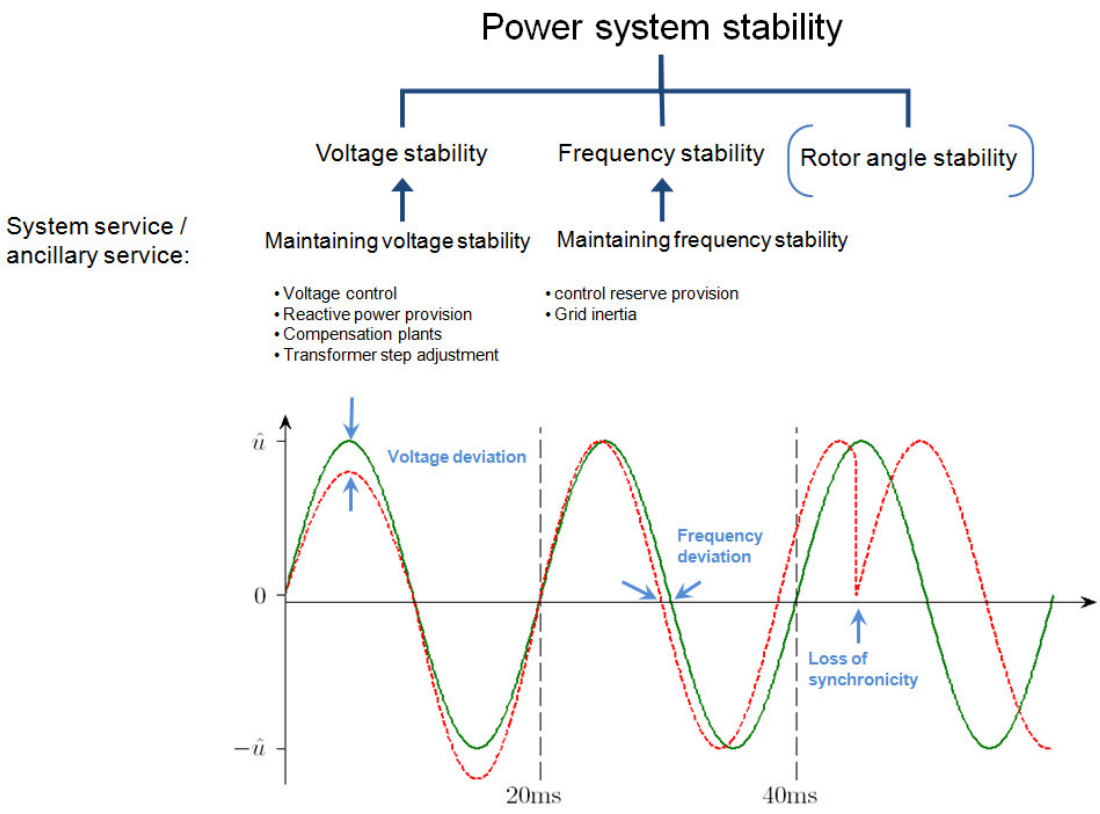

Figure 60: Explanations of the concept of grid stability

Ancillary services, also referred to as system services, maintain power system stability. According to their definition (e.g. according to [31]), ancillary services include maintaining frequency and voltage stability, the restoration of supply and system operations such as grid congestion management. The delivery of ancillary services is, according to the definition, a service of network operators using power generators. Sometimes is said that the services is provided by these power generation units directly when they are used for this. In Figure 60, possible measures for maintaining voltage and frequency stability are listed.

The scenario of a possible 100% renewable power supply compiled in Chapter 2 is examined below with regard to grid stability. The investigations include

- Control reserve for maintaining frequency stability (Chapter 3.1)
- Maintaining voltage stability and reactive power management (Chapter 3.2)
- Grid congestion management (Chapter 3.3)
- Restoration of supply (Chapter 3.4)

Apart from section 3.1.7, the investigations are limited to stationary or quasi-stationary analyses relating to events in the grid where it can be assumed that other rapidly changing events have no influence. Rapidly changing events, e.g. in milliseconds, so called transient or dynamic events, are also significant but are not dealt with in detail in this study. Among them is the behaviour during short-circuiting and voltage drops. In the grid codes ([31], [32], [58)]), the criterion that production plants have to meet to maintain power system stability are documented. In these documents one can find the requirements for their behaviour during transient faults such as the “fault-ride-through“. Short circuit power in the HV grid is not investigated in the modelled 100 % renewable power supply scenario. For this, the secondary voltage levels and the most remote edges of the European electricity network, the influence of the share of cabling, the degree of meshing, the spatial extent, switching statuses, neutral grounding, protection concepts and installation design (full power converters, DFIG, …) must be represented. A possible short circuit current flow with a 100 % renewable power supply represents yet another need for research.

3.1 Control reserve for maintaining frequency stability

This chapter contains several sections with various focus points that address the subject of control reserve (also referred to as operating reserve) by renewable energies in detail. After an introduction to current general conditions in section 3.1.1, in section 3.1.2 field tests on the delivery of control reserves with the RE installations with the Kombikraftwerk constructed for this project are described. The field tests and the concluding demonstration show the technical capabilities of delivering control reserve. The participation of RE installations in the control reserve markets is not part of the assessment. The assessment on this is shown in simulations in section 3.1.3 for selected types of installations. In section 3.1.4, feed-in forecasts for nine wind farms are calculated using two different methodologies. Potentials for the improvement of forecasts are pointed out, which would lead to a smaller control reserve requirement. Sections 3.1.5, 3.1.6 and 3.1.7 deal with the 100% RE scenario modelled in Chapter 2. In section 3.1.5, the control reserve requirement for the scenario is calculated. Subsequently, in section 3.1.6, meeting this requirement with the different power producers in the scenario is simulated. Section 3.1.7 considers the dynamic frequency stability of the 100% RE scenario and points out means of maintaining it.

3.1.1 Current framework conditions

Control reserves must be available to the grid in order to balance out frequency fluctuations caused by an unanticipated imbalance between consumption and production. This way the secure system operation can be guaranteed. Currently mainly large thermal power plants and pumped hydro storage deliver this ancillary service. The energy transition (“Energiewende”) changes not only the

power production but also the way control reserve is provided: Instead of individual large power plants, in future a varied system of renewable generators, storages and flexible backup power plants will be responsible for balancing the system. The purpose of using control reserves is to balance production and consumption and thus to maintain frequency. The geographical location of the delivery of the provision of control reserve is not important. Thus, for instance, a power plant in Spain could contribute physically to maintaining frequency in Germany.

The frequency of 50 Hertz in the European integrated network must be kept within a certain bandwidth (normally +/-0.2 Hertz) for the electricity supply system to remain stable. The frequency is not influenced as long as power production and consumption are in balance. Imbalances lead to frequency changes. An unplanned increase in consumption or the loss of generating capacity due to a breakdown will lead to a negative deviation from the nominal frequency. A tripping of an electric protection device could lead to an unplanned decrease in demand that leads to an increase in the frequency. In order to maintain the balance between production and consumption on short time scales, control reserve is kept available for this purpose. Control reserve may be positive or negative. Positive control reserve is additional dispatchable capacity, which causes an increase of the frequency, whereas negative control reserve results in a decrease in grid frequency.

Moreover, apart from the differentiation into positive control reserve to increase frequency and negative control reserve to decrease frequency, there are three different types of control reserve. They can be separated by their time constants. The transmission system operators, which are responsible for maintaining the frequency with in their control area, procure these three types of control reserve. They are called primary control reserve, secondary control reserve and tertiary control reserve [48].

Figure 61 depicts the temporal process of the three qualities of control reserve. During a frequency drop event in the network, e.g. due to a plant outage, the primary control reserve (primary control) is activated. This happens simultaneously throughout Europe in all power plants that deliver primary control reserve. Primary control is the fastest type of control reserve. It can be fully activated within 30 seconds.

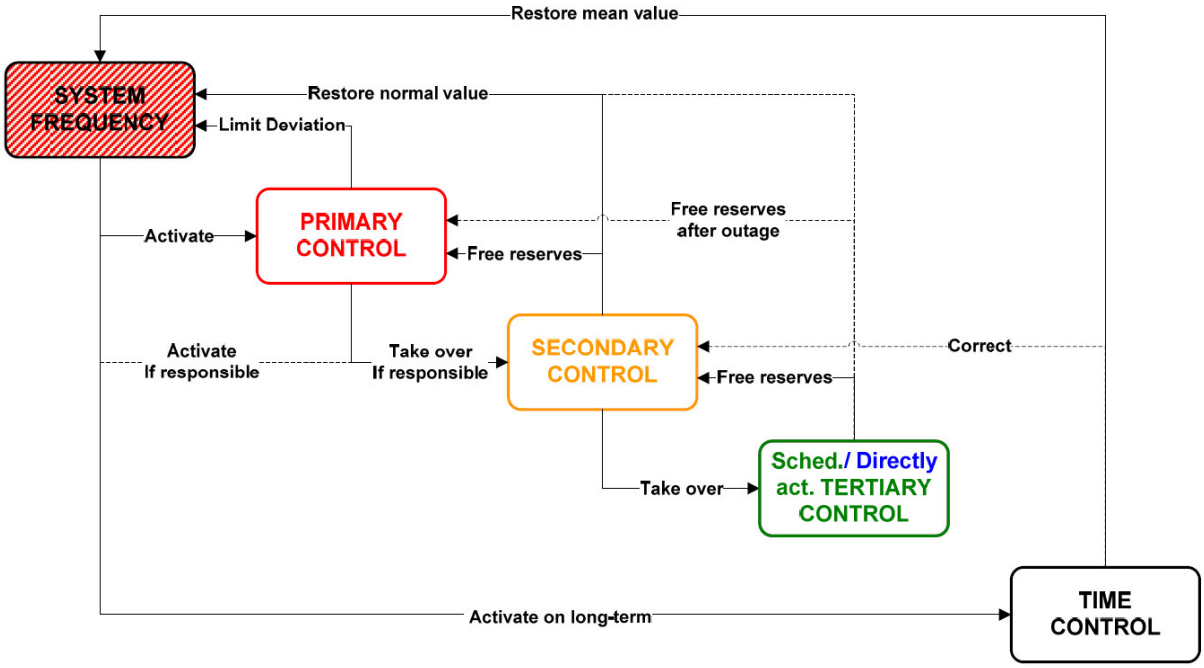

Figure 61: Temporal progress of the three qualities of control reserve [49]

Subsequently the secondary control reserve (secondary control) is activated, which has to be fully activated within five minutes. It has two functions. The first function is to release the primary control reserve and bring the frequency back to the target value of 50 Hertz. Secondly, it has to restore the planned power exchange on the interconnectors to neighbouring control areas back to target values. The last type of control reserve is the tertiary control reserve (in Germany often referred to as minute reserve). It has to be fully activated within 15 minutes and relieves the secondary control reserve in a control area, so it is available again.

Control reserve in Germany is procured through a tendering scheme; for all three product types separate tenders are executed. The control reserve tender is conducted jointly by all four transmission system operators on a common Internet platform (www.regelleistung.net). The tendered amount is determined every three months for the following three months, using the Graf-Haubrich method.

In Table 11, the most important characteristics of the three different types of control reserve are compared.

Table 11: Comparison of the three types of control reserve [85], [86], [87], [48], [88], [31], [77], [89])

	Primary control reserve	Secondary control reserve	Tertiary control reserve
Minimum offer	± 1 MW	5 MW	5 MW
Pooling	Yes, with control area.	Yes, with control area.	Yes, with control area.
Tendering period	1 week	1 week	Daily, except weekends and public holidays
Product length	1 week	High tariff (08:00 - 20:00 weekdays, otherwise low tariff)	6 daily blocks of 4 hours beginning at 00:00
Remuneration principles	capacity price	capacity and energy price	capacity and energy price
Auction criteria	lowest capacity price	lowest capacity price	lowest capacity price
Activation speed	30 seconds	5 minutes	7.5 to 15 minutes
Dispatch	De-centrally via frequency measurement	Signal from central network controller	Demand from TSO
Requested energy in 2011	-	1.600 GWh (pos.) and 4.500 GWh (neg.)	168 GWh (pos.) and 1.226 GWh (neg.)
Auctioned energy (4^{th} quarter 2012)	± 592 MW	2.109 MW (pos.) and 2.149 MW (neg.)	2.426 MW (pos.) and 2.413 MW (neg.)
Number of suppliers (4^{th} quarter 2012)	14	17	35

In order to offer control reserves, the market participants have to undergo successfully the pre-qualification procedure by the TSOs. Power plants have to prove that they are able to provide the contracted capacity within the time required for each product type.

Today most of the RE installations are technically capable of delivering control reserve. The possible power gradients of the weather-dependent RE installations are more than adequate; compared to the large power plants they are relatively small and can react quickly. In contrast to conventional sources however, the most important renewable energy sources sun and wind are not continually available. They are dependent on the natural resources. Weather-dependent RE can only supply control reserves when there is enough wind or solar irradiation. Additionally the controllable RE such as bio-energy and hydro energy are not depending on weather patterns. Weather-dependent RE installations can only provide positive control reserves if they have been curtailed in advance.

The power forecasts of wind and solar plants have been improved steadily over the last few years. This allows the short-term participation in the control reserve market (see section 3.1.8), given that the natural resource is available. They can therefore contribute to frequency control.

Currently neither wind energy nor photovoltaic plants deliver control reserve. The reason may be that there is no method for wind and photovoltaic installations to do this. Hence, in [60] a suggestion is developed for wind farms to deliver control reserve. This approach is also used in this project report. It is being tested on existing installations of a real VPP (see section 3.1.2). In these tests for the control reserve delivery, the suggestion of a verification procedure for control reserve delivery from [60] is implemented (see section 3.1.2.1). The suggestion of a bid procedure for control reserve delivery from wind farms from [60] is given in 3.1.2.1.

3.1.2 Field tests for delivery of control reserve

As part of the project, a VPP was formed including various RE installations in order to practically demonstrate the delivery of control reserves. The wind, solar and biogas installations were centrally controlled via a digital control centre of Fraunhofer IWES. The supervision and control was carried out in a set interval of 3 seconds. The description of the participating installations and their connection with the control centre, using communication technology, follows in section 3.1.2.2. The test processes and results are explained in section 3.1.2.3. The following section 3.1.2.1 shows the concept of control reserve provision and its novel methodology for proof of delivery, using the “available active power signal”. The new methodology improves the economics of a reserve provision and maximizes the electricity fed-in by wind and solar. The tests shown in this report are using this novel methodology.

3.1.2.1 The available active power signal as a prerequisite for the proof of control reserve dispatch

Two possible options for the proof of the delivery of RE control reserve are compared: the so-called “schedule” and “available active power” methods. The “schedule” methodology can take place via a previously announced schedule, which is sent to the transmission system operator (TSO) prior to generation (see Figure 62). The delivery of control reserve is proven when the difference between the schedule and the real generation equals the offered control reserve capacity. This is applicable for positive and negative control reserve. The feed-in of intermittent renewable energies can only be approximated. Using probabilistic forecasts allows announcing a schedule for the feed-in of fluctuating RE that is complying with the high degree of certainty required for the provision of control reserve. Probabilistic forecasts combine the forecasted power with a probability. The value that has a sufficient level of reliability will then be used as the schedule value. Maintaining the schedule value would require fluctuating RE to be curtailed to the probabilistic forecasted value. In Denmark and Great Britain, this system is already in use for the negative tertiary control reserve provision from wind farms ([61], [62]]) with the shortest-term forecast with a lead-time of one hour used, instead of the probabilistic forecast value. Evaluations for a 1 GW wind farm pool have shown though that deviations from this forecast of up to 15 % can occur in both directions. Single-valued expectancy forecasts should not be used for the schedules, as it might endanger the system security.

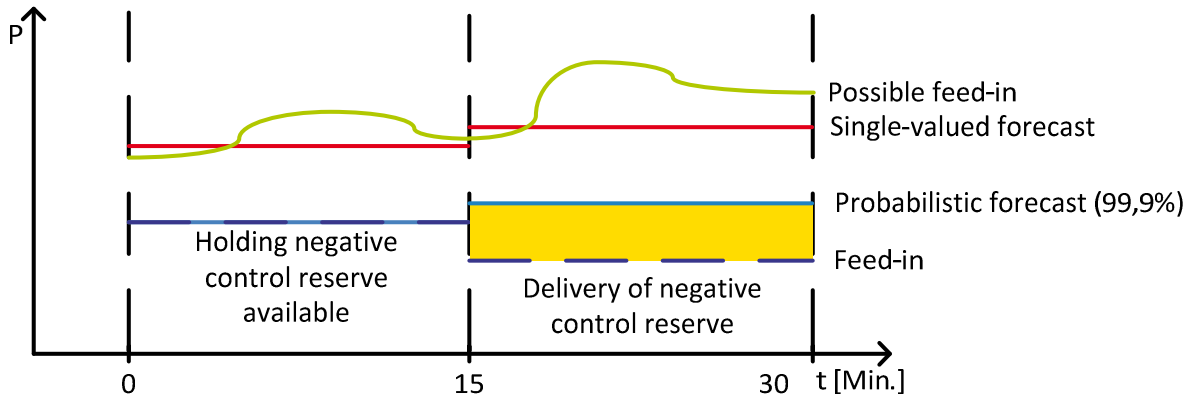

Figure 62: Illustration of the "schedule method"

Figure 63 clarifies the "schedule method" based on measurements from a wind farm [60]. In the illustration, the wind farm is down-regulated after 60 s from its very high feed-in level to the schedule level. It reaches this after approximately 15 s and keeps it very precisely. After approximately 210 s, 30 % of the installed capacity of the wind farm is dispatched as positive control reserve, which is a deviation from the schedule. The wind farm reaches this target value after approximately 10 s and, apart from initial overshooting, it adherers to it very precisely. A similar behaviour of the wind farm is shown when demanding negative control reserve after approximately 330 s. After approximately 450 s, the curtailment of the wind farm is relieved and it reaches its available active power. The possible feed-in of the wind farm during curtailment was not recorded or calculated and is represented in Figure 63 as the green broken line. The area named "wasted energy" between this "unknown available active power" and the recorded feed-in measured would have occurred the proof method "schedule" when delivering control reserve. It would have reduced the electricity provided to the grid.

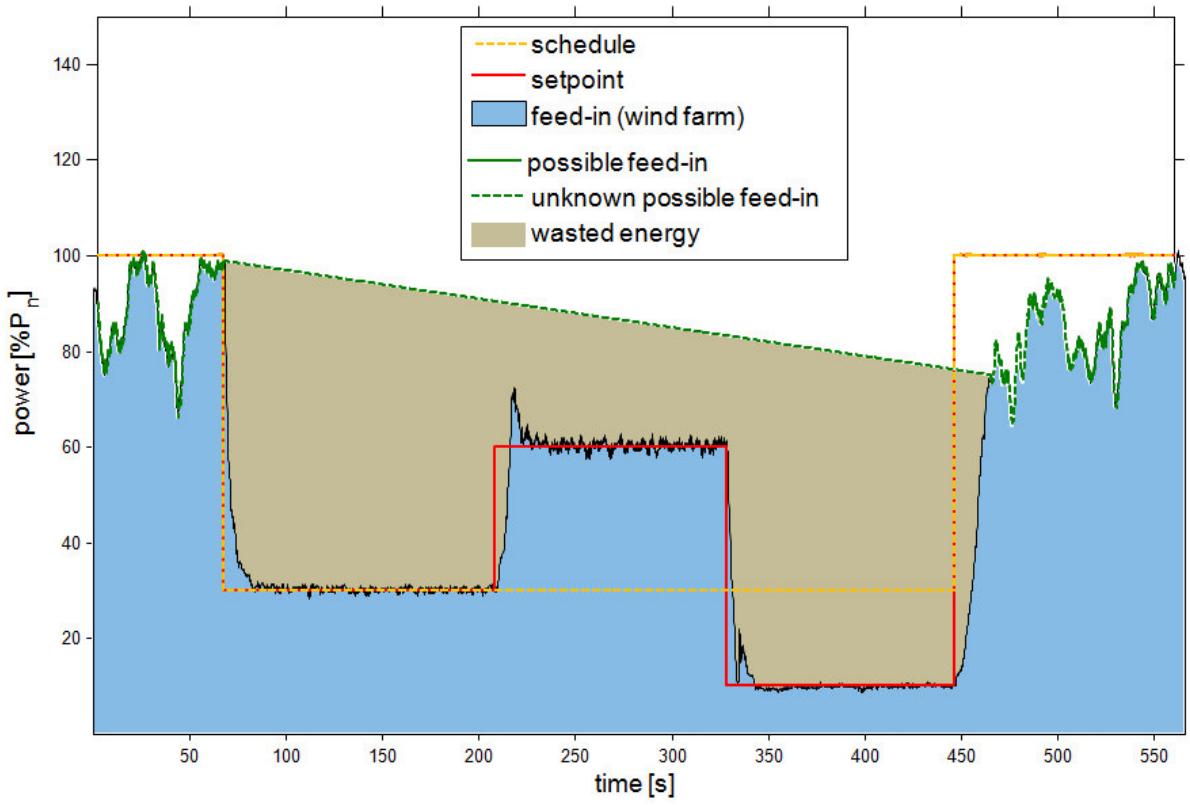

Figure 63: Control reserve delivery of a wind farm according to "schedule-method" [60]

The second option to prove the delivery of control reserve uses the so-called "available active power" signal. The available active power is the power the intermittent RE generators would have produced if they had not been curtailed. Delivery of control reserve is made in relation to the available active power by subtracting the dispatched control reserve from the available active power (negative control reserve) or by down-regulating the feed-in in relation to the available active power and lifting this curtailment by the amount of the dispatched positive control reserve (positive control reserve). The available active power is determined online.

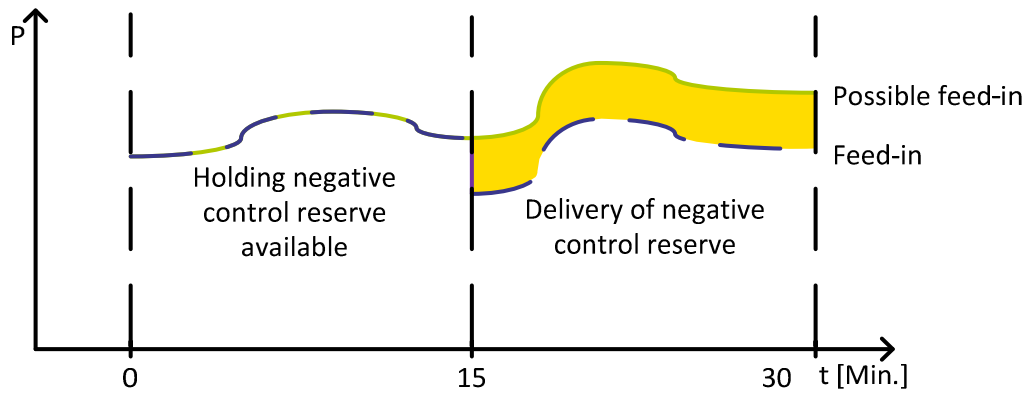

Figure 64: Illustration of the method "available active power"

The method “available active power” is tested in detail in section 3.1.2.

A criteria-based comparison was implemented in the project in order to identify which methodology is better for the entire system. The most important criteria to evaluate this are discussed in brief.

- Minimising energy losses: This criterion speaks against the “schedule” method, since large energy losses occur during curtailment to the schedule. Evaluations for 30GW of wind energy in Germany showed that losses amount to approximately 1 % of the nominal capacity.

- Security: Both methods are equally secure. It is prerequisite that the forecast error is taken into account when dimensioning the control reserve capacity for the “available active power” method. This is currently the case since the wind forecast error is not compensated on the level of the balancing areas. It is not relevant to system security whether the control reserve dispatch originates from non-fluctuating generators or by intermittent RE, using the available active power method. It is only important that energy is retrieved from the system (negative control reserve) or additionally fed into the system (positive control reserve).

- Cost effectiveness of suppliers: With the “available active power” method, lower cost-covering energy prices can be obtained, since energy losses that must be refinanced do not occur by complying with the schedule. Evaluations for 30GW of wind energy in Germany have shown that even in a large pool largely no cost-covering energy prices can be offered.

- Cost-effectiveness of the entire system: Three factors should be considered: First, the reduction in control reserve demand in the “schedule” method, caused by the compliance of weather-dependent RE with a schedule and thus not inducing a control reserve demand. Second, the production costs, which arise from balancing the energy losses. These arise from the curtailment with the “schedule” method. Third, the reduction in capacity and procurements costs for the TSOs if other operators are removed from the merit-order lists. Evaluations for 30GW of wind energy in Germany have shown that this criterion favours the “available active power” method.

- Technical feasibility: With the “available active power” method, the available active power must be determined online every three seconds (primary control reserve and secondary control reserve) or every minute (tertiary control reserve). Wake effects in the wind park increase the difficultly of the determination of the available active power signal. However, first evaluations lead to the assumption that available active power e.g. on wind farm level, can be determined with adequate accuracy [63] and thus this criterion does not speak against the “available active power” method.

- Equal market conditions for everyone: This criterion speaks for the “schedule” method because up to now operators also deliver control reserve in relation to a schedule.

Because of its benefits, the “available active power” method is used for the field tests in this section (3.1.2) and in the simulations for meeting demand in section 3.1.6.

3.1.2.2 Structure of VPP for control reserve delivery

The regenerative virtual power plant ("Kombikraftwerk") of the research project comprises a total of approximately 80 MW and consists of the following individual installations:

- Wind farm „Altes Lager" of ENERCON GmbH, Jüterborg (Brandenburg)

  18 turbines with a total of 37.2 MW output

- Wind farm „Feldheim" (Brandenburg) of energiequelle GmbH

  19 turbines with a total of 39.2 MW output

- Photovoltaics:

  12 photovoltaic plants in Kassel area, among them 9 installations on private residences and 3 photovoltaic large-scale plants with a total output of almost 1 MW

- Biogas plant "Wallerstädten" (Hesse)

  Output: 1.2 MW

- Biogas plant „Mittelstrimming" (Rhineland-Palatinate)

  Output: 0.5 MW distributed between 2 CHP with 0.2 and 0.3 MW

- Biogas plant „Zemmer" (Rhineland-Palatinate)

  Output: approximately 1.4 MW, of this 1 CHP with 889 kW and a satellite-CHP with 536 kW

- Biogas plant „Heilbachhof", Zweibrücken (Rhineland-Palatinate)

  Output: 0.5 MW distributed among 2 CHP with 250 MW each

Figure 65 shows the locations of the RE plants for the control reserve tests.

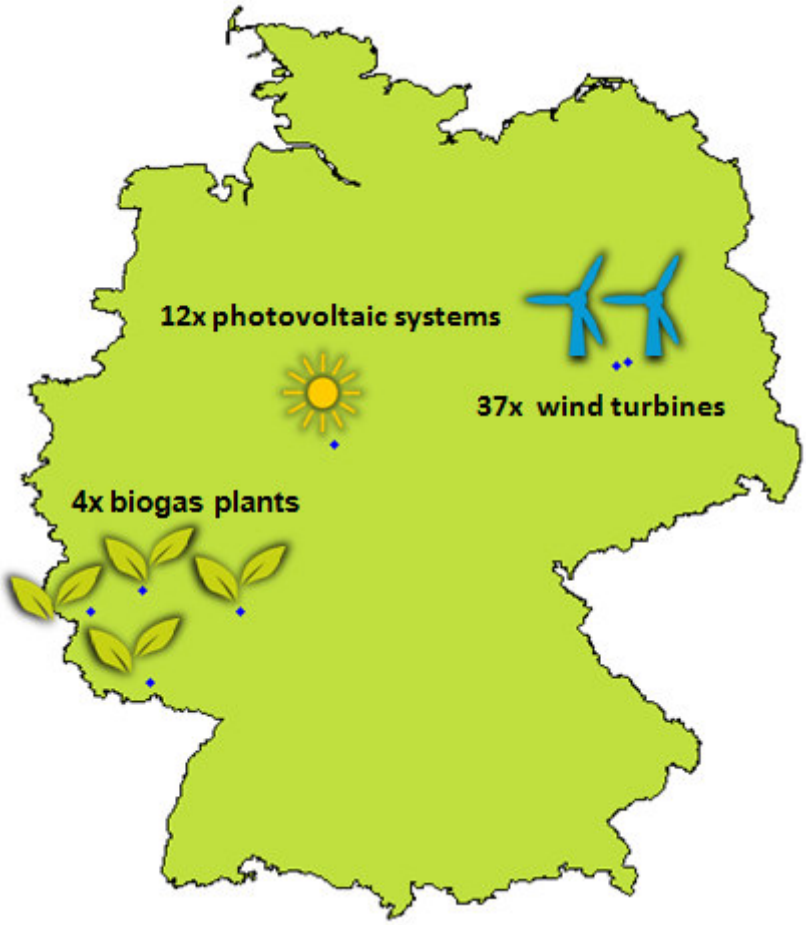

Figure 65: Locations of the RE plants for the control reserve tests

The plants have a high spatial dispersion, stretching the plant network over a large part of Germany. For the following study however, the locations are irrelevant as control reserve can be supplied independent of the location in the network. More significant for the study are the installed capacities of the individual plants and of the entire VPP. With a total output of approximately 80 MW, the delivery of the regenerative virtual power plant's control reserve cannot have a noticeable effect on network frequency as it depends on all the energy producers and consumers of the European integrated network. Influencing the network frequency through the virtual power plant (VPP), the 'Kombikraftwerk', is thus not the aim of these tests; the study focusses rather on the technical capabilities of the VPP to supply control reserve. The relationship between the installed capacities of the different plants shows a clear predomination of wind energy. Therefore, the shares are representative of a future power supply as it was the case in [1]. The relationship of the combined power generators to each other is clearly different from the scenario values in table 1. The composition of the VPP results from the plants that were available for the tests. Their use in the scientific study had to be authorized and organized by private operators. In addition, the test brought about unusual component load and generation loss (as during the test phases the plants were curtailed). However, decisive for the inclusion of RE plants into the VPP was not the operators' willingness to participate. The plants also had to possess the required technical facilities, which would make remote control via the VPP possible. Even if the following control reserve tests with the VPP are not representative in their composition for supplying control reserve in a future with a purely renewable power supply (see section 3.1.6 on this), they can demonstrate the technical

requirements and possibilities for renewable energies to participate in maintaining frequency stability.

It is a basic characteristic of a virtual or a VPP to encompass different, spatially distributed installations, which are regulated via a central control unit. For this, the generators must be linked to the control centre through communications technology. The control takes place via various communications protocols and must be encrypted following a security concept. In the control centre, various calculations are made (e.g. the set points for the plants), and active control measures and the reading of plant statuses is enabled via a user interface. Figure 66 shows the architecture of the VPP for the tests for the delivery of control reserve.

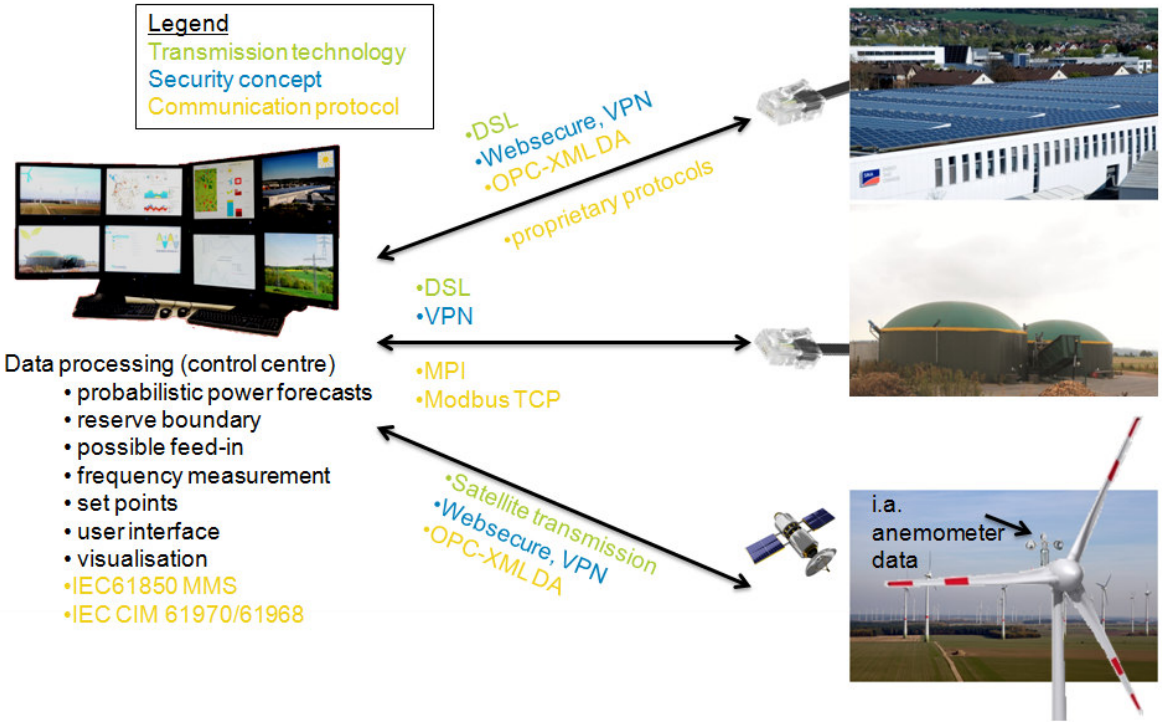

Figure 66: Structure of VPP for delivery of control reserve

The units of the VPP are linked to the control centre via various transmission technologies, using security concepts and communication protocols. Every individual type of plant had to be handled differently when connected to the control centre, which is very labour-intensive. Standardized communication technologies would have been more helpful and would simplify the structure of VPPs in future. At an interval faster than 3 s, the plants transmitted their current feed-in to the control centre in order to facilitate regulation in 3 second intervals. In the case of the wind energy plants, the data from the nacelle anemometers (enlarged in the diagram) were also transmitted. With these, the control centre calculates, according to [63], the available active power (see section 3.1.2.1) for the individual wind turbines on the basis of power curves compiled for each turbine on the basis of historical measurement data. The available active power from photovoltaic installations was transmitted directly to the control centre. For setting the available active power from the photovoltaic installations, the feed-in from several reference installations, which had not been curtailed, was measured. Based on these measurements, the available active power signal from near-by photovoltaic installations of the VPP can be estimated. In turns, only one reference plant was chosen to provide the value of the available active power signal.

The control centre also generates probabilistic feed-in forecasts for the following day. On this basis, the probability of weather-dependent RE plants feed-in a certain capacity with certainty can be calculated and the available capacity for control reserve for each individual plant determined. For the tests described below, a relatively wider control reserve band could be selected if high wind speeds or much sunlight was expected.

3.1.2.3 Test processes and results

The tests for control reserve delivery from the VPP uses the method based on available active power by the weather-dependent producers due to the advantages over the "schedule" method described in 3.1.2.1. Because of the continuously changing the set point, the process "available active power" places much higher demands on control speed and accuracy than the „schedule" method. Whether intermittent RE are able to deliver control reserve according to the "schedule" method, as conventional power producers do, is not investigated in this study. It is assumed that they can do so if they are able deliver control reserve according to the "available active power" method, as it is the more challenging one. An indication of the ability of a wind farm to deliver control reserve according to the "schedule method" is given in Figure 63 in section 3.1.2.1.

To investigate the technical abilities for delivering control reserve, the project tests were conducted with both individual plants and with the group of plants. In all test, a set point signal for control reserve was sent to the particular plants as can be seen in Figure 67.

The desired value signal is adapted from the pre-qualification procedure currently applied to conventional power plants in order to participate in the control reserve market in Germany. In Figure 67, this signal is depicted in standardized form for each generator. The control reserve delivery tests are divided into three phases. Before the start of the first phase, the control centre activated the individual plants in a standby mode for control reserve delivery. The plants reduce their feed-in to the level needed to deliver their full positive control reserve.

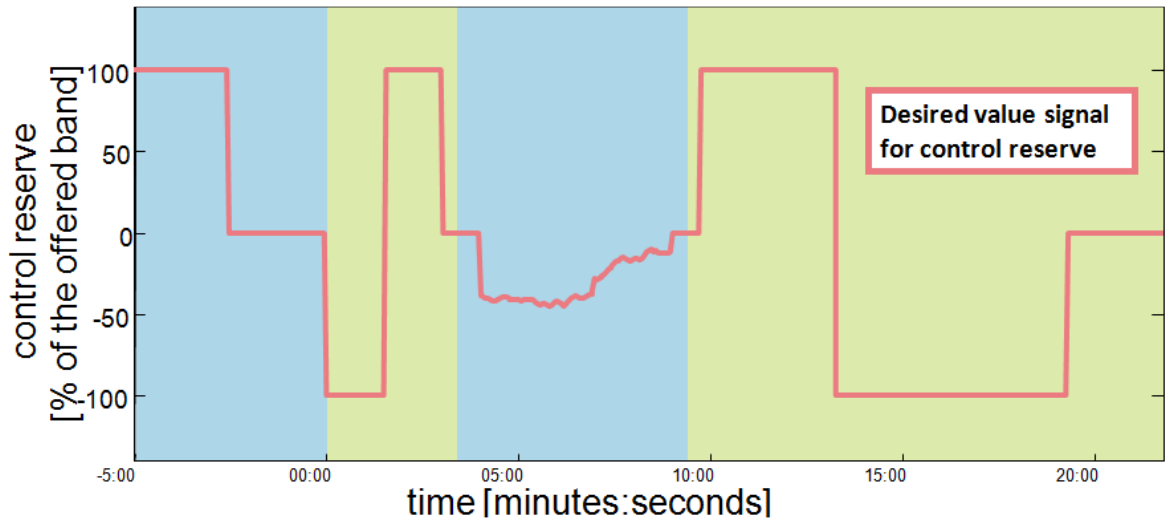

Figure 67: The three phases of the desired value signal for control reserve

The first phase begins with a call for the full activation of negative control reserve of the capacity band. It has to be fully activated for a minute and a half. Subsequently, also for a minute and a half, the full positive control reserve value is dispatched. The change in power output performed by the plants equals the sum of the negative and positive control reserve value. In the first testing phase, the response time of the plant and of the VPP for reaching the positive and negative control reserve is the focus. In the second testing phase, the delivery of control reserve is targeted towards the real network frequency measured during the test. This would be equal to the principles of delivering primary control reserve. The network frequency in this case is measured centrally by the control centre. A deviation from the 50 Hz network frequency triggers a proportional control reserve dispatch by the control centre. The amount of the negative or positive operating value depends on the extent of deviation from the network frequency of 50 Hz. The control of the VPP was configured for the tests such that with a deviation of at least ±0.05 Hz the full negative or positive control reserve is called. This may not reflect the parameters in [31], but it makes it possible that even in case of minimal frequency deviations the delivery of control reserve is visible. The third test phase is comparable to the first. The difference is in the sequence and duration of the positive and negative control reserve dispatch. The dispatch of positive control reserve is three and a half minutes in the positive and six minutes in the negative phase. In the third test phase, the ability of the plants and the VPP to maintain a constant level of control reserve delivery for a longer period is the focus of the study. The standardized dispatch signal was identical for all tests conducted, with the exception of the second test phase where the network frequency valid for the individual points in time was given.

Figure 68 illustrates the record of the control reserve tests, which was shown live to the public at the closing event of the project on 30/10/2013. Except for two biogas plants, all plants of the VPP took part at this demonstration.

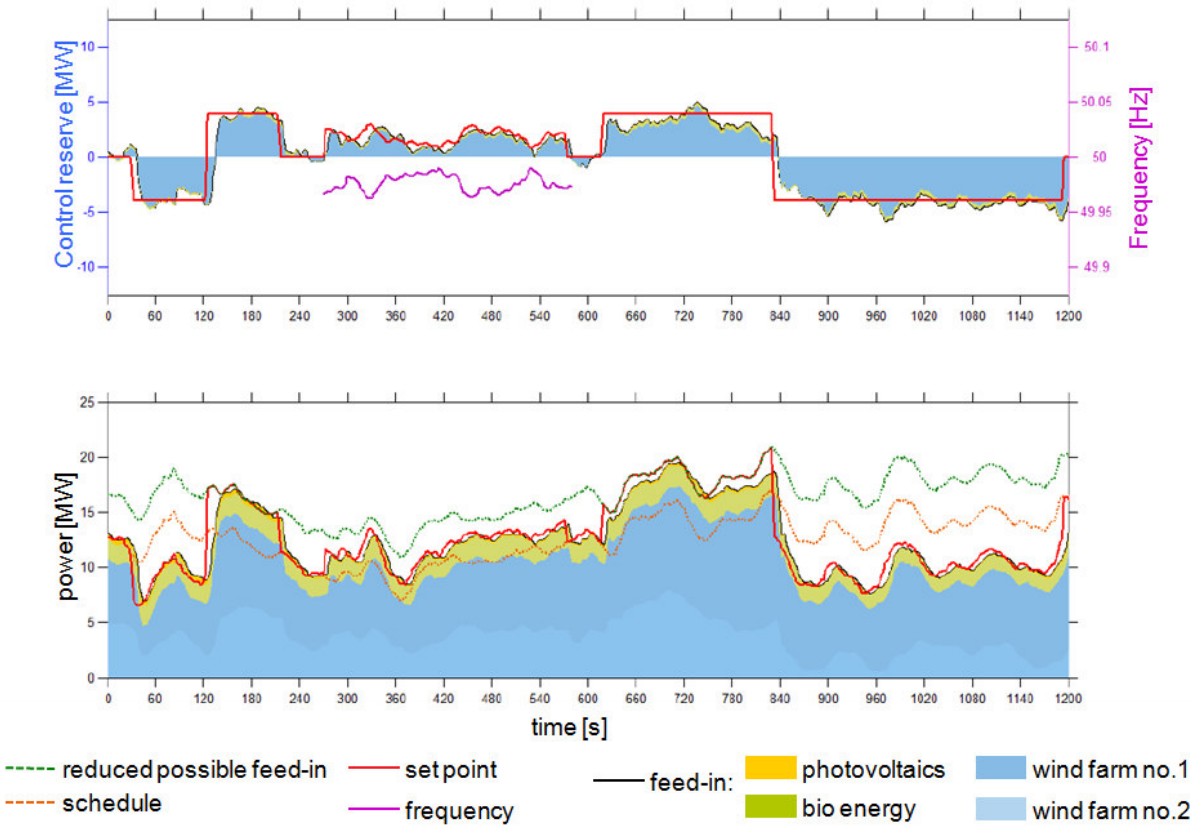

Figure 68: Record of demonstration of control reserve delivery by the VPP on 30/10/2013

In the top part of Figure 68 the delivery of control reserve is seen. The red line represents the desired value or set point signal for control reserve (cf. Figure 67). At the demonstration, the control reserve band covered the interval from -3,881 MW to 3,881 MW. The black line shows the delivery of the control reserve of the VPP. The delivery of control reserve approximates the set point signal but shows fluctuations around the plateau of the desired values and deviates some times more strongly from the set point. During the second test phase, the real deviation of the network frequency was continuously in the negative values, and the VPP exclusively delivered positive control reserve as a consequence.

The coloured areas reflect the different of the control reserve delivery by the individual types of RE. The blue area is clearly the largest, due to the large proportion of wind energy plants in the installed capacity of the VPP.

The lower part of Figure 68 does not reflect the control reserve but the active power values (actual feed-in) during the demonstration. The black line shows the feed-in of the VPP, the coloured areas below that the share of the individual types of RE. The weather conditions during the demonstration can be seen from although one has to take into consideration that the plants were running in curtailment mode. During the test, the possible feed-in of wind energy was approximately 12 to 25 % of its nominal capacity, which were not ideal wind conditions for the demonstration, as the wind turbines had to run in curtailment mode during the demonstration. This means that the wind feed-in had to be curtailed, e.g. in second 46 on average 6 % of their nominal capacity, with the danger of shutdown. In second 470, one turbine of the wind farm “Altes Lager” whose feed-in is shown in a slightly lighter blue in Figure 68, became inoperative, possibly for this reason, while by comparison, the turbines of the other wind farm “Feldheim” showed high feed-in at this point in time. The

curtailed turbine restarted only in second 895 and decreased the quality of the delivery of control reserve in the meantime. During the negative delivery of control reserve in the third testing phase, the feed-in from the wind farm “Altes Lager” lies at an average of approximately 5 % of its nominal capacity and at minimum of approximately 1.5 %. The feed-in of its individual turbines lies in part at even lower percentages of their nominal capacity. At such low feed-in levels it is very difficult to regulate the power output, especially as such low wind speeds tend to be very volatile. It seems improbable that wind farms would offer or even feed-in control reserve in future during such wind conditions. By comparison to wind energy, during the demonstration, the weather conditions were better for photovoltaics. During the demonstration, photovoltaics reached the maximum of its feed-in in second 186, with almost half of its installed capacity. Because of its small part in the installed capacity of the VPP, it is hardly visible in Figure 68.

The set point signal in the lower part of Figure 68, shown as a red line, is the feed-in that the VPP was set to follow. It is clear that the set points are not at a constant level, but changes dynamically over time. Despite the changing set point, the VPP was able to follow the set points relatively precisely (as can be seen when comparing the red and the black line), when disregarding a few deviations. It has to be noted that the feed-in follows the set points with a delay; the feed-in looks at many times like the delayed set point signal. This is caused by the time delay that the VPP needs to reach the set points. The deviations between the feed-in and the set point signal conform to those in the top part of the diagram with regard to their timing and dimensions.

The broken orange line reflects the so-called “real time schedule”. When deducted from the target values (red line), one gains the control reserve set points values in the upper part of the diagram. If it is subtracted from the feed-in (black line), the delivery of control reserve in the upper part of the diagram is obtained. During the demonstration, the real time schedule shown by the green dotted line is the “reduced calculated available active power” reduced by the full positive control reserve dispatch value.

This was calculated by the control centre for 3-second intervals and is the origin of the high dynamic of the feed-in control. The calculation of the originally uncurtailed available active power was carried out for the wind energy plants, using methods from [60]. This occasionally leads to an overestimation of the real maximum available active power from wind energy plants. To ensure that the full positive control reserve can be dispatched in spite of a possible overestimation, the available active power signal was reduced by a constant value of 7 % for the demonstration. The nominal capacity and so the “reduced available active power” was calculated subsequently.

In order to check investigate the accuracy of the VPP's delivery of control reserve, larger deviations from the control reserve set points are examined below:

1. Response time of delivery of control reserve

   The VPP cannot immediately deliver the instantaneously called positive and negative control reserve levels of testing phases 1 and 3. A certain reaction time is needed; also the technically feasible power gradients are limited, despite the fact that RE installations can react significantly faster than conventional large power plants. For the evaluation of the response time for the delivery of control reserves, different test periods of various measurement parameters were subsequently interpolated to every even second. This also explains the almost imperceptible increase and decrease of the control reserve set point signal in Figure 68, which was sent at 3 second intervals and changes abruptly in test phases 1 and 3. The interpolation facilitates the comparison of the various measurement values but also brings about that the subsequent data are only accurate to the second. Table 12 shows the key data for the response time evaluation of the delivery of the VPP's control reserves, which are clarified in Figure 69.

Table 12: Evaluation of response time of control reserve delivery

	Number of the target value step	1	2	3	4	5
1	Second of target value step	32	126	216	619	834
2	Second of first reaction, starting to approach the target value	35	126	217	621	834
3	Second of end of approaching the target value	42	142	225	628	841
4	Time delay to first reaction [s]	3	0	1	2	0
5	Duration of approach to target value	7	16	8	7	7
6	Exceeded performance at approach to target value [MW]	-3,93	7,78	-2,65	2,98	-4,35
7	Performance gradient [MW/s]	-0,56	0,49	-0,33	0,43	-0,62
8	Maximum performance gradient occurred [MW/s]	-0,78	0,72	-0,67	0,71	-1,17
9	Amount of quotient out of 3.881 MW to performance gradient	6,91	7,98	11,70	9,11	6,25

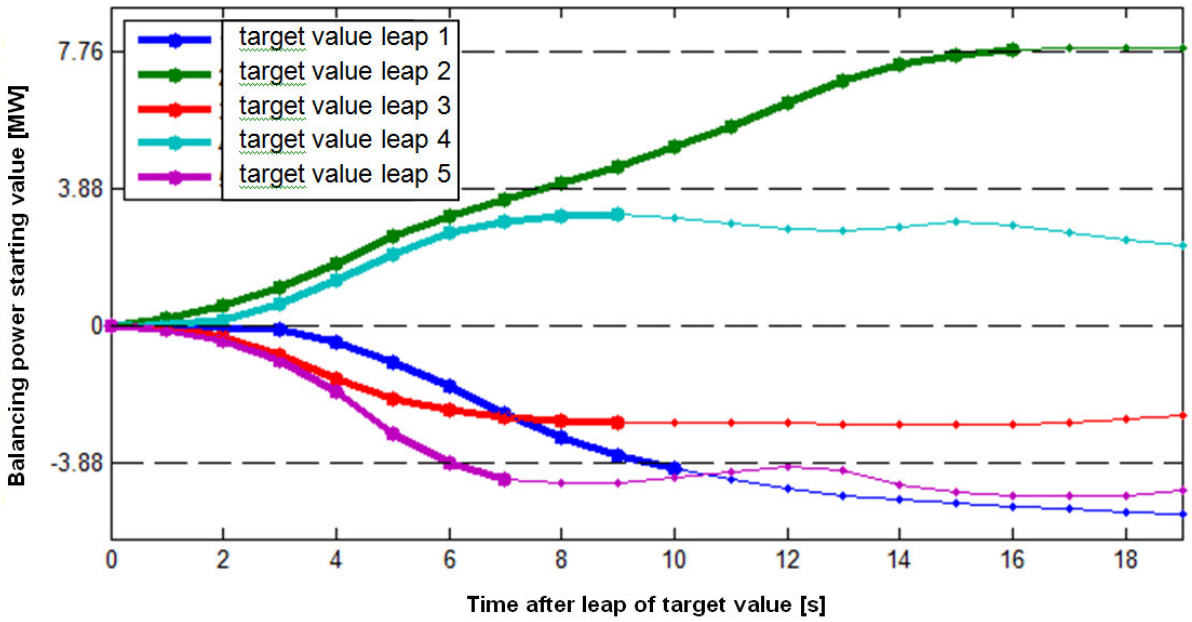

Figure 69: Approach of control reserve delivered to reference value plateau

In the first line of table 12, the times after the beginning of the demonstration are recorded to which a new control reserve reference value plateau was given. The second line specifies the seconds the feed-in from the VPP shows a first change towards the new the set point, thus does not feed in in the opposite direction or remain on the same level. A reason for the occurring time delay could be the duration of data transfer and the duration of calculations. For instance, the wind speed-readings must be transmitted to the control centre by the wind energy plants. As they cannot be acquired simultaneously from all wind turbines, the control centre has to wait for the necessary data. Only then, the available active power can be calculated, which are the basis for the set points for the wind energy plants. Another reason for the time delay could also be the short-term weather changes, which may work against the desired feed-in performance. A strong and sudden increase in wind speed, such a as wind gust, may be disadvantageous for a fast reduction in wind energy feed-in. In the third line of table 12, the times are noted at which the VPP either exceeds the demanded control reserve level for the first time, moves away from it or no longer approaches it. Lines 4 and 5 result from the difference between line 2 and 1 or 3 and 2. Line 6 displays the exceeded performance between the times from line and 3. Line 7 reflects the performance gradient in MW/s resulting from dividing the values from line 6 by the values of line 5. These performance gradients shall not be interpreted as maximum performance gradients of the VPP as the relevant time intervals also include times with the slow matching with the target value plateau. The maximum power gradients from one second to the next during the approach are recorded in line 8. As the VPP's control reserve delivery either does not reach or exceed the control reserve reference value plateau, the duration is calculated in purely mathematical terms in line 9. It is the time that the VPP would need to reach the control reserve reference value of ±3,881 MW exactly. This is assuming the same behaviour as in the previous line.

According to this, the VPP would need an average of 8.39 s to reach the control reserve reference value of ±3,881 MW. This, and the other values in table 12, are only valid for the

demonstration conducted and cannot be transferred uniformly to other weather situations or control reserve reference values.

The response time of the control reserve delivered by the VPP is sufficient for today's requirements as it lies clearly below the 30 s (see table 12) that are currently required for primary control reserve. Even higher control speeds can be expected when RE plants do not receive the reference values for the delivery of control reserve from a control centre but can compile it themselves (perhaps for primary control reserve performance). The same applies to calculating the available active power. Communication via DSL would also increase the control speeds. Faster reactions by the VPP installations would give better results in the second test phase too, as here the time delay is mainly due to the control centre's data collection and calculations. If individual plants were to measure the network frequency themselves and feed in according to a power-frequency-relation, fewer deviations could result. The advantage of the control centre measuring grid frequency is that only one frequency meter need be purchased.

2. Accuracy in adherence to constant control reserve reference values

Figure 70 shows the four control reserve plateaus of the control reserve reference value signal of four equally large images. The position of the four images during the tests is shown in the small image at the bottom. The starting times of the four images relate to the times from line 3 for the target value steps 1, 2, 4 and 5 in table 12. The dotted lines indicate bands around the control reserve reference values (black line), so-called tolerance bands. The distances of the bands from the reference value amount to multiples of 10 % of the reference value.

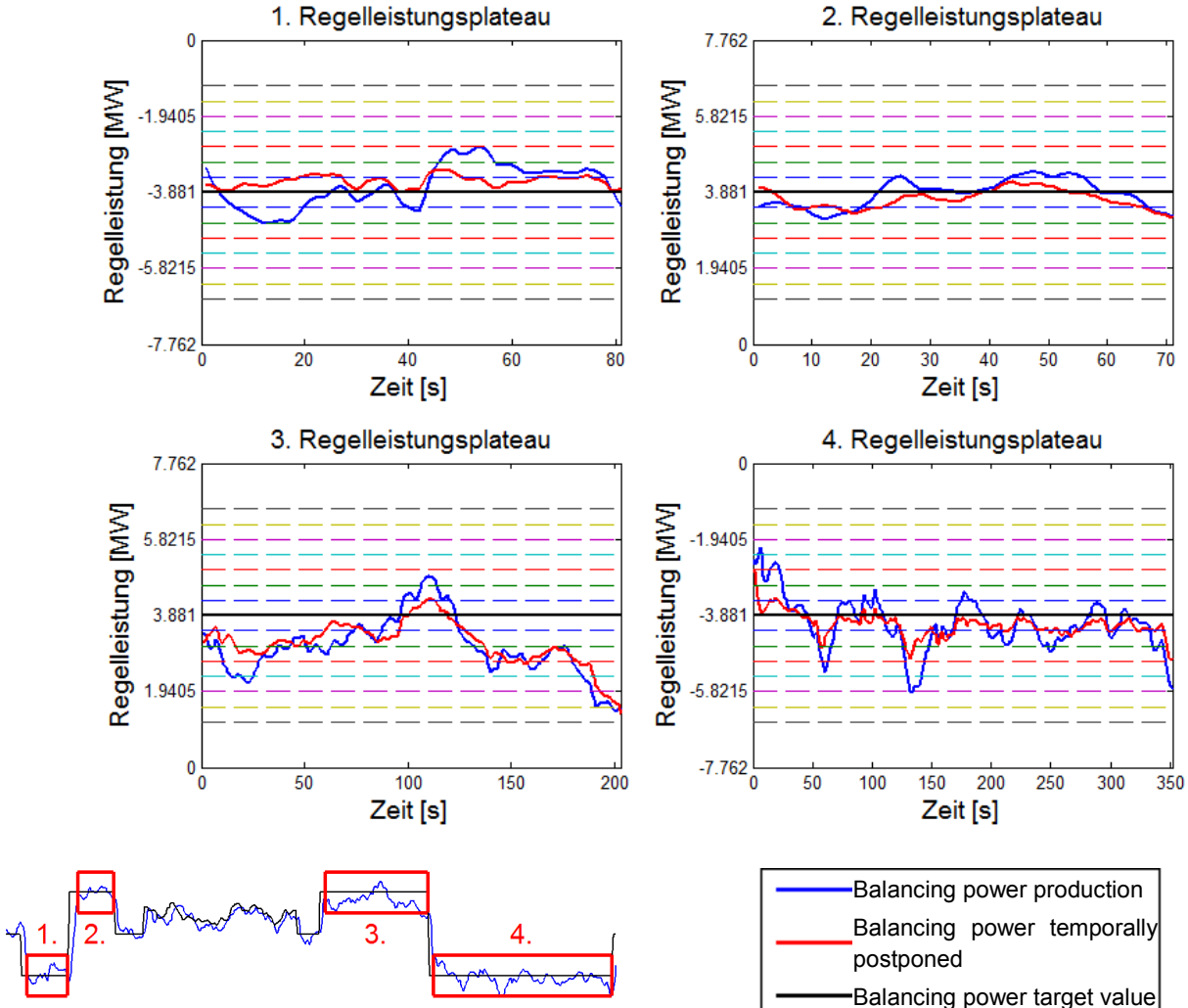

Figure 70: Accuracy in adherence to constant control reserve reference values

The control reserve of the VPP is shown as a blue curve in all illustrations. It is clear that the control reserve fluctuates around the target values (black line). The deviations are different for the various plateaus. While the deviations lie within the 30% tolerance band for the first two plateaus, and most of the time remain even in the 20% tolerance band, the deviations on plateau 3 and 4 are more pronounced. For plateau 3, the deviations are mostly negative. The cause of these deviations is due to an overestimation of the available active power in spite of the previously mentioned reduction of the signal. As can be seen in Figure 68 at the beginning of the third test phase, the wind energy plants are not able to increase the feed-in up to the target value. The wind speeds available were too low for this. For a more accurate feed-in of positive control reserve, either the available active power should have been calculated more accurately or its subsequent reduction should have been set higher. Both of these measures need to be studied further, which exceeds the scope of this study. The cause for the high deviations on the fourth control reserve plateau could be the above-mentioned very low wind speeds in one of the wind farms and the resulting reduced controllability of the wind energy plant in

these conditions. The VPP's reaction speed also influences all deviations shown in Figure 70; this is partially because the VPP's set pints could only be achieved with a time delay. To illustrate this influence and to emphasize the ability to maintain constant control reserve values, for the red lines in Figure 70, the reaction time of the VPP was mathematically reduced. This was achieved by shifting the VPP's feed-in by 6 s. As a result, the deviations have fewer peaks and are generally smoother.

According to today's requirements, the accuracy of the control reserve delivery by the VPP is not sufficiently adequate. Currently, an excessive over-production of a maximum of 10 % of the control reserve reference values is permitted for secondary control reserves, and 20 % for primary control reserve and tertiary control reserve. However, it should be investigated whether this stringent requirement for frequency stability in the power supply is necessary or whether it could be adjusted for the possible delivery of control reserve from weather-dependent RE. It should be borne in mind that deviations of seconds from the control reserve reference value would not cancel each other out stochastically between weather-dependent RE installations or other power plants. An increase in accuracy could be achieved by faster reaction times, increased precision of the calculation of the available active power signal, and an additional reduction of available active power and a (mathematical) smoothing of available active power.

The following illustrations show the recording of control reserve tests conducted with individual RE installations via control by the control centre.

Figure 71 shows the test result of a wind farm with higher wind speeds compared to Figure 68. Based on previous accuracy analyses, the available active power signal was reduced by 6 % of the nominal capacity. During the test, this meant that nominal capacity was not overestimated at any point in time. The wind farm did not only reach the target values for delivering positive control reserve but over-delivered, which was caused by the calculation methods used for issuing the set point. For the evaluation of speed and accuracy of the delivery of control reserve, a tolerance band is drawn in the top illustration of Figure 71, which includes the area of 30 s after a control reserve set point step and an area of 10 % over-delivery of control reserve reference values. The control reserve delivery is within the tolerance band regarding the response time and partly is beyond the tolerance band regarding the accuracy.

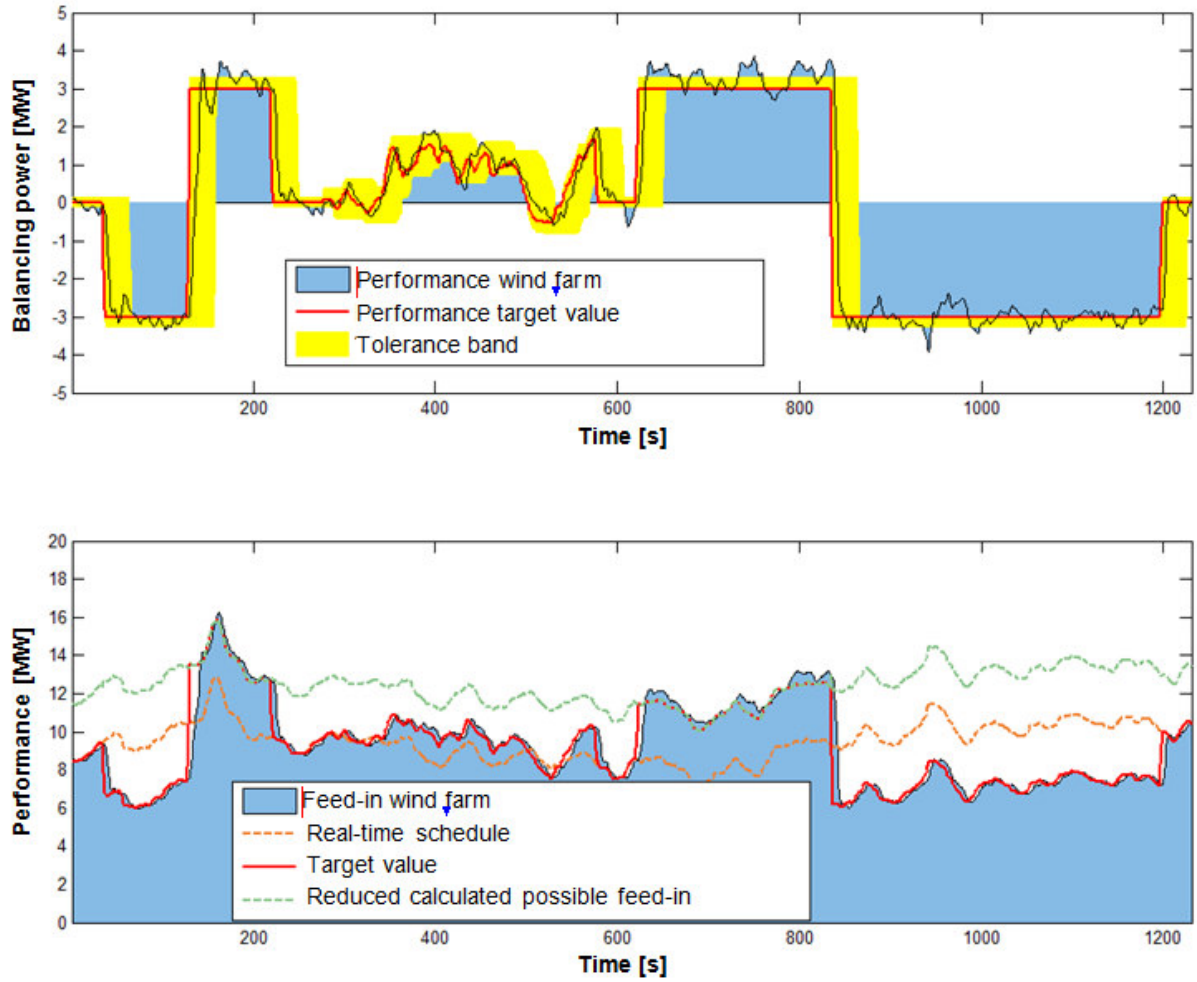

Figure 71: Record of a test for control reserve delivery with a wind farm on 11/10/2013

Figure 72 shows the recorded feed-ins and the feed-in set points of two biogas installations. A separate illustration of the control reserve delivery is not necessary for biogas installations as the delivery of control reserves conforms to the deviation from the constant (real time) schedule. As soon as it has reached the relevant level, the biogas installation shown in the upper illustration produces constant reference values with a very high degree of accuracy. The response time required to reach the reference values, however, is higher by comparison to PV and wind installations but lies within the expected range of values for continuous operation CHPs. The biogas installation in the diagram below shows a faster response time, keeping in mind that the total change in power output was lower as well. This biogas installation has a strong transient response, which is due to the internal control of the CHP, which could be adjusted. These two biogas installations are, however, older plants, which were optimized for continuous operation. Newer biogas CHPs have improved their reaction speed significantly and can sustain the set point much better as well.

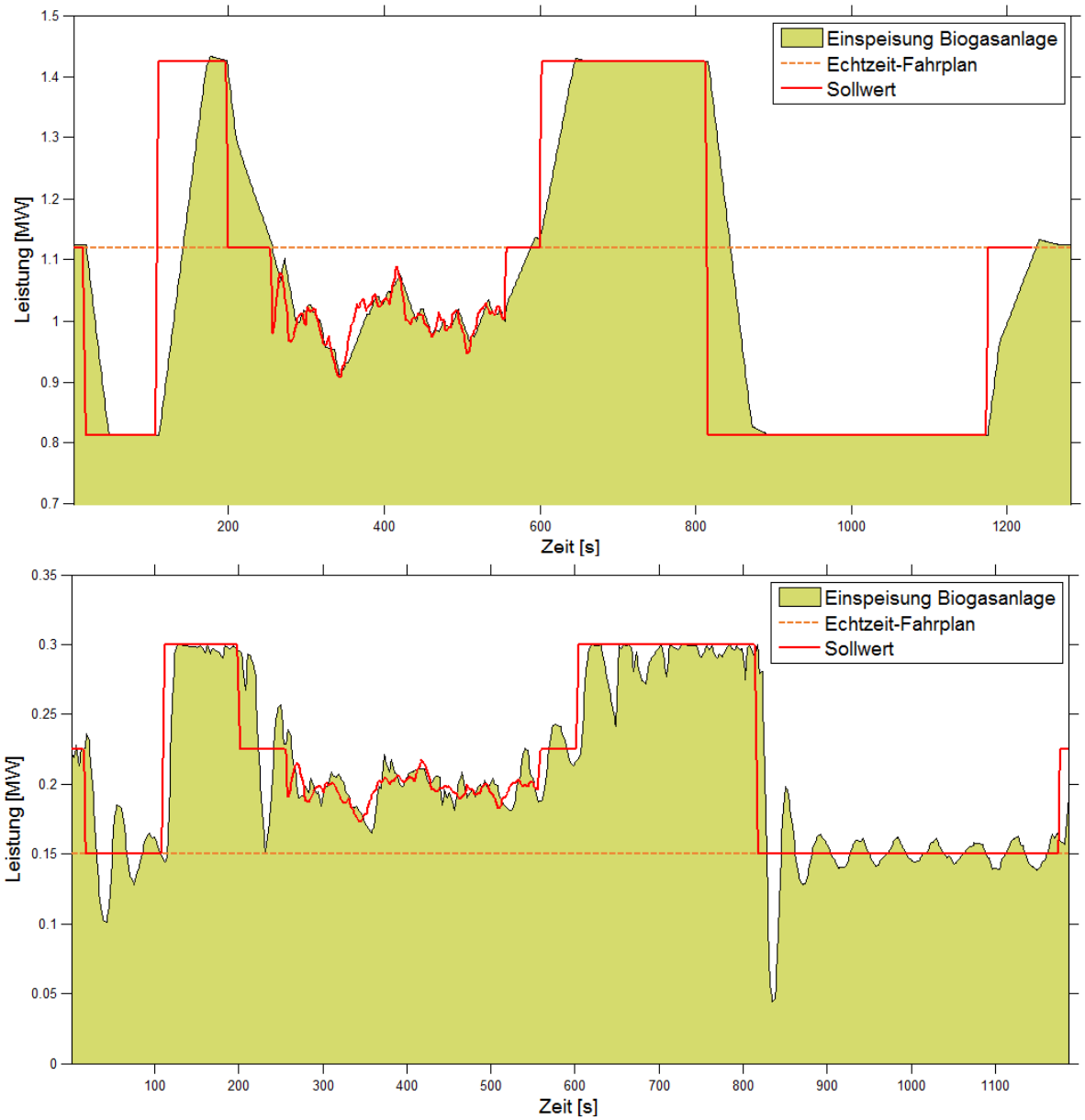

Figure 72: Record of a test for control reserve delivery with two biogas installations on 25.9.2013

Two additional biogas installations are not illustrated here, but show a similar behaviour to the upper biogas installation in Figure 72.

Figure 73 shows the result of a test with the photovoltaic installations from a screen shot from the VPP's control centre. The feed-in from the photovoltaic installations follows the course of the feed-in set points. The ability of the plants to implement extremely fast changes in feed-in can be seen. Photovoltaic installations can increase the accuracy of control reserve delivery by VPPs because they quickly balance out deviations from the control reserve reference value.

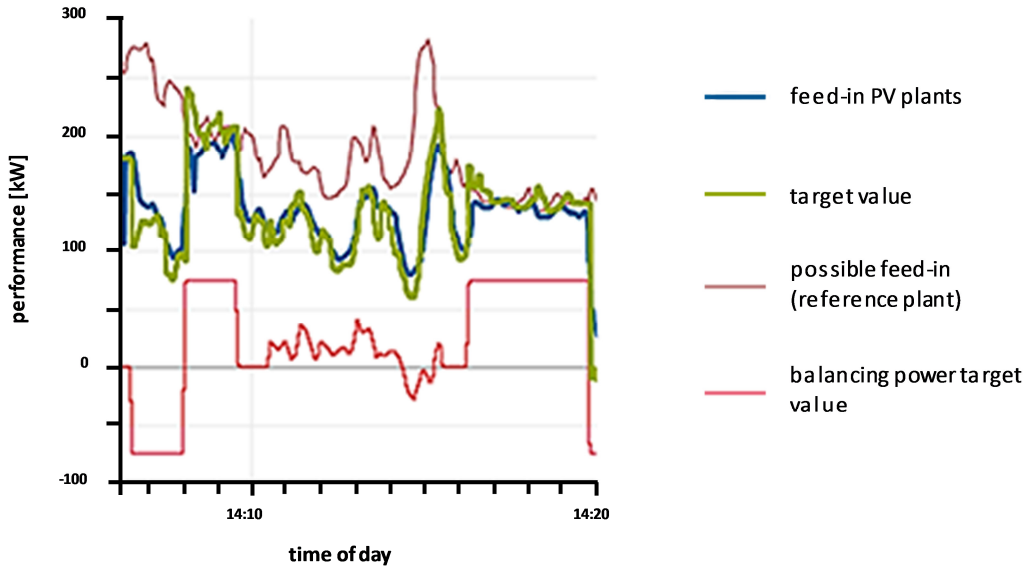

Figure 73: Record of a test for control reserve delivery with photovoltaic installations on 09/10/2013 (screen shots). A group of 11 small and 1 larger roof-installed plant was used (totalling 970 kW). It shows a good coverage of the reference value (red) derived from the control reserve reference value for PV installation feed-in (green) and the recorded actual feed-in from the PV installations (blue).

However, at the same time the recorded feed-in does show deviations from the reference value. With the aid of the individual tests implemented, the following influencing variables could be identified, which can contribute to more accurate control reserve delivery in future. The deviations correspond mainly to downturns in the control reserve delivery, which occur at regular intervals. They are caused by the cyclical switching of the reference plants for setting available active power signal. For the test, a relatively small number of installations were used so that the individual downturns could be observed. With more installations, clearly larger spatial balancing effects can be expected. To make the response time of photovoltaic installations usable for the VPP of the project, and to generally improve the control reserve delivery by photovoltaic installations compared to Figure 73, more research and development is needed. The main challenges are the short time spans for the VPP to react to weather changes and the need to process a large amount of data from different sources. The significance of fast communication, both within a photovoltaic power station and also to the outside, was also observed in other tests with other installations. Some of which were older and thus equipped with slower power inverters. Furthermore, the offered control reserve must be dimensioned with the aid of PV short-term power forecasts. This decision, whether and how much control reserve is offered by PV, requires high levels of reliability. The improvement of short-term forecasts is therefore a field of research that is key to the reliable delivery of control reserves from PV.

3.1.3 Simulations of the revenue situation for control reserve delivery by flexible energy plants

In a power supply system based on 100 % on renewable energies, decentralized renewable energy plants must be able to supply all ancillary services. The participation of RE plants in the control reserve market is thus an important building block on the way to the energy turnaround.

It is the aim of the studies to show:

- how flexibly renewable energy plants can participate in control reserve markets,
- what revenue they would have generated in the model year 2012 (the most current year with a complete data basis) and
- what adjustments are necessary to the German control reserve markets to deliver the necessary access.

The focus rested on five flexible types of plants in a possible supply system of 100 % renewable energies. These are:

- Electrical batteries
- Power-to-heat in a heat grid
- Power-to-gas / electrolyser
- Pumped hydro storage plants
- Flexible biogas plants with local conversion to power

CUBE Engineering developed market strategies for these five types of plants to achieve optimum revenue by participating in the control reserve markets, and completed simulations for the model year 2012. This is described in sections 3.1.3.1 to 3.1.3.11. In section 3.1.3.10 there is a more detailed description of strategies for weather-dependent RE delivering control reserve, and in section 3.1.3.11 inferences for the further development of the German control reserve markets are made.

3.1.3.1 Market access to control reserve markets

Markets investigated were the control reserve markets, i.e. markets for primary control reserve (PCR), secondary control reserve (SCR) and tertiary control reserve (TCR).

In order to maintain balance of power generation and consumption and maintaining grid frequency, the German TSOs put control reserve (CR) in these three qualities to tender. They differ with regard to activation principles. The current terms of trade on the control reserve markets can be outlined as follows: (see also Chapter 3.1): Prices are set on a pay-as-bid basis, i.e. each supplier gets its submitted price if the offer is accepted. In the case of SCR and TCR, provision of control reserve capacity and dispatched control energy are remunerated separately. However, for PCR only the provision is paid, the dispatched energy is not remunerated separately.

PCR and SCR are procured in weekly tenders, TCR in daily tenders. Furthermore, the products differ in the delivery periods. While successful offers of PCR have to be able to guarantee a provision over a weekly period from Monday 00:00 to Sunday 24:00, SCR is separated in two and TCR in six time slices procured as separate products. With SCR time slices are called peak or high tariff (HT) (Monday to Friday between 8:00 and 20:00) and off-peak or low tariff (LT) times (remaining time periods,

especially weekends and public holidays). TCR is traded in 4-hour blocks and tendered on the previous day. Close of trading for PCR is Tuesday of the previous week, for SCR it is Wednesday. While for SCR and TCR positive and negative control reserves are tendered separately and a minimum offer of 5 MW is set, for PCR a control reserve with a minimum offer of 1 MW is tendered symmetrically, i.e., 1 MW positive primary control reserve and 1 MW negative primary control reserve must be available simultaneously. The investigated power plants were only partially able to fulfil all requirements regarding the minimum offer amount (PCR, SCR and TCR) and product lengths (PCR and SCR). However, all control reserve markets permit pooled offers.

Participation in control reserve markets requires a combined trade on EPEX spot markets (intraday-trade and/or day-ahead spot market), in order to have the control reserves held at the offer period with the required 100 % energy availability.

3.1.3.2 Method of modelling and simulation

Modelling and simulation of market and operational management strategies was performed with the software energyPRO from EMD International A/S with the modules markets, operation and interface. Simulations were carried out based on time series with 15 minute resolution, using the model year 2012. For each type of plant and market strategy, a digital model with an individual optimization strategy was created. In many cases, several markets had to be served from one energy plant. These combined plant/market definitions were defined for each market, energy plant and direction of energy flow combination. Input values for the simulations were the technical plant characteristics, relevant economic core data, market offers and time series of market prices, activation quantities and the heat supply requirement.

In many cases, it was not possible to cover the entire time slice of a control reserve product with the full plant size. The required 100 % energy availability was reached by two separate ways:

1. In the first case, the control reserve was made available for a part of a time slice (e.g. the first six hours of a HT time slice for SCR), followed by a subsequent trade on the intraday market in order to recharge the buffer storage for the next phase of control reserve availability. Plant capabilities such as the maximum time of reserve provisions determined the length of time slice adjustment. In many cases, the buffer storage limits the duration of the reserve provision. In addition, for the biogas plants this restriction consists in the proportion of installed electrical CHP-output and installed capacity (“Bemessungsleistung” according to the German Renewable Energy Act “EEG”).
2. In the second instance, control reserve was held available continuously for the entire time slice, but the plant size was split in order to make an adequate offer of control reserve capacity. Only a part of the plant capacity was made available as control reserve and another part of the plant capacity served for a balancing intraday trade. The simulation of modelled market strategies was rolled over from time slice to time slice, and respectively in the case of a continuous control reserve availability, which occurred for all hours of the year, rolling in 3-day cycles with a daily output carried forward.

The results of the simulations gained from the use of software were available in form of time series graphics and tables. This applies to the daily operating times of the plants, the daily individual values of the produced, purchased and marketed amounts of energy and the costs. Summaries of the annual amounts were also available. These results were check for plausibility after each simulation.

As the market conditions on control reserve markets are presently undergoing major changes, the results can be only applied to the future to a limited extent. For further observations for the future, scenarios for the market development would have to be developed. This would be a research topic on its own and was not possible or planned as part of the project.

3.1.3.3 Assumptions about market prices, costs and market access

For all situational calculations, the assumption was made that the average capacity price [EUR/MW] is obtained on the control reserve markets and that each market offer is accepted. If only primary control reserve was offered by the pool, half the average capacity price was calculated.

In the simulations, the energy prices [EUR/MWh] for dispatched control reserve energy were constant throughout the year. For this, a sufficiently adequate estimate of an activation time series was calculated based on data published by the TSOs on various internet platforms. The calculation of the bids for the dispatch (energy price bids) included an optimization of yield from activation that result from the interaction of the bid price and the amount of energy activated. High bid prices cause low volumes activated and vice versa. The maximum income results from a specific bid price. It can be an advantage for storage and flexible electric loads to tender a negative operating price with the payment direction from plant operator (bidder) to the TSO, if activations for low-priced electrical energy can generate additional revenue. The simulation and the real participation in markets differ insofar, as the future trade period cannot be analysed at this stage. Instead, empirical values from the past had to be consulted.

It was assumed for the intraday trade that hourly trading takes place at the market clearing prices of the EPEX SPOT day-ahead auction. Ancillary costs such as the purchase of electrical energy, the (sur)charges and taxes, were based in the year 2012. Pumped and battery storage are exempted from these costs. Trading connection costs were not taken into consideration, as they have to be negotiated individually with the pool operator and depend on the market value of the power plant. Annual payments from depreciation of investments in the plant were also disregarded.

Regarding the conditions for access to the control reserve market – based on the market conditions of the model year 2012 – it was assumed that plants offer their control reserve within a control reserve pool. It was assumed that pool operators are in the position to provide suitable offers to all plant operators for the access to the control reserve pool. This consequently would allow the access to the control reserve markets. It was assumed that pool operators include both plants into the pool that either have limited volumes of control reserve to offer and/or are time-restricted or can only cover a part of the traded time slices. With these assumptions about the market access for the different types of plants investigated, an intermediate step between the current and the future market design was outlined. From the point of view of the plant operators, this would mean lower minimum bid sizes and shorter lead times before market gate-closure and shorter product time-slices. No simulations for scenarios of changed market designs were calculated since this would involve changed and unpredictable market prices and the results for market profits would have little significance.

3.1.3.4 Electrical batteries

The market participation of an electrical battery (BAT) in the medium voltage grid with a storage capacity of 40 MWh, an electrical loading and discharge capacity of 10 MW and a charge-discharge efficiency of 90 % was investigated. The fast response time enables a modulated operation between standstill and nominal load. For positive SCR, an energy price of 72.50 EUR/MWh is offered with the

payment direction from the TSO to the bidder (plant operator) (TB), for the negative SCR an energy price -12.50 EUR/MWh with the payment direction from the bidder to the TSO network (BT).

Market strategies

Reference: Arbitrage trading on EPEX day-ahead spot auction

BAT 1) Primary control reserve (PCR): Continuous offer of a symmetric control reserve band of 10 MW, i.e. 5 MW positive and 5 MW negative control reserve

BAT 2) Secondary control reserve (SCR): Continuous offer of a symmetric control reserve band of 10 MW, i.e. 5 MW positive and 5 MW negative control reserve

BAT 3) Secondary control reserve (SCR): Provision of positive secondary control reserve capacity for the first 3.5 hours of each HT phase, and negative secondary control reserve capacity in the 4 first hours of each LT phase. The maximum possible provision availability differs for positive and negative control reserve because of storage capacity and battery efficiency.

BAT 4) Secondary control reserve (SCR): Provision of negative secondary control reserve capacity during the first 4 hours of each LT and HT phase.

Table 13: Simulation results for market participation of the electrical battery related to the model year

	Reference	BAT 1)	BAT 2)	BAT 3)	BAT 4)
Net operating result in EUR	**305.687**	**823.067**	**1.386.517**	**542.702**	**544.172**
Profit versus reference (day-ahead spot only)	+/- 0%	+169%	+354%	+78%	+78%
Revenues activations + spot market [EUR]	355.687	151.828	821.035	448.493	372.982
of these activation of					
positive control energy [EUR]			1.241.459	288.231	0
negative control energy [EUR]			-201.206	-61.110	-93.847
spot market energy sale [EUR]	976.435	575.236	469.044	692.930	826.071
spot market energy purchase [EUR]	-620.748	-423.408	-688.262	-471.558	-359.242
Indicators (average for year):					
Energy production [EUR/MWh]	55,13	45,20	61,78	53,83	48,16
energy purchase [EUR/MWh]	28,40	26,94	26,02	23,69	21,44
Revenues of provision of CR-capacity in EUR	0	721.239	615.482	144.209	221.190
of this…					
positive control reserve EUR			110.052	16.189	0
negative control reserve EUR			505.430	128.020	221.190
Operating expenses in EUR	50.000	50.000	50.000	50.000	50.000

The best net operating results are obtained from the continuous availability of a symmetrical control band. Secondary control reserve obtains higher profits than primary control reserves (compare BAT 2 and BAT 1).

As an index the average annual prices realized for energy production and the purchase of electrical energy were calculated. For this, all profits from energy sold on the spot and control reserve markets were divided by the produced energy volume. The same method was applied for energy purchase. The total price obtained for energy production from control energy activations and spot market deliveries is (>60 EUR/MWh) for tendering secondary control reserve which, when compared to (45 EUR/MWh) for primary control reserve, is very high. For secondary control reserve, large volumes of energy are activated as positive control reserve and paid the bid price of 72.50 EUR.

3.1.3.5 Power-to-heat in the heat grid

An electric boiler (P2H) with a 1 MW performance and 98 % efficiency supplements a gas boiler of 10 MW_{th} and 90 % efficiency designed for peak load in a heat grid with 19.800 MWh_{th} annual consumption. The P2H installation possesses 500 m^3 heat buffer storage; its capacity of 13.76 MWh provides a buffer of >12 hours. For the negative secondary control reserve an energy price bid of 177.50 EUR/MWh (payment from TSO to bidder) is set; for the negative tertiary control reserve an energy price bid of 450 EUR/MWh (payment from TSO to bidder). The gas procurement price is 3.5 ct/kWh, the heat-selling price is 6 ct/kWh.

Market strategies

The power-to-heat plant offers negative control reserve around the clock throughout the model year. Based on the assumed pool concept, primary control reserve can also be offered for the negative part of the control reserve band only. Operations only occur during a dispatch of control reserve, with up to 100 % of the nominal load.

Table 14: Simulation results on market participation of the power-to-heat plant related to the model year

	Boiler operation	tertiary control reserve	secondary control reserve	primary control reserve
Net operating result in EUR	**419.235**	**468.163**	**525.613**	**458.482**
Profit versus reference	0%	+12%	+25%	+9%
Revenues of provision of CR-capacity [EUR]	0	26.654	101.094	72.124
Revenues of activation control energy [EUR]	0	29.363	12.893	0
Revenues heat energy sales [EUR] of these…	1.191.509	1.191.509	1.191.509	1.191.509
power-to-heat plant [EUR] boiler [EUR]	0 1.191.509	3.837 1.187.672	4.271 1.187.238	24.001 1.167.508
Ancillary costs for purchased electricity [EUR]	0	7.076	7.877	45.933
Costs gas for boiler [EUR]	772.274	769.787	769.506	756.718
Operating expenses electric boiler [EUR]	0	2.500	2.500	2.500

The configuration of the plant allows the control reserve activations free of any restrictions at any time. The exclusive boiler operation with natural gas states the reference case for the profits from the three control reserve markets.

For the assumed configuration of the plant, the operating profit is highest for negative secondary control reserve market as the income via the capacity price is higher than in the primary control reserve market, lower electricity costs at the same time.

3.1.3.6 Electrolyser

An electrolyser with an electrical capacity of 10 MW and 60 % efficiency and a control speed suitable for primary control reserve (control range from standstill to nominal load) feeds hydrogen into the natural gas network and thus possesses unlimited flexibility. For negative secondary control reserve an energy price of 227.50 EUR/MWh (TSO to bidder) is offered, for negative tertiary control reserve an energy price of 450 EUR/MWh (TSO to bidder). The gas sale revenue amounts to 3.0 ct/kWh.

Operational management strategy

The electrolyser offers negative control reserve around the clock throughout the model year. Operations only happen in case of control reserve activations, with up to 100 % of the nominal load.
As a reference for the profits on the three control reserve markets, a market participation in the EPEX day-ahead spot auction applies, where the electrolyser purchases energy only in the rare hours of market clearance prices below -94.44 EUR/MWh. This results from the marginal price for operating the plant, which is produced by the ancillary costs for electricity (charges, duties and taxes) and the gas sale revenue.

Table 15: Simulation results for market participation of the electrolyser related to the model year

	Spot market	tertiary control reserve	secondary control reserve	primary control reserve
net operating result in EUR	**-12.897**	**477.810**	**1.046.724**	**306.758**
Revenues capacity price in EUR	0	266.541	1.010.941	721.242
Revenues of activation control energy in EUR		299.250	104.167	0
Revenues spot market energy purchase in EUR	27.213			
Revenues gas sales in EUR	2.880	11.970	8.250	73.470
Ancillary costs for purchased electricity in EUR	17.990	74.951	51.634	462.954
Operating expenses in EUR	25.000	25.000	25.000	25.000

The electrolyser can make good profits on the secondary control reserve market, which are based mainly on revenues from the capacity price. For primary control reserve, the high ancillary costs for purchased electricity are a major cost factor. This also applies to the exclusive (reference) trade on the day-ahead spot auction, which causes a negative result.

3.1.3.7 Pumped hydro storage plant

The assumed pumped hydro storage plant (PSP) possesses an electrical connected load of 50 MW with an efficiency of 88 % in turbine operation and 42 MW with 75 % efficiency in pump operation (total efficiency is 75 %). The storage volume of 500 MWh in the top basin allows an energy dispatch of 8.8 hours in turbine operation and 14 hours in pump operation. For negative secondary control reserve, an energy price standardized over the year of -12.50 EUR/MWh (bidder to TSO) is offered. In the simulation PSP 1a and PSP 5, an energy price standardized over the year of 72.50 EUR/MWh (TSO to bidder) is offered for positive secondary control reserve. Differing from this, in the simulations for primary control reserve PSP 1b and primary control reserve PSP 3 a weekly changing energy price bid is offered, based on observations of the market price dynamics. For this purpose it is assumed that the plant operator is in a position to analyse the market developments on a weekly basis and able to adjust the offers accordingly. For the simulations, the energy price was optimized weekly according to the methodology outlined in Chapter 3.1.3.3. The assumed operating costs are 4 EUR/MWh.

Market strategies

Reference:	Arbitrage trading on day-ahead spot auction.
PSP 1a)+b)	Positive secondary control reserve, in each case the first 8 hours of each HT phase (turbine output).
PSP 2)	Negative secondary control reserve, in each case the first 12 hours per LT phase (pumped output).
PSP 3)	Positive secondary control reserve, in each case the first 5 hours of each HT phase (turbine output) and negative secondary control reserve, in each case the first 4 hours per LT phase (pumped output).
PSP 4)	Negative secondary control reserve, in each case the first 5 hours per LT phase with totalled turbine and pumping output where the turbine output is marketed day-ahead on the spot market.
PSP 5)	Continuously for all hours of the year, simultaneously positive secondary control reserve with partial turbine capacity bid of 15.7 MW and negative secondary control reserve with partial pump capacity bid of 21 MW.
PSP 6)	Continuous reserve analogous to secondary control reserve PSP 5 but exclusively negative secondary control reserve with full pump output of 42 MW.

The reference trade was not profitable due to the small price spread on the EPEX day-ahead spot auction (spread between peak prices and daily average price). This as was shown for the model year 2012. Observing the market and weekly adjustments of the energy price bids to the market conditions (PSP 1b) lead to significant profits (cf. to PSP 1a) for the positive secondary control reserve, where a higher annual average energy price for secondary operational reserve of 85,06 EUR/MWh is attained with a similar amount of 47 GWh activated. Negative secondary control reserve is more lucrative than positive control reserve, as is shown in strategy PSP 2 compared to PSP 1 as well as PSP 4 to PSP 3 and PSP 6 to PSP 5. Negative control reserve calls allow the acquisition of reasonably priced electricity for pumping. It was not determining for the net operating result whether only the pump output (PSP2) is made available as capacity for 12 hours per LT phase or the maximum of the turbine and pump output for 5 hours. Regarding the profits, it is advantageous to offer continuous control reserve with partial plant output (power slice) (PSP 5+6) over market participation with fragmented time slices with full plant output. In PSP 5 good average annual values were obtained for the energy production (63.26 EUR/MWh) and the energy purchases

(23.56 EUR/MWh). Compared to other strategies, the total traded volume of energy is high. At the same time, high profits are obtained from the capacity prices due to the continuous delivery of secondary control reserve. A technical precondition for this is the very fast controllability in all partial load areas of the pump and the turbine. If a pump turbine cannot accomplish that, a separate pump and turbine system with two downpipes are necessary, which is able to establish a hydraulic short circuit. Energy losses due to lower efficiency during partial load situations are disregarded in the simulation.

Table 16: Simulation results for market participation of the electrolyser related to the model year

	EPEX-Spot	PSP 1a	PSP 1b	PSP 2	PSP 3
Net operating result [EUR]	**1.204.045**	**1.351.215**	**1.971.228**	**3.379.455**	**3.022.243**
Profit versus reference	0 %	+12 %	+64 %	+181 %	+151 %
Revenues of CR-activations + spot market [EUR] of these…	1.823.927	1.918.762	2.546.304	2.401.934	2.682.888
positive control energy activation [EUR]		3.386.460	4.009.092		2.405.902
negative control energy activation [EUR]				-644.046	-256.667
spot market energy sale [EUR]		1.770.421	1.812.586	3.913.208	3.048.312
spot market energy purchase [EUR]	4.107.925	-3.238.119	-3.275.374	-867.228	-2.514.659
Indicators:	-2.283.998				
Energy production [EUR/MWh]	61.93	72.50	72.08	57.34	65.23
energy purchase [EUR/MWh]	25.77	30.27	30.31	16.66	24.84
Revenues of provision of capacity [EUR]	0	180.260	180.260	1.613.356	1.120.054
positive CR [EUR]		180.260	180.260	1.613.356	582.310
negative CR[EUR]		0	0		537.744
Operating expenses	619.882	747.807	755.336	635.835	780.699

	PSP 4	PSP 5	PSP 6
Net operating result [EUR]	**3.457.657**	**4.979.091**	**7.047.916**
Profit versus reference	+187 %	+314 %	+485 %
Revenues of CR-activations+ spot market [EUR] of these…	2.705.716	3.554.830	3.749.051
positive control energy activation [EUR]		3.912.250	0
negative control energy activation [EUR]	-682.878	-845.097	-1.690.189
spot market energy sale [EUR]	5.490.140	3.158.545	5.439.240
spot market energy purchase [EUR]	-2.101.546	-2.670.868	0
Indicators:			
Energy production [EUR/MWh]	71.29	63.26	53.60
energy purchase [EUR/MWh]	27.10	23.56	12.50
Revenues of provision of capacity [EUR] of this...	1.470.940	2.468.368	4.245.646
positive CR [EUR]		345.531	
negative CR [EUR]	1.470.940	2.122.837	4.245.646
Operating expenses	718.999	1.044.107	946.781

3.1.3.8 Biogas plant with local conversion to power

Since 01/01/2012, the EEG 2012 incentivises biogas installations to become more flexible. This allows a demand- and market adjusted production of electrical energy to balance out the fluctuating feed-in of wind and PV. This flexibility is achieved through additional installed capacity of the CHPs, gas storages and heat storages.

The objects of the study are three different configurations of flexibility of plants with identical biogas production in a fermenter of 1.35 MW per hour (availability of fuel or combined output). These three configurations of plants are compared based on their possible revenue on the control reserve markets.

Configuration 1 (non-flexible):
Biogas plant (BGP) without flexibilization, installed CHP capacity equals the installed capacity. 1 CHP with P_{el}=526 kW (originally as small CHP) with electrical efficiency of 39 % in nominal load and 37.9 % with 75 % nominal load. The provision of control reserve takes place 24 hours per day.

Configuration 2 (flexible):
BGP flexibilized, installed CHP capacity equals double installed capacity with 2 CHP of P_{el}=526 kW each (original small CHP plus identical small additional CHP). The provision of control reserve takes place over 12 hours per day.

Configuration 3 (very flexible):
BGP flexibilized, installed CHP capacity complies with four times the installed capacity. 1 CHP with Pel=1.560 kW_{el} with electrical efficiency of 41.7 % in nominal load and 40.8 % with 75 % nominal load, and a CHP with P_{el}=526 kW_{el} (large additional CHP plus original small CHP). The provision of control reserve takes place over 6 hours per day.

The usable biogas storage was assumed to have a net volume of 5.600 m^3 (equals 28.56 MWh). The modelled CHP minimum operating time is two hours – except where specified otherwise. It is assumed the CP can be controlled between 100 % and 75 % of the nominal capacity. As a larger control range enables larger control reserve provisions and one can anticipate technically improved engines in the future, cases BGP 1b and BGP 1a are investigated with a CHP control range between 100 % and 50 % of the nominal capacity. This allows investigating the sensitivity of this aspect. It is assumed that the electrical efficiency will decreases linearly between full load and partial load. In case of the large 1.56 MW-CHP the electrical efficiency is 38.0 % at 50 % of the nominal load. For the small 526 kW-CHP it is 35.4 % at 50 % partial load.

Market participation was simulated as follows: For both, secondary control reserve and primary control reserve, one of the CHPs within the plant´s configuration provides control reserve, which in configuration 3 would be the large one. The energy production in the periods of the control reserve provision is sold on the day ahead spot auction. Outside the provision periods, this CHP participates in the intra-day trading as well, taking into account that the biogas buffer storage's fill level guarantees the energy availability at the beginning of the next phase of providing control capacity. The second CHP participates only in the intra-day market. Ramp rates of the BGPs were not included in the simulations.

For positive secondary control reserve, an energy price of 72.50 EUR/MWh (TSO to bidder), for negative secondary control reserve one of 87.50 EUR/MWh (TSO to bidder) is offered. For negative tertiary control reserve the energy price is 175.00 EUR/MWh (TSO to bidder). 15 EUR/MWh were assumed for maintenance costs for the small 526 kW-CHP, and 10 EUR/MWh for the large one 1.56 MW-CHP. These standard amounts per MWh already include the increased maintenance costs for the starts and stops due to flexible operation or for the control reserve activation.

A special CHP design was assumed for the participation in the primary control reserve market. One of the CHPs of each plant configuration acts on the primary reserve market and is designed so that the highest electrical efficiency of 39 % lies at 87.5 % of the nominal load. At 100 % of the nominal capacity, 38.4 % of electrical efficiency is assumed, for 75 % of the nominal capacity 38.0 %. In this way, a symmetrical control reserve band of 12.5 % of the nominal load can be offered on the basis of normal operation at 87.5 % nominal load.

For tertiary control reserve, all plant configurations are optimized towards the income from EPEX spot price and negative tertiary control reserve capacity price, where daily varying 4-hour blocks for the provision of control capacity and plant operation are selected.

Market strategies

The following market strategies were simulated for the three plant configurations that differ in their flexibility as described above.

Reference:	EPEX day-ahead spot auction
BGP 1a:	Negative secondary control reserve (standard operation at nominal load; in case of activation 75 % of nominal load)
BGP 1b:	Negative secondary control reserve (like 1a, variant with a controllability up to a part load of 50 % of the nominal load, as described above)
BGP 1c:	Negative secondary control reserve (like 1b, variant with the opportunity of offering secondary control reserve by the hour and a controllability up to a part load of 50 % of the nominal load)
BGP 2:	Positive secondary control reserve (standard operation at 75 % of the nominal load, and in case of activation nominal load)
BGP 3:	Primary control reserve (symmetrical primary control reserve band between 75 % and 100 % of the nominal load while marketed on the day-ahead spot auction by 87.5 % of the nominal load at the CHP´s ideal efficiency level, see description above)
BGP 4:	Negative tertiary control reserve (standard operation at full load; in case of activation 0 % of nominal load)

Based on case BGP 1b, the effects of the possibility of offering negative secondary control reserve hour by hour were studied in the case of BGP 1c. The achievable annual hours of secondary control capacity provision and the annual revenue were enfocussed. Building on case BGP 1b, it was assumed that the minimum operating time of a CHP is one hour and secondary control reserve bids for each hour are possible. Model assumptions: The CHP offering secondary control reserve is marketing power production on the day-ahead spot market and provides negative secondary control reserve in the allocated hours (which assumes that secondary control reserve is traded analogue to the EPEX day-ahead spot market on the previous day, namely after-market clearing on the EPEX spot

market). In the simulation, the schedule optimization for the CHP providing secondary control reserve was carried out with the aim to maximize the total revenue from the spot market and the negative secondary control reserve capacity price market component. This led to a daily changing of the hours with control reserve provision. The second CHP only trades on the spot market, as elaborated before.

Results of simulations

The table below shows the results of the simulations with each market strategy in a separate line. Results are given for each of the three plant configurations above, each one of them in a separate columns. As mentioned before, plant configuration 1 shows no flexibility at all and configuration 3 has the highest degree of flexibility. The key performance indicator <energy production> (in italics) is the annual average price obtained in EUR/MWh for the total energy production. This includes the trading on the day-ahead and intra-day spot markets as well as the revenue from the control reserve dispatch.

Flexibilizing the plants increases the revenue from the day-ahead spot market since the hours with the highest price forecast prices can be used. This applies especially to configuration 3 with four times the installed capacity. Configuration 3 has sufficient flexibility to allow the plants to be operated during just a few hours a day. The power output is high in these hours. The higher electrical efficiency of the large CHP is a further advantage in configuration 3.

The additional offered negative control secondary reserve is beneficial for the least flexible plant (market strategy BGP 1a, configuration 1)., The more flexible plants (configuration 2 + 3) on the other hand do not achieve significantly higher revenues with a secondary control reserve market participation, as the additional expenses are not balanced by the additional income. This is based on based on the assumptions for market strategy BGP 1a whit a spot-only reference case (reference market strategy for configurations 2+3). This is under the assumption of a narrow control range between 100 % and 75 % of the nominal load. If partial loading of the plants was extended, the CHP were in a position to offer more secondary control reserve to the market within pre-qualification requirements. This would improve the economic situation significantly (market strategy BGP 1b). The delivery of secondary control reserve in twelve or six hour blocks and the associated operation restrict the optimal operation of the plants based on dynamically varying high-priced hours at the day-ahead spot market.

Assuming secondary control reserve markets that are tendered for each hour individually and the technical capability of the CHP to offer secondary control reserve hourly and further assuming a control range of 50 % of the nominal capacity (market strategy BGP 1c) would yield significant additional revenue for the plant configurations 2 + 3. Participation in the hourly secondary control reserve market removes the restrictions to maximize the income on the spot market. The CHP can provide control reserve in more hours of the year at the same time. Plant configuration 3 and BGP 1b with its continuous biogas production in the fermenter only allows for a continuous block of secondary control reserve over a period of six hours. This accumulates to 1.518 HT (high tariff) hours annually with control reserve provision. With the strategy BGP 1c the hours increase to 3.078 hours annually due to the flexibility of the market. The strategy for optimization also leads to secondary control reserve provision during LT (low tariff) when higher capacity prices are available. The

envisioned changes in the market design would result in increased provision of secondary control reserve but also will most probably decrease the market prices in general.

Table 17: Simulation results for market participation of biogas plant related to the model year

	Configuration 1	Configuration 2	Configuration 3
Reference: EPEX day ahead-spot			
Net operating result [EUR]	127.505	168.253	213.639
Revenue spot market [EUR]	196.811	237.551	265.460
maintenance costs [EUR]	69.306	69.299	51.822
energy production [€/MWh]	42.60	51.42	54.28
(operating hours):	(8.784)	(4.637)	(1.107)
BGP 1a: Secondary control reserves negative	HT+LT 24 hours	HT 12 hours	HT, first 6 hours
Net operating result [EUR]	143.433	167.510	208.832
Revenues CR capacity price [EUR]	13.242	3.597	5.338
Revenues CR energy price [EUR]	2.293	630	651
Revenues spot market [EUR]	196.811	232.544	254.252
Maintenance costs [EUR]	68.913	69.261	51.409
Energy production [EUR/MWh]	4.,34	50.66	51,83
		LT 12 hours	LT, first 6 hours
Net operating result [EUR]		151.617	182.577
Revenues CR capacity price [EUR]		7.376	10.958
Revenues CR energy price [EUR]		1.168	2.080
Revenues spot market [EUR]		212.464	232.813
Maintenance costs [EUR]		69.391	50.236
Energy production [EUR/MWh]		46.31	44.99
BGP 1b: Secondary control reserve negative/50% Pnom	HT+LT 24 hours	HT 12 hours	HT, first 6 hours
Net operating result [EUR]	159.456	176.247	219.051
Revenues CR capacity price [EUR]	26.586	7.212	10.691
Revenues CR energy price [EUR]	4.603	1.223	1.302
Revenues spot market [EUR]	196.784	237.244	260.738
Maintenance costs [EUR]	68.517	69.432	53.680
Energy production [EUR/MWh]	44.09	51.55	53.54
BGP 1c: Secondary control reserve negative/50% Pnom hourly secondary control reserve		optimized hourly	optimized hourly
Net operating result [EUR]		184.878	244.818
Revenues CR capacity price [EUR]		18.358	27.672
Revenues CR energy price [EUR]		3.488	5.924
Revenues spot market [EUR]		232.902	262.022
Maintenance costs [EUR]		68.870	50.801
Energy production [EUR/MWh]		51.19	54.47
BGP 2: Secondary control reserve positive	- / -	HT 12 hours	HT, first 6 hours
Net operating result [EUR]		169.077	206.110
Revenues CR capacity price [EUR]		707	1.041
Revenues CR energy price [EUR]		12.387	19.371
Revenues spot market [EUR]		225.098	235.840
Maintenance costs [EUR]		69.115	50.142
Energy production [EUR/MWh]		53.62	52.63

		LT 12 hours	LT, first 6 hours
Net operating result [EUR]		156.767	185.883
Revenues CR capacity price [EUR]		1.645	2.470
Revenues CR energy price [EUR]		15.205	20.217
Revenues spot market [EUR]		208.823	212.412
Maintenance costs [EUR]		68.906	49.216
Energy production [EUR/MWh]		51.26	47.92
BGP 3:			
Primary control reserve	HT+LT 24 hours	HT 12 hours	HT, first 6 hours
symmetrical		164.826	191.846
Net operating result [EUR]	120.683	3.200	4.814
Revenues CR capacity price [EUR]	9.376	230.046	259.662
Revenues spot market [EUR]	171.819	68.420	72.630
Maintenance costs [EUR]	60.512	50.43	53.63
Energy production [EUR/MWh]	42.59		
		LT 12 hours	LT, first 6 hours
Net operating result [EUR]		150.799	158.729
Revenues CR capacity price [EUR]		4.654	6.988
Revenues spot market [EUR]		214.752	224.517
Maintenance costs [EUR]		68.608	72.776
Energy production [EUR/MWh]		46.95	46.28
BGP 4:	24 hours	optimized 4 h blocks	optimized 4 h blocks
Tertiary control reserve negative			
Net operating result [EUR]	149.140	185.992	239.418
Revenues CR capacity price [EUR]	13.555	10.314	10.697
Revenues CR energy price [EUR]	8.975	15.671	25.954
Revenues spot market [EUR]	194.527	228.915	255.604
Maintenance costs [EUR]	67.917	68.909	52.837
Energy production [EUR/MWh]	45.46	53.24	58.40

It does not make sense for flexible biogas plants to provide secondary control reserve as in that case biogas produced in the fermenter would remain unused. During capacity provision times, the CHP of the flexible configurations 2+3 are also operated below the nominal capacity with decreased efficiency, and a smaller volume of electrical energy is also marketed day ahead; because of the interim intraday trade however, no biogas is lost. The revenues from the capacity prices for positive secondary control reserve are low when compared to the negative secondary control reserve. However, the revenues from the control reserve dispatch are considerably higher.

The additional effort for symmetrical primary control reserve offers does not pay off when compared to spot-only reference case. In the inflexible configuration 1, unused biogas equal to an electrical energy of 500 MWh must be burnt off since normal operation takes place at 87.5 % of the nominal load. Based on the assumptions made, the revenues from the capacity price for the flexible configurations 2+3 does not balance out the lower revenues on the spot market, when compared to the reference scenario. Compared to secondary control reserve, primary control reserve is additionally constrained by the requirement of symmetrical provision, according to the current tender conditions. One possibility would be to operate the biogas CHP according to the demand in nominal load and to offer negative primary control reserve.

As the assessment has shown, it is already possible to generate additional revenue by offering negative tertiary control reserves for highly flexible biogas plants under the current market conditions. The chosen strategy that both CHPs provide negative tertiary control reserve and select

those times with high income times from the combination of the revenues from the reserve and spot markets for four hour blocks has proven successful. Additionally, the revenues could potentially be increased further by offering positive tertiary control reserve during times of standstill of the flexible biogas plant.

3.1.3.9 Summarised result for flexible plants

From the operators' business point of view, it is possible to provide control reserves. A prerequisite for participating in the market is that the plant operators can also make offers for considerably shorter time slices than currently demanded by the tender conditions. Plant restrictions, such as the buffer storage sizes, limit the length of time slices that can be offered.

For the configurations of the types of plants studied here, electrical battery, power-to-heat, electrolyser and pumping storage plant, the secondary control reserves market promises the highest profitability when compared to other control reserve markets. The highest revenues are realised when negative secondary control reserve is offered continuously, at all hours of the year, even when this is only possible for a part of the plants' performance. The necessary continuous energy availability can be achieved by trading on the EPEX SPOT intra-day market simultaneously. This ensures that the secondary control reserve can be dispatched and the storage fill levels are balanced out. Then usable storage volume is reduced by the volume of energy that must be held available for the lead-time of the intra-day trade.

Biogas installations should be made flexible to be able to convert the dispatchable energy from biomass to electricity as needed. For highly flexible biogas installations, the delivery of secondary control reserves becomes profitable if the CHP continue to be developed further so that they are controllable and pre-qualify for a larger power ranges and the market conditions are adapted towards shorter time slices of 1 to 2 hours. If the minimum duration of holding power matched the product length of 1 hour on the day-ahead spot market, it would become possible to combine a demand-oriented operation, using the high price periods on the spot market, with providing secondary control reserve in such a way that from offering secondary control reserve does not decrease the revenue on the spot market.

Plants whose production is weather-dependent, thus fluctuates every hour, and needs to be forecast every day require appropriately adapted flexible control reserve markets with short lead times and product lengths. Apart from wind farms and PV installations, this applies to flexible methane CHP power plants with a heat storage and a district heating network where the heat demand is based on the outside. For this, it is possible to design plants with a high proportion of CHP links and high energy efficiency.

3.1.3.10 Offers by weather-dependent RE

Contractually, control reserve offers must be 100 % reliable [48]. However, this requirement can neither be fulfilled by weather-dependent RE nor by any other technical system. The risk to guarantee a delivery of control reserve is with the supplier and has to be managed accordingly. Therefore, a reliability of 99.994 % is assumed in the project. This value corresponds to an empirical value that was observed with other market participants [48]. The level of reliability of an offer by weather-dependent RE can be determined with probabilistic forecasts. The offering strategies, described in this section 3.1.3.10, are presented using the example of a wind farm pool. However, they can also be used for photovoltaic installations. In [67] the first investigations of the offering potentials potential have been conducted.

According to [60], six offering strategies are distinguished, three relating to day-ahead auctions and three for intraday auctions with a lead-time of one hour, as shown in blue below. The intraday auction is investigated since it is anticipated that an energy-only control energy market will be introduced in the near future, which will probably have a lead-time of one hour [64]. The day-ahead auction is studied here since the tertiary control reserve is already tendered on a daily basis. In the future, daily tendering of secondary control reserve is anticipated. For both time horizons, the intraday auction and the day-ahead auction, there are individual strategies named “full collateralization”, “partial collateralization” and “no collateralization”.

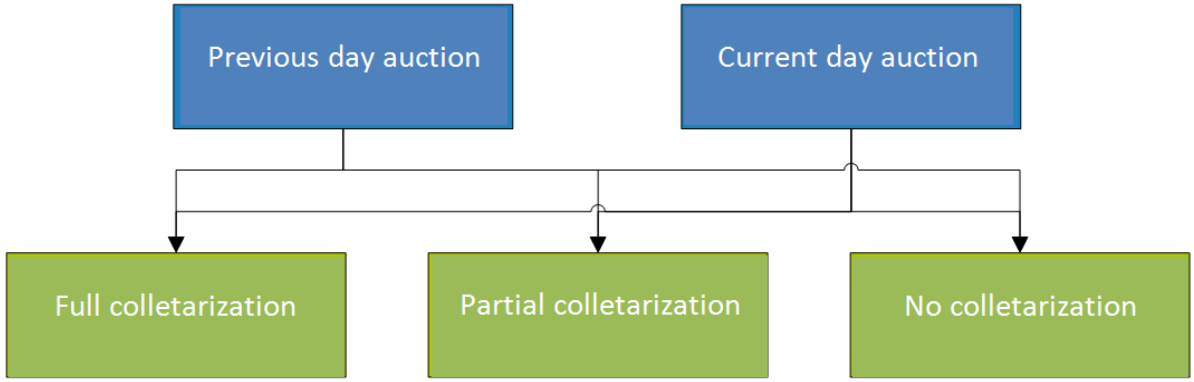

Figure 74: Overview of offer strategies

The strategy “full collateralization” requires the wind farm being part of a pool. The wind farm pool provides capacity that can be offered at a level of reliability of 99.8 %. If the largest output in the pool was (n-1)-collateralized and 20 % of the control reserve offered by the pool was collateralized (which may already be fulfilled by the (n-1)-collateralization), then the reliability of the pool’s offer would at least be 99.994 %.

The strategy “partial collateralization” requires that the probabilistic forecast of the wind farm pool is linked to the probabilistic forecast of other plants (e.g., methane power plants). Then the offer equals the output with a reliability rate of 99.994 %. The difficulty in this is the creation of the probabilistic forecast for the plants other than wind farms and PV systems. First evaluations of the development show that balancing effects can be accessed by pooling. These can be used to increase the offering potential in comparison to the individual participation in the control reserve market [66].

The strategy “no collateralization” requires that the wind farm pool offers the output corresponding to 99.994 % reliability. Evaluations show that 1 GW wind farm pool can offer an annual average of 3.7 MW (day-ahead auction) or 113 MW (current day auction). The Germany pool of wind farms, however, would have been able to offer 1.2 GW (day-ahead auction) or 3.7 GW.

Evaluations of offer strategies for day-ahead auctions show that the reliability can be increased if short-term forecasts are considered. This can be achieved by identifying possible violations of the day-ahead forecasts with the short-term forecasts for possible non-fulfilment (see Figure 75). The orange areas mark the only occasion during the year when the offer by German pool of wind farms would not have been available as offered. With the aid of probabilistic 1-h short-term forecast however, this would have been identified.

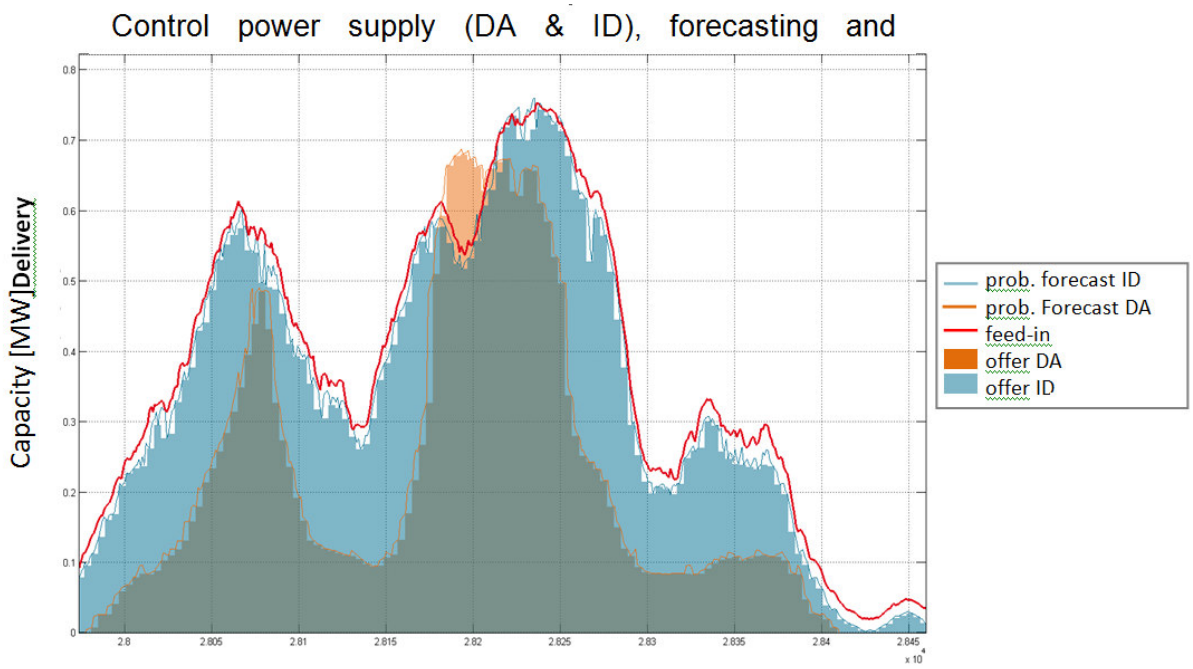

Figure 75: Illustration of probabilistic day-ahead forecast (orange) and 1-h forecast (blue) for a reliability of 99.994 % for the German pool of wind farms (30 GW)

The evaluation in [60] has shown that the offering potentials increase with decreasing product lengths and lead-time. Furthermore, the potentials depend on the size of the pool. This influence is less pronounced with decreasing lead times.

3.1.3.11 Conclusions for the further development of control reserve markets

The following conclusions and recommendations can be deduced from the study:

1. The lead times, product lengths and auction periods on the control reserve market must be shortened, in order to integrate wind farms, PV systems and controllable high efficiency CHP power plants into the control reserves market.

2. Publishing annual and monthly summaries of anonymized quarter-hour time series of medium and highest dispatch prices (similar to capacity prices) increases transparency of the control reserve market.

3. Introduction of an additional intra-day energy-only balancing market is recommended, which would allow the integration of short-term low-priced flexibility into the control reserve market (possibly following the Danish model).

4. The balancing energy price system should be structured in such way that balance responsible parties with wind farms or PV systems are incentivised to use 15-minute product trading and shortest-term forecasts, but disincentives the balancing of forecast errors on the level of the balance responsible party.

5. Integration of large loads (e.g., electrolysers, power-to-heat) into the control reserves market, including the market for primary control reserve.

3.1.4 Simulation for reducing control reserve demand through improved forecasts

An important building block of achieving a 100 RE energy supply is a reliable prediction of the energy production of wind energy installations for up to 72 hours in advance. This supports the estimation of network utilization on the short-term basis and provides an estimate of the possible control reserve delivery of wind farms. In the project Kombikraftwerk 2, CUBE Engineering focussed on forecasts for the following day. The quality of forecasts for power input is subject to spatial and temporal variations depending on many factors (characteristics of position, specifications of the wind energy plant, weather forecasts), which have been verified by real observations.

Wind output forecasts can be generated individually, for single wind turbines or for entire wind farms, using artificial neural networks or physically models. The forecasts by artificial neural networks are based on generation time series observed in past for at least one year, to cover all seasonal variations and thus guaranteeing the adequate training of the artificial neural networks. Physical models in general and the applied physical-statistic CUBE model specifically, do not have to be trained as their simulation results do not dependent on historical observations. This allows for a higher temporal flexibility with positive effects on marketing concepts. Dies impliziert eine Erhöhung der zeitlichen Flexibilität, was sich positiv auf Vermarktungskonzepte auswirkt

It is the aim of this study to verify the quality of the output of the neural network approach (Fraunhofer IWES) if this is trained with synthetic production time series of the CUBE-model, instead of real life observations. This approach aims at generating time series prior to the commissioning of a

wind farm in order to train the neural networks and thus be able to make feed-in forecasts shortly after commissioning (Figure 76).

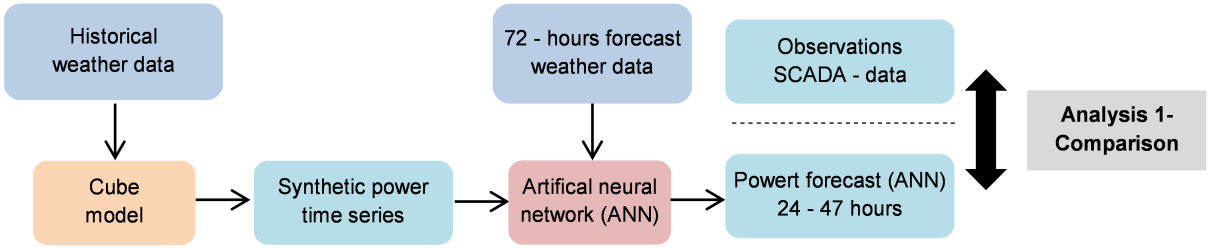

Figure 76: Scheme of analysis 1

Furthermore, in this study the modelled outputs are compared, one the one hand based on the CUBE model and on the other on neural networks. The ability of the models to describe the temporal and spatial variability in reality (Figure 77) is the focus.

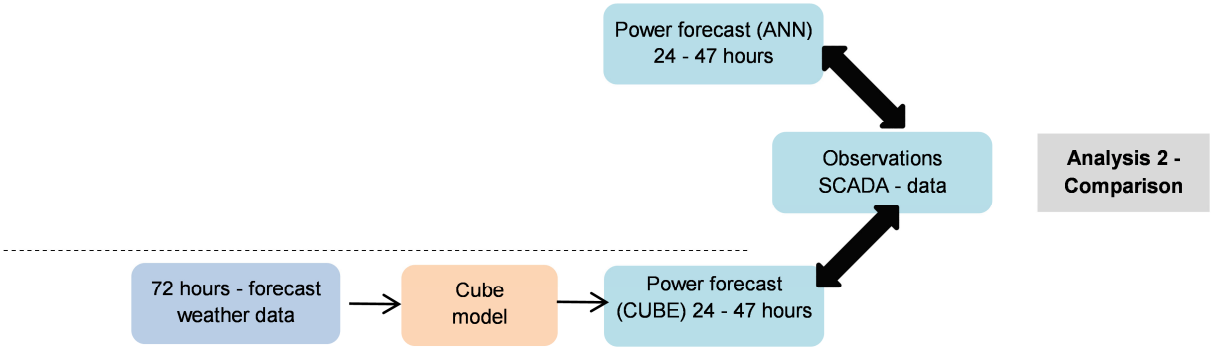

Figure 77: Scheme of analysis 2

Nine locations were analysed, for which the synthetic time series for the training of the networks were also compiled. The relevant SCADA data with a time resolution of 10 min were made available to CUBE by the project partner ENERCON. No individual wind turbines were studied, only entire wind parks. The locations and characteristics as well the relevant forecast-years are shown in Figure 78... Both models are based on forecasts of meteorological parameters by the German Weather Service (German: Deutscher Wetterdienst (DWD)) (COSMO-EU model), the forecast horizon is between 24 and 47 hours (forecast for next day).

Location	Characteristics	WEP-type (NH in m)	Forecast year
Wind farm 1	rolling hills	E-70/2MW (114)	2012
Wind farm 2	surrounded by forest	E-82/2MW (138)	2012
Wind farm 3	directly and indirectly influenced by forest	E-70/2MW (85,113)	2011
Wind farm 4	relatively even	E-70/2MW (98) E-82/2MW (138)	2011
Wind farm 5	relatively even	E-82/2,3MW(138)	2012
Wind farm 6	in forest	E-82/2MW (108)	2012
Wind farm 7	rolling hills	E-66/1,8MW (99)	2011
Wind farm 8	in forest	E-82/2MW (138)	2012
Wind farm 9	coastal location	E-66/15.66MW (67)	2009

Figure 78: Overview of wind farms used and table

As the SCADA data is the essential criterion for assessing the quality of the output forecasts, they were corrected and analysed in a preliminary step. During the assessment, it became evident that temperature data is not to be ignored. Figure 79 illustrates the dependency of the characteristic output curve with two selected classes of temperature. The blue line shows the average output of each class of wind speed for temperatures < 0°C and the orange line for > 20°C. The shape of the curve results from averaging. It can be seen that the output curve shifts to higher outputs with lower temperatures.

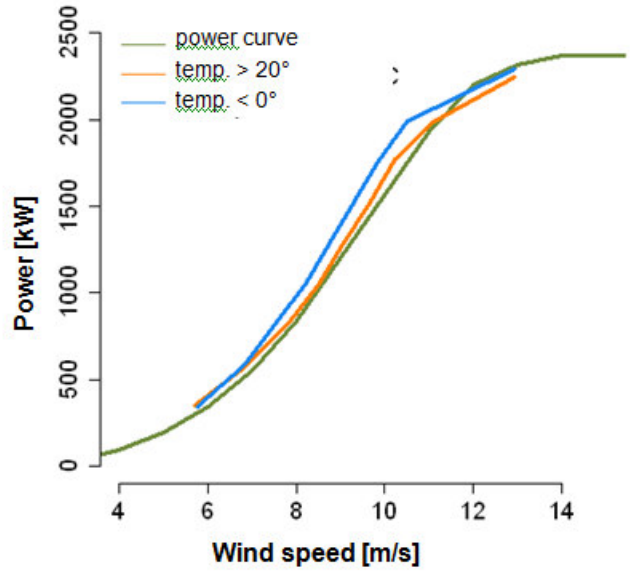

Figure 79: Characteristic output curve depending on temperature

Below the results of **Analysis 1** (Figure 76) are compiled. The output forecast is compared with the real observations (SCADA data).

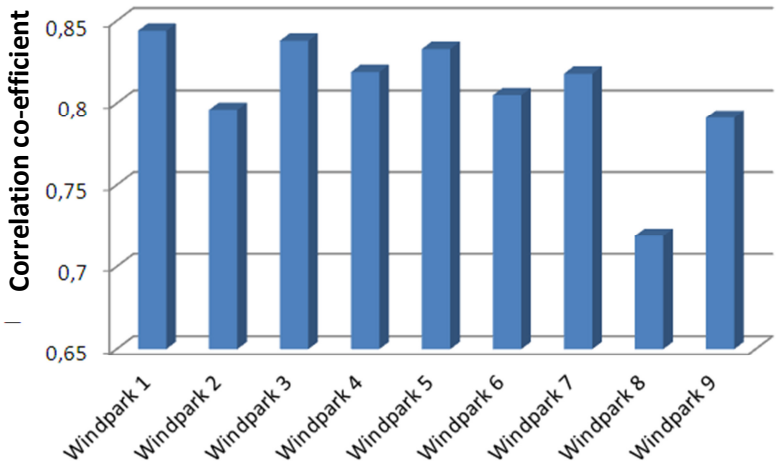

Figure 80: Correlation between forecast and observation

The first impression of the linear relation between forecast and observation shows the magnitude of the correlation coefficient for the nine wind energy parks studied, illustrated in Figure 80. With a correlation of 0.8 and more in six of the nine parks, a strong positive connection between forecast and observation can be seen; in the three other parks the linear connection is less distinct. The low correlation for wind farm 8 is caused by error propagation in the time series. The generation of the synthetic time series for wind farm 8, first the individual wind turbines were considered and then a time series was compiled for the entire wind park. For the other wind farms, the time series was modelled directly without the intermediate step. Below, wind farm 8 will continue to be shown, but will not be explained any further.

As the output depends on temperature in a way that cannot be ignored (Figure 79) the output is considered below not only for the entire period of study of a year but also monthly and for the time of day.

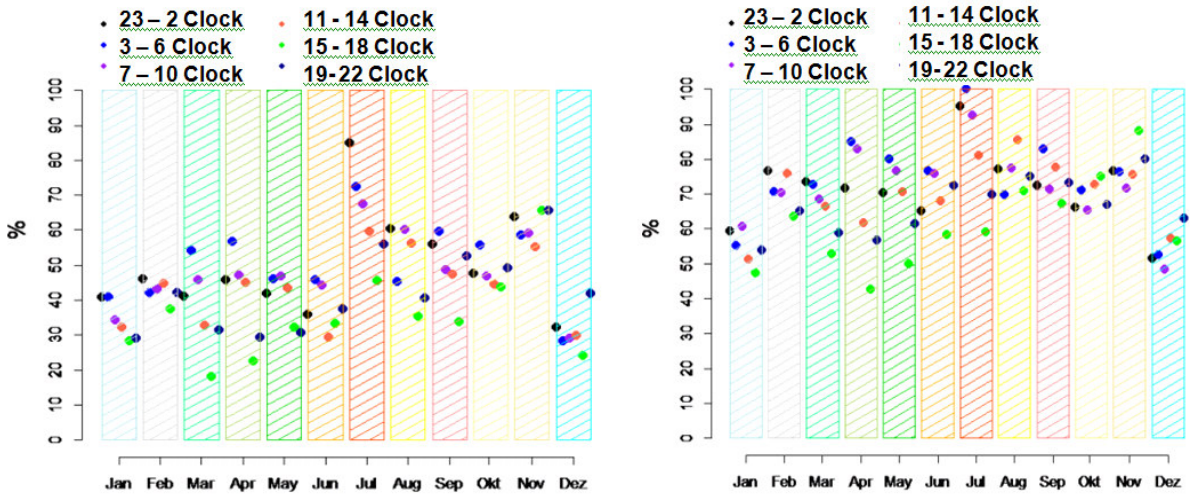

Figure 81: a) The difference between observation and forecast (set out in % of nominal capacity), smaller than 5 %. b) Difference between observation and forecast (set out in % of the nominal capacity) smaller than 10 % (in case of wind farm 3 – forecast year 2011)

An overview of the temporal and seasonal error distribution is given in Figure 81 (a) and (b) where the forecast for 2011 is illustrated in the example of wind farm 3. It is shown which percentage of the difference between observation and forecast are smaller than 5 % (or 10 %) of the nominal capacity of the wind farm. The number of these forecasts with relatively small errors fluctuates very strongly depending on the time of year (month) and time of day. For wind farm 3 the forecasts tend to be better during the night and better during summer months than in winter. However, this cannot be generalized when the analysis of the other wind farms are taken into account.

The 5% value (Figure 81 (a)) and the 10% value (Figure 81 (b)) give a good first impression and are compared in Figure 82 in order to compare the annual values of all wind farms. It can be seen that the number of forecasts with minor errors varies considerably from wind farm to wind farm. For wind farm 3, more than 40 % of the forecasts are different to observation by less than 5 % of the nominal capacity. For wind farm 2 this value only is approximately 25 %. Apart from wind farm 3 and 8, the 5% value moves between 22 % and just above 30 %, the 10 % value between 50 and 60 %. That means that between 50 % and 60 % of all output forecast values show a difference to the observed output of less than 10 % of the nominal capacity (exception Park 3).

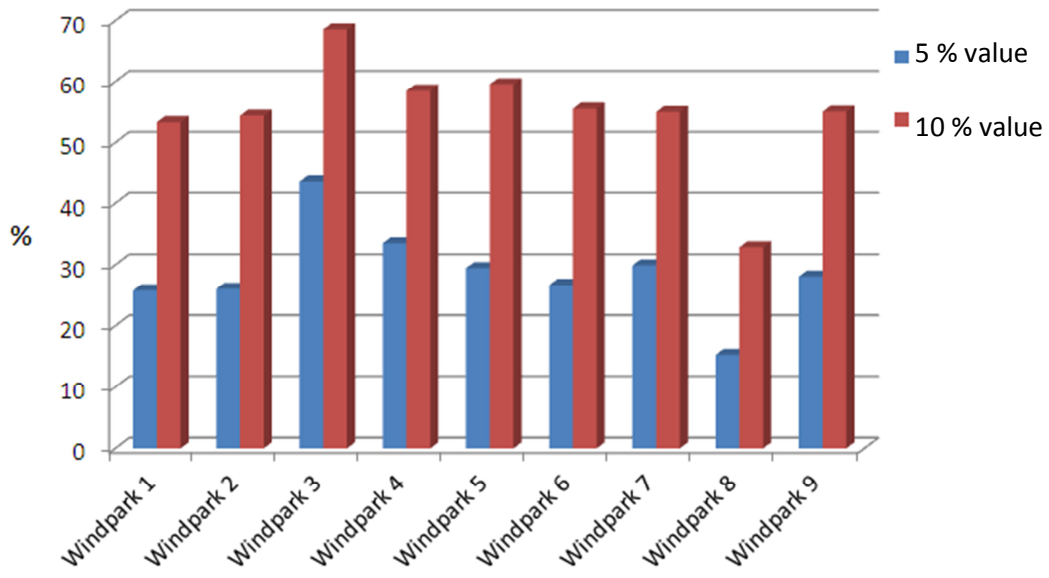

Figure 82: 5% and 10% value of all wind farms

In order to evaluate the quality of the forecasts, which belong to the 5% or 10% groups, the RMSE – with regard to the nominal capacity – is determined for these forecasts. The RSME is a measure used frequently for forecast quality assessment and is based on the squared difference between forecast and observation:

$$RMSE = \frac{1}{nominal\ capacity} * \sqrt{\frac{\sum(forecast_t - observation_t)^2}{n}}.$$

For an evaluation of the RMSE, it is necessary to include the forecast horizon. The wind power forecasts were generated using forecasts of meteorological parameters of the regional model COSMO-EU. The forecast horizon was 24 hours to 47 hours (forecast for next day).

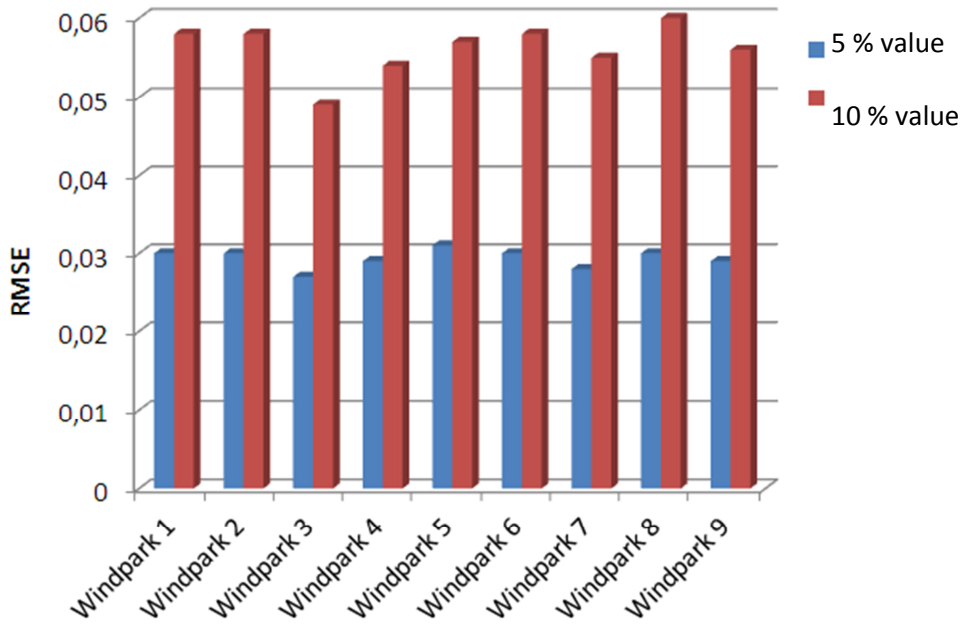

Figure 83: RMSE of the 5 % and 10 %-value of all parks

Figure 83 shows the RSME of the 5% and 10% values of all wind farms. According to [93], the RSME of Germany's total wind power feed-in is approximately 5 % of the installed capacity, where this value refers to the day-ahead forecast. For the evaluation of the RMSE for individual wind farms, it is important to note that the error in all of Germany is definitely smaller than the error observed at the individual wind farm level, due to balancing spatial effects of the forecast errors. Based on this RMSE analysis, both the 5% values with one RMSE below 3 % and the 10% values with an RMSE of between 5 % and 6 % must be judged as "very good" forecasts. In summary, the result of Figure 82 and Figure 83 shows that approximately 22 – 30 % of all forecasts have an RMSE smaller than 3 % of the nominal capacity and between 50 and 60 % of all forecasts have an RMSE smaller than 5.8 % of the nominal capacity.

A different picture is given by the RSME across all values of the forecast period. This was to be expected, since errors are quadratically weighted in the RMSE. In Figure 84, the RMSE is illustrated as an example for wind farm 4, depending on different months and time slices. The forecast horizon lies between 24 and 47 hours, so that the RMSE lies within the expected scope for individual wind farms with values of between 10 % and 25 %. The RMSE shows fluctuations both depending on the time of day and also in relation to the month. However, these fluctuations differ from one wind farm to the next. No functional relationship could be identified.

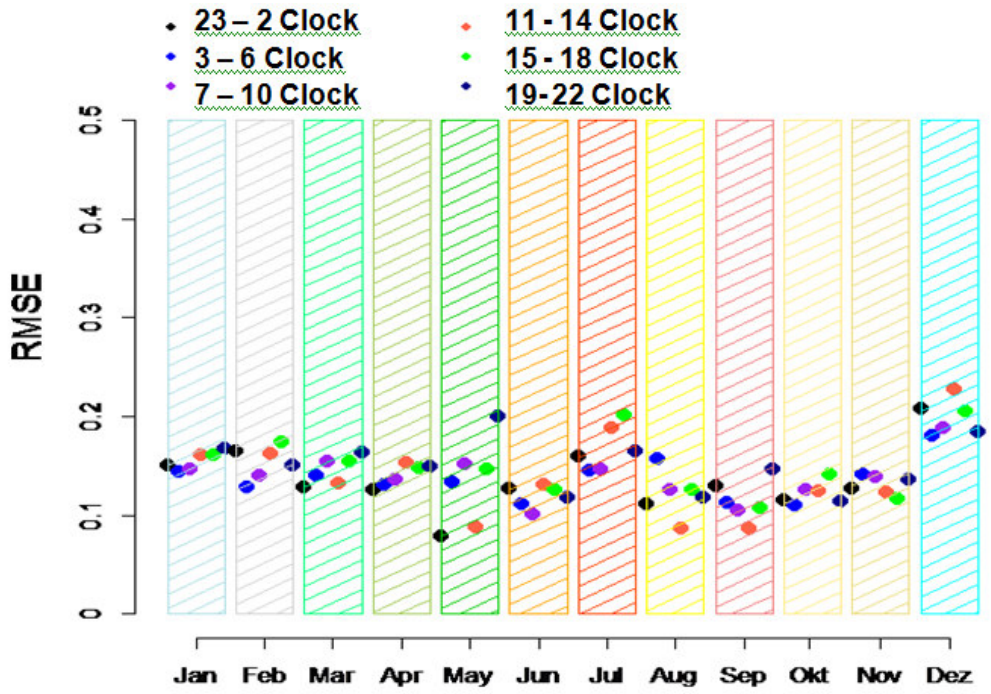

Figure 84: RMSE of the forecast for wind farm 4 – 2011

Figure 85 shows the RMSE for all wind farms. As was have already seen in the study of the 5 % and 10 % values, wind farm 3 stands out with a particularly good forecast. In the light of the forecast horizon of between 24 and 47 hours, the average RMSE for all wind farms can be seen as satisfactory with approximately 15 %, and also in relation with different regional conditions.

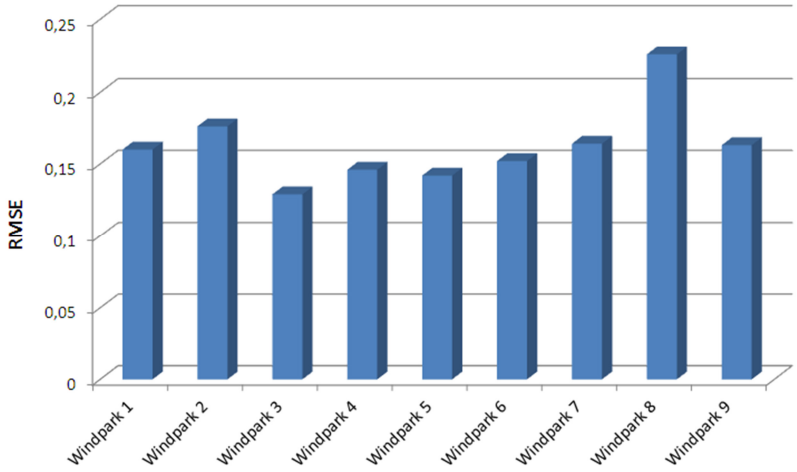

Figure 85: RMSE of forecast for all parks

The second analysis (Figure 77) compares the output generated by the artificial neural networks to the CUBE model outputs. The RMSE is used again to measure the data quality based on specific wind classes. The analysis of the modelled output, depending on wind speed, delivers an insight into the structure of the forecast models.

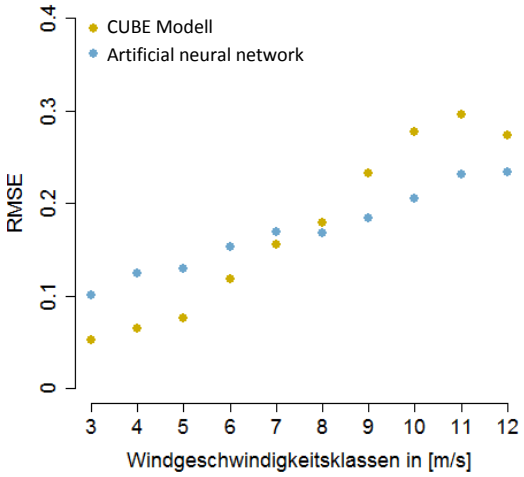

Figure 86: Wind-class specific RMSE for Park 4

Figure 86 shows the wind class specific RMSE using the example of wind farm 4. The RMSE differs from one wind farm to the next due to location-specific conditions. Depending on wind speed class, it can be observed that for all wind farms studied the increases in RMSE is less steep for the neural networks than for the CUBE model. From approximately 8 m/s onwards, the results from the neural networks have a smaller error, whereas below the CUBE model performs better.

The wind farm related analyses of the yield forecasts of the neural network – based on synthetic outputs of the CUBE model (analysis 1) – show a good correlation between the observation and forecast with correlation coefficients of between 0.78 and 0.84. Approximately one third of the forecast errors deviate from the nominal capacity of the park by a maximum of 5 % and is thus considered sufficient. There is an connection of the output forecasts quality to seasonal and time-of-day specific components (Figure 84). This link however has is influenced by park-specific components, which does not allows a clear conclusion in this study. It was shown that the synthetic output time series generated by the CUBE model are well suited as input for training the neural networks.

The comparison between neuronal networks and the CUBE model (analysis 2) shows that both models have their specific strengths and weaknesses. Further adjustments of the models and differentiated studies are needed in order to identify the origins of the differences between the two models. Overall, it is apparent that the quality of the models depends on numerous factors, which are not included in detail here. Within the scope of further studies, it is conceivable to link the two models to benefit from synergies. The essential factor for the quality of output forecasts is indeed the predicted wind speed, which must always be seen in relation to the particular weather conditions. Through this other meteorological parameters, such as the temperature and pressure gradients, also gain importance. Independent of the model approach or possible model-linking an optimization of meteorological input parameters is paramount, and attention should be paid to this in further studies.

3.1.5 Simulation of control reserve demand in 100% RE scenario

In this section the control reserve capacity demand for the 100 % renewable power supply scenario of Chapter 2 is determined. The results are to be found in section 3.1.5.2. In section 3.1.5.1, the current methodology as an innovative methodology for the determination of control reserve demand is described and applied.

It can be assumed that the demand for the necessary control reserve capacity would increase if the current dimensioning method was applied. This is due to the increasing share of weather-dependent RE in the future and the limited predictability of their feed-in beyond certain time horizons. Currently the demand for secondary control reserve and tertiary control reserve is dimensioned by TSOs using the Graf-Haubrich methodology ([68], [69]). The underlying idea is that there are various errors, which cause the control reserve demand. For these errors, probability density distributions are created, which are then combined to form an total probability density distribution, using a mathematical process (convolution). The errors taken into account are:

- Load noise: Load noise is the difference between a one-minute load and the 15-minute average of the load. The probability density distribution is determined by using a measurement of the vertical net load with the temporal resolution of one minute.
- Schedule step errors: This error is caused by the exchange of electrical energy with foreign countries. If at an hour-change a deviation occurs in the exchange of electrical energy, the change in the exchange is assumed a ramp. However, there are deviations from this assumption, which are taken into account via this error.
- Plant outages: This error is caused by power plant failure.
- Forecast errors: Forecast errors can be seen as consisting of wind, photovoltaic and load forecast errors. The distribution of errors is generated by using the deployed secondary operational reserve and tertiary control reserve.
- Hour-jumps: This error is due to the management of balancing responsible parties that produce hour products. As load varies within an hour, inevitably differences arise to the traded hour products, which have a constant value. These differences must be balanced by control reserve.

In order to determine the demand for secondary control reserve, the load noise, schedule jumps, power plant outages and the hour jumps are convoluted to form a joint error distribution. Using a defined surplus and deficit level, the demand for positive and negative secondary control reserve can be determined.

In order to determine the demand for tertiary control reserve, first the forecast errors, the load noise, the scheme schedule jumps and the plant outages are linked to form an overall error distribution. Here, too, the total positive and negative reserve is determined by using a surplus and deficit level. The difference between positive/negative total reserve and positive/negative secondary control reserve equals the demand for positive/negative tertiary control reserve.

As the control reserve demand is determined by using historical data, which cannot be extrapolated to different deployment levels of renewable energies, the demand for future scenarios cannot be determined using the Graf-Haubrich method. Therefore, in studies that determine the future demand a modified Graf-Haubrich method is used where forecast errors are differentiated as wind, photovoltaic and load forecast errors [16]. This method has been used here.

The disadvantage of the Graf-Haubrich method is that the demand for the following three months is dimensioned from past data. In this way, no forecasts for the feed-in from wind energy and photovoltaics can be used. Thus in this study, in addition to the modified Graf-Haubrich method (static method) a new approach has been developed and applied (dynamic method).

The concept behind the **dynamic method** is that the demand for every hour of the following day is dimensioned daily. In this way, forecast-dependent error distributions can be used. As tertiary control reserve is mostly tendered on an a daily basis already, and secondary control reserve will probably also be tendered daily in future, this is a realistic assumption.

In both the dynamic and the static method, the hour-error is disregarded. That can be justified as this error will become irrelevant in the future [70] since trading of 15-minute products solves the underlying error.

3.1.5.1 Description of process and data used

Below, the determination for error distributions of the dynamic and static method are compared

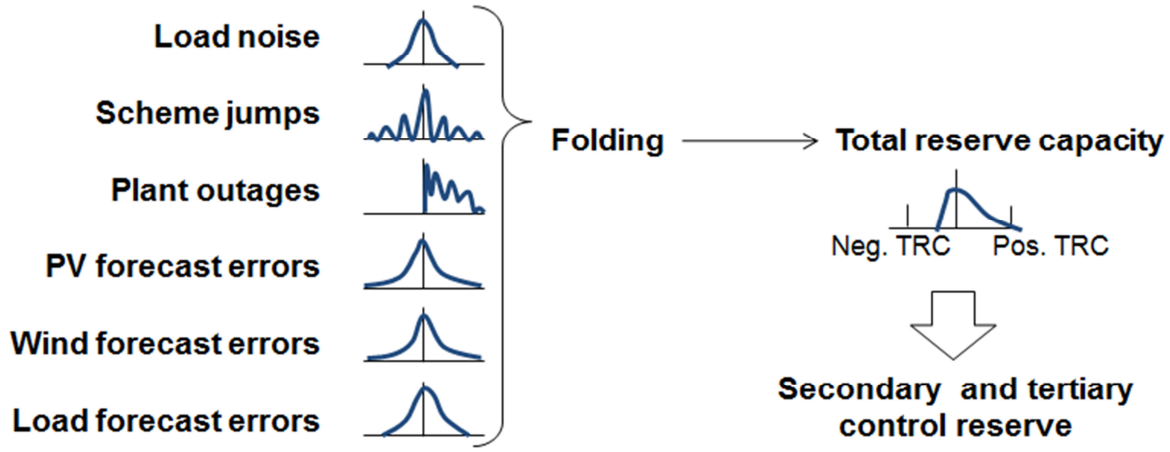

Figure 87: Method for dimensioning the static and dynamic demand for control reserve

Load noise

It is assumed that load noise is a Gaussian distribution with an expected value of 0.

The standard deviation amounts to 0.4 % of the annual peak load (static) or 0.4 % of the forecast load for any particular hour (dynamic) [16]. For the dynamic method, the load of a particular hour is used that is available in a time series.

Schedule step errors

Every hour has five schedule step errors as electricity is traded at 15-minute intervals. That is why in the dynamic method five quarter-hour jumps of each hour a used. Only half of the first and the last jumps come in because half of them lie in another hour's interval. In the case of the static method, all schedule step errors of the whole year are utilized. The error distribution is created using the ramp model [68].

The exchange with other European countries is determined by the power plant operational unit commitment planning. As this exchange of electricity is scheduled hourly, an interpolation delivers 15-minute values.

Power plant outages:

For the simulation of power plant outages, the distribution of methane power plants via the super grid nodes of the scenario (see Figure 42) is taken into account. For both the static and the dynamic method, initially an error distribution for each power plant is calculated; for the dynamic method only those power plants are included that are in operation at the particular hour. The error distribution consists of an outage probability, a partial outage probability, and a probability for normal operation. The probabilities are associated with the relevant capacity values. For instance, the probability for normal operation is associated with the nominal capacity. Individual error distributions are then linked to form a common error distribution for power plant errors (convolution).
For the dynamic method, feed-in time series of the methane power plants are used. The error time series needed to produce (partial) outage probabilities and the reduction in output in case of a partial outage can be seen in [68]. Full load hours are assumed to be 4,000 hours.

Load forecast errors

Equivalent to the load noise, it is assumed that the load forecast error will behave according to a Gaussian distribution. The standard deviation is 0.8 % of the highest annual load (statically) or 0.8 % of the forecast load for any relevant hour (dynamic) [16]. For the dynamic method, the load of the relevant hour is used for which there is a time series available. For the static method, the highest annual load is used.

Wind forecast errors

There is a great difference between the static and the dynamic method with regard to wind forecast errors. Nevertheless, for both methods the nRMSE scaling and kernel density estimation are required.

The **nRMSE-scale** is required if historical time series of the wind forecast error used for dimensioning has a nRMSE deviating from the nRMSE in the scenario.

The nRMSE is an indicator of the quality of an estimate and can thus be applied to a forecast. The nRMSE is calculated as follows:

$$nRMSE = \frac{\sqrt{\frac{\sum_{i=1}^{n}(x_{1,i}-x_{2,i})^2}{n}}}{x_{max}-x_{min}} x_1$$

x_1 is the estimator or forecast, and x_2 is the real value. n is the number of samples and x_{max} and x_{min} are maximum or the minimum value of the sample. With the static method, the 1-h forecast error is multiplied by the nRMSE-factor:

$$nRMSE\ factor = \frac{nRMSE_{scenario}}{nRMSE_{historical_{time}series}}.$$

For dynamic dimensioning two time series are used: The 1-h forecast error and the day-ahead forecast because the estimate of the 1-h forecast error is based on the day-ahead forecast. Exactly as with the static method, with the dynamic method the 1-h forecast error is multiplied by the nRMSE factor. In case of the day-ahead forecast, only the forecast error is multiplied by the nRSME factor. The forecast error that has been changed thus is then added to the feed-in in order to obtain the new forecast time series.

Using **the kernel density estimation** [71] a continuous distribution can be created from the sample. In case of the static method, the kernel density estimation is used to generate an error distribution of the 1-h forecast error. For the dynamic method, a two-dimensional error distribution is generated. One dimension is the day-ahead forecast; the other dimension is the 1-h forecast error.

Below, the kernel density is described using the dynamic method. Each value pair of data of the historical time series of the day-ahead forecast and 1-h forecast error is replaced by a two dimensional Gaussian kernel. All Gaussian kernels are then added to form a joint distribution.

$$f(y_1, y_2) = \frac{1}{n}\sum_{i=1}^{n} \frac{e^{-\frac{1}{2}(\frac{y_1-y_{1,i}}{h_1})^2}}{h_1\sqrt{2\pi}} \cdot \frac{e^{-\frac{1}{2}(\frac{y_2-y_{2,i}}{h_2})^2}}{h_2\sqrt{2\pi}}$$

f is the probability for the value pair (y_1, y_2). y_1 is the 1-h forecast error, y_2 the day-ahead forecast and n is the number of samples. h_1 and h_2 are the bandwidths for the 1-h forecast error and the day-ahead forecast error. The bandwidth must be greater than zero. The bandwidth h_1 is calculated as follows:

$$h_1=\left(\frac{4}{(d+2)n}\right)^{\frac{1}{d+4}}\sigma_1$$

The bandwidth h_2 for the day-ahead forecast is calculated using the same equation. d is the number of dimensions. In the dynamic method $d = 2$, with the static method $d = 1$. σ_1 is the standard deviation for the 1-h forecast error, which must also be calculated for the day-ahead forecast. The use of a robust estimate of the standard deviation allows the handling of possible extreme values. Thus, the standard deviation is calculated using the following equation:

$$\sigma_1 = \frac{median|y_{1,i} - \tilde{y}_1|}{0{,}6745}$$

$\tilde{y}_1$ is the median of the sample. The standard deviation of the day-ahead forecast is also calculated using this equation.

In a last step, based on the day-ahead forecast, the corresponding distribution of the forecast value is cut out of the two dimensional kernel density estimation. This distribution of the 1-h forecast error, which depends on the day-ahead forecast, is included in the dimensioning.

In case of the static method, the calculation of the error distribution, using kernel density estimation is reduced to:

$$f(y_1) = \frac{1}{n}\sum_{i=1}^{n}\frac{e^{-\frac{1}{2}\left(\frac{y_1-y_{1,i}}{h_1}\right)^2}}{h_1\sqrt{2\pi}}$$

Figure 88 illustrates an example of a two-dimensional kernel density estimation for the wind forecast error. It can be seen that the forecast error is small with both a high and a low forecast value.

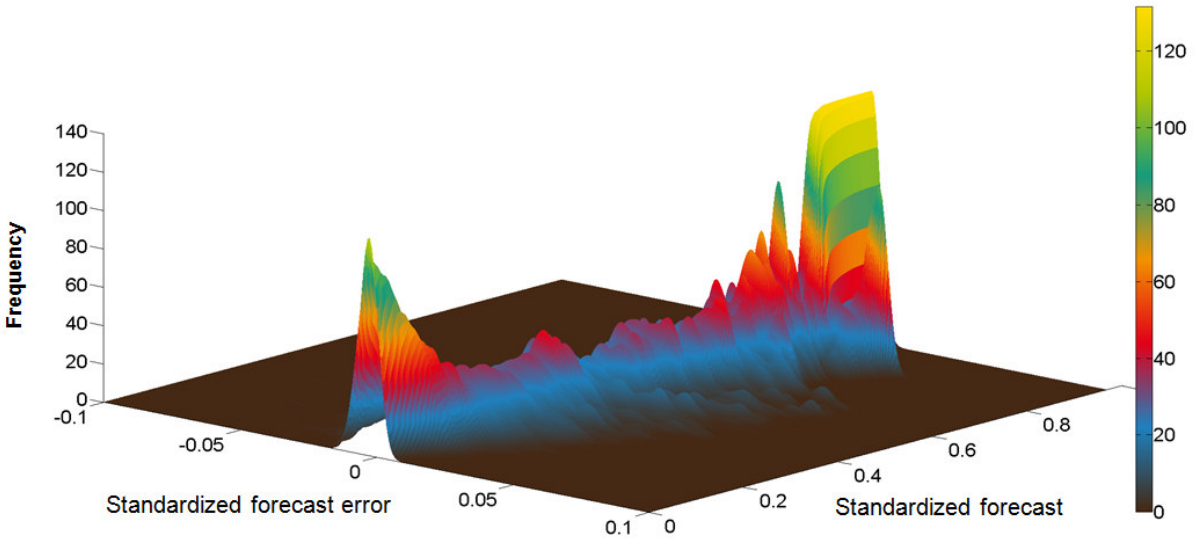

Figure 88: Illustration of a two-dimensional kernel density estimation for the wind forecast error

The historical time series for kernel density estimation are the forecast and feed-in values of the year 2010 for Germany. The day-ahead forecast and the feed-in values from wind energy can be found on

the EEX transparency platform [72]. For the generation of a short-term forecast a model developed at IWES was used, which was utilized e.g. in [90]. Because no forecasts were generated for the 100% RE scenario, the feed-in time series produced for the scenario, the day-ahead forecast is used for dimensioning. As the mean and the fluctuations around the mean are similar for the forecast and the feed-in, the use of feed-in instead of forecast will hardly influence dimensioning.

For the scenario, the nRMSE of 0.86 % assumed in [16] is set as maximum nRMSE of the 1-h forecast [16]. As this value applies to the year 2010, for the 100% RE scenario a mean (0.78 %) and a minimum nRMSE (0.69 %) are assumed. This is justified by forecast improvements due to an increased share of online-measuring of wind farms. Dimensioning is implemented for an nRMSE of 0.78 %, the maximum and minimum nRMSE are used for a sensitivity analysis. For the day-ahead errors, no improvements are assumed because in this case a more vigorous online capture is irrelevant.

Photovoltaic forecast errors

In producing an error distribution for the photovoltaic error, the method is identical as for wind forecast errors. The only difference is that for the dynamic method, the day-ahead forecast is not used directly but rather a day-ahead forecast value standardized for the feed-in performance. The maximum feed-in performance is given by the position of the sun. The advantage is that in this way it can be taken into account that, for instance, with maximum feed-in during morning hours no negative control reserves needs to be available. If only the performance was taken into account, this advantage could not have been realized as maximum feed-in during the morning hours corresponds to an average mid-day feed-in where negative control reserve must be available.

The historical time series for the kernel density estimation are the forecast and feed-in values of the year 2010 for Germany. The day-ahead forecast and the feed-in values from photovoltaics also can be found on the EEX transparency platform [72]. The 1-h forecast is calculated using a model that was constructed within the scope of a Master's thesis at IWES [91]. The model determines the short-term prognosis P_{PP} for the time $t + x$, having taken into account the last measured performance value $P_{feed-in}$ at the time t and the day-ahead forecast P_{DA} for the times $t + x$ and t.

$$P_{STF}\,(t+x) = P_{feed-in.}(t) + (P_{DA}(t+x) - P_{PDP}(t)) \cdot \frac{P_{feed-in.}(t)}{P_{DA}(t)}$$

An exception is made during morning hours as the term $\frac{P_{feed-in.}(t)}{P_{DA}(t)}$ can become very small or large here due to the low absolute values of both performances. To deal with this problem, for day-ahead forecast values smaller than 20 % of the maximum day-ahead forecast value a different approach is used. For this, the forecast value results from multiplying the day-ahead forecast with a factor and the above equation is multiplied by a 1-h factor. The factor is the quotient from the ratio between the day-ahead forecast value of the relevant hour and 20 % of the maximum day-ahead forecast value. Furthermore, short-term forecast values greater than the maximum feed-in given by the solar altitude are limited to the maximum feed-in. Using this method an nRMSE of 1.65 % could be obtained for the 1-h short-term forecast. The feed-in values required for dynamic dimensioning of photovoltaics may also be found in the 100% RE scenario.
The obtained nRMSE of 1.65 % is set as the maximum nRMSE for the 100% RE scenario. As solar irradiation forecasts have bigger errors than wind forecasts [76], an additional 30 % are added onto

the minimum and medium nRMSE for the 1-h wind forecast to obtain the medium and minimum nRMSE for the 1-h photovoltaic forecast. The medium nRMSE is thus 1.01 % and the minimum 0.89 %. The medium nRMSE is used for the dimensioning. The minimum and maximum nRMSE were used for sensitivity analyses.

Safety levels and scaling of the wind, photovoltaic, and load forecast error

In accordance with [69], for the entire reserve 0.0225 % is set as deficit / surplus probability and 0.0025 % for secondary control reserve.

In order to bring the ratio between secondary reserve and tertiary control reserve to a level comparable to the current one, the wind, photovoltaic, and load forecast errors are also taken into account in the dimensioning secondary control reserve. The distribution of these errors is multiplied by the factor 0.33 and is subsequently included into the convolution for the calculation of the distribution of secondary control reserve. The derivation of the factor is described in [6].

3.1.5.2 Results

Figure 89 and Figure 90 illustrate the results of the dynamic (continuous line) and the static (dotted line) method for the purely renewable power supply scenario from Chapter 2. Figure 89 comprises the results for the positive, and Figure 90 the results for the negative total reserve. The total reserve is equal to the sum of tertiary control reserve and secondary control reserve.

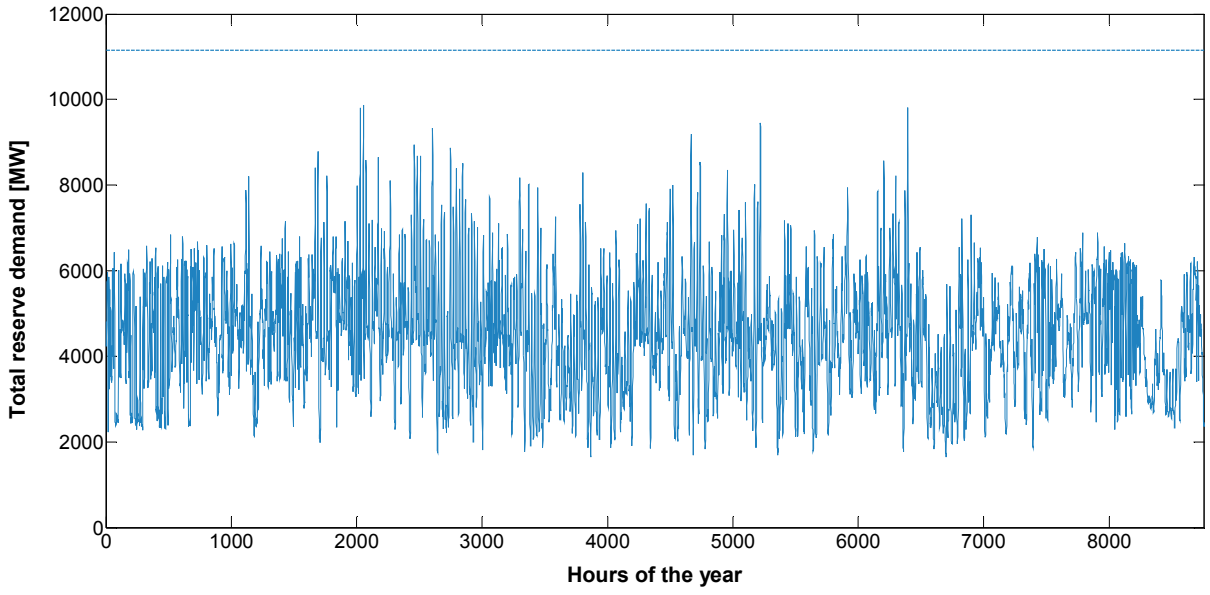

Figure 89: Progress for positive total reserve demand for the scenario year according to the dynamic (continuous line) and the static (dotted line) method

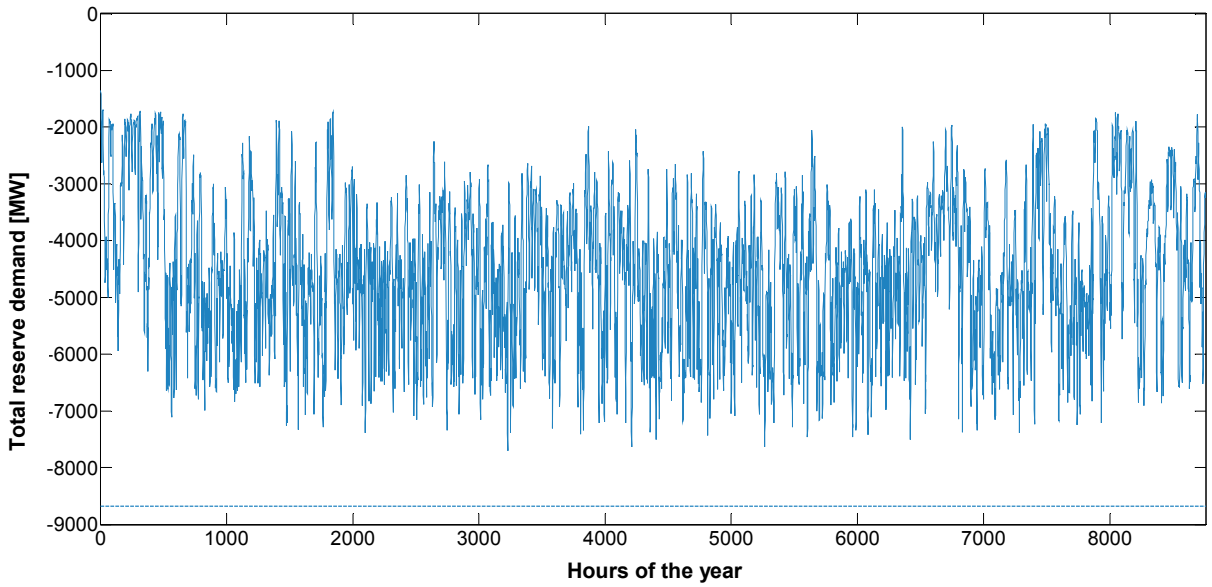

Figure 90: Progress for positive total negative reserve demand for the scenario year according to the dynamic (continuous line) and the static (dotted line) method

The results are remarkable:

- The average demand according to the dynamic method lies far below the demand according to the static method of 8.674 MW (neg.) and 11.149 MW (pos.) although the same level of reliability is applied.
- The maximum demand according to the dynamic method of 9.870 MW (pos.) and 7.702 MW (neg.) also lies below the demand according to the static method.
- The minimum demand according to the dynamic method of 1.650 MW (pos.) and 1.347 MW (neg.) even lies even below the currently tendered control reserve demand of approximately 4.500 MW.

Table 18 shows a comparison of the static and the dynamic method. The control reserve demand during the 4th quarter of 2012 is also illustrated.

Table 18: Comparison of the total reserve demand and the demand for tertiary control reserve, primary and secondary control reserve. The demands according to the static and the dynamic method are compared with the demand during the 4th quarter of 2012.

	Static (100% RE)		Dynamic (100% RE)		Demand (4th quarter 2012)	
	Pos. [MW]	Neg. [MW]	Pos. [MW]	Neg. [MW]	Pos. [MW]	Neg. [MW]
Ø total reserve	11.149	8.674	4.488	4.490	4.535	4.562
min total reserve	-	-	1.650	1.347	-	-
max total reserve	-	-	9.870	7.702	-	-
Ø Second control reserve	4.593	3.848	2.031	2.022	2.109	2.149
min Second control reserve	-	-	795	820	-	-
max Secondary control reserve	-	-	4.437	4.435	-	-
Ø Minute control reserve	6.556	4.826	2.457	2.468	2.426	2.413
Min Minute control	-	-	188	125	-	-

The advantage of the dynamic method can also be seen in the comparison of the table. If the static method were to be applied in the future, the demand would approximately double for the 4th quarter of the year 2012. The dynamic method however manages to keep the average demand constant.

Influence of individual errors on the total reserve demand

In order to be able to assess the influence of the individual errors on the total reserve demand, the period 2.000 hours to 2.400 hours was considered in more detail. This period was selected on purpose because here the influence of photovoltaics would not be overestimated (summer) or underestimated (winter).

Figure 91 and Figure 92 show – apart from the total reserve demand - also the demand for the individual errors if the same level of reliability is set that is used for the dimensioning of the total

reserve demand. The sum of the individual errors is greater than the total reserve demand as balancing effects are accessed by the convolution, which reduce the reserve capacity demand.

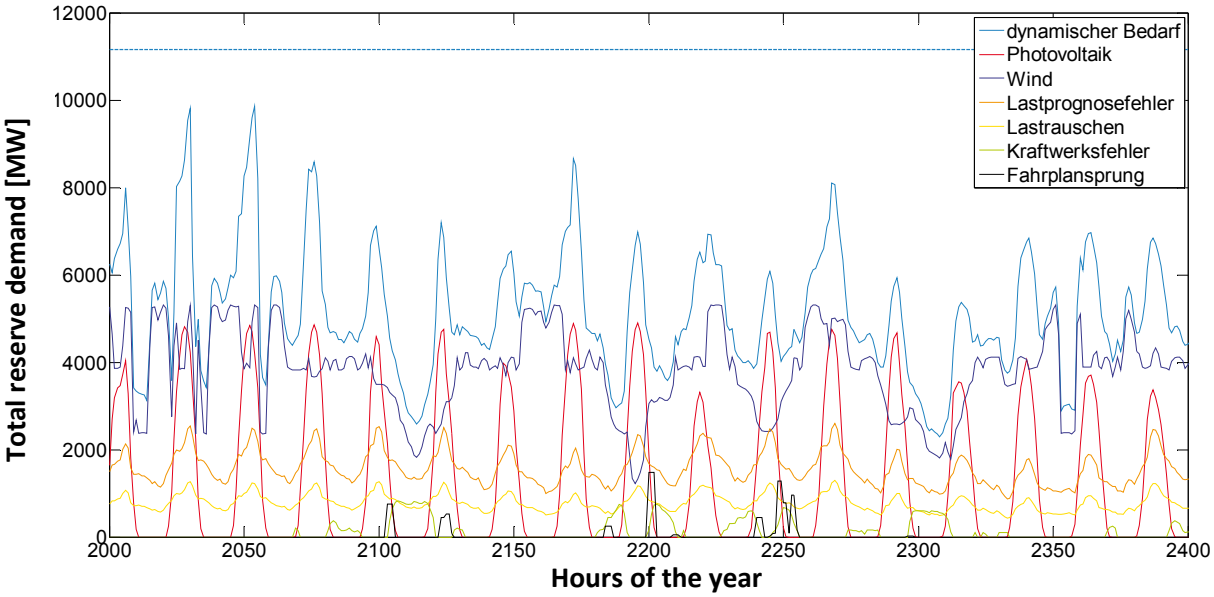

Figure 91: Illustration of the positive reserve demand and the demand for the individual errors

In Figure 91, it can be seen that the wind forecast error is the dominating error type. Furthermore, the trend of the load forecast error, the load noise and the photovoltaic forecast error show a daily cycle. This daily cycle can also be observed for the total reserve demand. A high total reserve demand always occurs when wind and photovoltaic errors are equally large. The power plant error and schedule step errors show little influence on the total reserve demand.

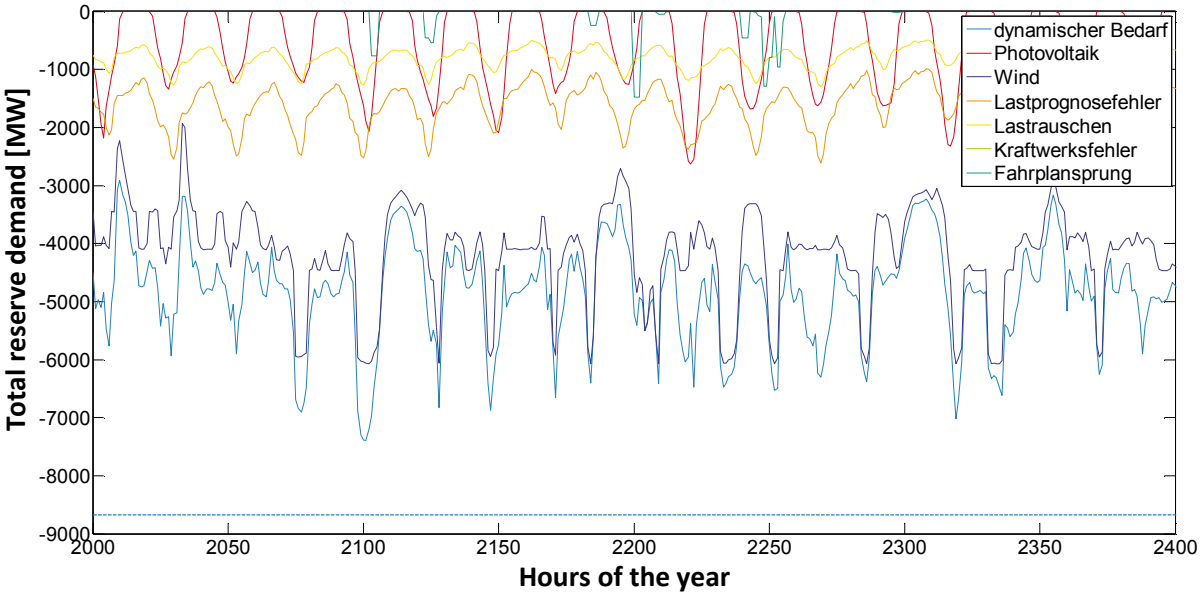

Figure 92: Illustration of the negative reserve demand and the demand for the individual errors

Based on Figure 92, showing the negative total reserve demand, it can be seen that the wind forecast error is also the dominating error. Here, too, photovoltaics and load forecast errors and load noise show a daily cycle. Together with the wind forecast error, these three errors are responsible for the peaks in total reserve demand. The schedule step errors show hardly any influence on the total reserve demand. The power plant errors do not apply in the case of negative control reserve.

Sensitivity analysis

For the sensitivity analysis, only variations in wind and photovoltaic errors are considered because they are the decisive factors as can be seen in previous evaluations.

Table 19: Comparison of average demand of total reserve with different nRMSE values of wind and photovoltaic forecast errors

		nRMSE wind forecast errors					
		0,69%		0,78%		0,86%	
		pos.[MW]	neg.[MW]	pos.[MW]	neg.[MW]	pos.[MW]	neg.[MW]
nRMSE photovoltaic errors	**0,89 %**	4.109	4.087	4.267	4.465	4.714	4.807
	1,01 %	4.172	4.113	4.488	4.490	4.774	4.831
	1,65 %	4.542	4.295	4.853	4.663	5.134	4.998

A maximum increase of the total reserve demand of 14.39 % (pos.) and of 11.31 % (neg.) results, compared to the reference values of 4.488 MW (pos.) and 4.490 ME (neg.). The minimum demand is 8.44 % (pos.) and 8.98 % (neg.) below the reference values.

Balancing forecast errors on the level of balancing responsible parties

Increasingly more wind and photovoltaic parks are marketed directly since the introduction of the market premium RE support scheme. The direct marketers are balance responsible parties that have the mandate to keep the balancing group schedule deviations as low as possible through thorough planning and forecasting applying best practice solutions [73]. There is no definition of best practice balancing for wind and photovoltaic parks. Shall forecast errors, which might arise after the last trading opportunity on the short-term spot market, be balanced by measures on the level of the balance responsible parties or not?

In order to help answer this important question, it was evaluated which additional control reserve demand would arise if the 1-h wind und 1-h photovoltaic forecast error were to be balanced by the balance responsible parties, using the dynamic and the static methodologies to establish. The additional control reserve demand arises due to the lack of balancing effects between different balance responsible parties if they have to balance the 1-h error themselves. Apart from the control reserve being dispatched by the TSO, reserve demand on the level of the balance responsible parties is also considered.

For the evaluation, it is assumed that all wind farms are located within one balancing responsible party and that all photovoltaic parks are located in another balancing responsible party. Further, it is assumed that balancing responsible parties have to balance out 1-h forecast errors to different degrees on balancing responsible party level. These are 95 %, 99 % and 99.95 %. With the static method, the distribution of the 1-h forecast error is utilized to read the performance on the safety levels 95 %, 99 % and 99.95 %. All other remaining errors must be covered by the TSOs. This is included in the calculation for control reserve demand, which takes into account that some of the

errors have already been balanced by the balancing responsible parties. The difference to the dynamic method is that here a forecast-dependent 1-h forecast error distribution is used.

In Figure 93, the clear increase in control reserve demand according to the static method can be seen when the 1-h forecast error is balanced on the level of the balancing responsible party. The bigger the degree of balancing on the level of the balancing responsible party is, the more the reserve demand increases.

With the dynamic methodology, the increase in demand for control reserve is different for every hour. On average the demand increases by 23.25 % (positive) and 17.56 % (negative) with a 99% share of the balancing on the level of the balancing responsible party.

The evaluations show that balancing the 1-h forecast error would cause a significant increase in the control reserve demand. For that reason, is not desirable to create regulations or financial incentives through the balancing energy pricing that would to increase the balancing efforts of the 1-h forecast error on the level of balancing responsible parties.

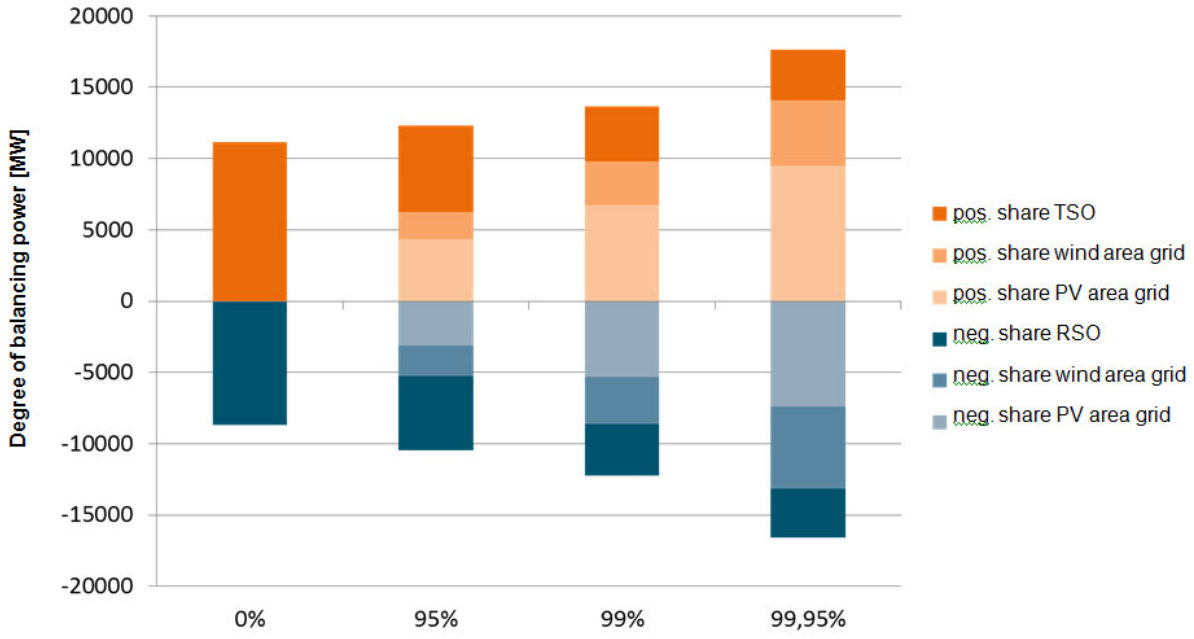

Figure 93: Control reserve demand with varying degrees of balancing the 1-h forecast error for wind energy and photovoltaics on the level of balancing responsible parties, utilizing the static method

Primary control reserve

The demand for primary control reserve is calculated by the ENTSO (European Network of Transmission System Operators for Electricity) and is addressing the outage of the two largest power plants in Europe. This capacity requirement is subsequently distributed to the countries in proportion of their individual share in the total power consumption of the UCTE area [74]. Germany's share amounted to ±592 MW in 2012 [75]. It is assumed that the demand for primary control reserve in the 100% RE scenario is not going to change, when compared with current demand.

3.1.6 Simulation of meeting demand for control reserve in the 100% RE scenario

For the calculation for meeting the demand for control reserve in the 100% scenario from Chapter 2, the power plant commitment plan by Siemens was used. For meeting the demand, the following power plant technologies are considered in the scenario: Methane power plants, biomass power plants, power-to-gas plants, batteries, pumped hydro storage and wind farms and photovoltaic parks. It is assumed that wind farms and photovoltaic parks provide control reserve according to the method “available active power” (see section 3.1.2.1).

Each plant can only supply a certain part of its capacity as control reserve. For the individual plants these parts are:

Wind- and photovoltaics parks

- Positive control reserve: the available active power minus the feed-in power yields the potential for positive control reserve.
- Negative control reserve: The potential is equal to the feed-in.

Pumped hydro storage and batteries

- Positive control reserve: The potential is equal to the maximum generation capacity minus the current output. In addition, the output of control reserve is limited by current storage fill state. Capacity can only be offered if the necessary energy for a complete hour is in the storage.
- Negative control reserve: The potential is equal to the maximum energy demand minus the current output. Storage capacity limitations are applied equally.

Power-to-gas plants

- Positive control reserve: The potential is equal to the energy demand.
- Negative control reserve: The potential is equal to the difference between the maximum energy demand and current energy demand.

Localized bio-energy plants

- Positive control reserve: The potential is equal to the difference between the nominal capacity of plants connected to the grid and their current feed-in. Because of the load gradients of these plants, the limitation exists that at maximum only ±20 % of the nominal capacity can be offered as primary control reserve.
- Negative control reserve: The potential is equal to the current feed-in. As with positive primary control reserve here, too, a limit of a maximum of ±20 % of the nominal capacity applies due to gradient limitations.

Methane power plants

- The production of control reserve from methane power plants is subject to the same conditions as bio-energy plants. Only the flexibility for primary control reserve is limited to 5 % of the nominal capacity as is typical for large, thermal plants with steam cycles.

The provision of control reserve is calculated during the general unit commitment planning of the scenario, see Chapter 2.1. The optimization goal of this calculation is minimizing the methane utilization. Hence, for the provision of control reserve, power plants that use as little additional methane as possible for the *dispatch* of control reserve are needed in the system and therefore selected first. For instance, positive control reserve is more likely to be offered with storages where – if available – no methane usage is needed in the system for the dispatch. This option is favoured over the curtailment of wind power plants, which would mean a certain loss of energy or methane production in power-to-gas installations. If no definite decision can be taken due to the (methane) costs of delivery, then the capacity decision is based on the methane consumption of the dispatch. The question of which plant hast the least methane consumption of dispatch is less important as the dispatch frequency of 10 % [77] is relatively low. Based on the methane consumption of a dispatch of control reserve, the following sequence for the control reserve dispatch is applied:

- Positive control reserve: Wind and photovoltaic parks, power-to-gas plants, batteries, pumped hydro storage, bio-energy plants and methane power plants.

- Negative control reserve: Methane power plants, bio-energy plants, pumped hydro storage, batteries, power-to-gas plants, wind and photovoltaic plants.

Furthermore, the so-called core part is considered in the assignment of the plants. The control reserve demand is divided into four control areas where 2/3 of the demand within one control area must be covered by plants within that control area.

Results

The results are shown below for the given assumptions for calculating the optimal techno-economic control reserve provision in the base line scenario (i.e. provision of a fixed volume of control reserve according to the current model). Furthermore, two variants were investigated, one using the dynamic provision of control reserve and one with the fixed (static) provision of control reserve, but in this case the batteries.

3.1.6.1 Results basis scenario (fixed control reserve demand)

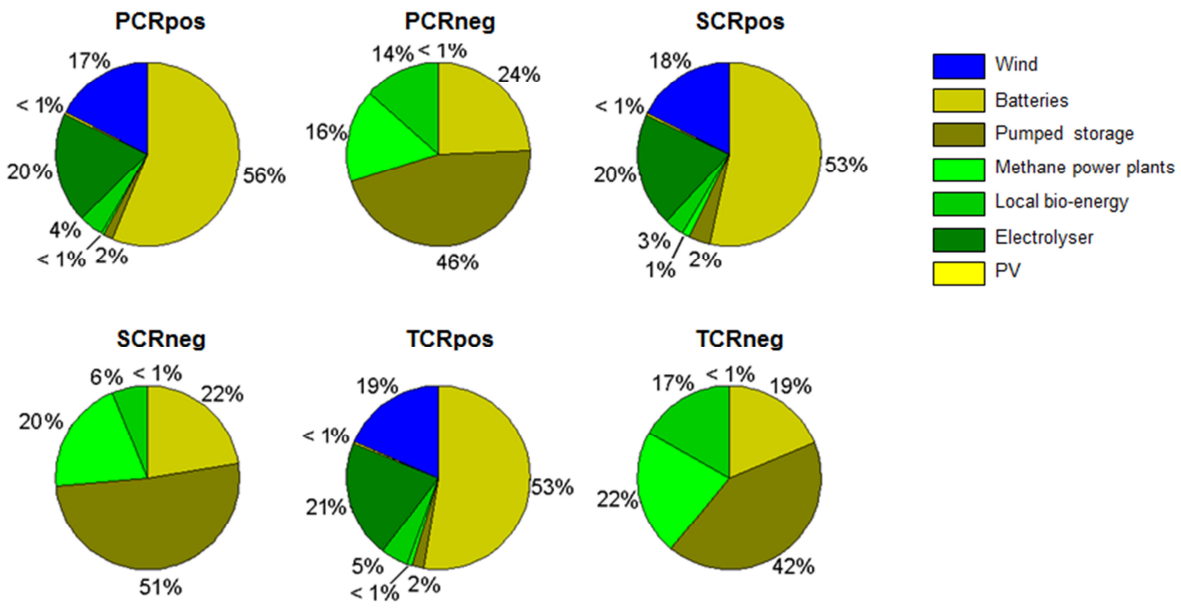

Figure 94: Average part of the various sources in producing the six simulated types of control reserves

In the optimization results in Figure 94, the high share of control reserve provision from storages, both pumped hydro storage and also decentralized batteries and the power-to-gas plants are remarkable. Together they provide almost 75 % of the sum of all types of control reserve.

At the same time, wind and photovoltaics play a significantly smaller part. They are used for control reserve only when they would also be curtailed, regardless of providing control reserve. In the calculations carried out, they are not used for negative control reserve.

This surprising result can be explained in the following way: With regard to positive balancing energy, costs for the delivery speak against wind farms and solar parks. In order to provide positive control reserve they have to operate in curtailed mode, i.e. there is the high probability that valuable energy is lost as the dispatch of positive control reserve is relatively rare. In the event of an additional power demand in the grid, a consumer should rather reduce his load, (e.g. a power-to-gas). Because of the low efficiency of power-to-gas plants, the loss of methane is substantially smaller. Of course, this argument is only valid for as long as the wind energy has not already been curtailed. The costs/energy losses in case of a dispatch of negative control reserve with wind and solar speak against their utilization. If at a point of time a thermal power plant is still in the grid, this plant should reduce its production and thus save fuel (costs).

In Figure 95, the simulated contributions for the delivery of control reserve from different sources are compared with the potential of each. All kinds of positive / negative balancing energy were summed and compared with the potential for the provision of tertiary control reserve.

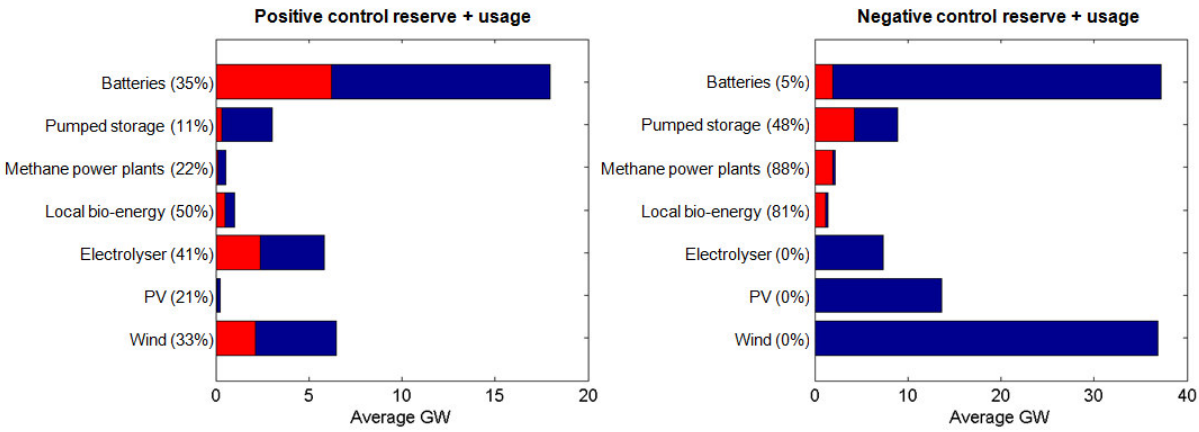

Figure 95: Simulated exploitation of existing potential for the delivery of control reserve from different sources

The extremely high potential of batteries is remarkable. Compared to its relatively low energy content, the total electrical capacity in the scenario with 55 GW (see section 2.6.3.1) is very high. On average, batteries are used for trans-regional balancing and are usually half charged. Therefore, they can provide high electrical capacities in both directions in very short times.

The wind and solar potential for negative control reserve is also very high on average. However, for the reasons discussed above, this potential is not used in the simulation.

The potential of methane and local bio-energy installations is small, as here only such periods are counted when the plants are in the grid connected (in order to reach operating points of the thermal power plants in the region of 50 to 100 % of their nominal capacity, in the simulation only a certain part of the installed power plants is marked as being in the grid connected). The necessity to provide control reserve does not increase the grid connection time of these power plants, as there are always enough other sources of control reserve in the scenario. The existing potential for control reserve of these sources is utilized to a comparatively high degree. Contrary to the initial intuition, above all the potential is used for negative control reserve provision as in this way fuel can be saved and there are usually enough other sources of positive control reserve.

One example of the computed regional production mix for generating control reserve is illustrated in Figure 96.

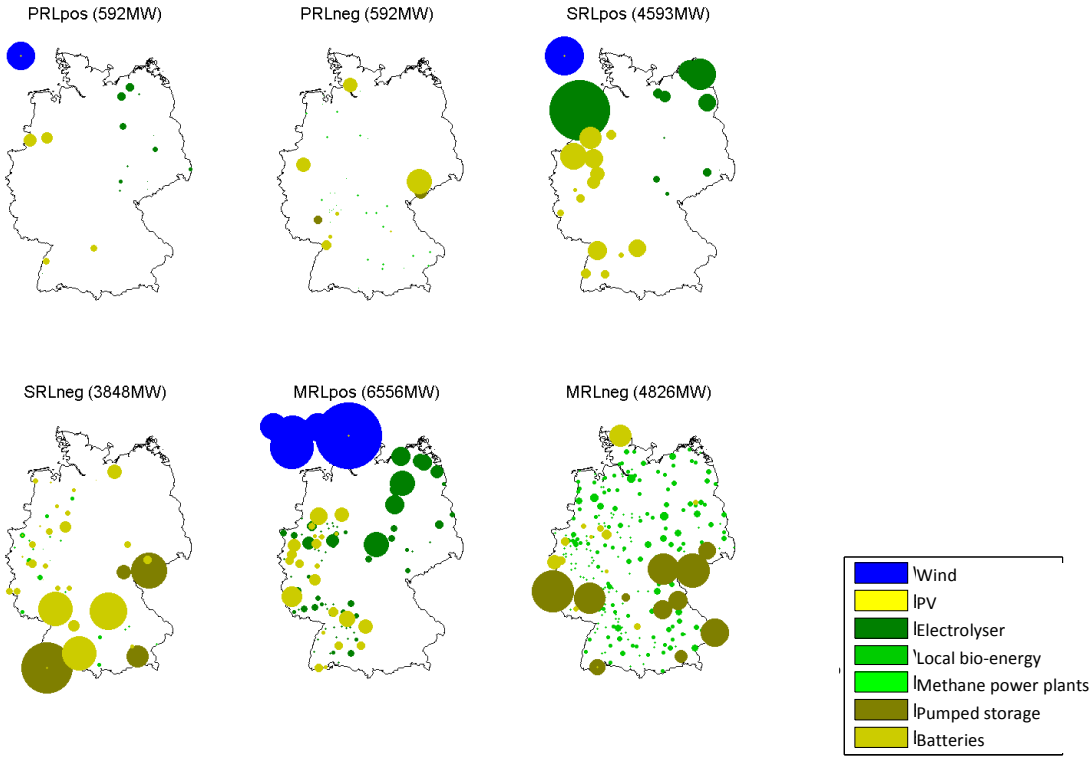

Figure 96: Distribution of simulated control reserve output for a point in time (1st Jan. 2:00) according to various locations and sources

3.1.6.2 Results – Variant: Dynamic control reserve demand

As described in section 3.1.5, the demand for control reserve was also calculated with the dynamic method. The results of this calculation of control reserve provision change in this respect that on average approximately half of the control reserve is required and thus the degree of utilization of the potential decreases. The biggest decrease regarding the provision of positive control reserve can be seen in the local bio-energy plants and methane power plants. The decrease of dispatch of negative control reserve is affective storages.

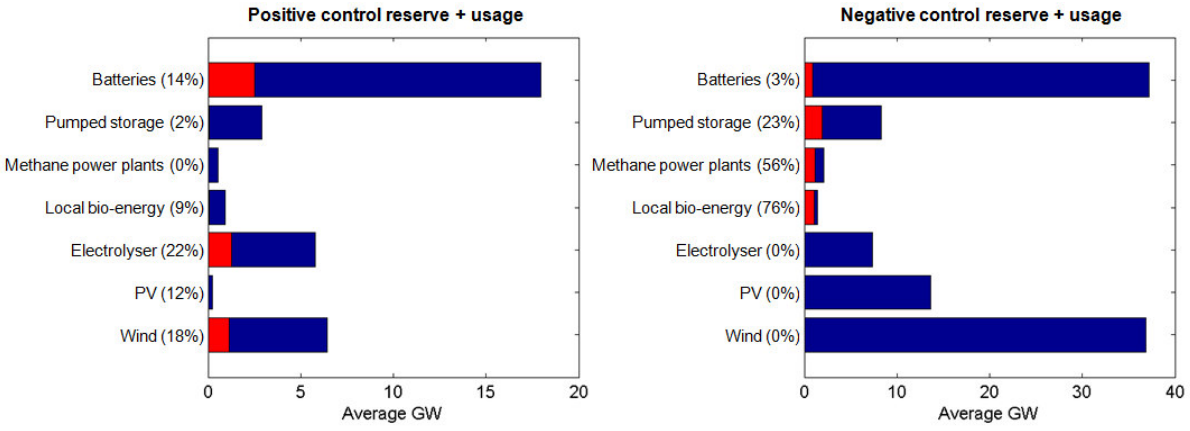

Figure 97: Simulated utilization of the existing potential for control reserve output of various sources for dynamic dimensioning of reserve power availability.

3.1.6.3 Results – Variant: Without batteries

Since the assumptions of the scenario on the installed capacity of decentralized batteries and their simultaneous access to the control reserve market are possible but currently uncertain, an additional variant without batteries for control reserve provision was calculated. For this, the basis scenario was used again, i.e. using a fixed dimensioning for control reserve.

In this way, both the relative distribution of the average control reserve sources and the utilization of the particular potential are changed significantly. Because much more is demanded of the remaining sources of control reserve, the share of wind and PV both of positive and negative control reserve increases. Even thermal power plants, local bio-energy and methane power plants are taken into the grid additionally so that positive control reserve can be provided during peak periods.

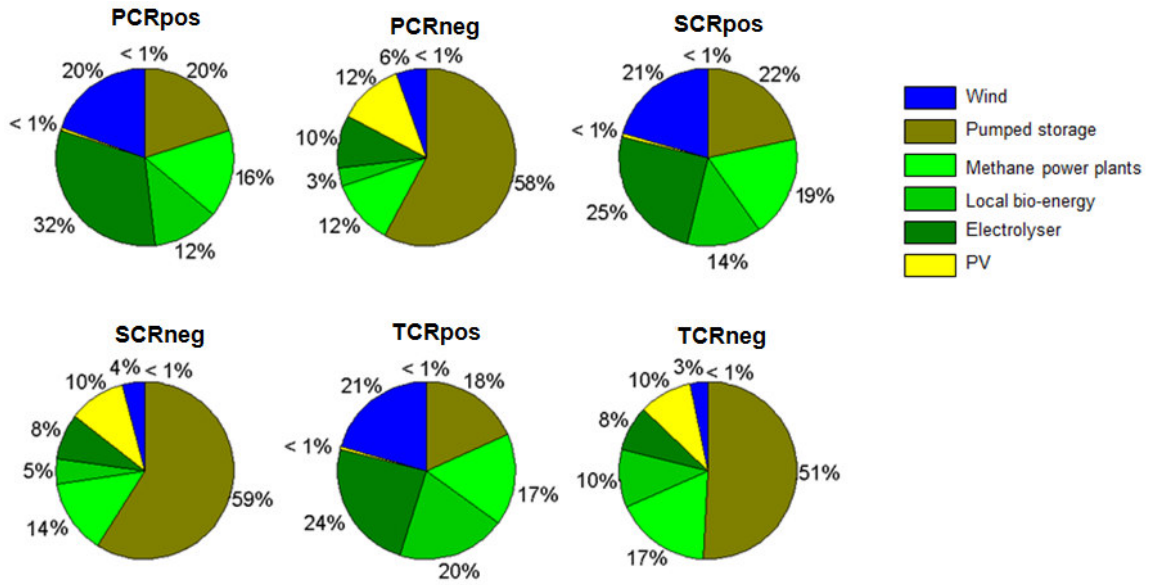

Figure 98: Average share of various sources in producing the six simulated types of control reserve, in case batteries are not included in control reserve production

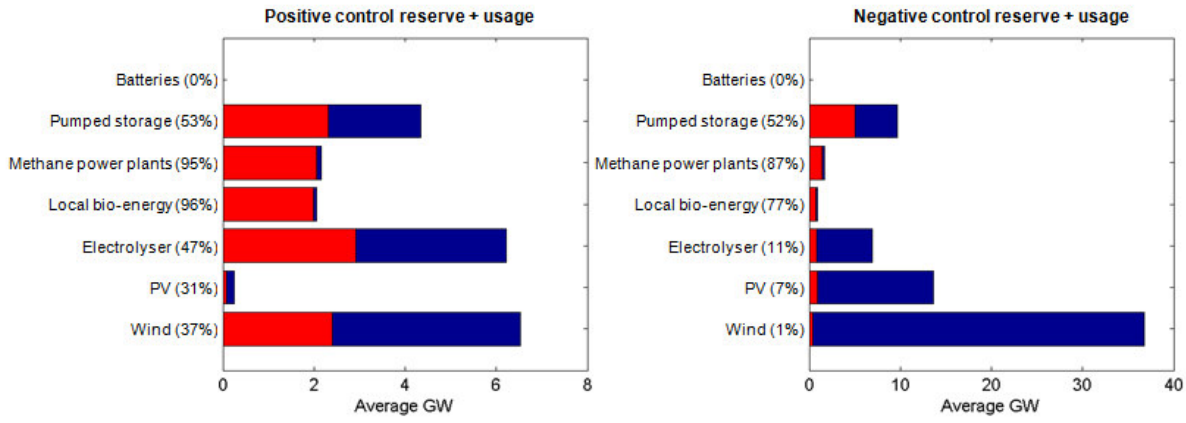

Figure 99: Simulated utilization of existing potential for producing control reserve of various sources, without considering batteries

3.1.6.4 Brief discussion

In the simulated baseline scenario, both the fluctuation and the thermal power plants, i.e. local bio-energy plants and methane power plants, play a smaller role with regard to control reserve provision. The reason is that the scenario assumes a high installed capacity of energy storages.

However, if this high storage capacity is not realized or is constructed slowly, particularly during the transition towards a 100% RE system, the finding changes significantly, as it is shown in the calculations for control reserve provision without batteries. In this case, the share of wind and solar for negative control reserve provision increases, which underlines the relevance of the field tests described in 3.1.2. For the provision of positive control reserve, the share of local bio-energy and methane power plants increases by 10 % each.

An adverse effect on market opportunities for the control reserve providers studied here would be the development of other flexible consumers for the control reserve market, which are not taken into consideration here. There certainly is a great potential in many industrial processes or in the area of power-to-heat for the production of control reserve, which could be utilized at relatively low cost which would represent economic competition for wind, solar and local bio-energy-/methane power plants.

3.1.7 Simulation of dynamic frequency stability in 100% RE-scenario

The concept of dynamic frequency stability is understood to be the characteristics of the grid and producers during malfunctioning of the power balance. Malfunctioning in the supply causes change in power frequency. In fault-free condition, the frequency f in the grid has the value of f = 50 Hz. The power in the grid is balanced. The rotational speed of the synchronous generators of conventional power plants is described by the differential equation as follows (point distribution model):

$$J\dot{\omega} = k(P_{\mathrm{mech}} - P_{\mathrm{el}})$$

Here the mass moment of inertia P_{mech} and the mechanical performance P_{el} the electrical power of the grid. The angular velocity of the synchronous generators is proportional to the grid frequency. Malfunction in the power balance influence the angular velocity of the generators. In case of a power plant, failure the mechanical performance decreases suddenly und causes the generators to slow down. In this kinetic energy from the rotating masses of the synchronous generators is exhausted. Thus the grid frequency drops and adjusts to a new end value since various consumers consume less power as the frequency decreases. The reduction in conventional power plants and move towards a 100% RE power supply leads to a decrease of rotating masses in the electrical energy system. The possibility of using kinetic energy from the rotating masses to limit frequency drops is drastically reduced. Pumped hydro storage power, biomass and methane power plants continue to make rotating masses available but the share of production units connected via converter-based systems is often significantly larger.

3.1.7.1 Current situation

Within the continental grid area (Synchronous Grid of Continental Europe) of ENTSO-E, according to appendix 1 of [33], a loss of production capacity totalling 3.000 MW is set as design-relevant malfunction in the grid area. This value is equal to 2 % of the minimum load of 150 GW in this grid

area. The minimum load represents the most critical design basis accident as in case of maximum load the malfunctioning of a larger number of power plants can be absorbed. As not the entire continental grid area but only the German grid area is studied in this project, the German share is assumed to have the current value of 592 MW (cf. section 3.1.5.2). The distribution of control reserve contributions amongst the grid operators in the continental Europe area is currently carried out in proportion to their annual energy production. A slightly different distribution does not influence the results from the following simulations, if the increase in converter-based generators is carried out to a similar degree throughout Europe.

The provision of kinetic energy, also called instantaneous reserve or inertia, is currently not a market product, but an inevitable result of the physical reality of power plants without converters, currently located high voltage and highest voltage levels of the grid. These days, wind energy plants are connected through converters, although a connection via conventional synchronous and asynchronous generators and thus direct linkage of the kinetic energy mass is possible. This has been practiced in the past but does not offer the necessary rotational speed variability required for optimum use of fluctuating wind energy potentials. Plants without rotating parts such as photovoltaic installations must be connected via a power converter.

Thus in case of an error less kinetic energy is available. Primary control reserve is currently tendered by the TSO on a market scheme (cf. section 3.1.1). According to [33], the capacity has to be able to be fully activated within 30 seconds. Figure 100 illustrates the calculated frequency function in design basis configuration with minimal load and a malfunction of 2 % and current minimum requirement for primary control reserve dispatch response time.

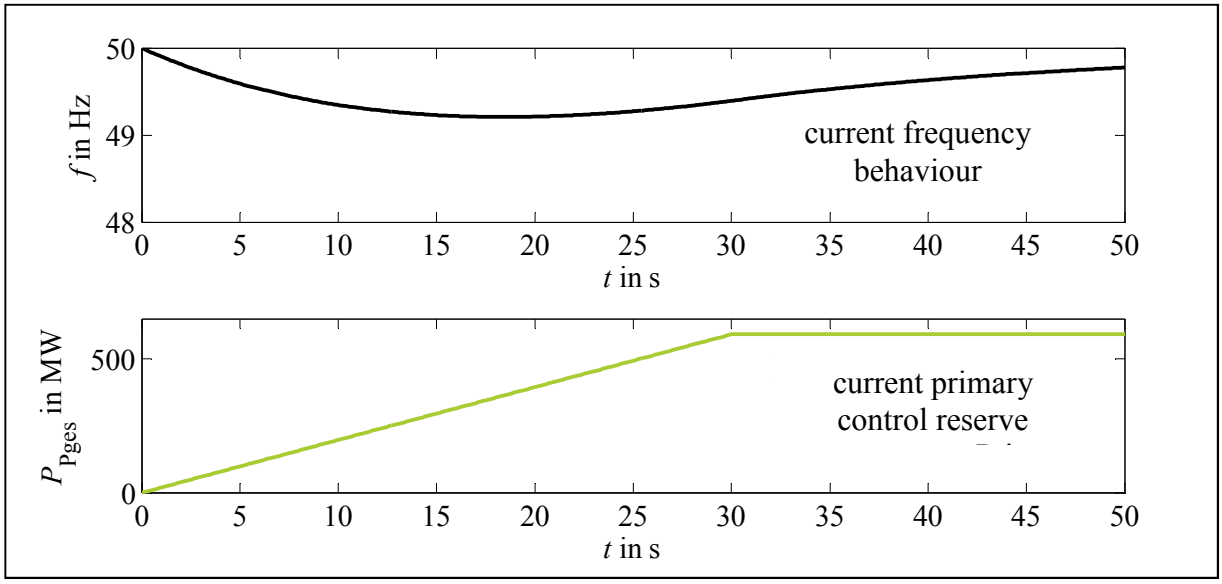

Figure 100: Frequency function and minimum requirements for primary control reserve delivery

The frequency may not be below 49.2 Hz at any time and must be brought back to 49.8 Hz by the primary control reserve. The changes induced by the 100% RE scenario from Chapter 2 are discussed in the following section.

3.1.7.2 Simulations

The simulations in this section are carried out using the so-called "aggregated grid model". This model is normally used for frequency stability studies and can be utilized when it can be assumed that all power plants studied form a so-called coherent group of generators, thus have a common angle hub. This assumption holds valid for a 100% RE scenario in Germany when the planned grid expansion at the highest voltage level is considered. In the aggregated grid model, balancing mechanisms between individual power plants are disregarded and all kinetic masses and capacities are included in a common mass model. For the current minimum load, a grid time constant T_n, which describes the inertia of the system for all aggregated kinetic masses, can be estimated as 10 s. In these studies, it is assumed that the grid time constant is composed of a 10 % share of load (e.g. rotating masses of directly linked asynchronous machines) and a 90 % share of generators. For all 8.760 hours of the scenario year, new grid time constants result from the ratio of the load P to minimum load P_{min} and the ratio of production of minimum load (which conforms to the minimum load production). Without a changed structure of the power plants, there would no change to the grid time, which would still be 10 s. The increasing number of converter-driven generators, however, reduces the number of power plants that have grid-connected kinetic masses. The following installations have directly linked kinetic energy: Biomass power plants, methane power plants, hydropower plants, geothermal power plants and pumped hydro storage power plants. Wind turbines, PV systems, power-to-gas installations, and batteries do not have a synchronous grid connection and therefore cannot have kinetic energy available to the grid. The following equation results for the grid constant of each point in time:

$$T = T_N \left(0{,}9 \cdot \frac{P_{\text{Biomasse}} + P_{\text{Methane}} + P_{\text{Water}} + P_{\text{Geothermics}} + P_{\text{Pumped hydro storage}}}{P_{\text{min}}} + 0{,}1 \cdot \frac{P_{\text{Load}}}{P_{\text{min}}} \right)$$

Here P_{min} is the output in case of low load. In times of high load and/or high output based on bio-mass, methane, water, geothermal leads to or pumped hydro storage in future grid time constants greater than 10 s are possible. However, at times with share converter-based generation grid time constants smaller than 10 s can result. Figure 101 illustrates the sorted course of grid time constants for the scenario year. Figure 101 shows the sorted progression of the grid time constant for the scenario-year.

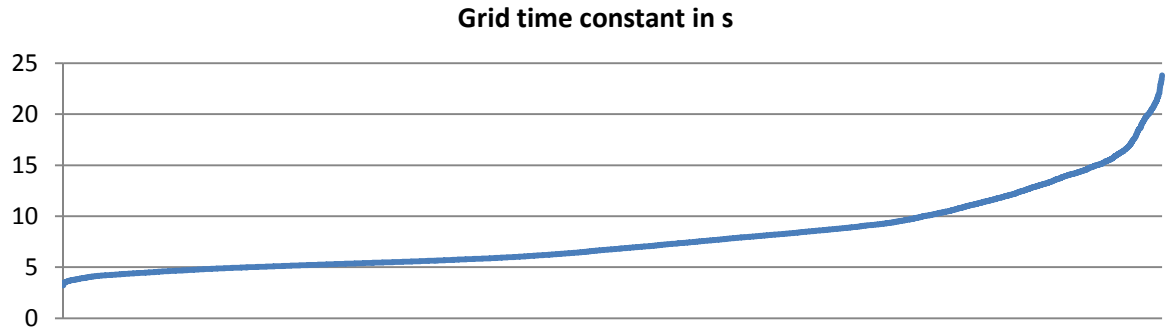

Figure 101: Sorted progression of grid time constants for the scenario year

In approximately 78 % of cases the grid time constant is smaller than 10 s so that frequency limit violations occur regarding the requirements of ENTSO-E specifications for primary control reserve. The loads in the grid also react to frequency changes. In the case of a frequency drop, the loads take up a little less power so that they slightly counteract a generation deficit. This effect is described as self-regulation effect of the power grid. For constant conditions, it can be assumed in simplified form that the load behaves proportionately to frequency changes.

$$P_{\mathrm{Last}} = k_{\mathrm{L}} \Delta f$$

The load KPI k_{L} is indicated as t $\frac{1\,\%}{Hz}$ in the design according to [33], so that this value for minimum load also in this study is used ($k_{\mathrm{L,min}}$). Dependent on the actual load however, the KPI is adjusted here according to the following equation:

$$k_{\mathrm{L}} = k_{\mathrm{L,min}} \frac{P_{\mathrm{Last}}}{P_{\mathrm{min}}}$$

Figure 102 shows the frequency progression f and the primary control reserve P_{Pges} applied to the 8760 points in time under the above-mentioned assumptions.

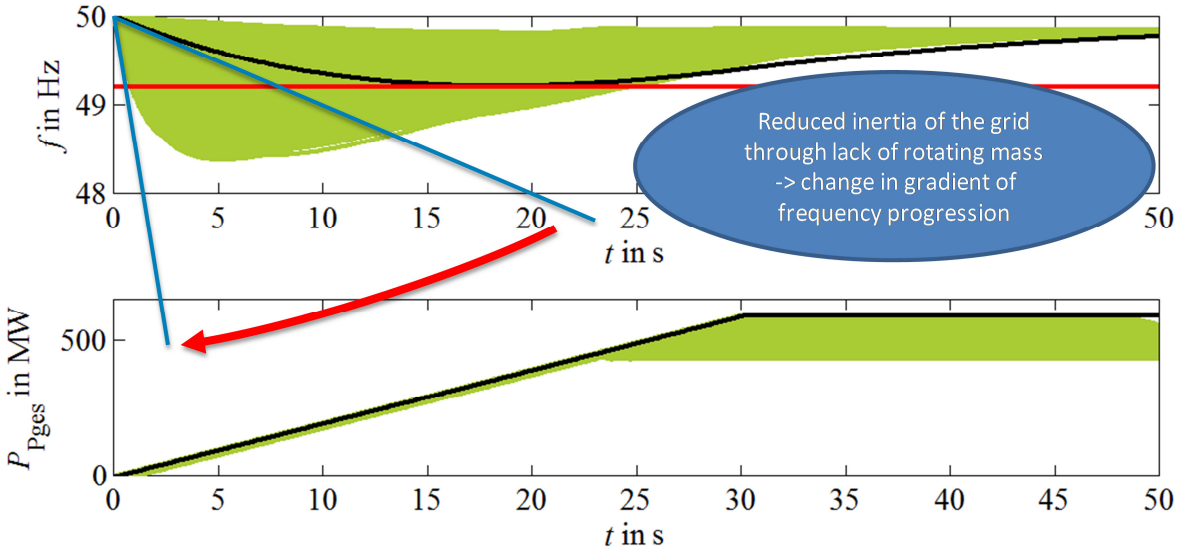

Figure 102: Frequency and output power progression in construction of conventional primary control reserve delivery.

The results show a number of points in time where the critical frequency of 49.2 Hz is violated. This was to be expected due to the decrease of kinetic energy and the reduction of grid time constants. A secure system operation is therefore not guaranteed in this way since the automatic load shedding would be triggered (not simulated here). The frequency and active power curves of different times are shown by the green areas. The difference between used primary control reserve and maximum primary control reserve (illustrated in black) in constant condition is caused by the differences in the efficacy of the self-regulation effect of loads.

The calculated frequency problems can either be counteracted through additional kinetic energy in the grid or by faster response time for dispatching primary control reserve. Additional kinetic energies do not necessarily require new grid components. Installations that are being taken out of operation or being newly built can be converted or planned in such a way that the generators (normally without turbines) can remain idling in the grid during critical times. Even though such measures cause operational losses they would have the advantage that idling generators - apart from their characteristic as oscillating weight - in most cases can also serve as phase shifters for reactive power provision (cf. Chapter 3.2). Plants optimised for oscillating weight are known as so-called flywheels. In this study, the description of different variants is omitted, as the 100% RE installations technically possess enough oscillating weight that can remain in the grid and as the primary control reserve provision can also be adjusted. Below, the potential of renewable energy installations are investigated to provide primary control reserve faster in order to counteract a dynamic frequency drop and to prevent frequency violation.

Power plants that do not have mass inertia but are entirely converter-based can adjust their output very quickly. Currently converters already have to remain connected to the grid in the event of short circuits and to adapt their active power output within a few milliseconds and provide a reactive power current. Based on a consultation with the power plant producers in the consortium of project partners, PV systems, power-to-gas power plants and batteries are able to deliver active power within seconds and without any almost any delay so that the use of this characteristic is studied below.

Wind turbines are, depending on their type, connected to the grid via a full power converter or a double fed asynchronous generator. In both cases, a change in power output is not possible immediately. Using the rotating mass of the rotor is possible via adaptive inverter control but it causes, apart from the desired power output from stored kinetic energy, also a change in the rotor speed. This changes the aerodynamics of the wind turbine from its optimal operating point to an inferior one, which decrease the power output. For smaller changes in the rotor speed, the advantage of additional power output outweighs the aerodynamics losses. However, beyond that even a small percentage change in the rotor speed increases the aerodynamic losses significantly. The simulations have shown that this can lead to unstable wind power plant behaviour and subsequently unstable system behaviour. Additional research is needed in this area regarding a possibly combined rotor speed and pitch angle control. Particularly in the event of an output surplus, the increase in plant revolution and thus the decreased power output with a worse aerodynamic operating point can be interesting. Wind energy installations can also decrease the dynamic frequency losses by other means, while not making primary control reserve available within 30 s but distinctly faster. After discussions with the wind power plant producer from amongst the group of project partners, wind energy plants could deliver primary control reserve by pitch angle changes even within 5 s.

Figure 103 illustrates the frequency curves with changed primary control reserve provisions by converters and wind energy plants. The generation schedule follows section 3.1.6. The 8760 hours in the year were divided into three groups (yellow, blue, green), with each group being dominated by one form of delivery.

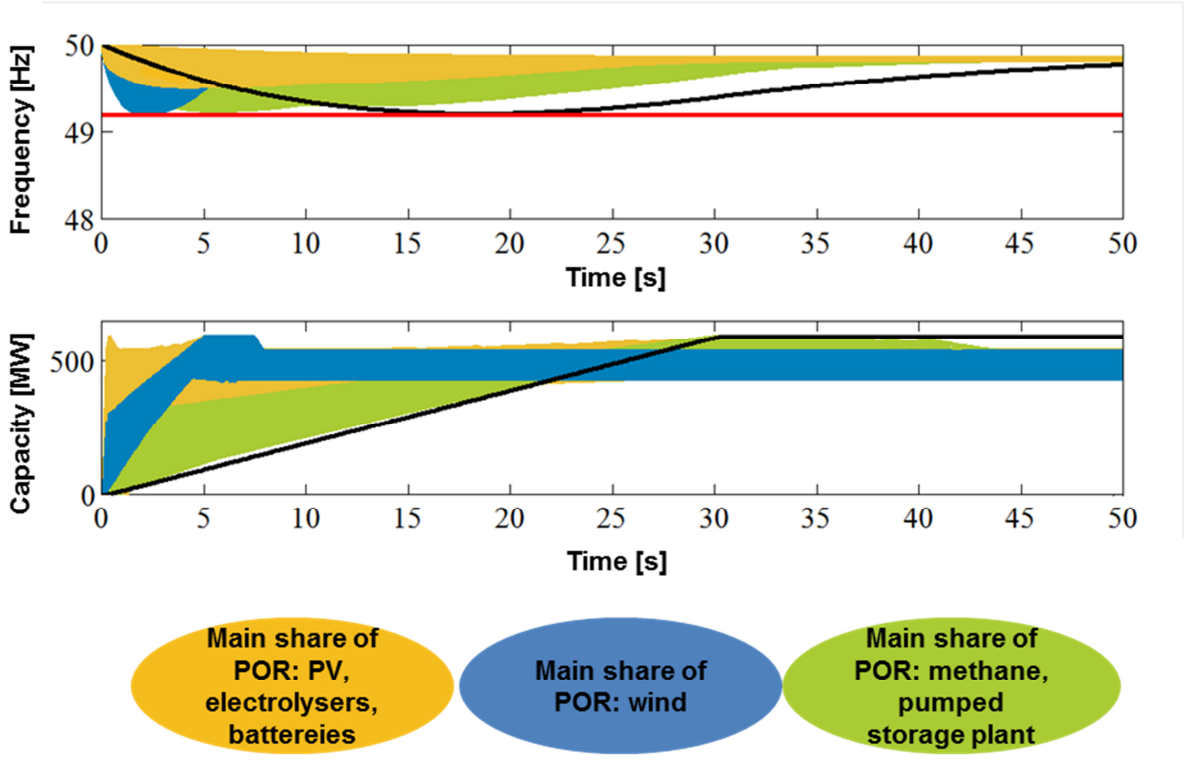

Figure 103: Frequency and delivery progress with changed primary control reserve delivery with identification of the major parts: converters, wind energy, rotating masses

The processes illustrated in Figure 103 shows the total used primary control reserve of the various energy sources. The main share among primary control reserve sources are marked in different colours according to their section. The first group represents the dominating primary control reserve use of the inverter-based plants (yellow area). It can be identified as a direct control reserve provider. The second group is dominated by the delivery of primary control reserve from wind energy (blue) and the third group through biomass, methane and pumped hydro storage power plants (green). The frequency curves are shown according to the division of the primary control reserve sources. After application of the measures described, the critical frequency of 49.2 Hz is not violated at any point in time. In order to further improve the sequence progress it is possible to shift the use of primary control reserve in favour of the quick converter- and/or wind energy plants. Current use is optimised economically and not technically. Such intervention could be called a “primary control reserve re-dispatch”.

3.1.8 Conclusions and recommendations

In this section, conclusions are drawn from the studies in all of Chapter 3.1 and based on that, recommendations are made on the subject of control reserve.

The **field tests** for the research project Kombikraftwerk 2 (section 3.1.2) show that renewable energies are currently technically able to deliver control reserve. Biomass installations are already used to deliver control reserve. The first plants have already prequalified for the delivery of primary control reserve. The delivery of control reserve from the weather-dependent renewable energies wind and sun is only possible and sensible with sufficiently high wind speed or solar radiation. If for the provision of control reserve and the proof with the available active power (see section 3.1.2.1) is used as reference value, the unavoidable energy losses of control reserve delivery can be kept to a

minimum. However, if fluctuation energy generators would receive a temporally constant schedule, as has been the case for suppliers of control reserve provision up to now, this would have the disadvantage that the fluctuating producers have to be curtailed to a constant level and thus available energy would remain unused. On the other hand, balancing effects between producers and consumers could not be used anymore. From the point of view of the whole system, the proof using the measure *available active power* is to be preferred (see section 3.1.2.1). The technical implementation of the measure *available active power* is, however, not yet adequate for delivering control reserve and thus must be improved. It should be implemented by the plants themselves and not by the control centre of the VPP in order to keep the time delay of control as brief as possible. In order to provide total positive control reserve in spite of certain current inaccuracies, in the tests the available active power was reduced by constant values. Depending on weather conditions, the amounts of these reductions and the control reserve bands should be calibrated and optimized in further tests. The use of available active power requires a scheme that has a high temporal variability. This high dynamic places high demands on the delivery speeds and accuracy for the plants so that delivering control reserve in the tests occasionally fell outside of current tolerances. Increasing accuracy in delivering control reserve could be achieved by more precise in-plant controls, faster reaction times, targeted short-term balance of deviations of one type of plant by another, but also by a mathematically decreased available active power dynamic or simply by using larger and additional VPPs. However, it must be investigated whether the current tolerances designed for conventional delivery of control reserve (proof method with the schedule) can be extended for fluctuation energy producers.

Because of the general conditions of the **control reserve market**, weather-dependent renewable energies are currently still prevented from offering their technical abilities for delivering control reserve and thus taking over the responsibility for stabilizing the system. Hence, the transformation of the energy system should include promoting the control reserve market and chances for the participation of fluctuating renewable energies should be created. By shorter tender periods, product lengths, lead times and auction times, photovoltaic systems and wind turbines, whose feed-in can only be predicted with a certain accuracy for short lead times of a few hours up to one day, could also participate in the control reserve market and the advantages of dynamic demand dimensioning could be used. Flexible installations that convert gas from renewable sources and are with a head demand operated highly efficient CHP, would have the opportunity of participating in the market. For these reasons, the ACER initiative for the introduction of a separate operating price with product lengths and lead times of one hour is to be welcomed. In order to further increase transparency of the control reserve market, the anonymized yearly and monthly time series of operating prices should be published. This simplifies market access for new participants. In future, large loads (power-to-gas, power-to-heat, etc.) should increasingly be included in the control reserve market, including for providing primary control reserve. For the integration of short-term low-priced available energy into the control reserve market, an additional intra-day market that is defined purely via operating prices (possibly following the Danish model) is to be recommended. It is also recommended that the symmetrical submission of tenders for primary control reserve be cancelled in order to enable an exclusively positive or negative delivery. The balancing energy price system should be structured such that specifically for balancing responsible parties with wind or PV installations there is an incentive for trading 15-minute products and using short-term forecasts but no incentive for balancing forecast errors on the level of the balancing responsible party.

In order for individual plants to dynamically calculate the possible control reserve delivery and the control reserve demand, highly accurate **forecasts** with information of confidence intervals is necessary. For this, high-resolution wind and PV output data (10 min to 1h) must be accessible to plant operators. Precise forecasts are also crucial for preparing offers in the control reserve market by wind and photovoltaic parks because then they can increase the offer with the same reliability. Regarding tendering, with the aid of probabilistic forecasts, wind farms can deliver control reserve as reliably as present suppliers. Furthermore, evaluations of demand dimensioning show that the forecast errors of photovoltaic and especially wind energy feed-in will in future make up a large portion of the demand for control reserve. For these reasons, forecast methods must continue to improve. In addition, for demand driven market participation of flexible installations with CHP, the forecast methods for the heat demand and the market prices must be optimized.

Although wind energy and photovoltaics will in future be the decisive factors in dimensioning demand, forecast errors should not be balanced out on the level of balancing responsible parties (see section 3.1.5.2). The reason for this is that no trans-regional balancing effects can be used that contribute to a reduction of demand for control reserve, where here the term control reserve also includes the balance energy in the balancing responsible parties. So the **balancing energy price system** should be structured such that specifically for balancing responsible parties with wind or PV installations there is an incentive for trading 15-minute products and using short-term forecasts, but no incentive for balancing of forecast errors on the level of the balancing responsible party.

With the aid of **dynamic demand dimensioning** (section 3.1.5) which specifies the demand daily for control reserve for the hours of the following day using forecasts, compared to the present there would be no increase in the average demand for control reserve with 100 % renewable energies. During individual hours, however, the demand may exceed present demand significantly. If the current method were not changed, the demand would approximately double. Hence, dynamic demand dimensioning should be introduced. Its implementation is already being investigated in a BMU project of Fraunhofer's IWES and the transmission system operator TenneT. The introduction of the dynamic demand dimensioning forces shorter deadlines for tendering and shorter a lead-time on the control reserve market (approximately 1 day).

The evaluations in section 3.1.6 show that **control reserve demand in a 100% RE scenario can always be met** without problems. For this purpose, wind and photovoltaic parks are needed to deliver control reserve where their share depends on the number of other flexibilities in the system.

The studies of **dynamic frequency stability** in section 3.1.7 show that the reduction of rotating mass can be compensated by the increased use of converter plants with faster delivery of primary control reserve by RE plants and storage. The dynamic frequency stability in the 100% RE scenario thus seems possible for the scenarios studied here. It is however suggested that the demand for primary control reserve be differentiated with regard to delivery according to the energy source. For RE and storage, a reduction in activation times should be designed within the framework of technical capabilities. According to the calculations, no change is necessary for power plants of conventional design. The difference in delivering time according to energy source may make "primary control reserve re-dispatch" necessary. The combined pitch angle and rotational speed control of wind energy plants needs further research. The conversion of synchronous generators of decommissioned power plants to rotating phase shifters could support the dynamic frequency stability by the associated increase in oscillating weight in the grid.

3.2 Voltage stability and reactive power management

In Chapter 2, for every hour of the scenario year a complete picture of the production and consumption was developed with a spatial resolution based on the level of highest voltage grid. The depth of detail of the scenario is a prerequisite for the following studies because, as opposed to frequency stability, voltage stability must be guaranteed locally and depends on the local conditions of the grid, and the energy producers and energy consumer structure. In this chapter, the resulting voltage bands (section 3.2.3) for the scenario and the reactive power demand (section 3.2.4) for each high voltage node and every point in time are determined by a complete power flow calculation (section 3.2.2). In section 3.2.5 investigations are presented that show how reactive power delivery from the lower voltage level to the high voltage level can be performed, how the future distribution of the energy producers to voltage levels is assumed, and the restrictions of voltage bands are estimated.

Voltage stability is the adherence to a voltage band at all nodal points. According to [31], the admissible voltage band is ± 10 % for the highest voltage level, where this does not only have to be guaranteed with (n-0) operation but also in all (n-1) cases. An excessively high voltage, e.g. through capacitive increase in voltage in idling or poorly utilized grid areas (Ferranti-effect), entails the risk of an isolation error and thus a short circuit. An excessively low voltage increases the danger of a voltage collapse: If constant energy must be transmitted via a transmission path, the adjustment of the current depends on the voltage level. If the voltage level at the initial node I high, as compared to low voltage, low current results, and this brings about a comparatively small reduction in voltage in the transmission path. If the voltage level decreases, then a larger power must flow with equal performance, which results in a bigger reduction in voltage and higher loss of active power and reactive power in the grid. A major decrease in the voltage causes a low level of voltage and larger current. If the voltage is too low, this effect reinforces itself and leads to a voltage collapse, e.g., if the load increases.

The equipment on the level of highest voltage consists of ohmic (lossy) as well as capacitive and inductive parts. Figure 104 illustrates the π-equivalent circuit diagram of a transmission line.

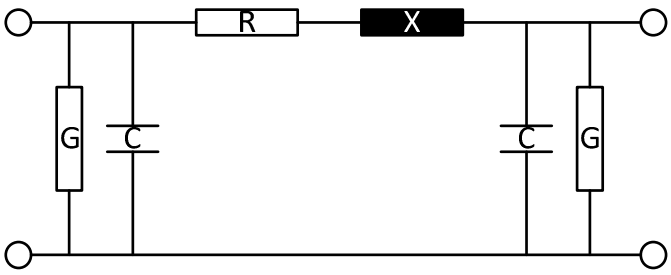

Figure 104: Single-phase π-equivalent circuit diagram of a transmission line

In the longitudinal section consisting of the resistance R and the reactant X, the inductive reactance predominates over the resistance because this is normally approximately 10 times as large on the highest voltage level. In the crosslink, the conductance G normally is negligible compared to the capacities C on the highest voltage level. As the capacitive demand for reactive power depends on the capacities of the attached voltage und thus is nearly independent of the load condition but the inductive reactive power demand of the reactance depends on the power in the longitudinal section and thus essentially depends on load condition, at idling the capacitive reactive power and in most

load cases the inductive reactive power predominates. Figure 105 illustrates the dependence of the reactive power demand Q on the transmitted active power in a 10 km long 380 kV transmission line:

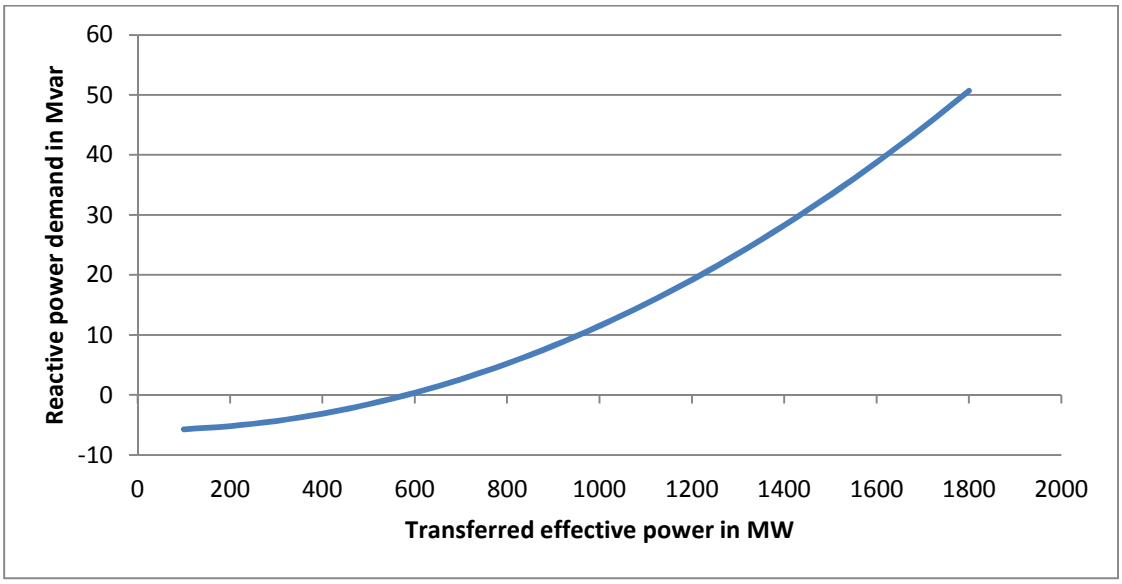

Figure 105: Reactive power demand in a 10 km long 380-kV transmission line in dependence on transmitted active power

In a poorly utilized operation, the line is capacitive (Q<0) and with increasing load an increasingly stronger inductive behaviour (Q>0) is shown.

3.2.1 Current general conditions

The reactive power delivery on the level of highest voltage is regulated in [31]. All production plants, from 110 kV to 380 kV-voltage level, and, depending on the grid voltage, must even in part load operation deliver reactive power according to agreed variant features. Production plants from secondary voltage levels are presently not usually used to deliver reactive power for the high and highest voltage level. Even though large power plants are also included on high and highest-level voltage in the 100% RE scenario, it cannot be assumed that they are in the grid at every point in time and that they will possess sufficient delivery potential for reactive power. Therefore, in section 2, the possibilities for delivering reactive power from secondary voltage levels are investigated, also qualitatively.

Apart from the potential for delivering reactive power the demand changes too: Because of the changed power flow situation in the grid consisting of AC and DC-transmission lines, because of network expansion and decentralized generation plants which, distributed over the entire grid, supply power, a changed grid situation and new demands for the target value calculation for voltage amounts and reactive power values arise.

3.2.2 Complete power flow calculations

After conducting the simplified power flow calculations (according to Chapter 2.1) for the simulation of the expansion of the modelled power grid (from Chapter 2.5) the grid model was expanded to include a complete AC-grid model for the simulation of voltage stability and reactive power delivery (including crosslinks) and it was so constructed that for conducting (n-1)-simulations each operating resource can be individually closed down. For the implementation of (n-0)- and (n-1)-power flow calculations on the basis of the Newton process “complete power flow calculations”, initially it was necessary to develop a strategy for distributing the loss of active power to plants and a strategy for voltage stability and reactive power. For this purpose, it was essential to prevent opposing regulations in order to prevent convergence problems in the total power flow calculations.

Active power strategy

Normally, as part of the power flow calculation a so-called “slack-node” is defined which takes over the power balance of the grid. Losses or surpluses deviating from the prognosis are balanced out via this node. In individual cases, this node must balance large amounts of power and the lines close to the node are loaded differently, possibly even overloaded. Thus a so-called “distributed slack” was implemented where in every iterative step of the power flow calculation the different power values of the grid were allocated to all energy producers and consumers that are used according to section 3.1.6 in delivering control reserve to the ratio of their power feed-in. This approach follows the assignment of delivering primary and secondary control reserve that balance different power values in the real grid. It implies a power flow situation that is (slightly) different with every iterative step, so that the reactive power to be fed in also has to interactively change, and its influence on grid losses reacts upon the “distributed slack”.

Reactive power strategy

As described at the beginning of this chapter, the plants must incorporate reactive power and hold it available in order to avoid surge voltages and power sags. As voltage does not adjust itself in an access node independently of neighbouring nodes, the situations in the grid and the reactive power availability influence each other within a node environment. Assuming that there was a central point in future, which could transmit an optimum reactive power nominal value to every plant at every

point in time without time delay, a global strategy for optimizing reactive power would be conceivable. In order not to assume this conjecture and to enable a feed-in of reactive power independent of the state of the entire grid which is made only on the basis of the voltage measurable at the grid connection point, a proportional regulation was designed, which, based on a co-efficient conditional on the grid connection point, defines the reactive power amount dependent on the voltage deviation from necessary nominal voltage at the point of connection. The co-efficient was identified by deducing the general power flow equations for the grid with nominal grid voltage at all nodes. Thus the coefficient is not exact for large voltage deviations, however, it still gives very good results as at least in a case of (n-0) the deviations in voltage at all nodes only amount to a few percentage points (cf. Figure 106 and Figure 107). The reactive power strategy by means of a P-controller is beneficial, as P-controllers do not regulate the nodes against each other and a P-controller does not carry out a return to target value (nominal voltage). A parameter of nominal voltage at all nodes would be advantageous from the point of view of voltage stability and was evaluated in the project. However, it necessitates unrealistically high feed-ins of reactive power and thus high grid losses, because the voltage drop caused by the active power flux would be compensated by additional reactive power feed-in. Due to the interactions between the active power and the reactive power household, the active power and reactive power strategies interact at every iterative step but do not regulate against each other.

As the grid losses and thus the necessary power loss demand have already been estimated within the framework of the simplified power flow calculations according to Chapter 2.1, section 4, no essential repercussions resulted from the effective and reactive power strategy on the application planning for the plants.

3.2.3 Simulation of voltage bands at the highest voltage nodes in the 100% RE scenario

The following graphics (Figure 106 and Figure 107) illustrate the percentual voltage bands of all 8.760 (n-0) cases in the scenario year for all nodes:

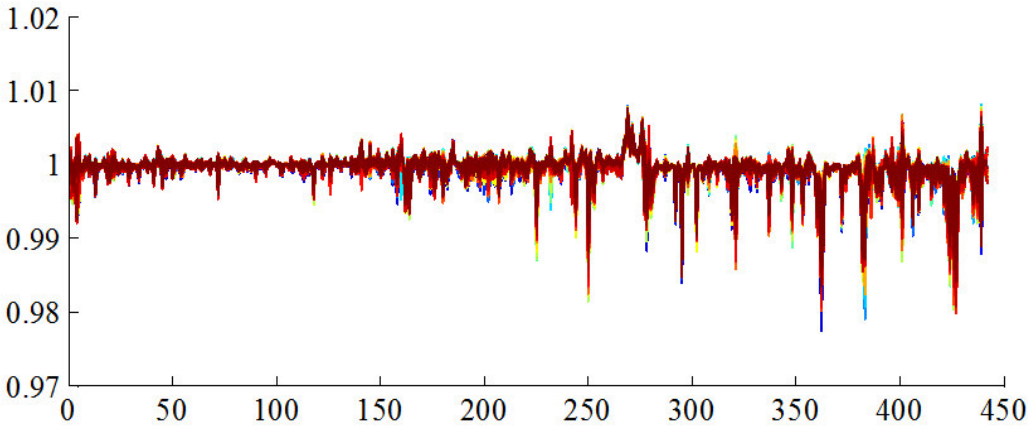

Figure 106: (n-0) voltage bands of all nodes for all points in time of the scenario year

The evaluations show that with the chosen strategy for voltage stability the voltage bands are not violated with the help of reactive power delivery by distributed power plants. Just a few nodes with increased voltage (typically feed-in nodes) or dropped voltage (typically load nodes) can be seen. In the following Figure 107, the same voltage bands of all nodes for all 8.760 points in time in the scenario year are show.

No seasonally dependent behaviour of the voltage bands can be observed. The minor voltage band distributions and the independence from seasons can primarily be attributed to the distributed reactive power strategy, which proportionately regulates voltage deviations on nodes or in grid areas.

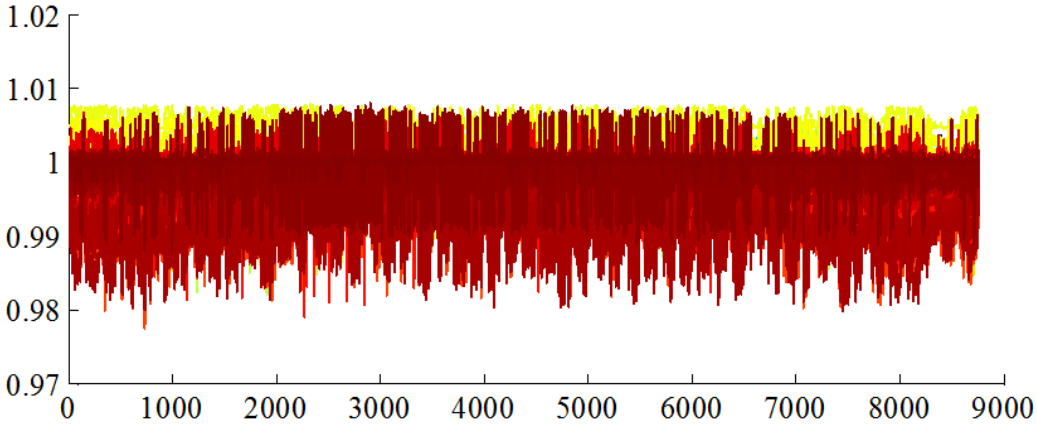

Figure 107: (n-0) voltage bands for all hours of the scenario year at all nodes

3.2.4 Simulation of reactive power demand in highest voltage in the 100% RE scenario

In analysing the reactive power demand, on the one hand the demand by the grid and on the other the demand by connected loads is assessed. Simplified, a $cos(\varphi) = 0.95\ ind$, is assumed for the

loads which is calculated for each node and each point in time. The reactive power demand by the grid depends on the loading situation of the grid, which in turn does not only depend on the load situation but also on the feed-in and storage situation and their geographical distribution. Figure 108 illustrates the average demand for reactive power of each node (left), the grid (middle) and their overlap (right).

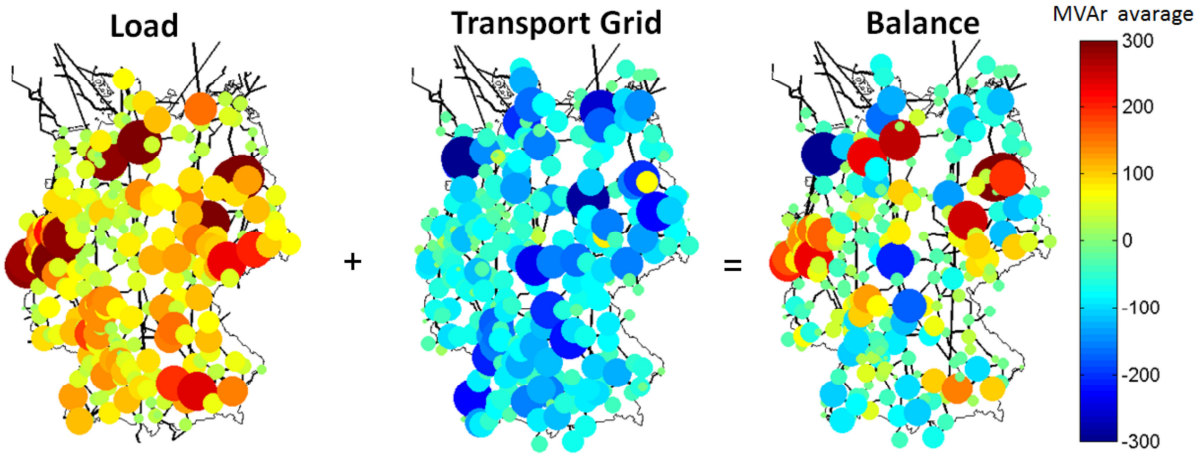

Figure 108: Simulated average reactive power demand of loads and the highest voltage grid in the 100% RE scenario and the balance. Positive reactive power implies an inductive reactive power, negative reactive power a capacitive reference.

The evaluations show an increased demand for reactive power in the same load regions with high industrial and population density that exist today. Figure 109 illustrates the entire demand for reactive power of the grid for all 8.760 hours of the year. The grid loading is stated as the product of transferred power times length of power totalled for all lines.

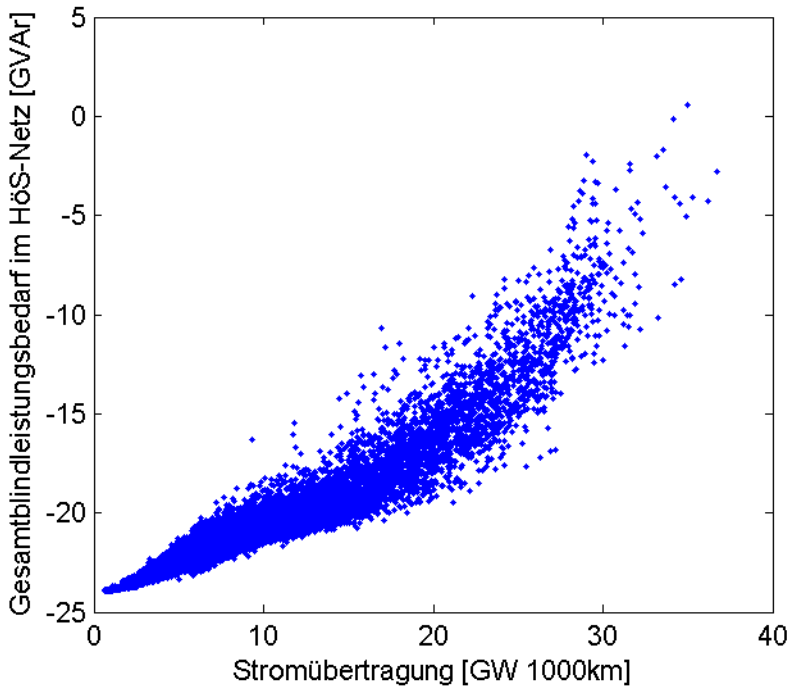

Figure 109: Simulated total reactive power reference of the highest voltage grid as function of the transport performance of the grid (negative values imply capacitive reactive power receipt)

On balance, the grid is at almost all points in time in a capacitive operational status, which at first seems surprising, as high capacity and transfer power especially over long distances in north-south direction are always assumed, and high transport capacity over long distances should require a big demand for inductive reactive power. The evaluation becomes transparent when it is taken into account that the network expansion according to Chapter 2.5 complies with extreme load scenarios, so that many sections are being expanded which are possibly used to full capacity only for a few hours per year. Altogether, the capacitive reactive power demand increases in the three-phase grid because there are more crosslinks (cf. Figure 104). In addition, through the expansion of high voltage direct current transfer systems a shift occurs in the long distance transfer of active power from the three-phase grid to the direct current grid. Often, the three-phase grid takes over the function of leading power to the direct current connections and away from them instead of transferring it. As power transfer in direct current systems does not require reactive power, the demand for inductive reactive power in the grid decreases. By contrast to the inductive reactive power in the grid, which occurs in high load scenarios, the demand for capacitive reactive power in low load times and regions occurs together with high voltages. Keeping to the (n-1) safety criteria for service security and the other grid safety parameters, it may be an advantage to shut down individual systems or whole sections in order to reduce the capacitive reactive power demand and associated active power losses.

3.2.5 Reactive power delivery in extra high voltage level

This section covers the study of how the demand for reactive power determined in the previous section can be met in the highest voltage nodes of the 100% RE scenario. The studies are limited to estimates and do not deliver concrete reactive current potentials because neither the current locations of the energy producers were illustrated for comparison with future locations, nor secondary distribution grids for highest voltage (i.e. the transport grid). Figure 110 firstly illustrates schematically the varying strong influence of “central” energy producers on the highest voltage level, and then “de-central” energy producers in the secondary grids on the delivery of reactive power (Q).

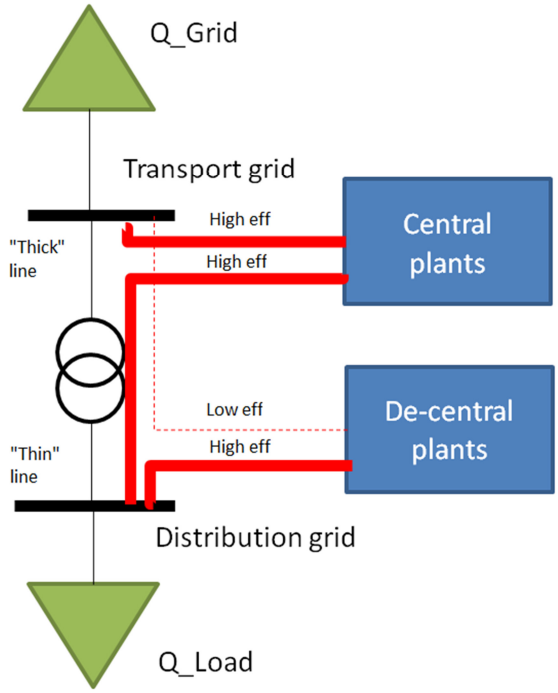

Figure 110: Schematic illustration of reactive power delivery of central and decentralized energy producers in the transport and distribution grid

While central power plants strongly influence both the transport and the distribution grid with regard to delivery of reactive power, the influence of decentralized plants – as is explained lower down – can be evaluated as strong only in the distribution grid, not, however, with regard to the transport grid.

Table 20 illustrates how producing power could change in future for the different energy producers when their performance is connected to voltage levels. In order to depict the current situation, the power plant list 2013 [80] and the EEG Statistics Report 2011 [81] were consulted. The statements for the 100% RE scenario were partially decided according to estimates; they result directly in part from the assumptions for the 100% RE scenario. For instance, the latter applies to photovoltaics where the distribution to the voltage levels in the 100% RE scenario is oriented to the ratio of open-site installations and installations on buildings.

As can be seen in the last column of Table 20, a large part of the nominal capacity in the power plant list is recorded without grid connection voltage. For the EEG Statistics Report however, a complete capture of the grid connection voltages is assumed. The power plant list does not include any data on low voltage either, thus the table was left blank in the relevant sections.

Table 20: Distribution of nominal capacity throughout Germany according to the Power Plant list 2013 [80] and the EEG Statistics Report 2011 [81] as well as the 100% RE scenario for the different energy producing technologies on grid or transformer level

Source	Designation energy source / energy production	nominal load (GW)	Percentage of nominal capacity							
			highest voltage	highest / high	high voltage (HV)	HV / MV	medium voltage (MV)	MV/ LV	low voltage (LV)	nominal capacity without voltage data
Power Plant List 2013	onshore wind energy	32,0	7	1	36	18	38			69
EEG Statistics Report 2011		28,5	3	1	31	14	50	0	0	0
100%-RE-scenario		87,0	10	0	60	0	30	0	0	0
Power Plant List 2013	offshore wind energy	0,5	88	0	12	0	0			0
EEG Statistics Report 2011		0,2	68	0	32	0	0	0	0	0
100%-RE-scenario		40,0	98	0	2	0	0	0	0	0
Power Plant List 2013	Photovoltaics	35,7	0	0	59	6	35			98
EEG Statistics Report 2011		23,9	0	0	4	1	25	3	67	0
100%-RE-scenario		133,7	0	0	2	0	33	0	65	0
Power Plant List 2013	Refuse	1,3	0	0	50	0	50			11
Power Plant List 2013	Mine gas	0,3	0	0	39	0	61			66
EEG Statistics Report 2011	Dump-, sewage-, mine gas	0,6	0	0	12	3	79	2	4	0
Power Plant List 2013	biomass	5,8	2	0	29	9	60			84
EEG Statistics Report 2011	biomass	5,4	0	0	6	4	75	4	10	0
100%-RE-scenario	bioenergy local	17,3	0	0	20	5	65	2	8	0
EEG Statistics Report 2011	Geothermics	0,1	0	0	0	0	50	13	38	0
100%-RE-scenario		4,7	0	0	0	0	50	13	38	0
Power Plant List 2013	storage water	1,4	82	0	17	0	1			6
Power Plant List 2013	running water	3,9	8	0	66	0	26			48
EEG Statistics Report 2011	water	1,4	0	1	9	6	64	3	17	0
100%-RE-scenario	Hydro energy	4,8	4	0	35	3	49	1	8	0
Power Plant List 2013	Pumped hydro storage	9,1	82	0	18	0	0			0
100%-RE-scenario		12,6	82	0	18	0	0			0
100%-RE-scenario	Batteries	55,0	0	0	2	0	33	0	65	0
Power Plant List 2013	natural gas	17,8	41	0	52	0	7			15
100%-RE-scenario	methane power plants	53,8	50	0	20	0	10	0	20	0
Power Plant List 2013	nuclear power	12,1	100	0	0	0	0			0
Power Plant List 2013	coal	19,7	82	0	17	0	1			0
Power Plant List 2013	lignite	17,8	97	0	2	0	0			0
Power Plant List 2013	several sources	14,6	38	0	49	0	13			1
Power Plant List 2013	mineral oil products	4,0	40	0	57	0	3			6
Power Plant List 2013	others	2,1	26	0	58	17	0			57

Table 20 delivers a general view of the energy producers connected to the respective voltage levels. Table 21 illustrates the difference between the current distribution of all energy producers on the voltage levels and the corresponding distribution in the 100% RE scenario. In case data for current distribution for one type of energy producer is given both on the power plant list and also on the EEG statistics report in table 20, a weighted average of the nominal capacities is generated, taking into account the percentage of existing voltage data.

Table 21: Distribution of total nominal capacities from Table 20 to the grid or conversion levels of the connection

	total	extra high voltage (EHV(	highest / HV	High voltage (HV)	HV / MV	Medium voltage MV	MV/ LV	Low voltage LV
Current nominal capacity (weighted average) [GW]	155,5	70,1	0,4	37,5	5,1	25,6	0,8	16,0
Proportion of total nominal capacity [%]	100,0	45,1	0,2	24,1	3,3	16,5	0,5	10,3
Nominal capacity in 100% RE scenario [GW]	408,9	85,3	0,0	74,9	1,0	109,7	1,0	136,9
Proportion of total nominal capacity [%]	100,0	20,9	0,0	18,3	0,2	26,8	0,2	33,5

It can be seen in table 21 that in the scenario more than 2.5 times the current performance is installed in Germany. This increase concerns all voltage levels apart from the conversion levels not included in the scenario assumptions. Thus, the installed capacity increases not only in low voltage but also in the highest voltage. This suggests that also in a 100% RE scenario an adequate reactive power delivery can be delivered on highest voltage level by energy producers although the locations of the plants in highest voltage, the reactive power demand at the respective highest voltage nodes and the structure of the secondary grid must be taken into account. With regard to the delivery of reactive power from wind energy and photovoltaic installations, it must be noted that their potential for delivering reactive power cannot be directly related to the weather as their effectiveness (P) can. Photovoltaic installations can, thanks to their power inverters, feed in their full reactive power amount (Q) during the night, just like wind energy plants, even with low wind speeds (see e.g. PQ diagram in Figure 130).

Looking at the share of the voltage level in the total nominal power in Table 21, the shift from the current situation to the scenario becomes apparent. While currently the share of connected installed capacity continually decreases from highest voltage level to lowest voltage level – disregarding the transformer levels – in the scenario, this share shows an upward trend. The implementation of this change and continued stable voltages on all levels is one of the great challenges of the energy turnaround (“Energiewende”) and still needs intensive studies, bearing in mind relevant factors in the various distribution grids.

The delivery of reactive power for the highest voltage level will continue to come primarily from plants connected to the highest voltage level possible because they have the greatest effect on the highest voltage level. To increase the reactive power potential it is also possible to convert

decommissioned power plants, or plan new power plan in a way that the generators (normally without turbines) remain in the grid when idling during critical times in the power grid. Even though such measures cause operational losses they would have the advantage that idling generators - apart from their characteristic as inertia - can in most cases also serve as phase shifters for reactive power delivery (cf. section 3.1.7). Converters also have potentials for delivering reactive power in the intended high voltage direct current transmission (cf. Chapter 2.5), which, depending on design, permit a 4-quadrant operation and thus large-scale reactive power delivery and in highest voltage instead of in secondary grids.

In spite of the above-mentioned possibilities, for times when insufficient reactive power potential is available or it cannot or should not be used due to financial restraints, the study below showcases the effects, potential and restrictions of a reactive power delivery from secondary voltage levels.

Here an “average highest voltage node” is studied to which secondary voltage levels are connected which contain loads and production plants. The following study shows the effects of decentralized generators and possible reactive power delivery. However, for specific observations on the individual nodes or grid areas individual conditions must be studied that cannot be generalized. A possible meshing or link to several nodes, especial of high and medium voltage, is omitted here. These exclusions must not occur in concrete studies of real grid areas but they have little effect on the basic approach in this section.

For the study, the following tree structure was set for the grid:

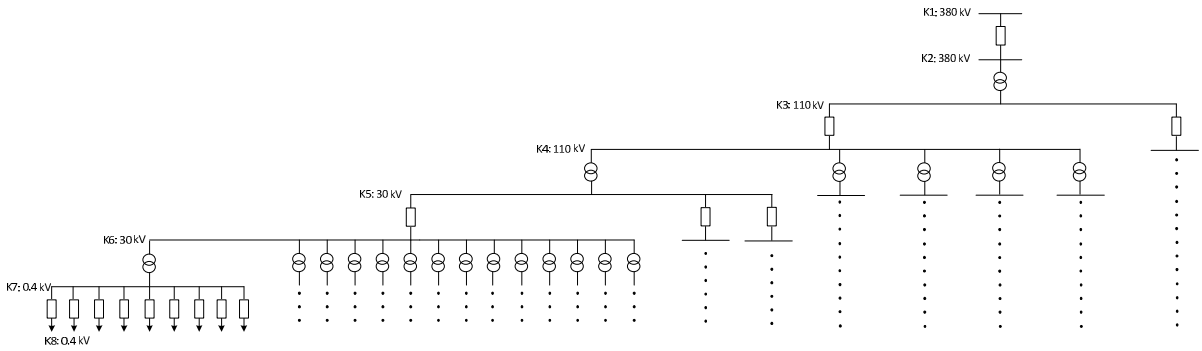

Figure 111: Grid model showcasing secondary voltage levels of a highest voltage node

In the simplified string diagram, crosslinks and different ohmic and inductive parts are not shown. However, they were taken into account in the grid calculations. For line lengths, number of parallel resources and resource parameters either usual values or literature values were used. The lengths and number of overhead lines and cables were estimated using ENTSO-E data [40] and [94].

Below, various scenarios are applied to the “average grid” in order to evaluate their effect on the voltage bands of the various voltage levels.

First, a basic load case with loads in all voltage levels is illustrated. Here an average strong load is assumed. The maximum load in Germany amounts to approximately 80 GW. Divided into 501 highest voltage nodes, approximately 160 MW result which are taken off in various voltage levels. The allocation to the grid nodes of the voltage levels follows the ratio of the assumed average numbers and rated output of transformers and pipe runs. Because of the total symmetry of the example grid

in Figure 111, the evaluation of the voltage band of the grid levels is shown for one of each of the grid nodes.

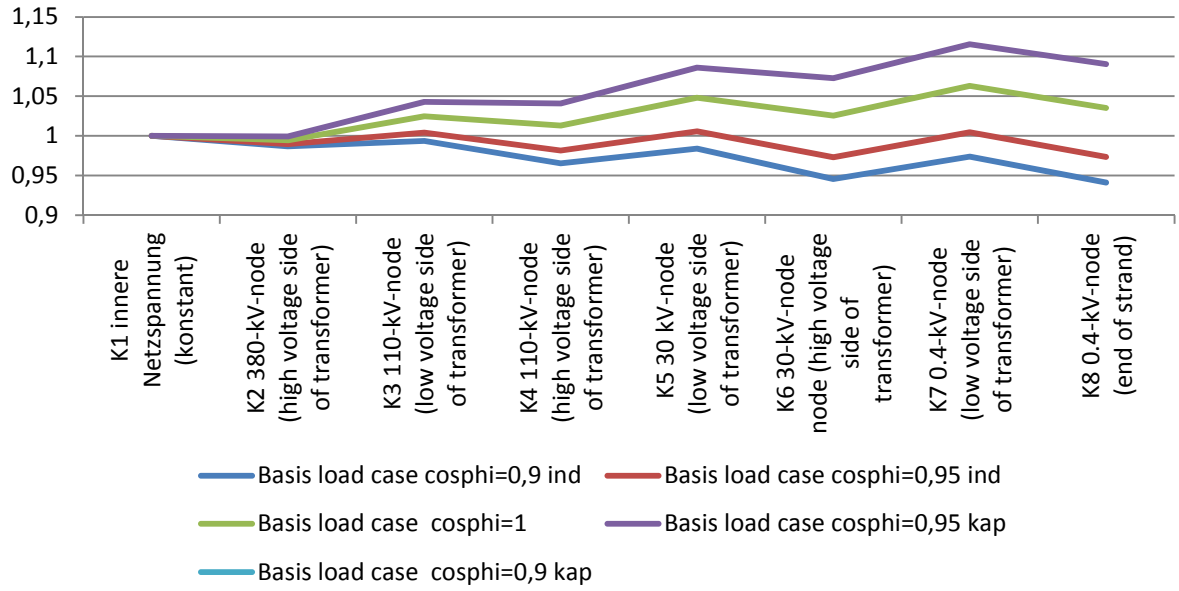

Figure 112: Voltage band of the example grid for the basic load situation

The evaluations in Figure 112 show that the voltages obtained from the power flow of loads decrease in the operating sources. In order for the voltage not to sink too low at the end of a string, the stages of the transformer are adjusted so that they do not correlate with the ratio of the nominal voltage but a ratio larger than 100 %. The influence of the power flow on the voltage at the connecting node of the highest voltage grid (node 2) is low when compared to the influence on local voltage. In the basic load situation there is still a safe distance to the voltage band limits and to possible inductive behaviour of the loads. A capacitive behaviour of the loads leads to voltage band violations while maintaining transformer step range. Thus in a next step the basic load situation is studied in connection with the three previously mentioned variants with changed transmission situations. A transformer, which up to now increased secondary voltage to 105 %, is now run with a transmission ratio which increases the voltage to 100 %.

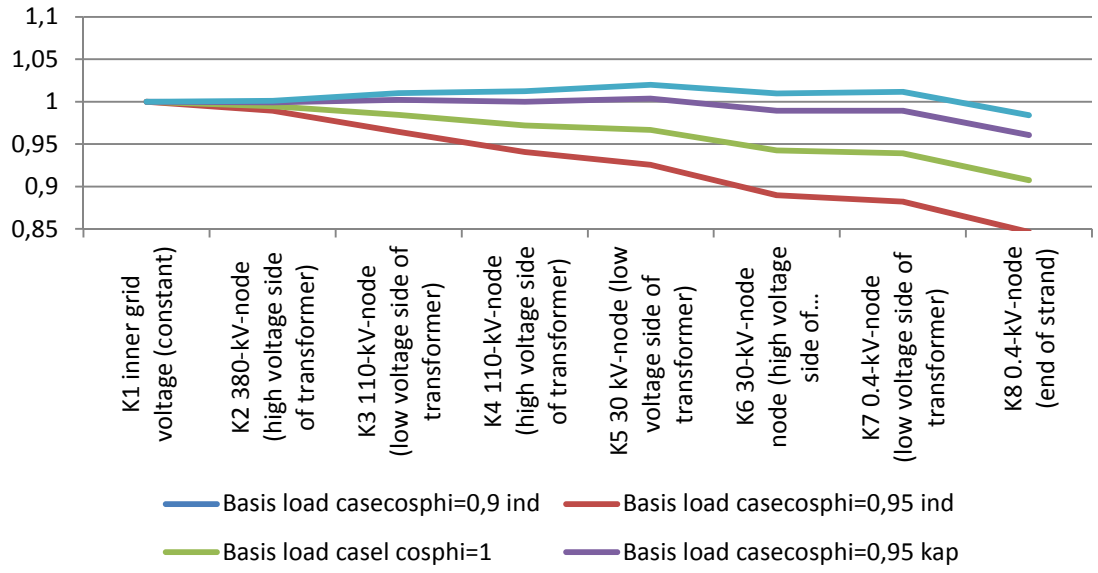

Figure 113: Voltage band in the example grid for the basic load case with changed transformer step range

Even small changes in the transformer step range show the great sensitivity of the voltages. A permissible system operation with ohmic inductive load is not possible with this step range. However, the loads can show ohmic-capacitive behaviour to a greater measure.

In a following step, the feed-in variants are investigated where active power input corresponds to the reverse basic load flow. Thus a feedback to all levels of voltage occurs. The variants differ in their reactive power feed-in.

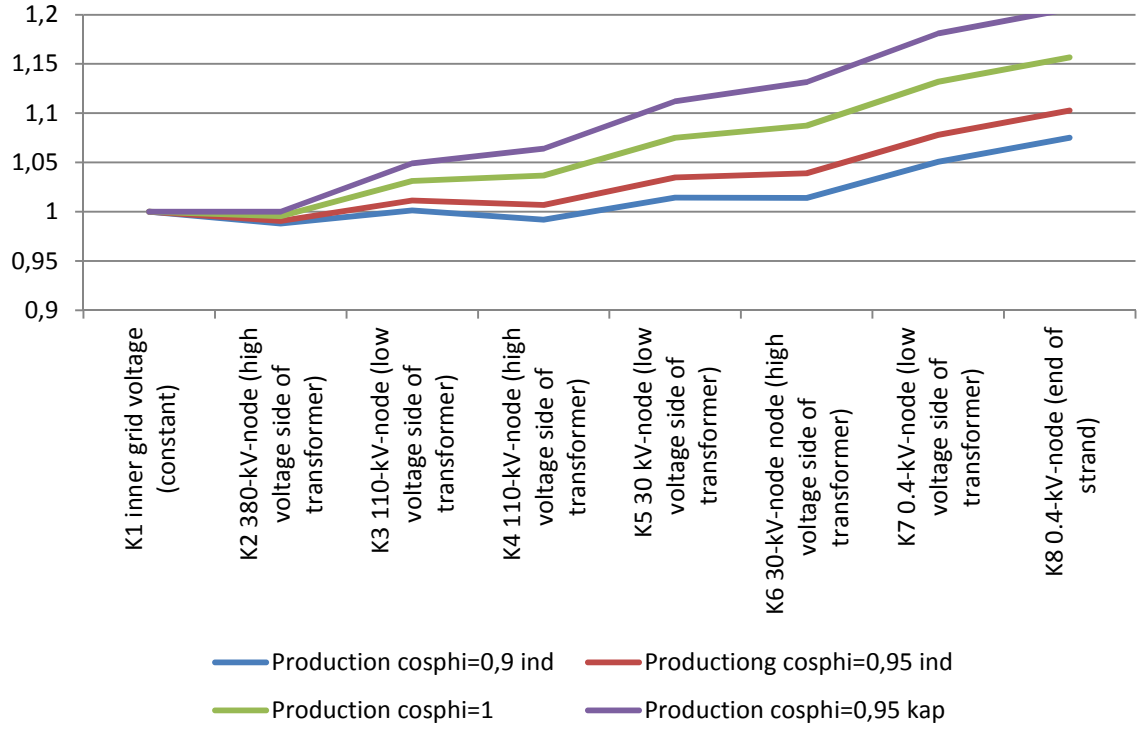

Figure 114: Voltage band of example grid in 4 production variants

The evaluation in Figure 114 show that the obtained voltages increase through decentralized feed-in. With strong feedback by production plants the voltage bands are not adhered to without voltage reducing reactive power feed-in (thus $cos(\varphi) = 1$). In this case, capacitive behaviour of production plants aggravates the voltage band violations and permits no acceptable system operation and thus no capacitive reactive power delivery for the highest voltage level. Only an inductive behaviour of the decentralized production plants with high feed-in, like it is being demanded currently, permits an acceptable system operation within voltage band limits. The decentralized reactive power delivery shows a strong influence on local voltage bands and only a moderate influence on the voltage on highest voltage level.

It can be seen that the delivery of capacitive reactive power by decentralized production plants is to be seen as critical with regard to the voltage bands in the secondary grid levels. The back-feeding active power flow from decentralized production plants causes an increase in voltage, already in the secondary voltage levels. In addition, there are the transformer transmission conditions, which are normally designed for load cases and have a step range different to the ratio of the rated voltage of more than 100 % in order to support the secondary voltages in load cases. Thus, the adjustment of transmission conditions by controllable transformers offers a potential opportunity of adjusting the voltage. Below, the three above-mentioned variants are studied with altered transmission conditions. A transformer, which up to now increased secondary voltage to 105 %, is now run with a transmission ratio, which increases the voltage to 100 %.

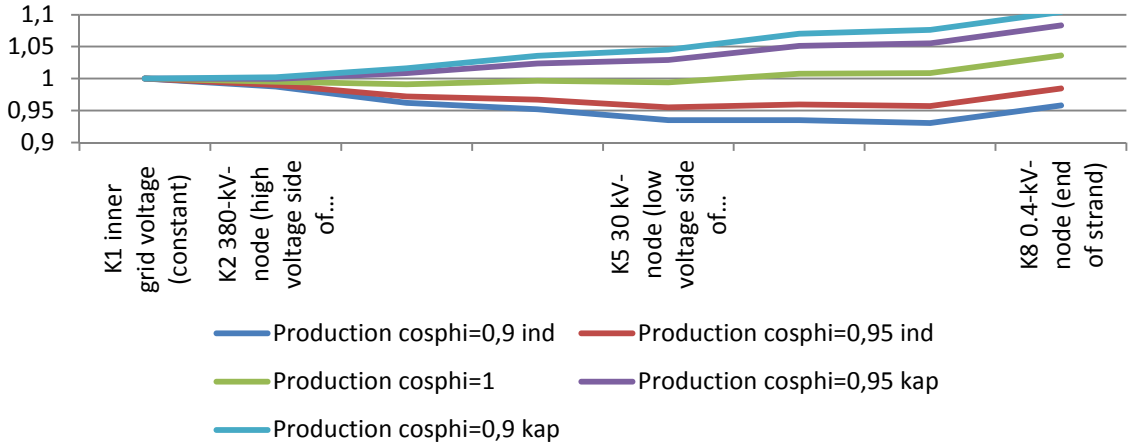

Figure 115: Voltage band of the example grid in 5 production variants with changed transformer steps.

The results in Figure 115 show that with changed step ranges of the transformers feed-in of capacitive reactive power is possible within the limits of the voltage bands. The feed-in operation with inductive reactive power is still acceptable with this step range. The decentralized delivery of reactive power shows a strong influence on local voltage bands and only a moderate influence on the voltage in the highest voltage bands. If an individual case permits it, greater step ranges could help deliver larger amounts of reactive power.

A decentralized delivery of reactive power is transferred through the voltage levels up to highest voltage level unless it is not first compensated by other reactive power measures. However, such a reactive power transmission requires active power losses and changes to the voltage in all voltage levels involved. The following evaluations show the relevant grid loss changes in the example grid according to Figure 111 for different capacity angles $cos(\varphi)$ and the two different transformer step ranges starting from the basic load case of the example grid:

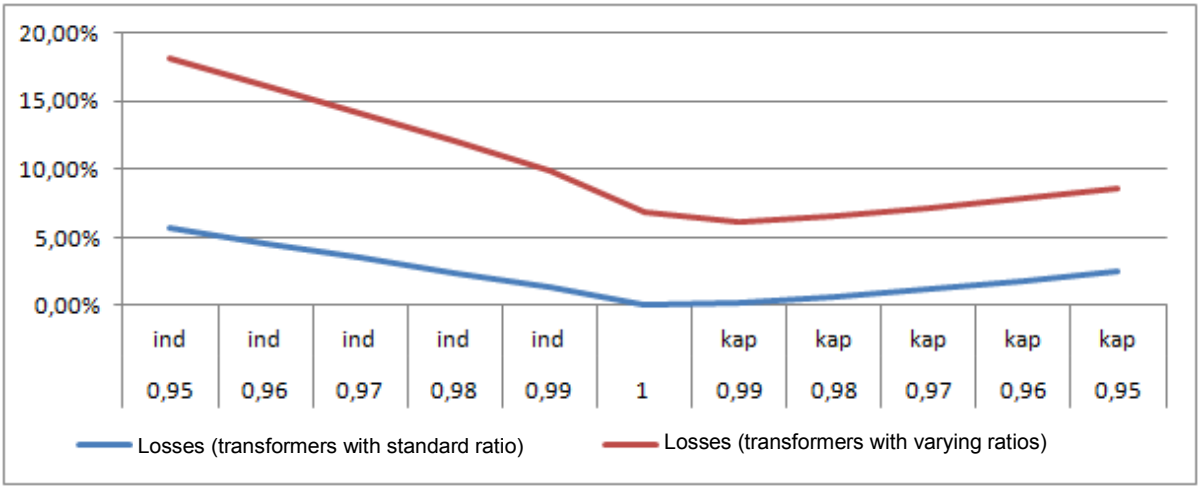

Figure 116: Grid losses through reactive power delivery in secondary voltage levels.

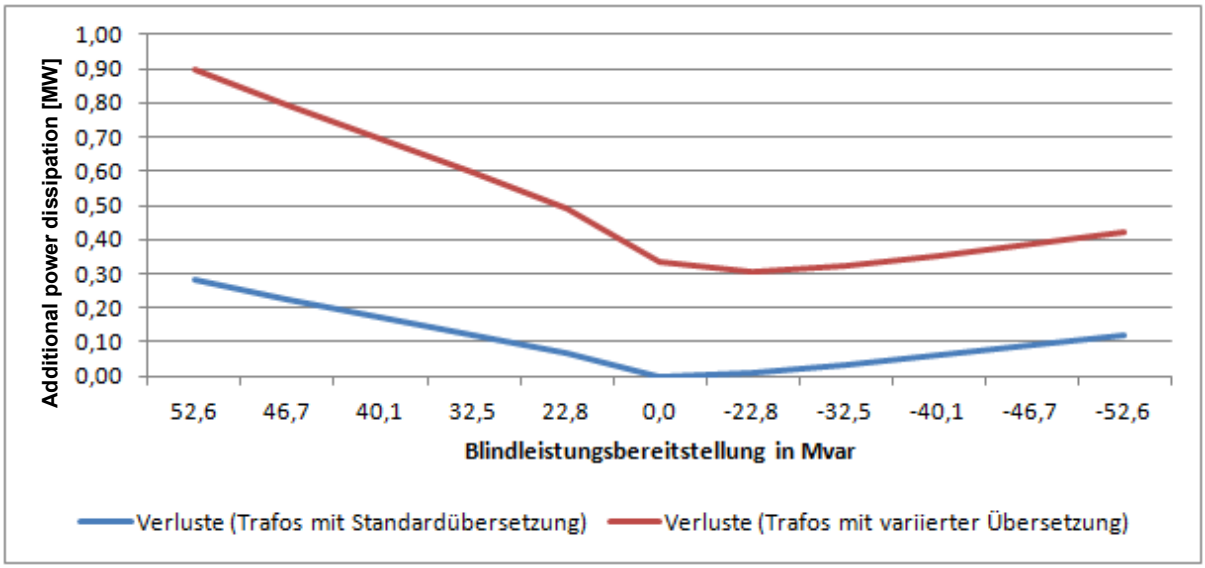

Figure 117: Grid losses through reactive power delivery in secondary voltage levels

The evaluations show that major increases in losses in part must be anticipated so that the delivery of reactive power from secondary grid levels, apart from the possible negative effects on local voltage bands, also affects the losses negatively, and should be deployed subordinately to reactive power potentials in the highest voltage level. The losses arising in the real individual case can also vary strongly depending on individual active power flow situation, the lengths and cross sections of the grid components, the degree of meshing, the expansion of cable or overhead lines, the transformer transmission situation and the state of reactive power. Figure 116 however, shows basic connections. The greater loss increase with inductive producer behaviour compared to the increase in losses with capacitive producer behaviour can be explained by basically higher losses with consistent power transmission on low voltage level, which is caused by inductive producer behaviour.

In summary, it can be said that the transmission of reactive power from secondary voltage levels to the highest voltage level is feasible. However, the interactions and limitations of reactive power, voltage stability and grid losses must be taken into account. A robust, general statement on the potential of this attempt is not possible in this project. The dependence of the individual active power flow situation on the lengths and cross sections of the grid components, the degree of meshing, the expansion of cable or overhead lines, the transformer transmission situations and the state of reactive power is too individual.

It was shown that for the modelled average distribution grid with appropriately optimized step range of the transformers a cos (φ) of 0.9 in both capacitive and inductive direction will be possible at any time. With regard to rated output of 160 MW for this partial grid, a reactive power potential of ±70 MVAr is available for the simulated grid node. A linear extrapolation for all of Germany shows a potential of 35 GVAr reactive power in both directions at any time. The calculated reactive power demand by the highest voltage grid node in the project varies between up to 25 GVAr capacitive and 10 GVAr inductive (e.g., see Figure 109) of more or less equal magnitude. The calculations allow the assumption that the secondary grid level will in future be able to make an important contribution to the voltage stability in the transmission grid. However, this will partly demand a significant restructuring of the distribution grids (dynamical transformer tap changers, distinctly extended degree of automation).

The precise potential for the delivery of reactive power from the individual distribution grids will have to be clarified in other studies, as is already being planned.

3.2.6 Conclusions and recommendations

In this section, the voltage bands and the demand for reactive power in the highest voltage nodes of the 100% RE scenario from Chapter 2 were determined. The requirements for this were precise grid-node simulations of power production and consumption and the calculation of the resulting power flows in the highest voltage grid model, which was determined using complete power flow calculations, and strategies of dealing with effective and reactive power (see section 3.2.2). The evaluations in section 3.2.3 show that the voltage bands can securely be observed to ensure voltage stability, using the chosen strategy for pertinent reactive power delivery. The evaluations in section 3.2.4 show that the demand for reactive power in the highest voltage nodes of the scenario occur particularly in a capacitive direction and this is essentially the result of using the planned direct current lines. In how far this demand can be met at any time could, however, not be finally ascertained in the studies. In section 3.2.5 it was estimated for the set scenario how much power generation capacity will be connected to the various voltage levels in Germany. The calculations

show that thanks to a massive increase in the total generating capacity there is an increase in the generation capacity on the level of highest voltage. Thus, the plants in highest voltage will probably, in conjunction with other operating sources (e.g., high voltage direct current transmission, FACTS, new compensation plants), be able to continue to meet most of the transmission grids future demand for reactive power, even with few operating hours. Further, the challenges in reactive power delivery for highest voltage from secondary grid levels were clarified. However, the precise potential of this decentralized concept must be determined with precise, locality-specific grid calculations in ongoing research projects.

In summary, it was shown that the grid voltage probably could continue to be kept in acceptable boundaries even in a purely regenerative power supply. However, new voltage stability strategies will be necessary. A decisive role in maintaining voltage stability will be played by the planned direct current/DC lines, which presently can solve reactive power problems in transmitting power over long distances and thus will lead to a changed reactive power demand in the highest voltage grid. Many power producers will be connected to low voltage levels and should be used there to compensate inductive reactive power demand of loads and operating sources. The power producers linked to the grid by converters should be able to contribute to the grid's reactive power household, even if they do not provide active power at that moment. Here, flexible transformer tap changers increase the chances of voltage stability in the distributions grids. In selecting grid connection points for new producers, their benefits to voltage stability and reactive power delivery should be kept in mind. To this effect, connection to high voltage levels is beneficial. Building additional compensation plants and restructuring existing power plants into rotating phase shifters represent further means of ensuring future voltage stability.

3.3 Grid congestion management

To ensure secure system operation, load limits for all operating sources in the grid must not be exceeded. Normally these are thermal load limits and the voltage bands in node voltages, where exceeding and/or not reaching tolerances e.g., in an overhead line where due to high heat the strength or life of the cable can have a negative impact and/or lead to cable sag. In the current grid operation, pilot projects in so-called dynamic line rating (DLR) or overhead line monitoring evaluate the environmental factors such as wind and environmental temperature, not using worst-case-values but their actual values in order to obtain higher load limits on the line. Particularly high feed-in from wind energy plants, which lead to a high loading of the line, correlates with the wind-related cooling of the overhead line. Even if it is to be expected that better utilization of the sources is possible through DLR, these potentials are not included in this feasibility study which does not claim to determine optimal operational strategies as the technology is not available yet. This guarantees that the findings are feasible with current technologies. This also applies to the consideration of high temperature overhead cables, which offer higher load tolerances. Due to reasons of voltage stability and the (n-1) criterion, they cannot be used in all parts of the meshed transmission grid.

The failure of a grid component, e.g. due to a short circuit error or snapped overhead line cannot be excluded, even if overhead lines have a high reliability of more than 99,99289 % (outage: 0,6234 h/a) [94]. The outage of a production resource (in case of overhead cables, the outage of a power circuit) is called a (n-1)-case because in this case one grid components less than intended for normal operation is in the grid. For instance, for this purpose two systems of one transmission path count as two grid components. The guaranteed availability of high voltage DC transmission is set to 98 %,

according [95] (outage: 175 h/a), where the down time essentially is caused by scheduled maintenance and servicing. Whether a (n-2)-study will become necessary in future to ensure secure system operation with high voltage DC transmission due to the almost 300 times higher outage probability compared to overhead line three phase power transmission, must be decided on the basis of increasing operational experience and/or the possible technical advances until the 100% goal has been reached. As this project assessed all 8.760 hours of the year, complete (n-1)-studies of the grid are carried out for all 8.760 points in time, and relevant measures for establishing the (n-1)-security are taken.

3.3.1 Current general conditions

According to [31] a congestion occurs when the operational (n-1) criterion is not observed due to existing load flow in the studied grid, i.e., when the grid cannot transport the produced power because of the outage of an individual cable. In addition, there is a congestion when the TSO can anticipate that on acceptance of all schemes the operational (n-1) criterion cannot be observed.

In the course of managing the system serving the secure operation of the entire system, the TSO is obliged to conduct a congestion prognosis and deriving from it, take congestion management measures. Congestion management includes all measures taken by a network operator in order to avoid, or prevent congestions, e.g., auctions, re-dispatch, countertrading or market splitting [31].

In order to be able to adopt measures for eliminating congestions and ensuring security or reliability, TSO are entitled and obligated under § 13. par. 1 and par. 2 EnWG (Energy Operations Act) to initially conduct grid-related, and if this not sufficient, market-related measures, and thus to intervene in market-related power plant application planning.

3.3.2 Simulations

In DC grid expansion simulation (Chapter 2.1 point 4), the grid was initially so designed for the 100% RE scenario that at all 8.760 points in time no congestions (n-0) would occur. For this, the current transmission grid with a length of approximately 43,100 km was increased by approximately 16,000 in the AC grid and approximately 17,400 km in the DC grid. This is in line with scenario B 2023 of the grid development plan [43], as well as an additional expansion in the AC grid to the extent of 3.800 km (cf. Table 10 in Chapter 2.5). This network expansion depends strongly on power consumption (Chapter 2.3), the composition and regional distribution of generators of the various energy sources (Chapter 2.4), and the capacity allocation and the unit commitment planning of energy storage (Chapter 2.6). This means that the grid scenario is just one of the possible grid expansion scenarios for 100 % renewable energies. As it is only one scenario, it is possibly not the best one. The grid expansion strategy, which includes (n-1) security in addition to (n-0) security, could conceivably also be used to reduce the re-dispatch demand for achieving the (n-1)-security described below.

In order to monitor and achieve (n-1)-security, (n-1) power flow calculations were conducted for the outage of each individual power resource. In order to attain a set of grid data where at all 8760 points in time there would be no (n-1) case for island grid formation, voltage band violations or lacking re-dispatch potential, a further 1.078 km AC grid expansion was necessary. Particularly in critical locations in addition to the initial grid expansion, totalling 3,800 km to create (n-0) security via grid expansion in Chapter 2.5. In this way, an additionally of 4.878 km of grid expansion is necessary beyond the grid expansion of scenario B 2032 of the grid development plan [43]. The grid scenario will be referred to as “KK2-(n-1) scenario”. A grid expansion to this extent does not indicate that

there would be no congestions at all. Instead, during simulations the load on grid components showed that in all (n-1) scenarios there were many points in time that congestions occurred (Figure 118) and many grid components at many points in time showed congestions as well (Figure 119). Detailed evaluations have shown that congestions in AC grid components with (n-1) failures of HVDC transmission systems occur less often since no parallel systems are directly affected, as opposed to a failure in an AC system. The lacking DC power flow is evenly distributed widely to different systems, as HVDC connected areas far apart from one another.

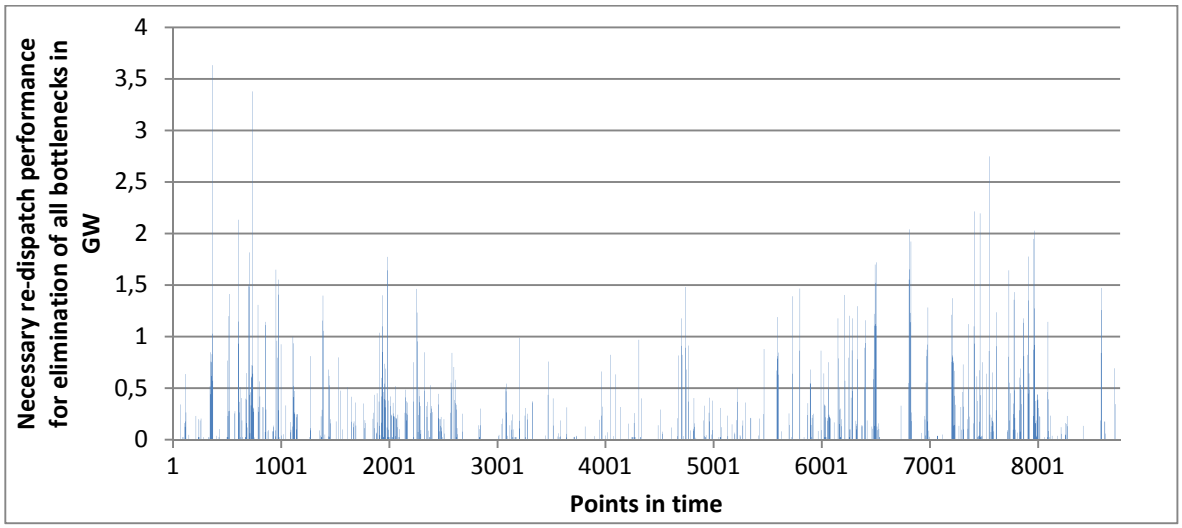

Figure 118: Necessary re-dispatch performance per point in time to eliminate all (n-0)- and (n-1)-congestions in the KK2 (n-1)-scenario

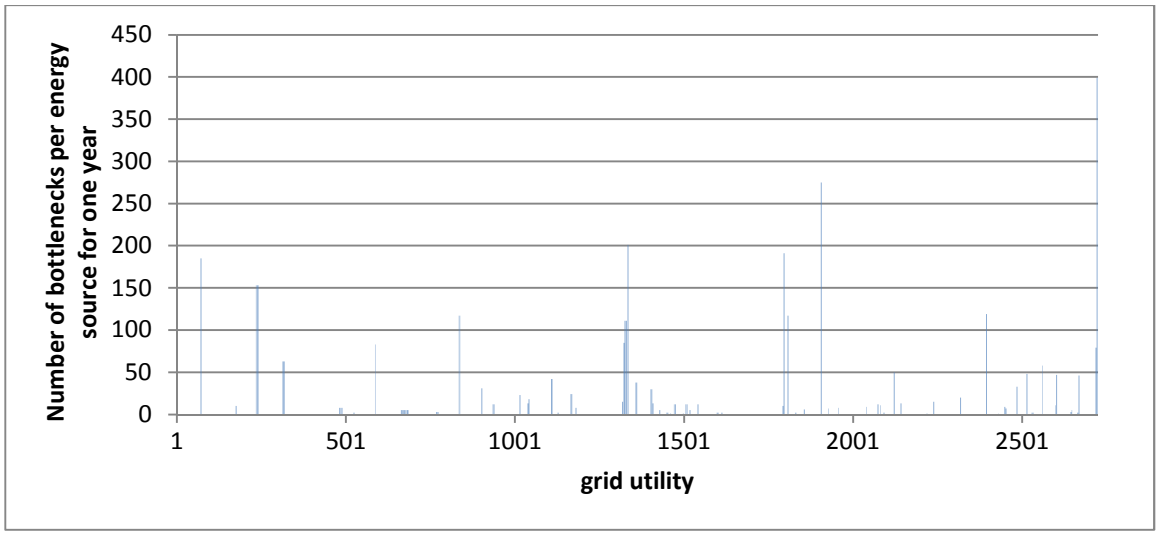

Figure 119: Number of congestions per energy source for a year in KK2-(n-1)-scenario

In this model, congestions in (n-0) and (n-1) scenarios are cured exclusively through re-dispatch. A re-dispatch means that a feed-in or a load (e.g. power-to-gas plant or pumped hydro storage in pumping mode) which causes the congestion is curtailed and a feed-in or load removes the congestion (or loads it less) is increased. The increased output must be equal to the reduced output. To simplify, the feed-ins and loads are uniformly referred to below as plants. Switching, stepping transformers and other grid-technical measures are not described, as these potentials are generally not used in planning process but in the real time management of congestions. Thus, the considerations within the project are designed for security.

Removing all (n-0) and (n-1) congestions at a point in time is a sophisticated problem of optimization as each re-dispatch measure affects all resources in the grid. Therefore, the optimum re-dispatch measure for one congestion event can affect other bottlenecks negatively or even produce new bottlenecks. A singular curing strategy for congestions for each congestion site works for small grids and a low number of congestions but fails with multiple large congestions in a meshed grid. As each re-dispatch measures change the optimum application scenario (or a market result) this causes economic costs. Thus, it is necessary not only to find a possible re-dispatch configuration but also the minimum re-dispatch configuration. Figure 120 shows the incoming and outgoing values for optimizing multiple congestions of a point in time.

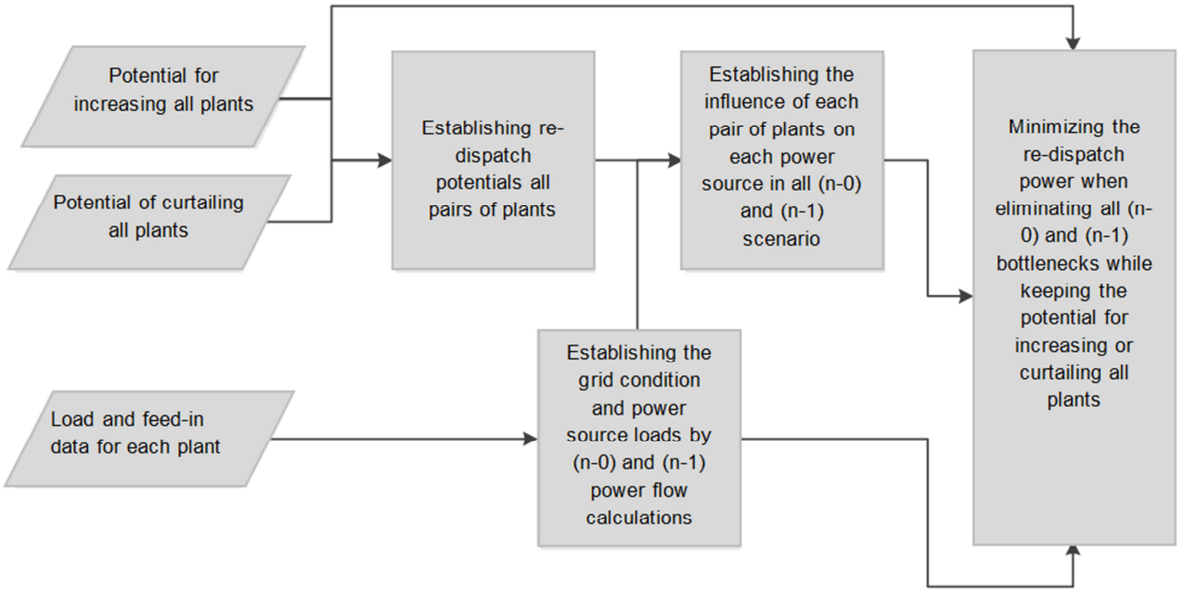

Figure 120: Process for optimization of multiple congestions

The influence of each plant on a congestion at a re-dispatch is just a rough approximation, independent of the choice of "partner plant". This assumption of independence particularly implies a power imbalance in the grid, which may not occur during re-dispatch. Especially for a spatially extensive and heavily meshed grid, as the already existing model for the German transmission grid, the influence of a congestion has to be assessed in the system context. This means that not only each plant individually has to be assessed, but also each combination of a plant with all other plants. Furthermore, the adjustment potentials of a pair of plants in dependence on the adjustment potentials of the "partner plant" are varied. Additionally one has to note the influence of a pair of plants on the voltage level and grid losses is depending whether plant 1 increases its out and plant 2 decreases its output and vice versa. This means that the number of pairs of plants is squared to the number of plants. For each (n-0) and (n-1) scenario the influence of all pairs of plants on all power resources must be calculated separately and included in the optimization.

Beside the maximum power resource load in all (n-0) and (n-1) cases, the plant's modulation limits must be taken into account as basic conditions since a plant cannot be operated above its maximum capacity or below its minimum capacity. A further condition of a re-dispatch is that the power in the grid must be balanced.

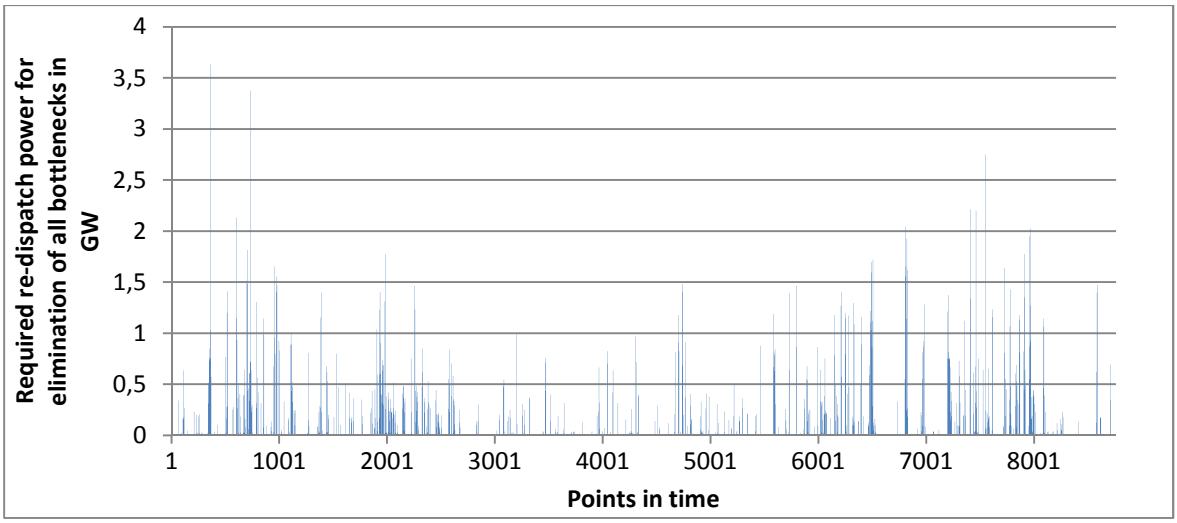

Figure 121: Required re-dispatch power per point in time for elimination of all (n-0) and (n-1) congestions in KK2-(n-1) scenario

The evaluations in Figure 121 show that in part re-dispatch performance totalling several gigawatts (GW) is required in order to ensure secure grid operation, although in the KK2-(n-1)-scenario a further 4.878 kilometres of power lines have been added in terms of scenario B 2032 of the grid development plan [43]. A secure system operation is possible at all times during the year as adequately high re-dispatch potentials are available although their utilization may create high costs.

As described in Chapter 2, the condition of the grid depends largely on network expansion and the input data of the 100% RE scenario. Thus the re-dispatch demand, too, depends heavily on these data. In this point, there is a certain degree of freedom in designing and optimization, in relation to all other energy sectors, that will require further examination on the path to a 100 % RE supply. Figure 122 and Figure 123 show the dependence of the annual re-dispatch work and the annual congestion hours of an ongoing grid expansion for the 100% RE scenario.

To get an idea of the magnitudes in Figure 122 and Figure 123, these can be compared to the current numbers of the Bundesnetzagentur (Federal Republic Grid Agency). For 2010, the number of hours with congestion 3,671 hours and the energy content of it as 2,137 GWh [94]. For 2011, the number of hours with congestion is approximately 5,000 hours [77] and for 2012 is 4,769 hours with an energy content 2.566 GWh [78].

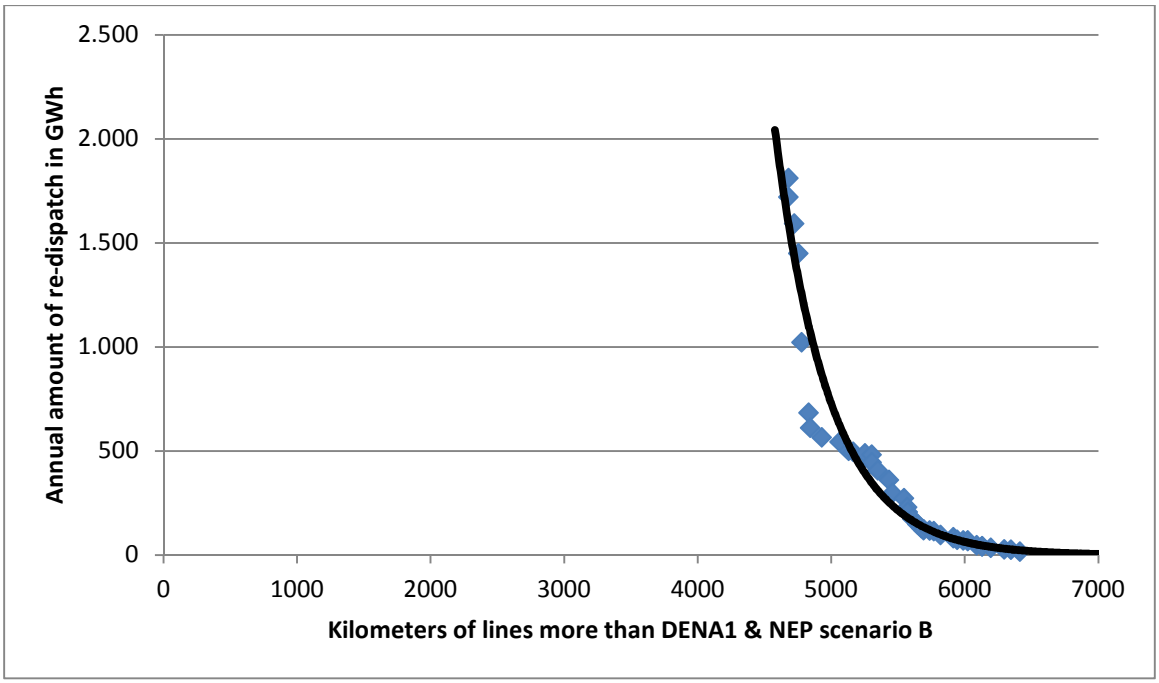

Figure 122: Annual re-dispatch quantities in depending on further network expansion

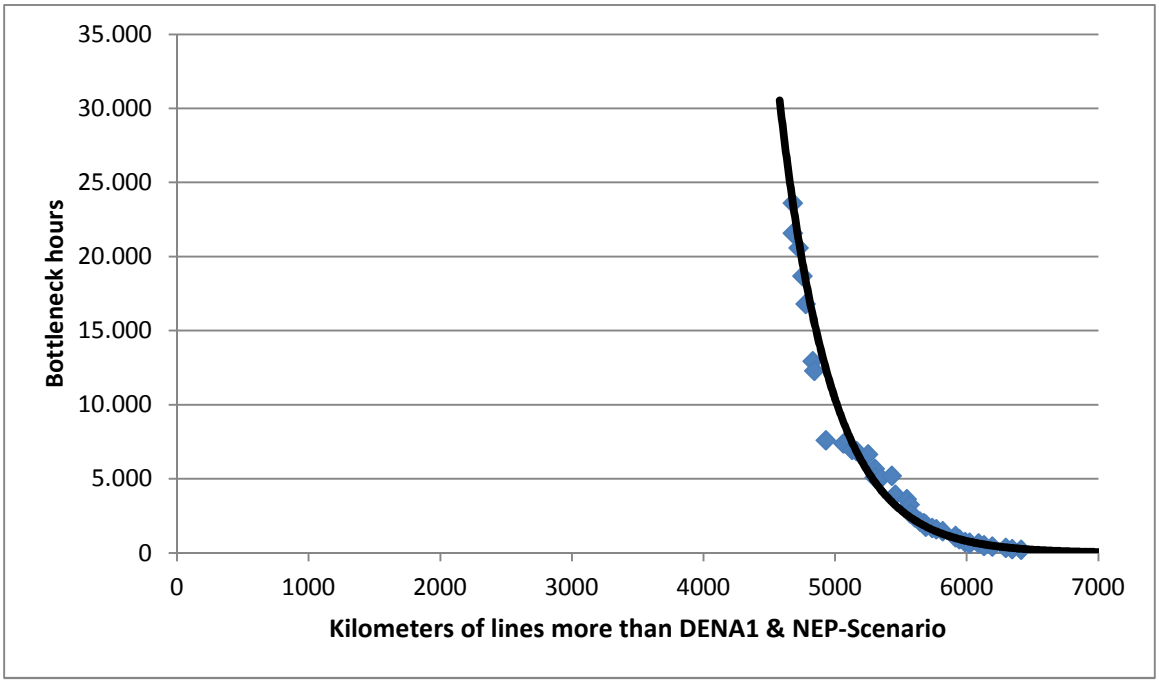

Figure 123: Annual number of congestion hours depending on further network expansion

The fact that the number of congestion hours in the 100% scenario for the assumed network expansion is higher than current numbers, but the annual re-dispatch quantity is lower can be explained. In the assumed scenario congestions occurred more often, but most of them with a negligible energy contents. The higher energy contents of the current situation is characterized by some particularly affected congestion areas or simultaneous congestions on several grid components, as pointed in the publications [77], [78]. This also means that a particular re-dispatch measure benefits more than one single congestion area. To get an idea of the magnitudes, it should also be noted that the grid expansion in this chapter has been preceded by the grid expansion described in Chapter 2.5. This grid dispatch was already necessary to guarantee (n-0) secure grid operation. Further, because of the integration of the high voltage DC current transmission in the AC

grid, a strongly divergent grid situation exists than in [77] and [78]. In Figure 123, congestion hours result that are higher than the annual number of hours of 8.760. These results are based on the fact that congestion hours do not indicate the number of hours that are subject to congestions but the sum of hours in which congestions occur on any grid component. If congestions occur in a large number of hours per year on more than one grid component, congestion hour numbers greater than annual hours occur. The evaluations for the 100% scenario show a strong non-linear dependence of annual congestion amounts and congestion hours on implemented grid expansion measures which would tend to continue in this area with less than the 4.878 km expansion. Once more, one sees the interaction between the target values for each energy source, the utilization of storages and their geographical allocation as well as the grid expansion.

3.3.3 Conclusions and recommendations

While in the scenario, the flexible producers and storages are allocated and deployed in such way that grid loads remain minimal, in reality the expansion could happen differently. Furthermore, the grid expansion going beyond the scenario B 2032 grid development plan [43] is difficult to estimate and strongly depends on costs. All these factors influence each other as well as the re-dispatch demand. Studies of different pathways of different 100% RE and storage scenarios, as well as scenarios on the road to a supply 100 % RE power supply as well as different grid expansion scenarios should be carried out. This allows carrying out the grid expansion in an economically optimized way, which evaluated the congestions against a possible grid expansion. In such studies, apart from congestion management, other grid parameters and ancillary services such as voltage stability and reactive power management (cf., section 3.2) should also be taken into account. Voltage stability and reactive power management could be secured for the study of variants in section 3.3.2 for all grid expansion and (n-1) scenarios. However, a review of the provision potentials (cf. section 3.2.5) was not carried out. Here not only the German but also the entire European grid should be investigated with the use of a combined congestion management strategy. Additionally, the effects and/or potentials of an ever-increasing connection of the power sector to the heat and also the transport sectors should be explored.

The simulations conducted in this project did not include monitoring of overhead lines (dynamic line rating), which will probably be rolled out in the future. This measure will probably lead to an increase in thermal load limits on overhead lines, especially in windy periods, and thus improve the capacity utilization of the overhead lines. The positive effects of high temperature conductor lines can lead to additional capacity of the power grid, thus reducing the risk of congestion. In future, both are to be evaluated further so that the support potentials can be quantified more effectively.

3.4 Restoration of supply

On average, currently power does not reach consumers for approximately 15 minutes per year [29]. In most cases, power outages affect individual streets or residential areas, more seldom whole suburbs or towns areas. The causes of such outages are usually faults in the low or medium voltage grid; the voltage in adjacent grids is usually not affected, i.e. it is stable and can be used to reinstate power to the affected area. In case of the rare occurrence of a supra-regional power outage, a major disruption ([30],[31]), when even the high and highest voltage grid is without power, the restoration of supply is more complicated. In that case, the power plants can no longer receive the power they need for their own operation from the grid. As a result, the power plants either fail or stabilize themselves at self-consumption levels, only generating the power necessary for their own operation. In this last case, the power plants have separated from the meshed grid and are able maintain a small island grid. The power supply has then closed down in a large area. In addition, if no neighbouring grid exists which specifies the voltage, phase position and frequency for their operation, the restoration of supply must be handled by the power plants that are in self-consumption island mode operation or by power plants that are able to black-start. Black-start ability is the technical property to start independently from the grid. Currently, mainly gas, run-of-river and pumped hydro storage power plants are able to do this. On principle however, all power producers can be enabled to black-start if they are equipped with grid-independent power supply, such as a batteries or an emergency generators, which serve provide power for the starting process. During the restoration of supply process, the black-start power plants or those working in self-consumption first form their own island grid. These power plants are capable of establishing nominal voltage or frequency levels without external inputs. They are therefore called grid-forming. Now the crucial challenge in the restoration of the power supply is the coordination of the reconnection of loads, other power plants and grid components. If, for instance, large loads are connected too fast, the frequency can deviate from the nominal tolerances, which in turn would stop resynchronisation of the grid and potentially lead to additional outages. To avoid this, reconnected generators are required to be able to operate in island mode and support the grid ([31], [32]), i.e., that they contribute to frequency and voltage stability. During the restoration of supply, all requirements of grid stability have thus to be met by the rebuilt smaller island grids, though adapted to the special conditions of this case. Each of these grids must be operated in a stable manner. For the connection of two island grids it is necessary to ensure that the voltage amplitudes, phase angles and grid frequencies are not too dissimilar on the connections or that they meet within allowable deviations. So-called synchronizing devices serve to establish this synchronism.

3.4.1 Current general conditions

The approach of the transmission system operators with regard to major disruptions is recorded in [31] and [33]. Initially a major outage must be kept under control. In case of a major disruption with a frequency drop, the TSO have developed the so called “5-step plan” which specifies how much load must be shed with specific low frequencies. When the grid frequency falls below 47.5 Hz, all power producers are disconnected from the grid; then, at last, a large-scale power outage has occurred. For the subsequent restoration of supply the TSOs have prepared situation-specific concepts and coordinated and trained them with the power plant and distribution grid operators involved. Initially at a large-scale power outage, the grid situation is analysed and depending on that, a grid-reconstruction concept is applied in cooperation with other TSOs and the operators of the generators and secondary distribution grids. Here a fail-safe communication system that will function during a power outage is extremely important. Therefore, it must have its own power supply. The

TSOs' procedure for restoration of supply is described in detail in [30] and [34]. Here two types of restoration of supply are differentiated. One is with the external setting of the default voltage values and one without it. Additionally, the technical problems of the restoration of supply with regard to balancing reactive and active power, transient procedures and the behaviour of electric safeguards are clarified.

Currently large power stations on highest voltage level normally handle the restoration of supply. These power plants specify voltage, phase position, and frequency; the secondary grids are then successively connected. The restoration of supply thus happens "from the top down". Power generation however will shift with the increase of renewable energies from the higher to the lower voltage levels. Even if the restoration of supply can continue to take place from the top down (as there will still be generators connected to the highest voltage levels), the importance of the restoration of supply from the bottom is going to be more important than it is today. On the one hand, this allows the stable operation of island grids when the rest of the grid is without voltage. On the other hand, it simplifies the reconnection of island grids as they are stable and have a secure generation and consumption balance.

3.4.2 Laboratory test

In order to determine the requirements for re-establishing power to a distribution grid using renewable energies, a laboratory test is being conducted by the Design Centre for Modular Supply Technology (DeMoTec) [53] of the Fraunhofer IWES and the University of Kassel (see Figure 124). For the test, an exemplary distribution grid was implemented which functioned in island operation mode during the restoration of supply.

Figure 124: The Design Centre for Modular Supply Technology (DeMoTec)

The laboratory test has a disadvantage over a field test, as it takes place under artificial conditions and is not directly transferable to the real operation. On the upside it has distinctive features that are necessary to demonstrate a restoration of supply by RE. These are:

In the laboratory environment, grid conditions can be tested that lie outside of the admissible limits of the integrated grid. Specifically, the laboratory grid can be disconnected from the integrated grid, which is the prerequisite for tests for the restoration of supply.

The grid reproduced in the laboratory can be designed and adjusted in such a way that the influence of the power plants registers on the power flows in the grid. In the real integrated grid, there are usually such high power flows that for experimental purposes a comparatively small VPP has hardly an influence.

The plants of the laboratory test all feed into the same distribution / laboratory grid. Through the island operation of this grid, the interplay of the plants can be analysed, and this takes centre stage in investigations for a VPP.

The components used for the test are, apart from extensive communication and regulation infrastructure, a greatly simplified replica for a biogas plant, replicas for wind energy installations, controllable and non-controllable loads as well as a synchronisation unit (see Figure 125). Below, more detail is given on the individual components and their control concepts for the restoration of supply.

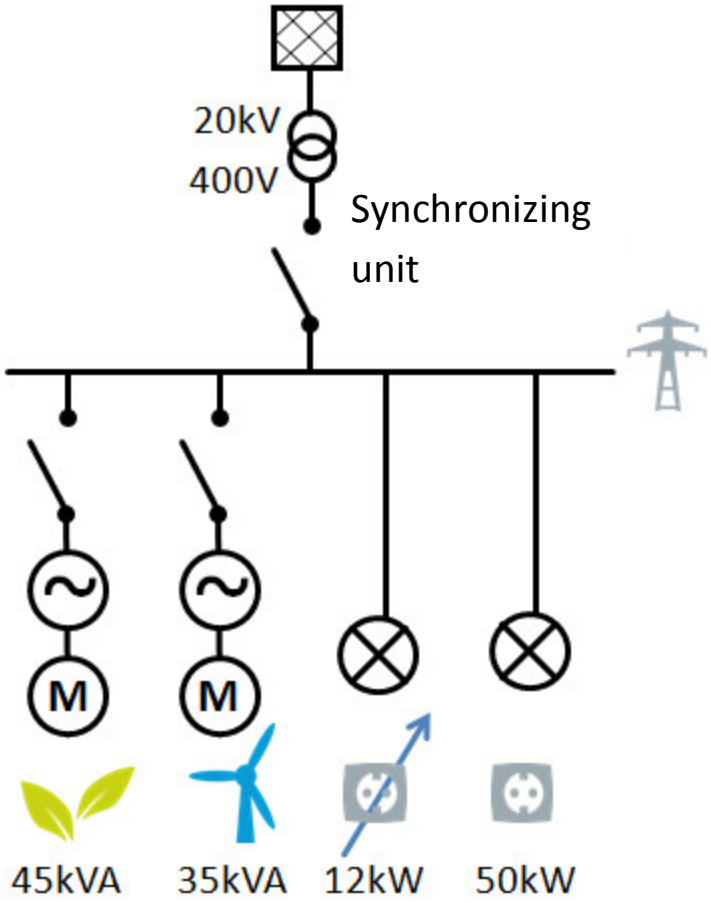

Figure 125: Structure of the laboratory test for the restoration of supply

3.4.2.1 Description of test environment

Below is a description of the experimental setup. The test environment consists of various installations and loads connected to the experimental grid, which are controlled by the communication and control infrastructure, described the in next section.

Communication and control infrastructure

For the transfer of measured values and set points for the restoration of supply by RE, an extensive communication and control infrastructure (CCI) is necessary because all components have to be controlled in a synchronized manner. The CCI used in the laboratory experiment is shown in Figure 126. Below, the individual CCI components are described: the communication system, the data capturing system, the remote control terminals and the SCADA-system.

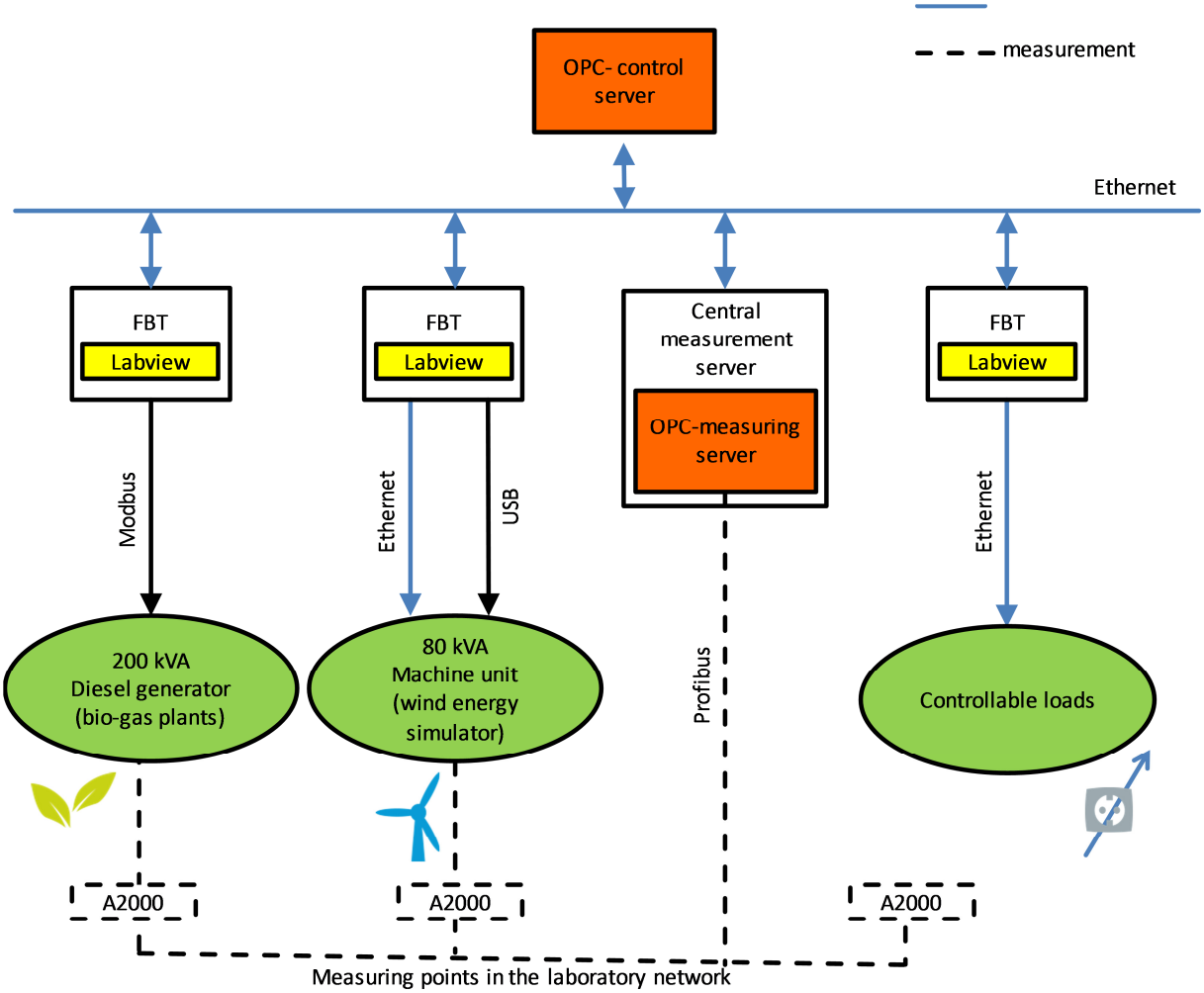

Figure 126: Communication and control infrastructure of the laboratory test

Communication system

For communication between generators, loads and control centres an Ethernet/Local Area Network to the standard IEEE802.3 is utilized. The information exchange between the different elements takes place via OPC-interfaces (Open Process Control). Using this open interface format permits the integration of the most varied applications developed on different platforms. The grid is connected to an OPC server, the so-called control server. All elements of the grid can access it for entering and reading set points and measured values.

Data capturing system

The central data capturing system of the test measures the performance and other values of the laboratory test. The data capturing system consists of several measuring devices (A2000), a Profibus-network, and a Profibus/OPC server, the so-called measuring server. The measuring devices situated at the connecting points of the generators and the controllable loads measure the following values:

- active and reactive power of each phase

- frequency
- voltage of each phase

All data of all measuring devices are transferred to the central measuring server via the Profibus network. This central measuring server logs all measured data and saves them in an OPC-server located in the same casing.

Remote control terminals

The remote control terminals (RCT) serve as interface between the control server and the power producing units or the controllable loads and were developed in the programming system Labview. They are adapted to the special characteristics of the power producing units and the shiftable loads and will be explained in the relevant sections.

SCADA System

The SCADA system controls the producers' feed-in and records the measured data of the RCT and the measurement server. Its functions are:

- Central and synchronous control of effective and reactive power from the plants via the target value specification. These specifications are read from text files.
- Access to measuring data in the measurement server and the RCTs and synchronization of measured data.
- Visualization and
- Human-machine-interface-functions

The SCADA system communicates with the control server in order to control the generators and the loads via their RCTs. The SCADA system also communicates with the measuring server to capture the data from the measuring devices.

Biogas installation

The biogas installation was reproduced by a 200 kVA diesel unit and basically consists of a combustion engine and a generator. In order to keep the biogas installation to the scale of the other test components only 45 kVA of the possible 200 kVA are utilized. The biogas installation has key role to play in test for the restoration of the power supply, as it represents a grid-forming unit and can control frequency and voltage. It is equipped with a battery that it can use to black-start. The battery serves as a starter-battery for the biogas installation and as source of energy for the gas carrying components such as the compressor, measuring technology etc. The biogas power plant is connected to the consumers or rather the island-/laboratory grid. The biogas power plant features an integrated control (IC) installed by the manufacturer with the Modbus-protocol communication protocol type. In order to access the biogas power plant's integrated control, an interface is necessary which translates between the Modbus-(RS-232) and the OPC-protocol. For this purpose, the system is equipped with an RTU, which is also used to expand the control options of the biogas installation with regard to the restoration of supply.

The biogas installation's RTC enables the following basic functions:

Grid-connected operation

With grid-connected operation, the active and reactive power of the unit is controlled by the integrated control. Grid-connected operation can function directly after the start or after the island operation. After the start, as soon as the unit runs flawlessly and the actual values for voltage and frequency are correct, the unit is connected to the grid. The same applies to island operation but in this case, the integrated control receives a synchronization permission signal before synchronization with the grid takes place.

- Active power regulation

  The RTU controls the feed-in of active power when the unit is running connected to the grid. In this case, the nominal value is transferred from the SCADA system to the unit's integrated control.

- Reactive power control

  For the control of reactive power, two pulse signals are transmitted to the integrated control; one signal for increase, one signal for decrease of the reactive power delivery. The reactive power is controlled by the integrated control through these signals. The limits of the operation regards delivery of reactive and active power was defined in the RTU as in the following illustration:

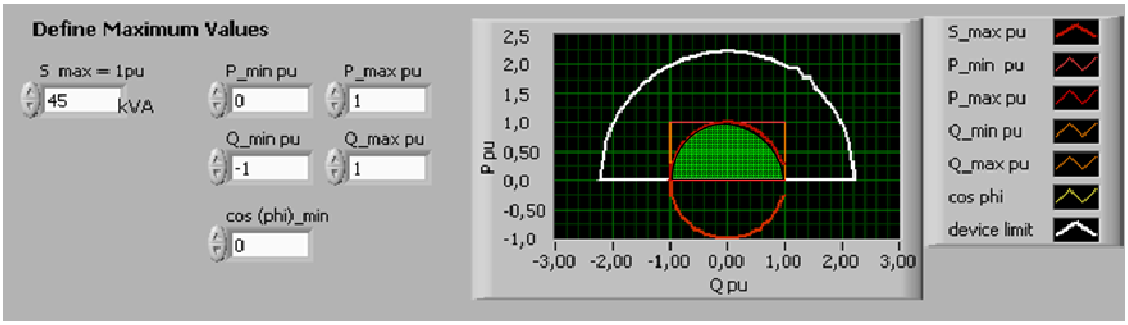

Figure 127: Set P/Q diagram of the biogas installation

The green area (interface) is the area where the biogas plant can operate during the test. The white line is the actual physical limit of the diesel unit. In Figure 127 it can also be seen that the limits regarding the cos(φ), the reactive power and the active power can be predetermined.

Island operation

During island operation, the unit reproduces the grid using frequency and voltage control.

- Frequency control

  Via the unit's RTU a Δf/P static ("droop") can be set to control the frequency. By this it can be established which frequency the plant provides to the unit, depending on the load of its generator. Since the connection of other generators leads to a load relief for the biogas plant's generator, no communication technology between the various generators is necessary to regulate frequency via the static.

  In the illustration above in Figure 128, the configured Δf/P-static of the biogas plant is shown. The grid frequency is regulated by the load of the biogas plant. If the active power produced in the plant is 45 kW, the frequency is set to 10 % below the target value. For idling, a frequency of 52.5 Hz is set.

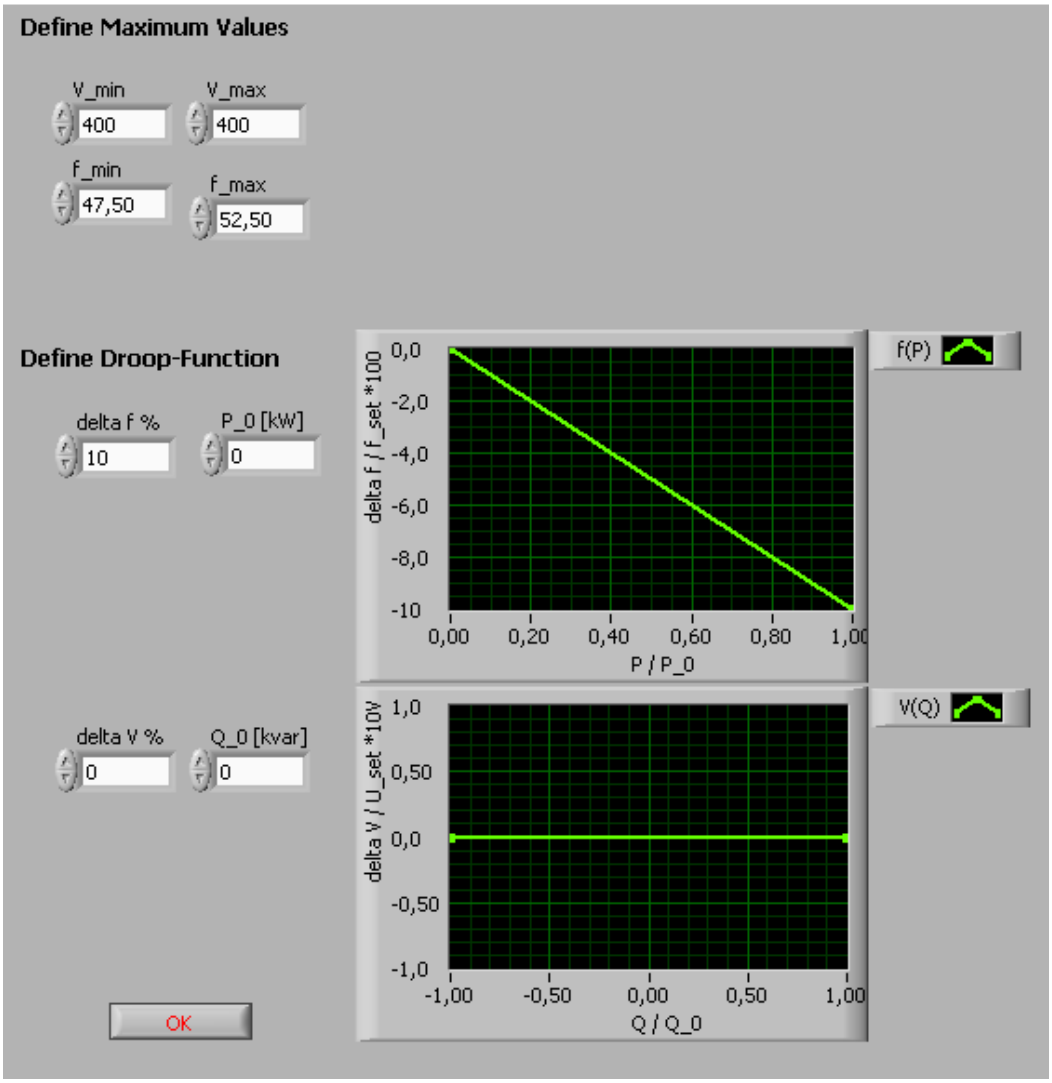

Figure 128: Set statics of the biogas plant

Voltage control

A comparable behaviour can be realised for the voltage control. Depending on the reactive power delivery, the voltage can be changed according to the set reactive power static (ΔV/Q-static). In the illustration in Figure 128 below, the chosen reactive power static is shown. It is visible that no control actions were realised for the reactive power static.

Measurement data transmission

All measurements in the biogas plant are recorded by their integrated control and read by the RCT. After that, the measurements are transmitted to the KRI.

Monitoring

The RCT also serves to read the status information on the biogas plant from the integrated control, which is coded in a 32-bit long word. This includes information on alarms, trip conditions, reports, the current operating mode, and the switch status. In order to avoid problems during the restoration of supply, it is very important for the coordination of the restoration of supply always to know the status of the grid-forming units.

Switch control

The RCT permits opportunity of controlling of switches. For this purpose, there is a bit; if it is set to 1, the switch is closed, if set to 0, the switch opens. The synchronising unit, too, which is a switch between the laboratory grid and the integrated grid is switched in this way.

Wind energy plant

The wind energy plant is reproduced by a 80 kVA machine unit of which only 35 kVA are used in order to keep the size of the wind energy plant similar to that of the other test components. The machine consists of a variable-speed DC electric motor, which is controlled by four quadrant converters. The DC motor is linked to a flywheel and a synchronous generator. The reproduced wind energy plant functions as grid-supporting unit for the restoration of supply. It can feed active and reactive power into the grid and replicate the frequency-dependent power control of a wind turbine.

Figure 129: The 80 kVA machine unit as replica of a wind energy plant

Similar to the biogas plant, the RCT enables a number of basic functions for the wind energy plant.

The wind energy plant can be started and stopped by the RCT. Via the wind energy plant's RCT, the feed-in of reactive and active power can be controlled. For this, a programmable logic controller (PLC) is used, which regulates the rotational speed and the torque of the DC motor via the converter. The excitation of the synchronous generator is controlled via signals. The status of the switch is monitored by digital signals. Apart from the control of active and reactive power, the PLC is also used for the display of its temporal progress, frequency and voltage.

In addition, the remote control terminal shows a P/Q diagram which is oriented to the characteristics of [55] (see Figure 130).

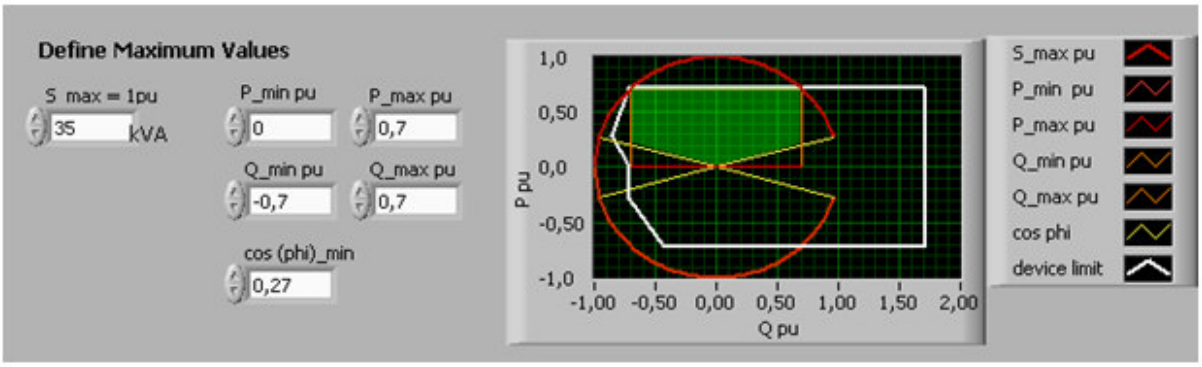

Figure 130: Set PQ diagram of wind energy plant

The green area relates to the possible operating points of the wind energy plant. If index values occur during the test that fall outside of this area, initially the active power and then the reactive power is limited to the nearest valid value.

In Figure 131 the set effective control of the reproduced wind energy plant is shown.

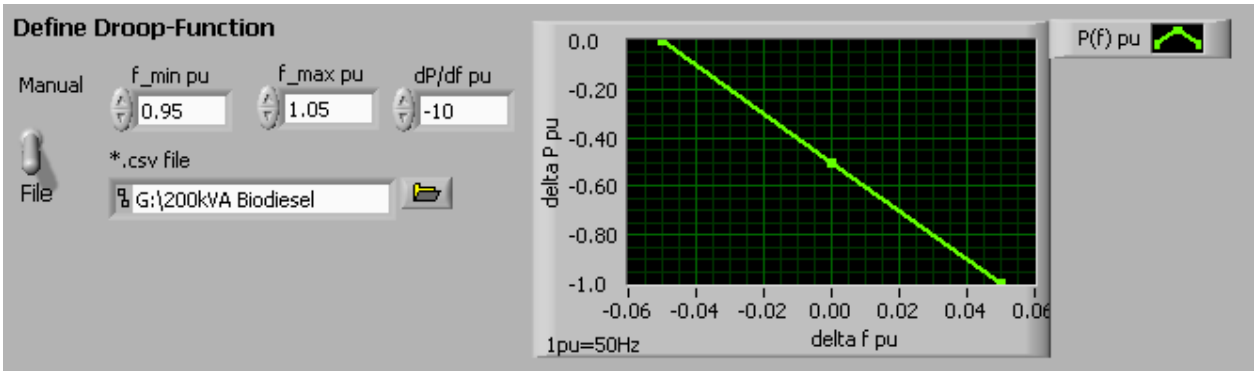

Figure 131: Set ΔP/Δf-static of the wind energy plant

It can be seen in the diagram that the wind turbine is permanently limited. The full wind energy is fed-in only when the frequency is at lowest limit. When the frequency value is at the highest limit, the wind energy plant no longer feeds-in any power.

If the plant is idling, the RCT takes over its synchronization with the laboratory grid and re-connects when synchronicity is achieved. In the laboratory, a synchronising unit is used for this. In reality, the synchronisation can be carried out by the wind energy plant's converter. When the wind energy plant has been synchronised with the grid, it begins to feed in power – analogous to the measured process in an actual wind energy plant.

The wind energy plant's operation during which the signals from the control OPC server are also processed is shown in Figure 132. Depending on whether the plant is connected to the grid or not and whether the stop procedure has been activated or not, various operational modes are set.

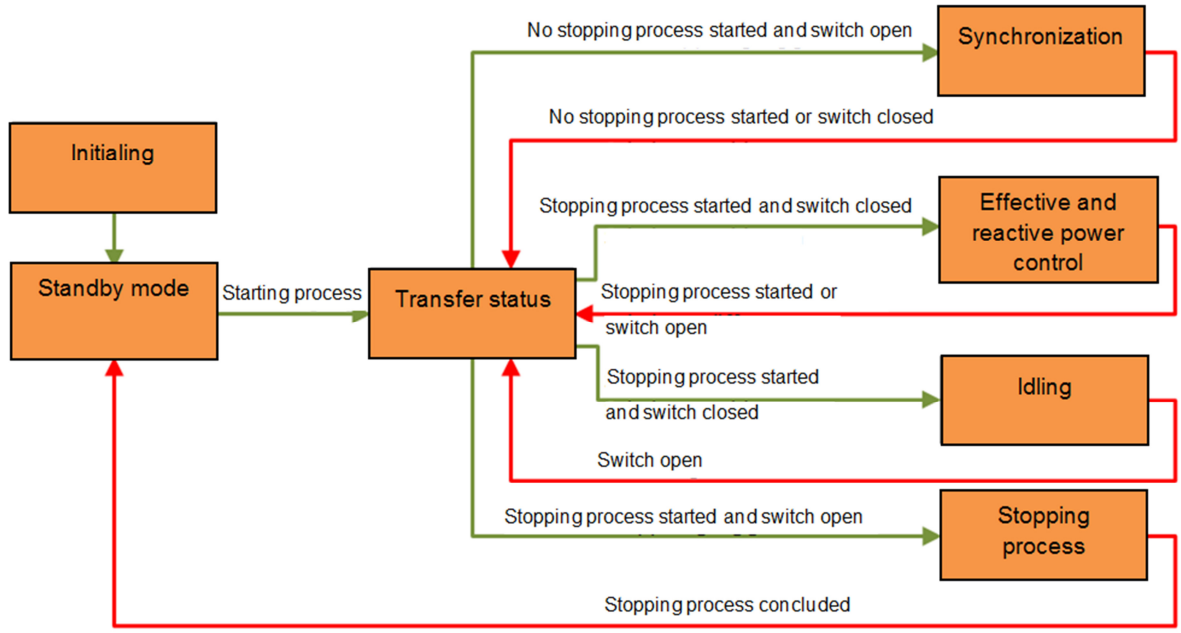

Figure 132: Status transition diagram of wind energy plant

Electrical grid

In the test for the restoration of supply, the grid is represented by a simple coupling section (crossbar distributor). Its line impendences are of minor importance due to the interaction of the producers and consumers (not the voltage stability) are the focus of the study. The coupling section consists of three bus bars of 630 A each, connecting the producers and consumers by means of an individual line. The nominal voltage of the grid is 400 volt in all three phases.

Non-controllable load

The consumers are represented in the supply restoration test by ohmic loads. These are differentiated as controllable and non-controllable loads. Consumers that cannot be influenced by load management are reproduced as non-controllable loads of a total of 50 kW ohmic load. In the laboratory test, two non-controllable loads of each 20 kW and one of 10 kW are used.

Controllable load

The controllable loads have a maximum capacity of 12 kW that can be controlled in three steps of 300 W. The represent temporally shiftable loads that can be controlled by load management. Just like the other units in the supply restoration test, for the controllable loads an interface is developed in Labview, in this case between the Interbus-OPC server of the loads and the control OPC server of the KRI. The load control is also programmed in Labview; their basic idea is to make loads dependent on the frequency.

Via the remote control terminal (see Figure 133), the controllable loads have a $\Delta P/\Delta f$-static allocated, which controls the load, depending on the frequency. If the frequency value is greater than 50 Hz, additional load up to 12 kW (1.2 PU) is added and vice versa. If the frequency falls below 50 Hz, the load is reduced.

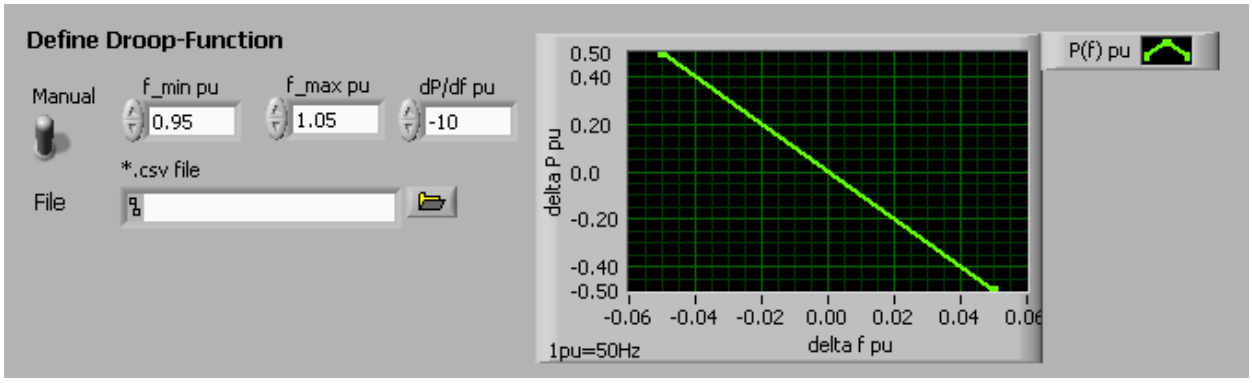

Figure 133: Set $\Delta P/\Delta f$-static for controllable loads

If the frequency falls outside of the limits set by the static, a load shedding/adding load concept is applied. Load shedding is a strategy, which is used to guarantee the security of supply if the load in a grid is too high. By shedding certain loads, an outage of the grid can be prevented [54]. There are many possibilities of implementing such a load shedding concept, such as, for instance, using different levels of load that are switched off at different frequency levels. The correct dimensioning of a load-shedding concept depends on the requirements and the characteristics of the relevant grid.

The load shedding concept for the test of restoration of supply needs the definition of three different parameters: The frequency limits (upper and lower limit), the time delay and the extent of the load levels. If the frequency falls below the lower limit of 48.5 Hz in the test, and the time of this under-frequency lasts for more than 10 seconds, one load level is disconnected. If the frequency is above the upper limit of 52.5 Hz for longer than 10 seconds, the opposite happens: a frequency level is switched in. The extent of the load levels was fixed to a value of 2.1 kW maximum load. Figure 134 illustrates the procedure of load shedding.

Figure 134: Status transition diagram of load shedding

Synchronizing unit

The synchronizing unit serves to reconnect the island grid to the integrated network. The reconnection takes place when the integrated network is (again) available and the laboratory grid conditions have been fulfilled with regard to frequency, voltage, and absence of alarms. Then central control will send a signal to the synchronizing unit. This will carry out the synchronization and switches the laboratory grid back into the integrated grid.

3.4.2.2 Test process and results

At the beginning of the test, the laboratory grid is disconnected from the integrated network and is then without voltage. The biogas plant starts up with the aid of its battery and begins to reproduce an island grid in island operation. Now already one level of passive, non-controllable load is covered, the so-called cold load. The controllable loads, too, become active. The wind energy plant now has a voltage at its grid connection. It starts, synchronises itself with the laboratory/island grid and connects with it. Their $\Delta P/\Delta f$ control starts. The following temporal progression during which loads are switched on and off again, depending on the frequency, is illustrated in Figure 135. It can be seen how the various units interact to produce frequency stability during the restoration of supply.

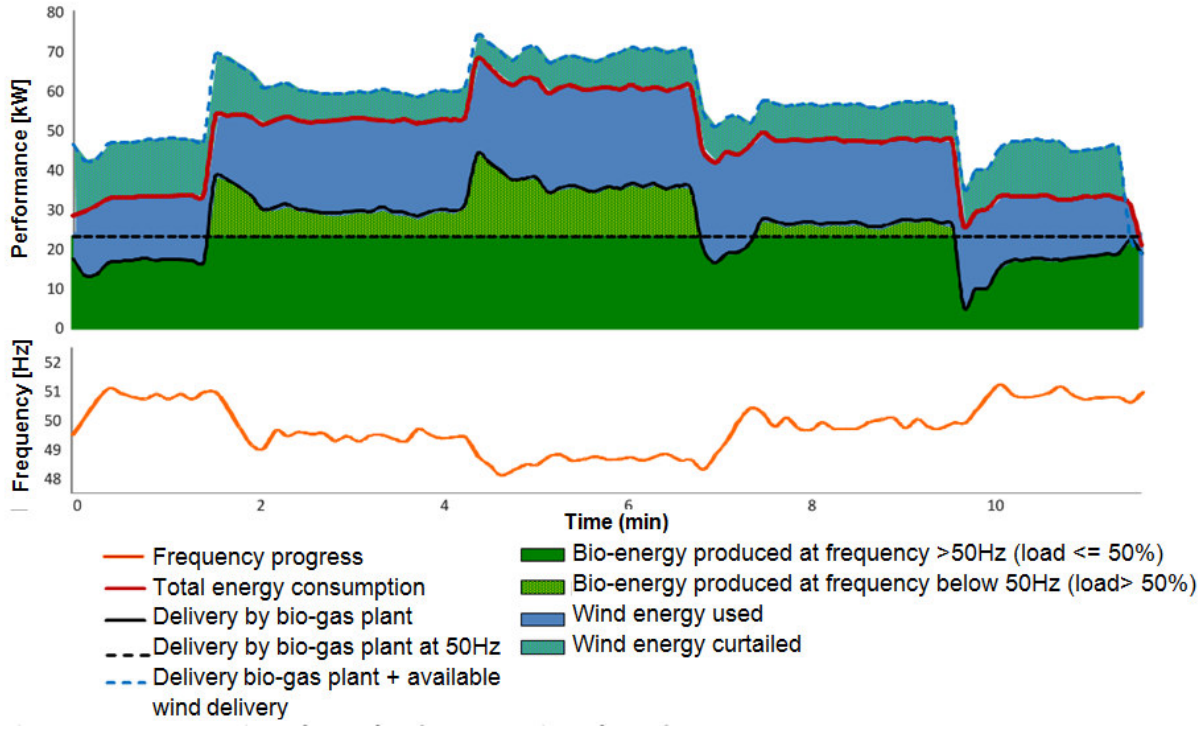

Figure 135: Progression of tests for the restoration of supply

If the load in the biogas plant is below 50 %, grid frequency is increased in order to communicate the requirement for regulation to the other producers and the need for additional load to the controllable loads. This sequence is set by the static of the biogas plant and can also be changed via this. In setting this property, a decisive role is played by the efficiency curve and the overload capacity of the biogas plant.

In case of the wind energy plant it can be seen how its reserve changes in dependence on the progression of the frequency. An increase in frequency goes hand in hand with the growth of capacity reserve of the wind energy plant and vice versa. Thus in case of high frequencies, a smaller part of the available wind energy is used than with lower frequencies.

Figure 136 illustrates the progression of energy used by the loads. The non-controllable loads have a strong influence on the loading of the entire system as can be observed by reference to the progression of the frequency.

The contribution by controllable loads to the frequency stability can also be observed. Towards the middle of the test, a part of the controllable load is shed due to under frequency. When the frequency increases again but also at the beginning of the test, load is added.

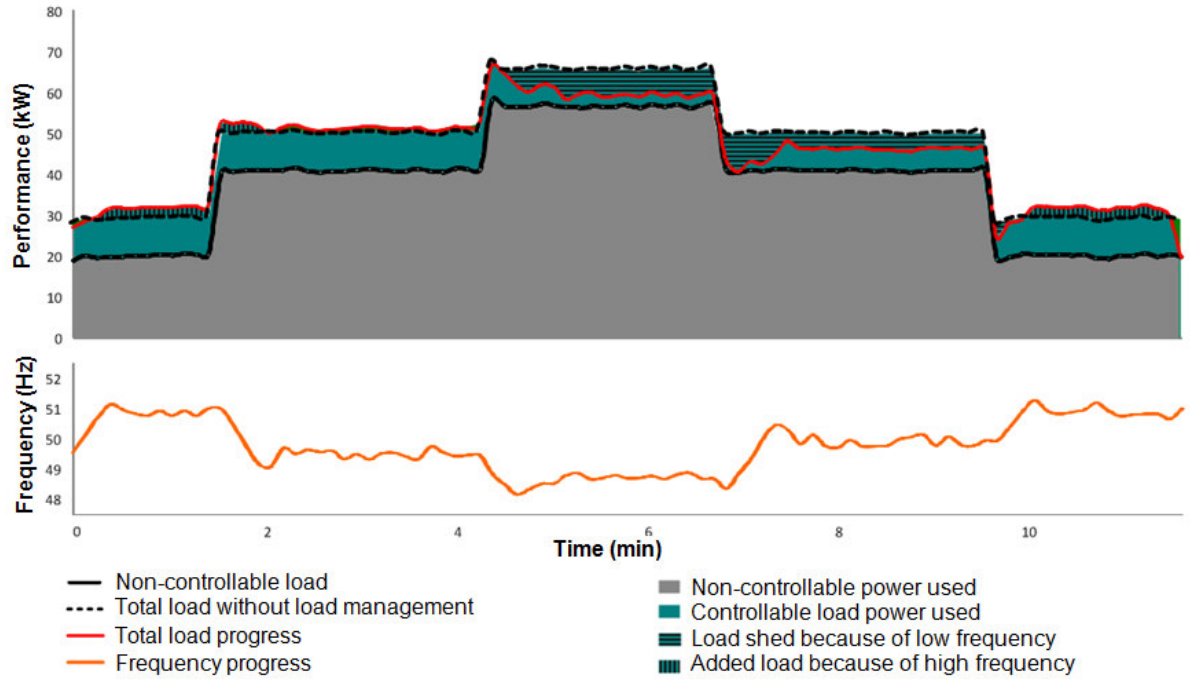

Figure 136: Progression of energy usage

At the end of the test, frequency and voltage of the laboratory grid lie within tolerance limits. The synchronizing unit reconnects the laboratory/island grid with the integrated network. The biogas plant then changes over to grid-connected operation. The frequency and voltage control mode is disabled.

3.4.3 Conclusions and recommendations

The laboratory tests for the restoration of supply were carried out successfully. From the successful test, it can be concluded that the technical potential for the restoration of supply through renewable energies exists. However, the test results cannot simply be transferred to real distribution grids but are valid only for the test configuration studied. Real distribution grids have a power grid which includes spatial extension and various voltage levels whereby the voltage stability – which was not investigated further in the tests – is made more complicated, and on the other hand production and consumer structures are very different. In principle, a distribution grid can only recreate itself from its own resources if it consists of more energy producers than consumers. Distribution grids with fewer generators than loads always depend on help, i.e. the delivery of energy from the outside, to completely re-establish power. However, the power producers of such distribution grids can act as support in the restoration of supply. For a distribution grid to re-establish power by itself there must be at least one energy producer that succeeds in creating its own requirements after a power outage or is able to go into black start mode and can act as a grid creating capacity.

The switching of power producers and power consumers into the that is maintained by the grid-creating unit requires it to have a sufficiently large frequency and voltage stability capability. This allows it to control the frequency and voltage within the limits of tolerance despite constant active and reactive power changes. Regarding frequency and voltage stability during the ongoing re-creation of the grid, additional grid-supporting power producers are helpful. They should be in a position to continuously support frequency and voltage, as was achieved in the test by the set statics.

During the restoration of supply with renewable energies, it is also helpful to know their available active power (see 3.1.2.1) in order to be able to estimate how much active and how much reactive power can be expected from them. The necessary proportions of grid-creating and grid-supporting power producers and of switchable and non-switchable power consumers for the restoration of supply was shown in the test by means of an example, which not varied or optimized and could be very different for real distribution grids. With regard to that, there is a continued need for studies on the transfer to distribution grids in Germany.

Another area for necessary study exists with regard to the behaviour of the parameters of protective devices at island operation and the necessary number of synchronizing units for the German grid. In addition, the role of the increasing number of CHP plants, storages, and especially batteries on the restoration of supply, needs to be studied. These could increase the black start capabilities significantly and contribute to the formation of smaller island grids, e.g. for individual buildings. It became apparent during the test that the restoration of supply needs a high degree of communication, which can be applied to real grids.

The control of grid-creating and grid supporting units, switching on and off of loads and receiving and forwarding of situational measured values must take place by means of a communication system that is reliable and above all, that functions even during an outage. It is of course a prerequisite that the communication infrastructure exists. The high communication and control-technical effort for the restoration of supply, in a distribution grid using decentralized energy producers, can be limited if the network operators do not have to communicate directly with all producers and consumers in the grid, but only to existing VPPs. These can take over the control of their plants and offer reliable ancillary services for the restoration of supply to the network operator.

Another development requirement exists in the area of technical implementation of creating island grids in biogas plants. Although biogas CHP which are designed to create island grids and are available for emergency standby operations already exist, biogas plants still feature various loads such as agitators, pumps, compressors that have to be managed appropriately. This has to be included in the implementation of a biogas plant control.

4 Summary, recommendations and outlook

The power production in Germany is in a period of transition. In future, fossil fuels are to be replaced almost completely by renewable energy sources – this is what the government and a great majority of the population strive for. It is foreseeable that the changes in the power supply will lead to new, untested situations in the grid. These situation may create concerns about power outages in the future, which are understandable. In order to ensure that the power supply remains reliable in future, it is necessary to assess the future grid stability with forward-looking studies that assess the possibilities at this point in time. This is no easy task by any means, as grid stability has many aspects and depends on all components of power supply, such as the producers, the storages, the consumers and the grid itself and its grid components that might be in different states.

In order to approach this task, a consistent scenario and an associated model of a future, purely renewable power supply for Germany were developed for this study. The model features has a high energy-geographical degree of detail, both with regard to the spatial resolution and with regard to the variety of technologies included. Even though a model obviously cannot describe the future reality precisely, important conclusions for the design of the power supply can be gained. This can be seen in the conclusions and recommendations of the scenario in Chapter 2. The scenario model was explored, using common / accepted and partly innovative scientific methods, concerning important though non-exhaustive aspects of grid stability. The conclusions that were drawn from the calculations for grid stability may be found in the relevant sections, namely 3.1.8, 3.2.6, 3.3.3 and 3.4.3.

The results of calculations in the study in hand suggest that a secure and stable power supply for Germany on the basis of 100 % renewable energy sources is technically possible, and that a relevant adjustment of the system will not compromise the accustomed high service quality in Germany.

No model can deliver complete assurance in this matter – it has to be proven in practice. However, further forward-looking studies to assess the future grid stability in Germany are advisable and should include the following topics as an extension of the implemented calculations:

- Necessary number of grid-forming inverters
- Voltage stability in secondary grids through interaction with the transmission grid
- Studies on short-circuit current
- Simulations of dynamic frequency stability with a non-aggregated model and the oscillations identified from it

Further information on the organization of the energy turnaround (“Energiewende”) would also deliver an extension of the scenario model developed here. Apart from modelling of other 100%-RE electricity supply scenarios based on a further optimization of certain values and conditions, modelling of the development of power supply from the current state to the desired 100 % RE state would deliver important insights into the technical feasibility for the transition period in between.

The precise investigation of the connection between the power supply with the energy consumer sectors heat and transport continues to be of special significance since these are the key to the success of the energy turnaround. The extension of the model to Europe would also deliver extensive information about the stability of the grid, which does not end at Germany's borders but is part of an interconnected system across Europe. Finally, the economic consequences of the energy turnaround on energy trading and grid operations should be investigated carefully.

Apart from the simulations, part of the project in hand was dedicated to testing the technical capabilities of providing ancillary services under laboratory conditions (for the test of the restoration of supply in Chapter 3.4) and with real RE plants (for control energy in section 3.1.2). Particularly the tests and the concluding demonstration of providing control reserve from the Kombikraftwerk show that renewable energy technologies already possess the necessary technical capabilities, which can be used to guarantee grid stability. For instance, they can increase and decrease their feed-in extremely quickly and also can maintain constant feed-in levels over a longer period of time.

It can thus be concluded that renewable energies are already technically able to provide important ancillary services. However, it was also made clear in the study (section 3.1.8) that for this, the conditions for integrating them into the market and system would have to be adjusted.

The much-discussed disadvantages for grid stability, due to the reduction of rotational energy in the system, can largely be compensated by the technical abilities of RE power plants, which in part exceed the current requirements for delivering ancillary services.

Thereby, the commitment of RE units must be controlled actively, regardless whether security of supply, ancillary services or grid stability are concerned.

In order to guarantee grid security, decentralised RE-plants would have to be monitored and controlled by secure and efficient communication standards.

Only then can they assume the responsibility for the stability and security of the power supply. Uniform communication standards facilitate the technical implementation and should be valid in the long term. The communication link between RE plants is also the basic step towards forming VPPs. The disadvantages of the individual plants, such as faulty forecasts, schedule deviations or outages can be counterbalanced through coordination within the group and thus the services offered is reliable with reduced external communication requirements.

As a result of the aggregation in VPPs, renewable energies have the ability to guarantee the safe operation of the grid.

However, to reach the goal of an energy turnaround, political, economic, and technical efforts will have to be made during the next years and decades. The challenges of maintaining grid stability that are posed by the change in electricity supply are less to be seen in RE themselves as they already fulfil the necessary technical requirements today. The new structure of the future power production and distribution requires a re-evaluation of the organisation of the system. The transformation of the system requires that the fluctuating feed-in from wind and photovoltaic (PV) systems are seen as an essential supporting pillar. Flexible biomass (biogas and solid mass) and bio-methane power plants form an important part of the energy system and contribute to secure the necessary capacity. For this reason, continuing developments are necessary to make biomass plants more flexible. Without

an appropriately adapted expansion of the electricity grid with all its components, adapting regulations and the creation of both adequate flexibilities and a power storage system, the turnaround in the electricity supply will not succeed. As a reward for these efforts, a modern, clean, and stable power supply can be achieved.

5 Definition

The concept **VPP** has not been defined unambiguously. The meaning of the parts of the word which make up the whole suggest using it for a power plant, which combines either various processes or various energy sources. For this reason, the term is occasionally used for “combined gas-steam power plants” (GAS power plants) or combined heat and power units (CHP) but it is also synonymous with a “virtual power plant”, particularly in connection with renewable energies. The concept “virtual power plant” has established itself in science for a group of decentralized plants which are centrally controlled via a control centre, even though it is not easy to define it [56] and the term “virtual” is misleading as real power plants are involved which really feed energy into the grid. For this reason the term “VPP = Kombikraftwerk” has been maintained as it also is the name of the research project. If a VPP has been established which is composed entirely of renewable energies, the term will expand to “Kombikraftwerk”. These days, VPPs usually are formed by an operator of one type of plant (for instance, a wind farm) who would add other types of plants (for instance, photovoltaics or biogas plants) to his portfolio in order to increase his scope. As a rule, the plants are connected to a control centre by communication technology for purposes of maintenance and control and this is the fundamental prerequisite for running a VPP. Among the typical operators of VPPs are specifically communal energy supply companies, e.g. public utility companies that are usually allocated a complete medium voltage power grid. By linking different RE plants into one VPP the individual strengths of wind and sun energy, biomass, geothermal and hydropower, storage and backup-power plants can be pooled. Such a Kombikraftwerk cannot only produce reliable power but also ancillary services such as delivering control reserve. A further advantage of such a link is the spatial balance – for instance, if wind farms from different regions are linked, it would be very rare if all of them in all locations were to experience calm simultaneously. In addition, the weather is easier to forecast with fewer errors for larger areas.

6 References

[1] R. Mackensen, K. Rohrig, H. Emanuel: "Das regenerative Kombikraftwerk - Abschlussbericht", Institut für solare Energieversorgungstechnik (ISET) (2008), Kassel, http://www.kombikraftwerk.de/fileadmin/downloads/2008_03_31_Ma__KombiKW_Abschlussbericht.pdf

[2] A. Schwab: „Elektroenergiesysteme – Erzeugung, Transport, Übertragung und Verteilung elektrischer Energie“, 3., neu bearbeitete und erweiterte Auflage, Springer DE, 20.07.2009, ISBN 978-3-540-92226-1

[3] G. Büttner et al.: “Corine Land Cover 2006 Technical Guidelines”, European Environment Agency - Technical report , 2007, http://www.umweltbundesamt.at/umwelt/raumordnung/flaechennutzung/corine/, besucht am 22.3.2011

[4] Bundesamt für Kartographie und Geodäsie, Digitales Basis-Landschaftsmodell BASIS-DLM, Frankfurt am Main, 14.10.2008

[5] BMU, BMWi: „Energiekonzept – für eine umweltschonende, zuverlässige und bezahlbare Energieversorgung“, Bundesministerium für Umwelt, Naturschutz und Reaktorsicherheit (BMU) und Bundesministerium für Wirtschaft und Technologie (BMWi), September 2010

[6] DLR, Fraunhofer IWES, InfE: „Leitstudie 2010 - Langfristszenarien und Strategien für den Ausbau der erneuerbaren Energien in Deutschland bei Berücksichtigung der Entwicklung in Europa und global“, Schlussbericht BMU - FKZ 03MAP146, 2010

[7] Th. Klaus et al.: „Energieziel 2050: 100% Strom aus erneuerbaren Quellen“, Publikation des (Deutschen) Umweltbundesamtes. Dessau-Roßlau, 2010.

[8] BDEW, „Verteilung des Netto-Stromverbrauchs in Deutschland auf die Kundengruppen in Mio. kWh“, http://www.bdew.de/internet.nsf/id/DE_Energiedaten

[9] Statistische Ämter des Bundes und der Länder: „Regionaldatenbank Deutschland“, https://www.regionalstatistik.de/genesis/online

[10] Entso-E, „Consumption Data“, https://www.entsoe.eu/resources/data-portal/consumption/

[11] S. Bofinger, D. Callies, M. Scheibe, Y.-M. Saint-Drenan, K. Rohrig: „Studie zum Potential der Windenergienutzung an Land“ – Kurzfassung, Kassel, 2011

[12] K. Einig et al.: „Wieviel Platz braucht die Windkraft“, neue energie – das magazin für erneuerbare energien, Nr. 8/2011, http://www.neueenergie.net/fileadmin/ne/ne_inhalte/dokumente/neue_energie_08_2011_S.34-37.pdf

[13] S. Bofinger et al.: „Potenzial der Windenergie an Land - Studie zur Ermittlung des bundesweiten Flächen- und Leistungspotenzials der Windenergienutzung an Land“, Umweltbundesamt, September 2013, http://www.umweltbundesamt.de/publikationen/potenzial-windenergie-an-land

[14] J.-P. Schulz, U. Schättler: „Kurze Beschreibung des Lokal-Modells Europa (LME) und seiner Datenbanken auf dem Datenserver des DWD“, Deutscher Wetterdienst (DWD), Offenbach, 15.01.2009

[15] M. Baldauf, J. Förster et al.: „Kurze Beschreibung des Lokal-Modells Kürzestfrist COSMO-DE (LMK) und seiner Datenbanken auf dem Datenserver des DWD“, Deutscher Wetterdienst (DWD), Offenbach, 31.03.2011

[16] „dena-Netzstudie II – Integration erneuerbarer Energien in die deutsche Stromversorgung im Zeitraum 2015-2020 mit Ausblick auf 2025“, Deutsche Energie Agentur, Berlin, 2010, http://www.dena.de/themen/thema-esd/publikationen/publikation/dena-netzstudie-ii

[17] Bundesamt für Seeschifffahrt und Hydrographie (BSH), 2011, www.bsh.de

[18] Offshore-Wissenschaftliches Mess- und Evaluierungsprogramm (Offshore˜WMEP) , 2011, www.offshore-wmep.de

[19] Bundesverband WindEnergie: „Potenzial der Windenergienutzung an Land“ – Langfassung, http://www.wind-energie.de/shop-potenzial-der-windenergienutzung-land, Artikelnummer: ST-PO-13, ISBN: 978 3 94257993

[20] UpWind – “Design Limits and Solutions for Very Large Wind Turbines”, März 2011, http://www.ewea.org/fileadmin/ewea_documents/documents/upwind/21895_UpWind_Report_low_web.pdf

[21] N.O. Jensen: “A Note of Wind Generator Interaction”, Technical Report M-2411, Risø National Laboratory, Roskilde, Dänemark, 1983

[22] M. Braun et al.: „Vorstudie zur Integration großer Anteile Photovoltaik in die elektrische Energieversorgung“, Studie im Auftrag des BSW - Bundesverband Solarwirtschaft e.V., Berlin

[23] EEG-Anlagenstammdaten, Informationsplattform der deutschen Übertragungsnetzbetreiber: „EEG / KWK-G“, http://www.eeg-kwk.net/de/Anlagenstammdaten.htm

[24] Solar Radiation Data: „Einstrahlungsdaten“, Paris, http://www.soda-is.com, letzter Zugriff: 3. Mai 2010

[25] S. Bofinger: „Rolle der Solarstromerzeugung in zukünftigen Energieversorgungs-strukturen - Welche Wertigkeit hat Solarstrom?“, Studie im Auftrag des Bundesministeriums für Umwelt, Naturschutz und Reaktorsicherheit, Berlin, 2008

[26] T. M. Klucher: “Evaluation of Models of Predict Insolation on Tilted Surfaces”, Solar Energy, 23:111-114, 1979

[27] H. Schmidt, D. U. Sauer: „Wechselrichter-Wirkungsgrade“, 1996, Sonnenenergie 4, 43-47. Berlin

[28] Beyer et al.: “A Robust Model for the MPP Performance of Different Types of PV-modules Applied for the Performance Check of Grid Connected Systems”, EUROSUN 2004, ISES Europe Solar Congress, Unter Mitarbeit von G. Heilscher, S. Bofinger und H.G. Beyer, Freiburg, 2004

[29] Bundesnetzagentur: „Versorgungsqualität - SAIDI-Wert“, 2012, http://www.bundesnetzagentur.de

[30] F. Prillwitz, M. Krüger: "Netzwiederaufbau nach Großstörungen." Universität Rostock, Institut für Elektrische Energietechnik, 2007

[31] Verband der Netzbetreiber VDN e.V. beim VDEW: „TransmissionCode 2007 Netz- und SysteTCRegeln der deutschen Übertragungsnetzbetreiber“, Berlin, 8.2007

[32] Bundesverband der Energie- und Wasserwirtschaft (BDEW): „Technische Richtlinie Erzeugungsanlagen am Mittelspannungsnetz - Richtlinie für Anschluss und Parallelbetrieb von Erzeugungsanlage am Mittelspannungsnetz“, Berlin, Juni 2008

[33] UCTE: "Operation Handbook", 2004, https://www.entsoe.eu/publications/system-operations-reports/operation-handbook/

[34] M. Krüger, H. Weber, Harald et al.: "Wiederaufbau von Übertragungsnetzen nach Großstörungen", ETG-Fachbericht-Netzregelung und Systemführung, 2008

[35] Fachverband Biogas: „Branchenzahlen 2011 und Branchenentwicklung 2012/2013"

[36] J. Witt, C. Hennig, N. Rendsberg, A. Schwenker, F. Scholwin: „Monitoring zur Wirkung des EEG auf die Entwicklung der Stromerzeugung aus Biomasse", Deutsches Biomasse Forschungszentrum (DBFZ), 2010

[37] BMVBS: „Globale und regionale Verteilung von Biomassepotenzialen, Status-quo und Möglichkeiten der Präzisierung", BMVBS-Online-Publikation, 27/2010, 2010

[38] ITAD - Interessengemeinschaft der thermischen Abfallbehandlungsanlagen in Deutschland e.V.: „Übersichtskarte der ITAD-Mitglieder-Anlagen", http://www.itad.de/itad/mitglieder/79.Mitglieder.html

[39] H. Paschen, D. Oertel, R. Grünwald: „Möglichkeiten geothermischer Stromerzeugung in Deutschland.", Sachstandsbericht Deutscher Bundestag, Ausschuss für Bildung, Forschung und Technikfolgenabschätzung, TAB-Arbeitsbericht 84, 2003

[40] ENTSO-E Grid Map, European Network of Transmission System Operators for Electricity, http://www.entsoe.eu, 1.7.2011

[41] Verband der *Elektrotechnik,* Elektronik und Informationstechnik e.V.: „Deutsches Höchstspannungsnetz – Übersichtsplan", 1.1.2012

[42] Deutsche Energie Agentur: „dena-Netzstudie I - Energiewirtschaftliche Planung für die Netzintegration von Windenergie in Deutschland an Land und Offshore bis zum Jahr 2020", Berlin, 2005

[43] 50Hertz Transmission GmbH/ Amprion GmbH/ EnBW Transportnetze GmbH/ TenneT TS0 GmbH: „Netzentwicklungsplan Strom 2012 – Entwurf der Übertragungsnetzbetreiber", 30.5.2012

[44] Bundesverband der Energie- und Wasserwirtschaft: „Liste der Stromnetzbetreiber„ 1.8.2012

[45] B. R. Oswald: „Skript Freileitungen-Vorlesung elektrische Energieversorgung I.", Institut für Energieversorgung und Hochspannungstechnik, Universität Hannover, 2005

[46] D. Heide, L. von Bremen, M. Greiner, C. Hoffmann, M. Speckmann, S. Bofinger: „Seasonal Optimal Mix of Wind and Solar Power in a Future, Highly Renewable Europe", Renewable Energy 35 (11), 2010, 2483 - 2489

[47] P. Kundur et al.: "Definition and Classification of Power System Stability", IEEE/CIGRE Joint Task Force on Stability Terms and Definitions, IEEE Transactions on Power Systems, Vol. 19, No. 3, S. 1387-1401, 8.2004

[48] TransmissionCode 2003. Anhang D 1: „Unterlagen zur Präqualifikation für die Erbringung von Primärregelleistung für die ÜNB", Stand August 2003

[49] Handbook, UCTE Operations. "P1–Policy 1: Load-Frequency Control and Performance [C]." Version: v3. 0 rev 15.01.04 (2009), https://www.entsoe.eu/fileadmin/user_upload/_library/publications/entsoe/Operation_Handbook/Policy_1_final.pdf

[50] Bundesverband Erneuerbare Energie e.V.: „Stromversorgung 2020 – Wege in eine moderne Energiewirtschaft, Strom-Ausbauprognose der Erneuerbaren-Energien-Branche“, Berlin, 2009

[51] E. Wagner, U. Rindelhardt: „Stromgewinnung aus regenerativer Wasserkraft in Deutschland – Überblick“, In: ew - das Magazin für die Energiewirtschaft, Jg. 106(25-26), 2007, S. 52-57

[52] GtV – Bundesverband Geothermie: „Tiefe Geothermieprojekte in Deutschland, Liste der tiefen Geothermieprojekte in Deutschland 2013 nach Projektname“, http://www.geothermie.de/wissenswelt/geothermie/in-deutschland.html, Stand: Oktober 2013

[53] M. Braun, R. Estrella Navarro, M. Jentsch, und C. Bünsow, „Specification of Laboratory Test“, Kassel, Deliverable, 11.2008

[54] S. Hirodontis, H. Li, und P. A. Crossley, „Load Shedding in a Distribution Network“, in Sustainable Power Generation and Supply, SUPERGEN'09 - International Conference, 2009, S. 1–6

[55] ENERCON GmbH, Datenblatt, Enercon Windenergieanlagen, E-101 / 3050 kW / FTQ, Netztechnische Leistungsmerkmale, 2011

[56] C. Kieny, B. Berseneff, N. Hadjsaid, Y. Besanger, J. Maire: “On the Concept and the Interest of Virtual Power Plant: Some Results from the European Project FENIX”, IEEE PES Gen. Meet. 2009

[57] F. Steinke, P. Wolfrum, C. Hoffmann: „Grid vs. Storage in a 100% Renewable Europe“, Renewable Energy 50, 2013, S.826-832

[58] VDE, Verband der Elektrotechnik Elektronik Informationstechnik e.V.:“ Entwurf - Erzeugungsanlagen am Niederspannungsnetz – Technische Mindestanforderungen für Anschluss und Parallelbetrieb von Erzeugungsanlagen am Niederspannungsnetz“, Berlin, 7.2010

[59] Verband der Netzbetreiber VDN e.V. beim VDEW: „DistributionCode 2007 – Regeln für den Zugang zu Verteilungsnetzen“, Berlin, 8.2007

[60] Fraunhofer IWES, Amprion, TenneT, Enercon, Energiequelle: „Regelenergie durch Windkraftanlagen. Abschlussbericht“, 2013

[61] P. Sorknæs, A. N. Andersen; J. Tang, S. Strøm:”Market Integration of Wind Power in Electricity System Balancing”, In: Energy Strategy Reviews (0), 2010, Online verfügbar unter http://www.sciencedirect.com/science/article/pii/S2211467X13000072

[62] BM Intermittent Gen WG: “BM Uni Data from Intermittent Generation - final”, Working Group Report, 2010

[63] D. Schneider, K. Kaminski, M. Siefert, M. Speckmann: “Available Active Power Estimation for the Delivery of Control Reserve by Wind Turbines”, EWEA 2013, Wien, 4.2. - 7.2.2013

[64] ACER: „Framework Guidelines on Electricity Balancing“, 2012

[65] Bundesnetzagentur: „Eckpunktepapier zur Weiterentwicklung des Ausgleichsenergiepreissystems, BK6-12-024“, 2012

[66] M. Jansen, M. Speckmann: “Wind Turbine Participation on Control Reserve Markets”, EWEA 2013, Wien, 2013

[67] M. Jansen, M. Speckmann: "Participation of Photovoltaic Systems in Control Reserve Markets", 22nd International Conference on Electricity Distribution, Stockholm, 10.6. - 13.6.2013

[68] Consentec: „Gutachten zur Höhe des Regelenergiebedarfs", Im Auftrag der BNetz-A, 2008

[69] Consentec: „Gutachten zur Dimensionierung des Regelleistungsbedarfs unter dem NRV", Untersuchung im Auftrag der BNetz-A, 2010

[70] P. Zolotarev, D. Schlipf: "Marktseitige und technische Maßnahmen zur gesamtwirtschaftlichen Optimierung der Lastdeckung im liberalisierten Strommarkt", 9. Fachtagung Optimierung in der Energiewirtschaft 2011 - VDI, 2011

[71] A. W. Bowman, A. Azzalini: "Applied Smoothing Techniques for Data Analysis. The Kernel Approach with S-Plus Illustrations", Oxford, New York, Clarendon Press, Oxford University Press, 1997

[72] EEX-Tranzparenzplattform, Online verfügbar unter http://www.transparency.eex.com/de/, zuletzt geprüft am 06.01.2013

[73] Bundesnetzagentur: „Bilanzkreisvertrag - Anlage zum Beschluss BK6-06-013", 2011

[74] UCTE: "P1 - Policy 1: Load-Frequency Control and Performance", 2009

[75] regelleistung.net: „Ausschreibungsübersicht", Online verfügbar unter https://www.regelleistung.net/ip/action/ausschreibung/public, zuletzt geprüft am 04.12.2012

[76] Fraunhofer IWES: „Energiewirtschaftliche Bewertung von Pumpspeicherwerken und anderen Speichern im zukünftigen Stromversorgungssystem", Endbericht, 2010

[77] Bundesnetzagentur, Bundeskartellamt: „Monitoringbericht 2012. Monitoringbericht gemäß § 63 Abs. 3 i.V.m. § 35 EnWG und § 48 Abs. 3 i.V.m. § 53 Abs. 3GWB", 3. Auflage, 5.2.2013

[78] Bundesnetzagentur: „Bericht zum Zustand der leitungsgebundenen Energieversorgung im Winter 2011", 12. 03.05.2012. Online verfügbar unter: http://www.bundesnetzagentur.de/cln_1932/DE/Allgemeines/DieBundesnetzagentur/Publikationen/Berichte/berichte-node.html, Zugriff am 12.06.2013

[79] K. Schaber, F. Steinke und T. Hamacher: "Managing Temporary Oversupply from Renewables Efficiently: Electricity Storage Versus Energy Sector Coupling in Germany", 32nd International Energy Workshop (IEW 2013), Paris, Frankreich, 2013

[80] Kraftwerksliste der Bundesnetzagentur, http://www.bundesnetzagentur.de, Stand: 16. Oktober 2013

[81] Bundesnetzagentur: „Statistikbericht EEG - Jahresendabrechnung 2011", http://www.bundesnetzagentur.de

[82] Erneuerbare Energien-Statistik (AGEE-Stat): „Zeitreihen zur Entwicklung der erneuerbaren Energien in Deutschland", Stand Juli 2013

[83] M. Scheftelowitz, J. Daniel-Gromke, M. Beil, W. Beyrich, W. Peters: „Stromerzeugung aus Biomasse – Zwischenbericht 2013", Deutsche Biomasse Forschungszentrum (DBFZ), 2013

[84] Verbundprojekt: DEA-Stabil: „Beitrag der Windenergie und Photovoltaik im Verteilungsnetz zur Stabilität des deutschen Verbundnetzes Teilvorhaben: Bewertung und Abhilfemaßnahmen", Laufendes Forschungsvorhaben des BMU, FKZ 0325585

[85] Bundesnetzagentur - Beschlusskammer 6 (2011a): „Festlegung zu Verfahren und Ausschreibung von Regelenergie in Gestalt der Minutenreserve“, 2011

[86] Bundesnetzagentur - Beschlusskammer 6 (2011b): „Festlegung zu Verfahren zu Ausschreibung von Regelenergie in Gestalt der Primärregelleistung“, 2011

[87] Bundesnetzagentur - Beschlusskammer 6 (2011c): „Festlegung zu Verfahren zu Ausschreibung von Regelenergie in Gestalt der Sekundärregelung“, 2011

[88] FNN: „TransmissionCode 2007. Anhang D2 Teil 2: Anforderungen für die Umsetzung des SRL-Poolkonzepts zwischen ÜNB und Anbietern“, 2009

[89] regelleistung.net: „Minutenreserveleistung. Gemeinsame Ausschreibung Minutenreserveleistung“, Online verfügbar unter https://www.regelleistung.net/ip/action/static/ausschreibungTCRl, zuletzt geprüft am 04.12.2012

[90] J. Dobschinski, E.D. de Pascalis, A. Wessel, L. von Bremen, B. Lange, K. Rohrig, Y.-M. Saint-Drenan: “The Potential of Advanced Shortest-term Forecasts and Dynamic Prediction Intervalls for Reducing the Wind Power Induced Reserve Requirements”, In: European Wind Energy Conference and Exhibition, 2010

[91] F. Sandau: „Entwicklung einer Simulationsumgebung zur dynamischen Berechnung des Regelleistungsbedarfs, sowie deren Anwendung auf ein Szenario mit einer erneuerbaren Energieversorgung“, Masterarbeit an der TU Berlin, 2013

[92] P. Andres, M. Spiwoks: „Prognosegütemaße: State of the Art der statistischen Ex-post-Beurteilung von Prognosen“, Sofia-Studien zur Institutionenanalyse Nr.00-1, Darmstadt, 2000

[93] B. Lange et al.: „Prognosen der zeitlich-räumlichen Variabilität von Erneuerbaren. Transformationsforschung für ein nachhaltiges Energiesystem“, FVEE-Themen, 2011, S. 95-96

[94] Bundesnetzagentur, Bundeskartellamt: „Monitoringbericht 2011. Monitoringbericht gemäß § 63 Abs.3 i.V.m. § 35 EnWG und § 48 Abs. 3 i.V.m. § 53 Abs. 3GWB“, 3. Auflage, 5.2.2013

[95] DVGW: Arbeitsblatt DVGW-G 260 „Gasbeschaffenheit “, Deutscher Verein des Gas- und Wasserfaches e.V., Bonn, 2008

[96] 50hertz u.a.: „Bericht der deutschen Übertragungsnetzbetreiber zur Leistungsbilanz 2013 nach EnWG § 12 Abs. 4 und 5“, Online verfügbar unter http://www.bmwi.de/BMWi/Redaktion/PDF/J-L/leistungsbilanzbericht-2013,property=pdf,bereich=bmwi2012,sprache=de,rwb=true.pdf, Stand 30.09.2013